Emission Factor Documentation for AP-42
Section 7.1

Organic Liquid Storage Tanks

Final Report

For U. S. Environmental Protection Agency
Office of Air Quality Planning and Standards
Emission Factor and Inventory Group

September 2006

Emission Factor Documentation for AP-42
Section 7.1

Organic Liquid Storage Tanks

Final Report

For U. S. Environmental Protection Agency
Office of Air Quality Planning and Standards
Emission Factor and Inventory Group
Research Triangle Park, NC 27711

Attn: Mr. Michael Ciolek

September 2006

TABLE OF CONTENTS

TABLE OF CONTENTS (continued)

LIST OF FIGURES

LIST OF FIGURES (continued)

LIST OF TABLES

LIST OF TABLES (continued)

LIST OF TABLES (continued)

LIST OF TABLES (continued)

EMISSION FACTOR DOCUMENTATION FOR AP-42 SECTION
Organic Liquid Storage Tanks

1.0 INTRODUCTION

The document *Compilation of Air Pollutant Emission Factors* (AP-42) has been published by the U. S. Environmental Protection Agency (EPA) since 1972. Supplements to AP-42 have been routinely published to add new emission source categories and to update existing emission factors. AP-42 is routinely updated by EPA to respond to new emission factor needs of EPA, State and local air pollution control programs, and industry.

An emission factor is a representative value that attempts to relate the quantity of a pollutant released to the atmosphere with an activity associated with the release of that pollutant. The emission factors presented in AP-42 may be appropriate to use in a number of situations, such as making source-specific emission estimates for areawide inventories for dispersion modeling, developing control strategies, screening sources for compliance purposes, establishing operating permit fees, and making permit applicability determinations. The purpose of this report is to provide background information to support revisions to AP-42 Section 7.1, Organic Liquid Storage Tanks.

This background report consists of six chapters. Chapter 1 includes the introduction to the report. Chapter 2 gives basic descriptions of fixed roof tanks, floating roof tanks, variable vapor space tanks, and horizontal tanks. It also includes descriptions of the different types of rim seals and deck fittings on floating roof tanks. Chapter 3 presents the emission estimation procedures for each tank type, as well as the methodology for hazardous air pollutant (HAP) speciation. Chapter 4 provides an evaluation of the equations that predict standing storage and working losses from fixed roof tanks. Chapter 5 provides an evaluation of the equations that predict standing storage and withdrawal losses from floating roof tanks. Chapter 6 is a summary of changes to the section since the previous edition of AP-42 (February 1996).

2.0 STORAGE TANK DESCRIPTIONS

2.1. INTRODUCTION

This chapter presents basic descriptions of fixed-roof tanks (vertical and horizontal); internal, external, and domed external floating roof tanks; pressure tanks; and variable vapor space tanks. In addition, the chapter provides descriptions of perimeter seals and fittings for internal, external, and domed external floating roofs.

2.2. TYPES OF STORAGE TANKS

Seven types of vessels are used to store volatile organic liquids (VOL):

1. Fixed-roof tanks;
2. External floating roof tanks;
3. Internal floating roof tanks;
4. Domed external floating roof tanks;
5. Horizontal tanks;
6. Pressure tanks; and
7. Variable vapor space tanks.

The first four tank types are cylindrical in shape with the axis oriented perpendicular to the foundation. These tanks are almost exclusively above ground. Horizontal tanks (i.e., with the axis parallel to the foundation) can be used above ground and below ground. Pressure tanks often are horizontally oriented and "bullet" or spherically shaped to maintain structural integrity at high pressures. They are located above ground. Variable vapor space tanks can be cylindrical or spherical in shape. The discussion below contains a detailed description of each of these tank types.

2.2.1. Fixed-Roof Tanks

Of currently used tank designs, the fixed-roof tank is the least expensive to construct and is generally considered the minimum acceptable equipment for storing VOL's. A typical fixed-roof tank, which is shown in Figure 2-1, consists of a cylindrical steel shell with a cone- or dome-shaped roof that is permanently affixed to the tank shell. Most recently built tanks are of all-welded construction and are designed to be both liquid- and vapor-tight. However, older tanks may be of riveted or bolted construction and may not be vapor-tight. A breather valve (pressure-vacuum valve), which is commonly installed on many fixed-roof tanks, allows the tank to operate at a slight internal pressure or vacuum. Breather vents are typically set at 0.19 kPa (0.75 in. w.c.) on atmospheric pressure fixed-roof tanks.[1] Because this valve prevents the release of vapors during only very small changes in temperature, barometric pressure, or liquid level, the emissions from a fixed-roof tank can be appreciable. Additionally, gauge hatches/sample wells, float gauges, and roof manholes provide accessibility to these tanks and also serve as potential sources of volatile emissions. Breather vents may be called conservation vents, although hardly any conservation of vapors occurs at such low pressure settings. Generally, the term conservation vent is used to describe a pressure setting of 17 kPa (67 in. w.c.) or less. Vents with settings greater than 17 kPa (67 in. w.c.) are commonly called `pressure' vents.

2.2.2 External Floating Roof Tanks[2]

A typical external floating roof tank consists of an open-topped cylindrical steel shell equipped with a roof that floats on the surface of the stored liquid, rising and falling with the liquid level. The floating roof is comprised of a deck, fittings, and rim seal system. Floating roof decks are constructed of welded steel plates and are of three general types: pan, pontoon, and double deck. Although numerous pan-type decks are currently in use, the present trend is toward pontoon and double-deck type type floating roofs. The two most common types of external floating-roof tanks are shown in Figures 2-2 and 2-3. Manufacturers supply various versions of these basic types of floating decks, which are tailored to emphasize particular features, such as full liquid contact, load-carrying capacity, roof stability, or pontoon arrangement. The liquid surface is covered by the floating deck, except in the small annular space between the deck and the shell; the deck may contact the liquid or float directly above the surface on pontoons. External floating roof tanks are equipped with a rim seal system, which is attached to the roof perimeter and contacts the tank wall. The rim seal system slides against the tank wall as the roof is raised and lowered. The floating deck is also equipped with fittings that penetrate the deck and serve operational functions. The external floating roof design is such that evaporative losses from the stored liquid are limited to losses from the rim seal system and deck fittings (standing storage loss) and any exposed liquid on the tank walls (withdrawal loss).

2.2.3 Internal Floating Roof Tanks[3]

An internal floating roof tank has both a permanent fixed roof and a floating roof inside. There are two basic types of internal floating roof tanks: tanks in which the fixed roof is supported by vertical columns within the tank; and tanks with a self-supporting fixed roof and no internal support columns. The fixed roof is not necessarily free of openings but does span the entire open plan area of the vessel. Fixed roof tanks that have been retrofitted to employ an internal floating roof are typically of the first type, while external floating roof tanks that have been converted to an internal floating roof tank typically have a self-supporting roof. Tanks initially constructed with both a fixed roof and an internal floating roof may be of either type. An internal floating roof tank has both a permanently affixed roof and a roof that floats inside the tank on the liquid surface (contact deck) or is supported on pontoons several inches above the liquid surface (noncontact deck). The internal floating roof rises and falls with the liquid level. A typical internal floating roof tank is shown in Figure 2-4.

Contact-type decks include (1) aluminum sandwich panels with a honeycombed aluminum core floating in contact with the liquid; (2) resin-coated, fiberglass-reinforced polyester (FRP), buoyant panels floating in contact with the liquid; and (3) pan-type steel roofs, floating in contact with the liquid with or without the aid of pontoons. The majority of contact internal floating decks currently in VOL service are pan-type steel or aluminum sandwich panel type. The FRP decks are less common.

Several variations of the pan-type contact steel roof exist. The design may include bulkheads or open compartments around the perimeter of the deck so that any liquid that may leak or spill onto the deck is contained. Alternatively, the bulkheads may be covered to form sealed compartments (i.e., pontoons), or the entire pan may be covered to form a sealed, double-deck, steel floating roof. Generally, construction is of welded steel.

Noncontact-type decks are the most common type of deck currently in use, and typically consist of an aluminum deck laid on an aluminum grid framework supported above the liquid surface by tubular aluminum pontoons. The deck skin for the noncontact-type floating decks is typically constructed of rolled aluminum sheets (about 1.5 meters [m] [4.9 feet (ft)] wide and 0.58 millimeter [mm] [0.023 inches (in)] thick). The overlapping aluminum sheets are joined by bolted aluminum clamping bars that run perpendicular to the pontoons to improve the rigidity of the frame. The deck skin seams can be metal on metal or gasketed with a polymeric material. The pontoons and clamping bars form the structural frame of the floating deck. Deck seams in the noncontact internal floating roof design are a source of emissions. Aluminum sandwich panel contact-type internal floating roofs also share this design feature. The sandwich panels are joined with bolted mechanical fasteners that are similar in concept to the noncontact deck skin clamping bars. Steel pan contact internal floating roofs are constructed of welded steel sheets and therefore have no deck seams. Similarly, the resin-coated, reinforced fiberglass panel decks have no apparent deck seams. The panels are butted and lapped with resin-impregnated fiberglass fabric strips. The significance of deck seams with respect to emissions from internal floating roof tanks is addressed in Chapter 5.

The internal floating roof physically occupies a finite volume of space that reduces the maximum liquid storage capacity of the tank. When the tank is completely full, the floating roof touches or nearly touches the fixed roof. Consequently, the effective height of the tank decreases, thus limiting the storage capacity. The reduction in the effective height varies from about 0.15 to 0.6 m (0.5 to 2 ft), depending on the type and design of the floating roof employed.

All types of internal floating roofs, like external floating roofs, commonly incorporate rim seals that slide against the tank wall as the roof moves up and down. These seals are discussed in detail in Section 2.3.2. Circulation vents and an open vent at the top of the fixed roof are generally provided to minimize the accumulation of hydrocarbon vapors in concentrations approaching the flammable range.

Flame arresters are an option that can be used to protect the vessel from fire or explosion. When these are used, circulation vents are not provided. Tank venting occurs through a pressure-vacuum vent and flame arrestor.

2.2.2. Domed External Floating Roof Tanks[4]

Domed external floating roof tanks have the heavier type of deck used in external floating roof tanks as well as a fixed roof at the top of the shell like internal floating roof tanks. Domed external floating roof tanks usually result from retrofitting an external floating roof tank with a fixed roof. A typical domed external floating roof tank is shown in Figure 2-5.

As with the internal floating roof tanks, the function of the fixed roof is not to act as a vapor barrier, but to block the wind. The type of fixed roof most commonly used is a self supporting aluminum dome roof, which is of bolted construction. Like the internal floating roof tanks, these tanks are freely vented by circulation vents at the top of the fixed roof. The deck fittings and rim seals, however, are basically identical to those on external floating roof tanks.

2.2.5. Horizontal Tanks

Horizontal tanks are constructed for both above-ground and underground service. Figures 2-6 and 2-7 present schematics of typical underground and above-ground horizontal tanks. Horizontal tanks are usually constructed of steel, steel with a fiberglass overlay, or fiberglass-reinforced polyester. Horizontal tanks are generally small storage tanks with capacities of less than 75,710 L (20,000 gallons). Horizontal tanks are constructed such that the length of the tank is not greater than six times the diameter to ensure structural integrity. Horizontal tanks are usually equipped with pressure-vacuum vents, gauge hatches and sample wells, and manholes to provide accessibility to these tanks. In addition, underground tanks may be cathodically protected to prevent corrosion of the tank shell. Cathodic protection is accomplished by placing sacrificial anodes in the tank that are connected to an impressed current system or by using galvanic anodes in the tank. However, internal cathodic protection is no longer widely used in the petroleum industry, due to corrosion inhibitors that are now found in most refined petroleum products.

The potential emission sources for above-ground horizontal tanks are the same as those for fixed-roof tanks. Emissions from underground storage tanks are mainly associated with changes in the liquid level in the tank. Losses due to changes in temperature or barometric pressure are minimal for underground tanks because the surrounding earth limits the diurnal temperature change and changes in the barometric pressure would result in only small losses.

2.2.6. Pressure Tanks

Two classes of pressure tanks are in general use: low pressure (2.5 to 15 psig) and high pressure (higher than 15 psig). Pressure tanks generally are used for storing organic liquids and gases with high vapor pressures and are found in many sizes and shapes, depending on the operating pressure of the tank. Pressure tanks are equipped with a pressure/vacuum vent that is set to prevent venting loss from boiling and breathing loss from daily temperature or barometric pressure changes.

2.2.7. Variable Vapor Space Tanks[5]

Variable vapor space tanks are equipped with expandable vapor reservoirs to accommodate vapor volume fluctuations attributable to temperature and barometric pressure changes. Although variable vapor space tanks are sometimes used independently, they are normally connected to the vapor spaces of one or more fixed roof tanks. The two most common types of variable vapor space tanks are lifter roof tanks and flexible diaphragm tanks.

Lifter roof tanks have a telescoping roof that fits loosely around the outside of the main tank wall. The space between the roof and the wall is closed by either a wet seal, which is a trough filled with liquid, or a dry seal, which uses a flexible coated fabric.

Flexible diaphragm tanks use flexible membranes to provide expandable volume. They may be either separate gasholder units or integral units mounted atop fixed roof tanks.

Variable vapor space tank losses occur during tank filling when vapor is displaced by liquid. Loss of vapor occurs only when the tank's vapor storage capacity is exceeded.

2.3. TYPES OF FLOATING ROOF PERIMETER SEALS

2.3.1 External and Domed External Floating Roof Rim Seals[2,6,7]

Regardless of tank design, a floating roof requires a device to seal the gap between the tank wall and the deck perimeter. A rim seal, or in the case of a two-seal system, the lower (primary) rim seal, can be made from various materials suitable for organic liquid service. The basic designs available for external floating roof rim seals are (1) mechanical (metallic) shoe seals, (2) liquid-filled seals, and (3) (vapor- or liquid-mounted) resilient foam-filled seals. Figures 2-8 and 2-9 depict these three general types of seals.

One major difference in seal system design is the way in which the seal is mounted with respect to the liquid surface. Figure 2-8 shows a vapor space between the liquid surface and rim seal, whereas in Figure 2-9, the seals rest on the liquid surface. These liquid-filled and resilient foam-filled seals are classified as liquid- or vapor-mounted rim seals, depending on their location. Mechanical shoe rim seals are different in design from liquid-filled or resilient foam-filled rim seals and cannot be characterized as liquid- or vapor-mounted. However, because the shoe and envelope combination precludes contact between the annular vapor space above the liquid and the atmosphere (see Figure 2-9), the emission rate of a mechanical shoe seal is closer to that of a liquid-mounted rim seal than that of a vapor-mounted rim seal.

2.3.1.1. Mechanical Shoe Seal. A mechanical shoe seal, also known as a "metallic shoe seal" (Figure 2-9), is characterized by a metallic sheet (the "shoe") that is held against the vertical tank wall. Prior to 40 CFR 60 Subpart Ka, the regulations did not specify a height for mechanical shoe seals; however, shoe heights typically range from 75 to 130 centimeters (cm) (30 to 51 in.). The shoe is connected by braces to the floating deck and is held tightly against the wall by springs or weighted levers. A flexible coated fabric (the "envelope") is suspended from the shoe seal to the floating deck to form a vapor barrier over the annular space between the deck and the primary seal.

2.3.1.2. Liquid-Filled Seal. A liquid-filled rim seal (Figure 2-9) may consist of a tough fabric band or envelope filled with a liquid, or it may consist of a flexible polymeric tube 20 to 25 cm (8 to 10 in.) in diameter filled with a liquid and sheathed with a tough fabric scuff band. The liquid is commonly a petroleum distillate or other liquid that will not contaminate the stored product if the tube ruptures. Liquid-filled rim seals are mounted on the liquid product surface with no vapor space below the seal.

2.3.1.3. Resilient Foam-Filled Seal. A resilient foam-filled rim seal is similar to a liquid-filled seal except that a resilient foam log is used in place of the liquid. The resiliency of the foam log permits the seal to adapt itself to minor imperfections in tank dimensions and in the tank shell. The foam log may be mounted above the liquid surface (vapor-mounted) or on the liquid surface (liquid-mounted). Typical vapor-mounted and liquid-mounted seals are presented in Figures 2-8 and 2-9, respectively.

2.3.1.4. Secondary Seals on External Floating Roofs. A secondary seal on an external floating roof consists of a continuous seal mounted on the rim of the floating roof and extending to the tank wall, covering the entire primary seal. Secondary seals are normally constructed of flexible polymeric materials. Figure 2-10 depicts several primary and secondary seal systems. An alternative secondary seal design incorporates a steel leaf to bridge the gap between the roof

and the tank wall. The leaf acts as a compression plate to hold a polymeric wiper against the tank wall.

A rim-mounted secondary seal installed over a primary seal provides a barrier for volatile organic compound (VOC) emissions that escape from the small vapor space between the primary seal and the wall and through any openings or tears in the seal envelope of a metallic shoe seal (Figure 2-10). Although not shown in Figure 2-10, a secondary seal can be used in conjunction with a weather shield as described in the following section.

Another type of secondary seal is a shoe-mounted secondary seal. A shoe-mounted seal extends from the top of the shoe to the tank wall (Figure 2-10). These seals do not provide protection against VOC leakage through the envelope. Holes, gaps, tears, or other defects in the envelope can permit direct exchange between the saturated vapor under the envelope and the atmosphere. Wind can enter this space through envelope defects, flow around the circumference of the tank, and exit saturated or nearly saturated with VOC vapors.

2.3.1.5. Weather Shield. A weather shield (see Figure 2-9) may be installed over the primary seal to protect it from deterioration caused by debris and exposure to the elements. Though the NSPS's 40 CFR 60 Subparts Ka and Kb do not accept the installation of a weather shield as equivalent to a secondary seal, there are a large number of existing tanks not affected by the NSPS that have this configuration. Typically, a weather shield is an arrangement of overlapping thin metal sheets pivoted from the floating roof to ride against the tank wall. The weather shield, by the nature of its design, is not an effective vapor barrier. For this reason, it differs from the secondary seal. Although the two devices are conceptually similar in design, they are designed for and serve different purposes.

2.3.2. Internal Floating Roof Rim Seals[3,7]

Internal floating roofs typically incorporate one of two types of flexible, product-resistant rim seals: resilient foam-filled seals or wiper seals. Similar to those employed on external floating roofs, each of these seals closes the annular vapor space between the edge of the floating deck and the tank shell to reduce evaporative losses. They are designed to compensate for small irregularities in the tank shell and allow the roof to freely move up and down in the tank without binding.

2.2.2.1. Resilient Foam-Filled Seal. A resilient foam-filled seal used on an internal floating roof is similar in design to that described in Section 2.3.1.3 for external floating roofs. Resilient foam-filled seals are shown in Figures 2-8 and 2-9. These seals can be mounted either in contact with the liquid surface (liquid-mounted) or several centimeters above the liquid surface (vapor-mounted).

Resilient foam-filled seals work because of the expansion and contraction of a resilient material to maintain contact with the tank shell while accommodating varying annular rim space widths. These seals consist of a core of open-cell foam encapsulated in a coated fabric. The elasticity of the foam core pushes the fabric into contact with the tank shell. The seals are attached to a mounting on the deck perimeter and are continuous around the roof circumference. Polyurethane-coated nylon fabric and polyurethane foam are commonly used materials. For emission control, it is important that the mounting and radial seal joints be vapor-tight and that the seal be in substantial contact with the tank shell.

2.2.2.2. Wiper Seals. Wiper seals are commonly used as primary rim seals for internal floating roof tanks. This type of seal is depicted in Figure 2-8.

Wiper seals generally consist of a continuous annular blade of flexible material fastened to a mounting bracket on the deck perimeter that spans the annular rim space and contacts the tank shell. The mounting is such that the blade is flexed, and its elasticity provides a sealing pressure against the tank shell. Such seals are vapor-mounted; a vapor space exists between the liquid stock and the bottom of the seal. For emission control, it is important that the mounting be vapor-tight, that the seal extend around the circumference of the roof, and that the blade be in substantial contact with the tank shell.

Three types of materials are commonly used to make the wipers. One type consists of a cellular, elastomeric material tapered in cross section with the thicker portion at the mounting. Rubber is a commonly used material. All radial joints in the blade are joined.

A second type of wiper seal construction uses a foam core wrapped with a coated fabric. Polyurethane on nylon fabric and polyurethane foam are common materials. The core provides the flexibility and support, while the fabric provides the vapor barrier and wear surface.

A third type of wiper seal consists of overlapping segments of seal material (shingle-type seal). Shingle-type seals differ from the wiper seals discussed previously in that they do not provide a continuous vapor barrier.

2.2.2.3. Secondary Seals for Internal Floating Roof Tanks. Secondary seals may be used to provide some additional evaporative loss control over that achieved by the primary seal. The secondary seal is mounted to an extended vertical rim plate, above the primary seal, as shown in Figure 2-10. Secondary seals can be either a resilient foam-filled seal or an elastomeric wiper seal, as described in Sections 2.3.2.1 and 2.3.2.2, respectively. For a given roof design, using a secondary seal further limits the operating capacity of a tank due to the need to maintain contact with the tank shell or keep the seal from interfering with IFRT fixed-roof rafters when the tank is filled. Secondary seals are not commonly used on internal floating roof tanks that are not affected by the NSPS (40 CFR 60 Subpart Kb).

2.3. TYPES OF FLOATING ROOF DECK FITTINGS

2.3.1. External and Domed External Floating Roof Deck Fittings[2,6,7]

Numerous fittings penetrate or are attached to an external floating roof deck. These fittings accommodate structural support components or allow for operational functions. These fittings can be a source of emissions in that they must penetrate the deck. Other accessories are used that do not penetrate the deck and are not, therefore, sources of evaporative loss. The most common fittings relevant to controlling vapor losses are described in the following sections.

2.3.1.1. Access Hatches. An access hatch consists of an opening in the deck with a peripheral vertical well attached to the deck and a removable cover to close the opening as shown in Figure 2-11. An access hatch is typically sized to allow workers and materials to pass through the deck for construction or servicing. The cover can rest directly on the well, or a gasketed connection can be used to reduce evaporative loss. Bolting the cover to the well reduces losses further.

2.3.1.2. Gauge Float Wells. Gauge floats are used to indicate the level of stock within the tank. These usually consist of a float residing within a well that passes through the floating deck, as shown in Figure 2-11. The float is connected to an indicator on the exterior of the tank via a tape passing through a guide system. The float rests on the stock surface within the well, which is enclosed by a sliding cover. Evaporation loss can be reduced by gasketing and/or bolting the connection between the cover and the rim of the well. The cable passes through a bushing located at the center of the cover. As with similar deck penetrations, the well extends into the liquid stock on noncontact floating decks.

2.3.1.3. Gauge Hatch/Sample Ports. Gauge hatch/sample ports provide access for hand-gauging the level of stock in the tank and for taking samples of the tank contents. A gauge hatch/sample port consists of a pipe sleeve through the deck and a self-closing gasketed cover, as shown in Figure 2-11. Gauge hatch/sample ports are usually located under the gauger's platform, which is mounted on the top of the tank shell. The cover may have a cord attached so that it can be opened from the gauger's platform. A gasketed cover reduces evaporative losses.

2.3.1.4. Rim Vents. Rim vents are found on tanks equipped with a rim seal system that creates a vapor pocket, such as a mechanical shoe seal or double wiper seal system. The rim vent is connected to the rim vapor space by a pipe and releases any excess pressure or vacuum that is present (Figure 2-12). The rim vapor space is bounded by the floating deck rim, the primary-seal shoe, the liquid surface, and the primary-seal fabric. Rim vents usually consist of weighted pallets that rest on the gasketed surface.

2.3.1.5. Deck Drains. Deck drains permit removal of rainwater from the surface of floating decks. Two types of floating roof drainage systems are currently used: closed and open. Closed drainage systems carry rainwater from the surface of the deck to the outside of the tank through a flexible or articulated piping system or through a flexible hose system located below the deck in the product space. Since product does not enter this closed drainage system, there is no associated evaporative loss. Open drainage systems, consisting of an open pipe that extends a short distance below the bottom of the deck, permit rainwater to drain from the surface of the deck into the product. Since these drainpipes are filled with product to the product level in the tank, evaporative loss occurs from the top of the open drainpipes. Two types of roof drains are commonly used in open drainage systems: flush drains and overflow drains. Flush drains (Figure 2-12) have a drain opening that is flush with the top surface of the double deck. They permit rainwater to drain into the product. Overflow drains (Figure 2-12) consist of a drain opening that is elevated above the top surface of the deck, thereby limiting the maximum amount of rainwater that can accumulate on the deck and providing emergency drainage of rainwater. They are normally used in conjunction with a closed drainage system. Some open deck drains are equipped with an insert to reduce the evaporative loss.

2.3.1.6. Deck Legs. Deck legs prevent damage to fittings underneath the deck and allow for tank cleaning or repair by holding the deck at a predetermined distance from the tank bottom. These supports consist of adjustable or fixed legs attached to the floating deck as shown in Figure 2-12. For adjustable deck legs, the load-carrying element passes through a well or sleeve in the deck.

2.3.1.7. Slotted and Unslotted Guide Poles and Wells. Antirotation devices are used to prevent floating roofs from rotating and potentially damaging roof equipment and rim seal systems. A commonly used antirotation device is a guide pole that is fixed at the top and bottom of the tank (Figure 2-13). The guide pole passes through a well in the deck. Rollers attached to the top of the well ride on the outside surface of the guide pole to prevent the floating roof from

rotating. The guide pole well has a sliding cover to accommodate limited radial movement of the roof. The sliding cover can be equipped with a gasket between the guide pole and the cover to reduce evaporative loss. The guide pole well can also be equipped with a gasket between the sliding cover and the top of the well to reduce evaporative loss. Openings at the top and bottom of the guide pole provide a means of hand-gauging the tank level and of taking bottom samples. In the slotted guide pole/sample well application, the well of the guide pole is constructed with a series of drilled holes or slots that allow the product to mix freely in the guide pole and thus have the same composition and liquid level as the product in the tank. Evaporative loss from the guidepole can be reduced by modifying the guidepole or well, or by placing a removable float inside the pole. Deck fitting factors for slotted guidepoles without pole sleeves were determined from test data on fittings where the float top or float wiper was positioned at or above the sliding cover elevation. Tests were not conducted with floats where the top of the float or wiper was below the sliding cover elevation ("short" floats); emissions from such a configuration are expected to be somewhere between those for guidepoles with and without floats, depending upon the float height. When a pole sleeve is used, the evaporative loss will not be affected by the height of the float within the well, since the purpose of the pole sleeve is to restrict the flow of vapor from the vapor space below the deck into the slotted guidepole.

2.3.1.8. Vacuum Breakers. The purpose of a vacuum breaker is to allow for the exchange of vapor and air through the floating roof during filling and emptying. Vacuum breakers are designed to be activated by changes in pressure or liquid level, or strictly by mechanical means.

Mechanical vacuum breakers are activated when the deck is either being landed on its legs or floated off its legs to equalize the pressure of the vapor space across the deck. This is accomplished by opening a deck penetration that usually consists of a well formed of pipe or framing on which rests a cover (Figure 2-12). Attached to the underside of the cover is a guide leg long enough to contact the tank bottom as the external floating deck approaches the tank bottom. When in contact with the tank bottom, the guide leg mechanically opens the breaker by lifting the cover off the well. When the leg is not contacting the bottom, the penetration is closed by the cover resting on the well. The closure may or may not have a gasket between the cover and neck. Since the purpose of the vacuum breaker is to allow the free exchange of air and/or vapor, the well does not extend appreciably below the deck. The gasket on the underside of the cover, or conversely on the upper rim of the well, provides a small measure of emission control during periods when the roof is free floating and the breaker is closed.

2.3.2. Internal Floating Roof Fittings[3,7]

Numerous fittings penetrate or are attached to an internal floating deck. These fittings serve to accommodate structural support components or to allow for operational functions. The fittings can be a source of evaporative loss in that they require penetrations in the deck. Other accessories are used that do not penetrate the deck and are not, therefore, sources of evaporative loss. The most common fittings relevant to controlling vapor losses are described in the following sections.

The access hatches, deck legs, vacuum breakers, and automatic gauge float wells for internal floating roofs are similar fittings to those described earlier for external floating roofs. Therefore, the discussion is not repeated.

2.3.2.1. Column Wells. The most common fixed-roof designs (Figure 2-4) are normally supported from inside the tank by means of vertical columns, which necessarily penetrate the

floating deck. (Some fixed roofs are entirely self-supporting and, therefore, have no support columns.) Columns are made of pipe with circular cross sections or of structural shapes with irregular cross sections (built-up). The number of columns varies with tank diameter from a minimum of 1 to over 50 for very large tanks. A typical fixed roof support column is shown in Figure 2-11.

The columns pass through deck openings via peripheral vertical wells. With noncontact decks, the well should extend down into the liquid stock. Generally, a closure device exists between the top of the well and the column. Several proprietary designs exist for this closure, including sliding covers and fabric sleeves, which must accommodate the movements of the deck relative to the column as the liquid level changes. A sliding cover rests on the upper rim of the column well (which is normally fixed to the deck) and bridges the gap or space between the column well and the column. The cover, which has a cutout, or opening, around the column, slides vertically relative to the column as the deck raises and lowers. At the same time, the cover slides horizontally relative to the rim of the well. A gasket around the rim of the well reduces emissions from this fitting. A flexible fabric sleeve seal between the rim of the well and the column (with a cutout, or opening to allow vertical motion of the seal relative to the columns) similarly accommodates limited horizontal motion of the roof relative to the column. A third design combines the advantages of the flexible fabric sleeve seal with a well that excludes all but a small portion of the liquid surface from direct exchange with the vapor space above the floating deck.

2.3.2.2. Sample Pipes or Wells. A sample well may be provided to allow liquid stock sampling. Typically, the well is funnel-shaped to allow for easy entry of a sample thief. A closure is provided, which is typically located at the lower end of the funnel and which frequently consists of a horizontal piece of fabric slit radially to allow thief entry. The well should extend into the liquid stock on noncontact decks.

Alternately, a sample well may consist of a slotted pipe extending into the liquid stock equipped with an ungasketed or gasketed sliding cover.

2.3.2.3. Ladder Wells. Some tanks are equipped with internal ladders that extend from a manhole in the fixed roof to the tank bottom. The deck opening through which the ladder passes is constructed with similar design details and considerations to those for column wells, as discussed in Section 2.4.2.1. A typical ladder and well are shown in Figure 2-14.

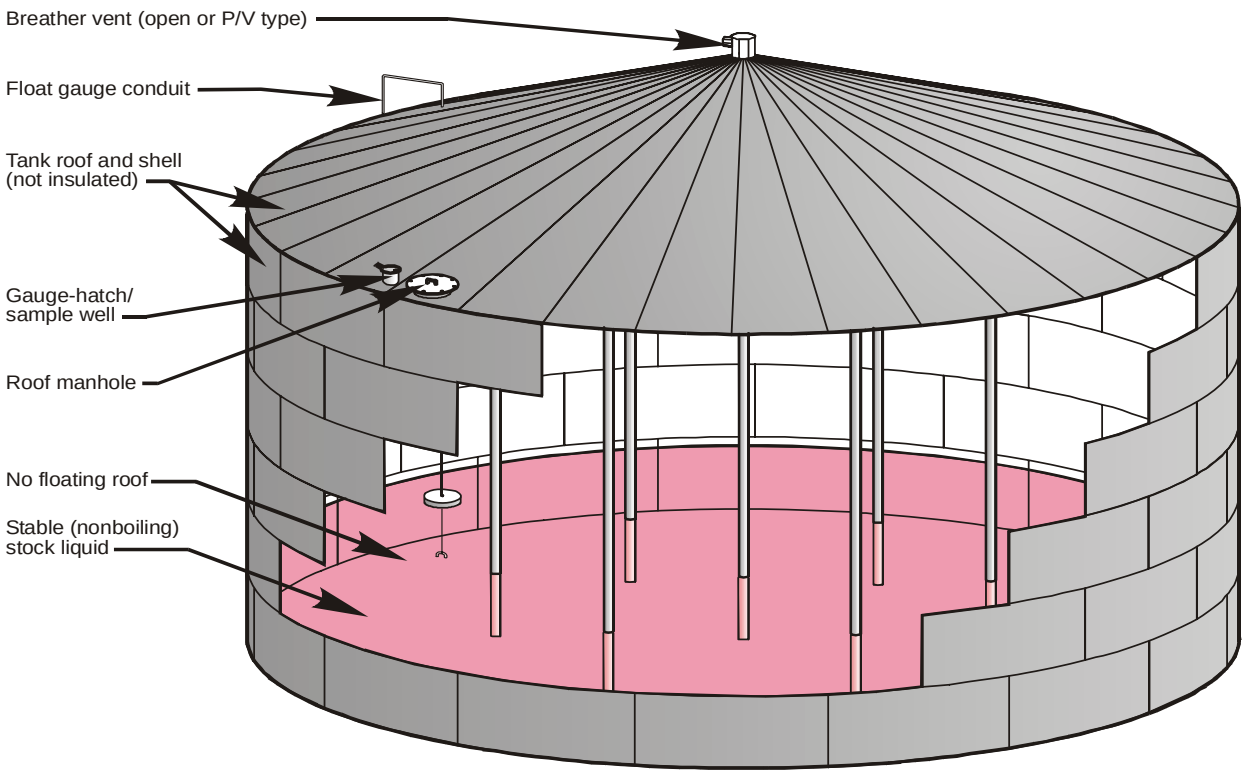

Figure 2-1 Typical Fixed Roof Tank

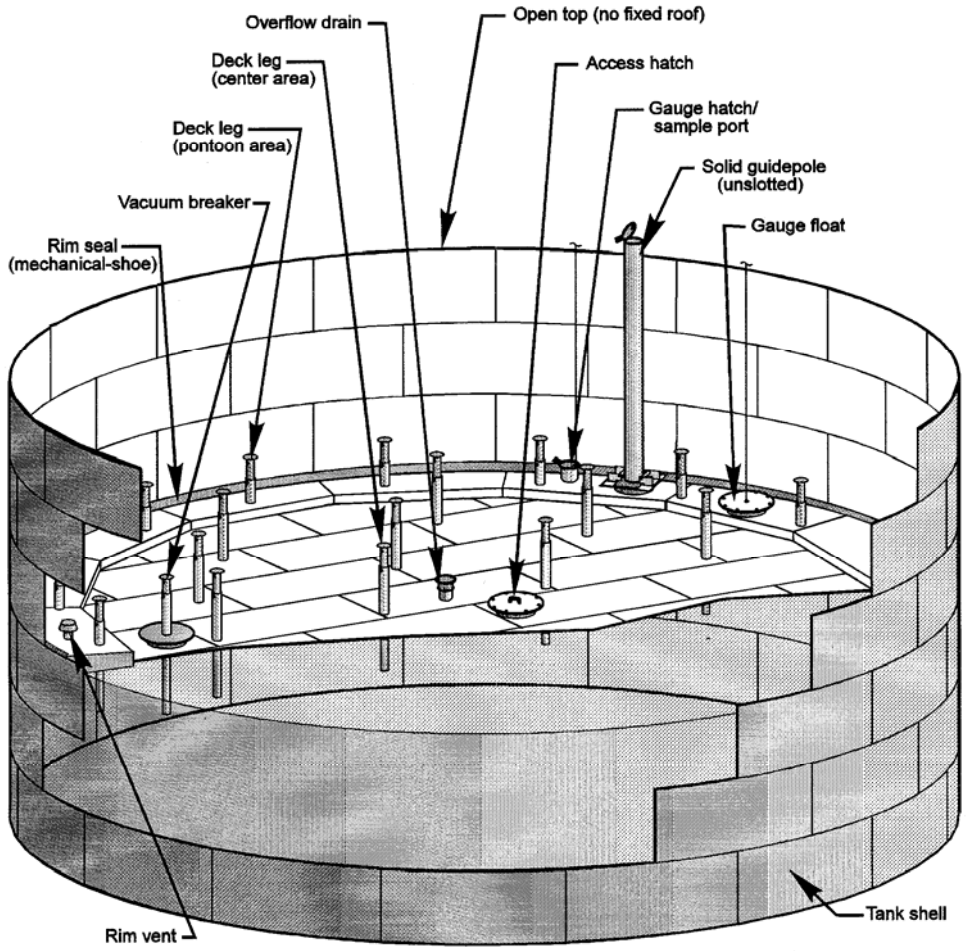

Figure 2-2. External floating roof tank (pontoon type).[11]

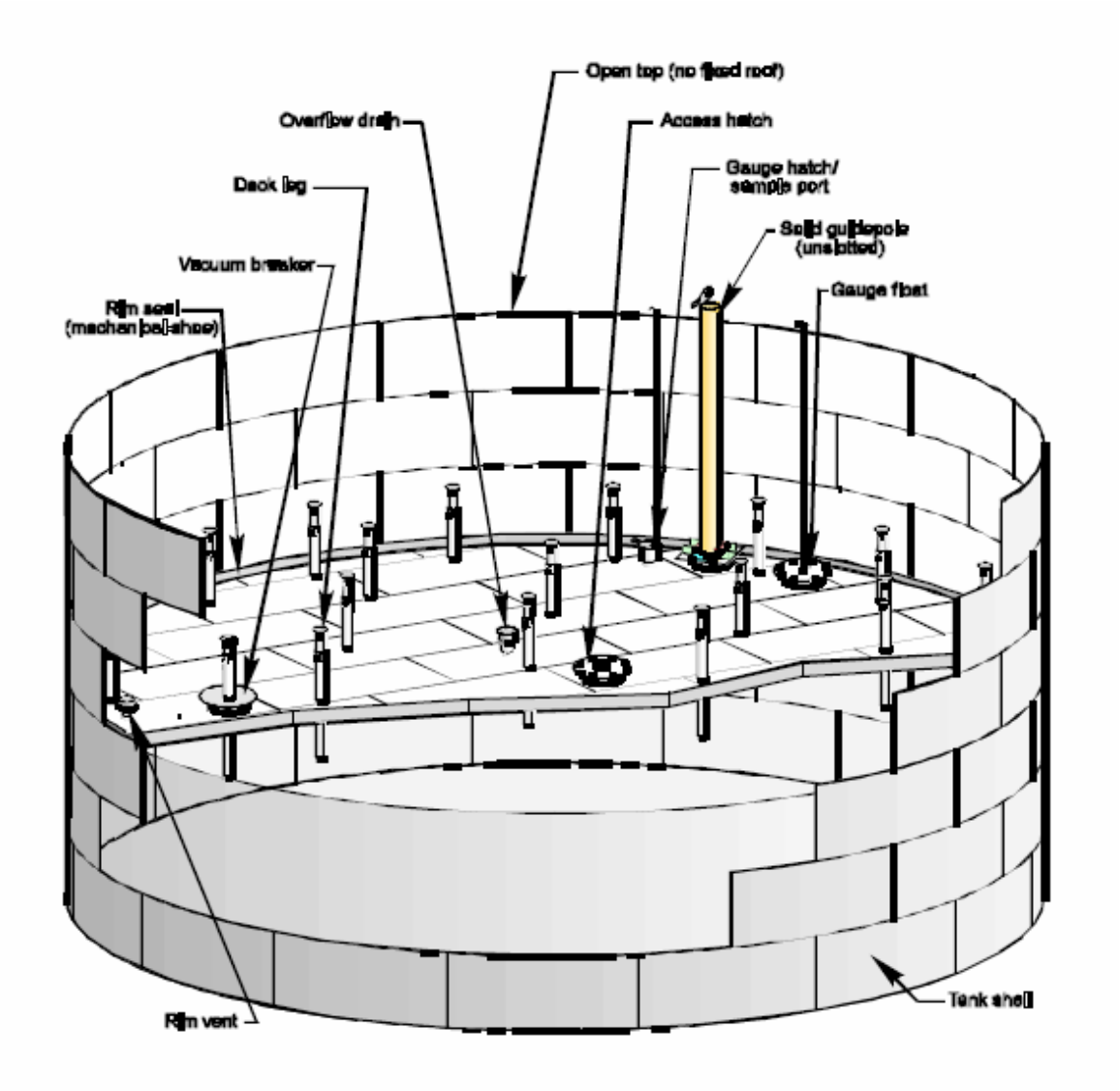

Figure 2-3. External floating roof tank (double-deck type).[11]

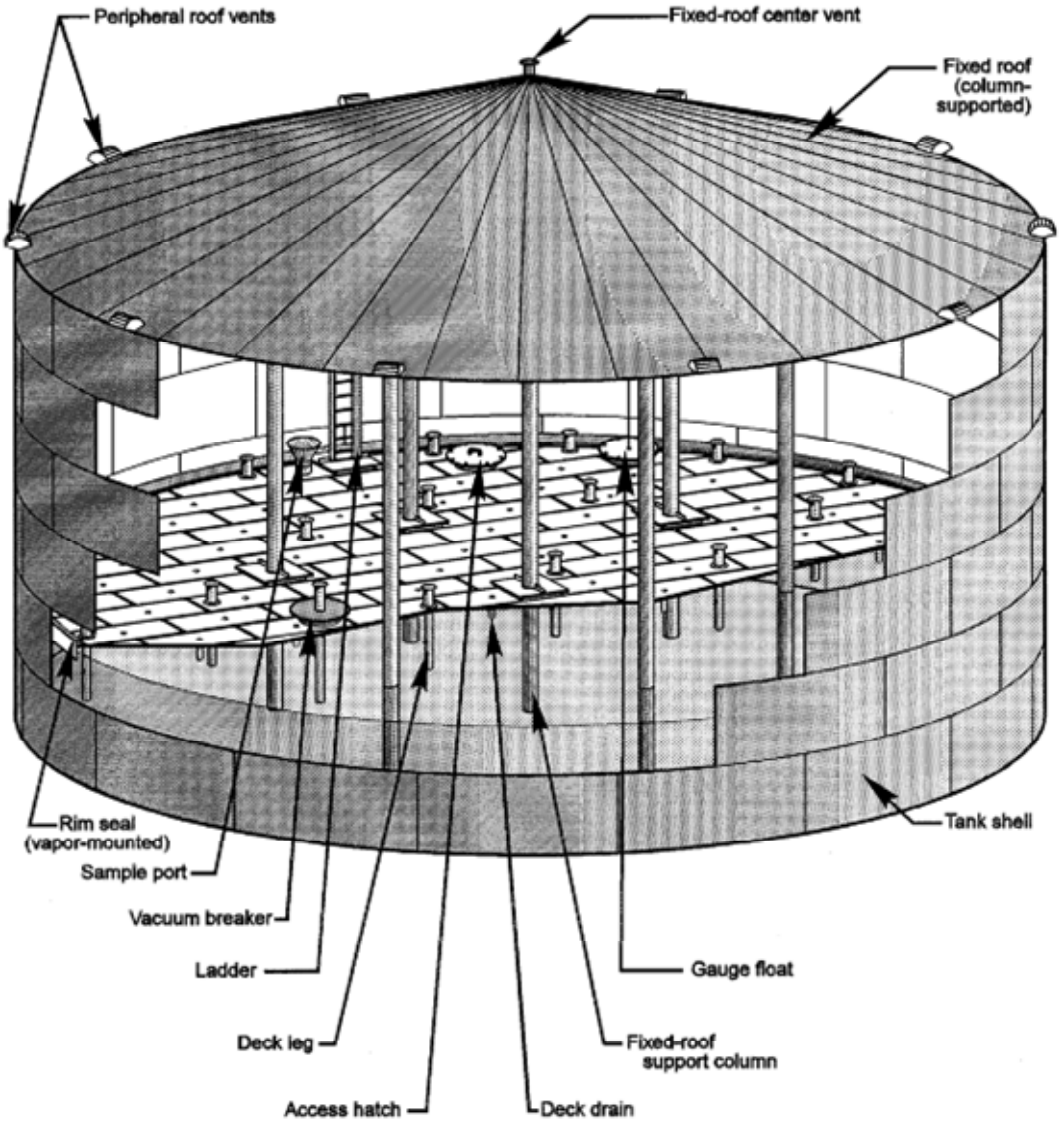

Figure 2-4. Internal floating roof tank.[11]

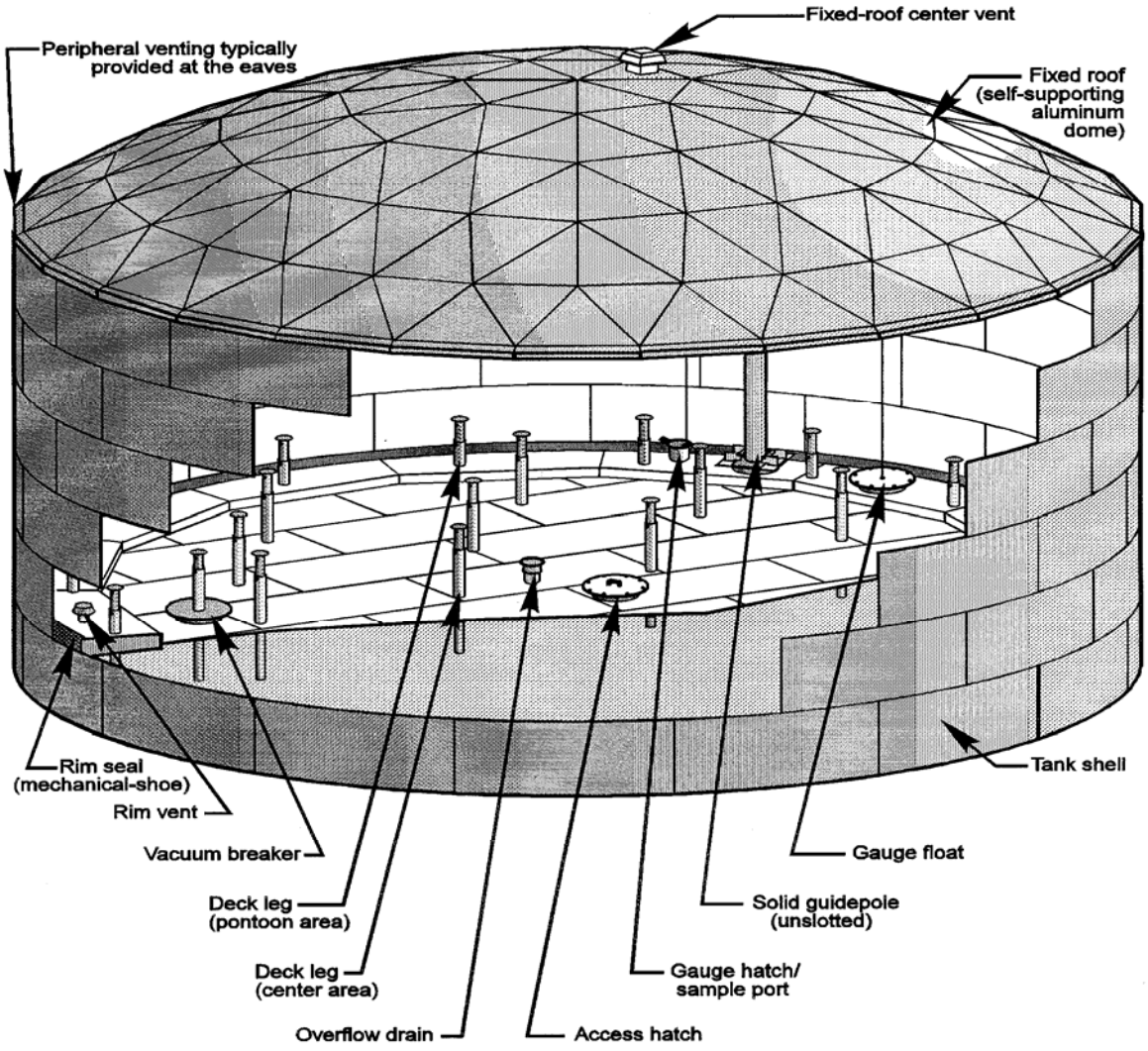

Figure 2-5. Domed external floating roof tank[11].

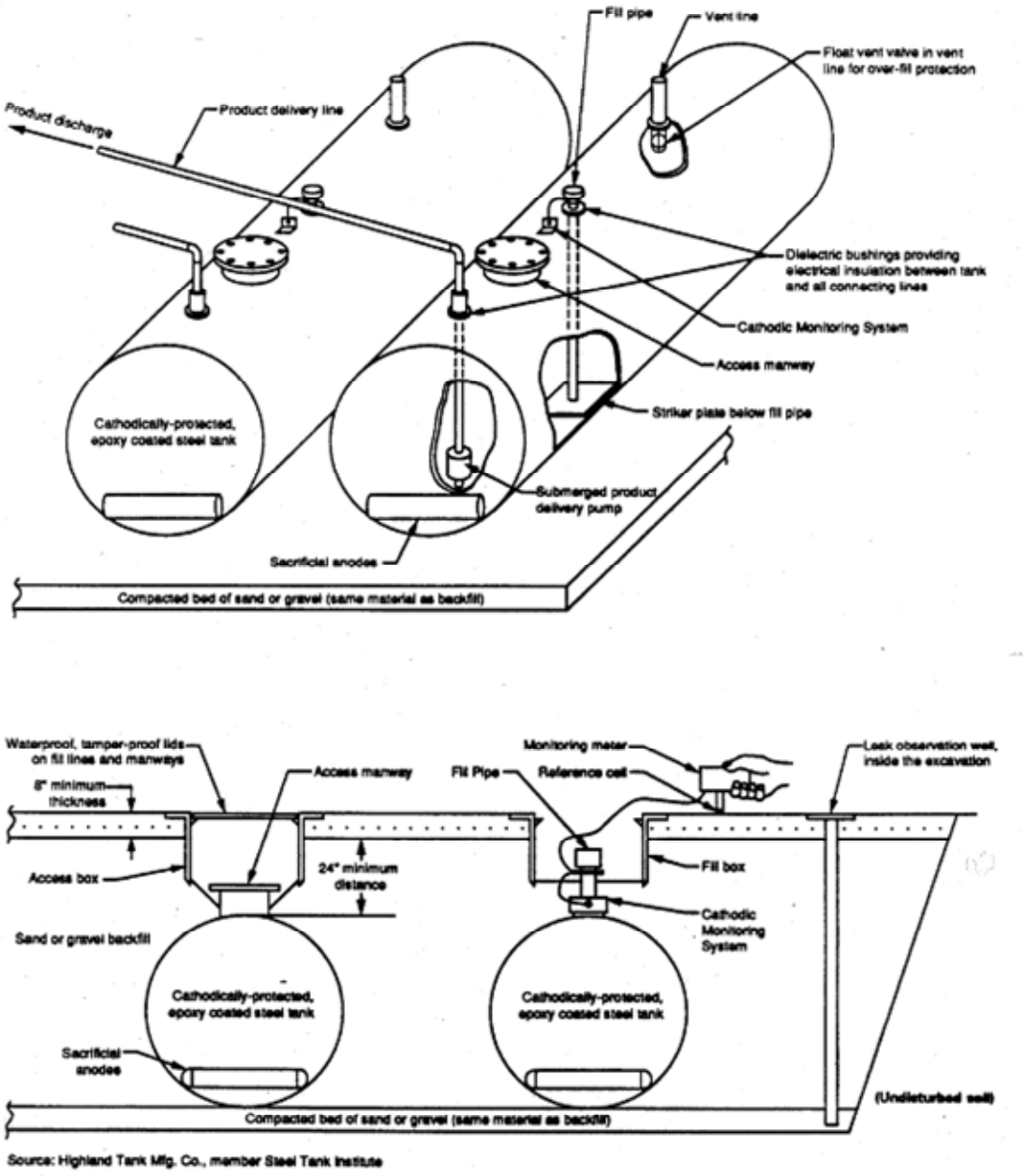

Figure 2-6. Typical underground storage tank.

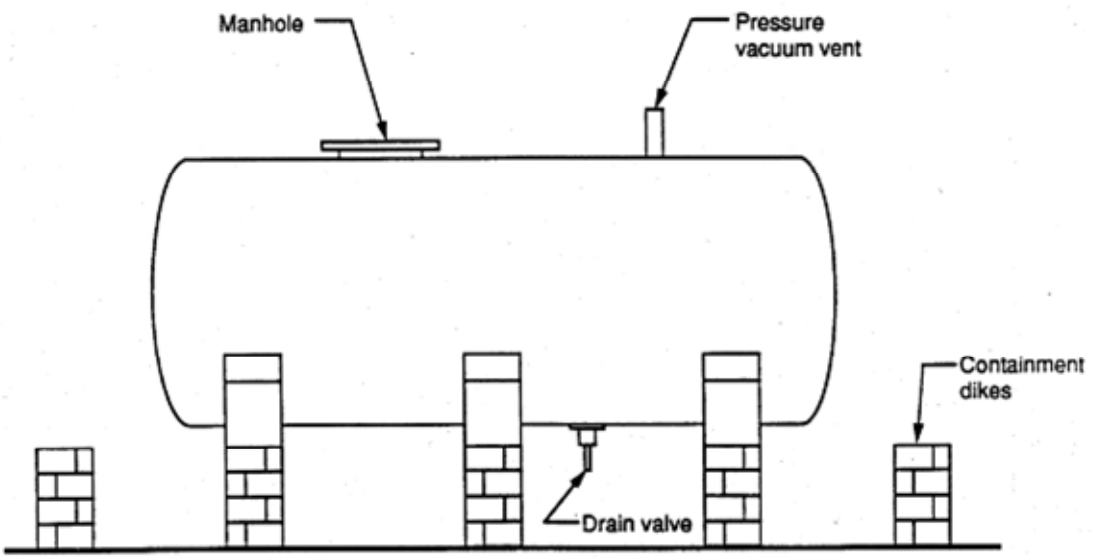

Figure 2-7. A typical above-ground horizontal tank.

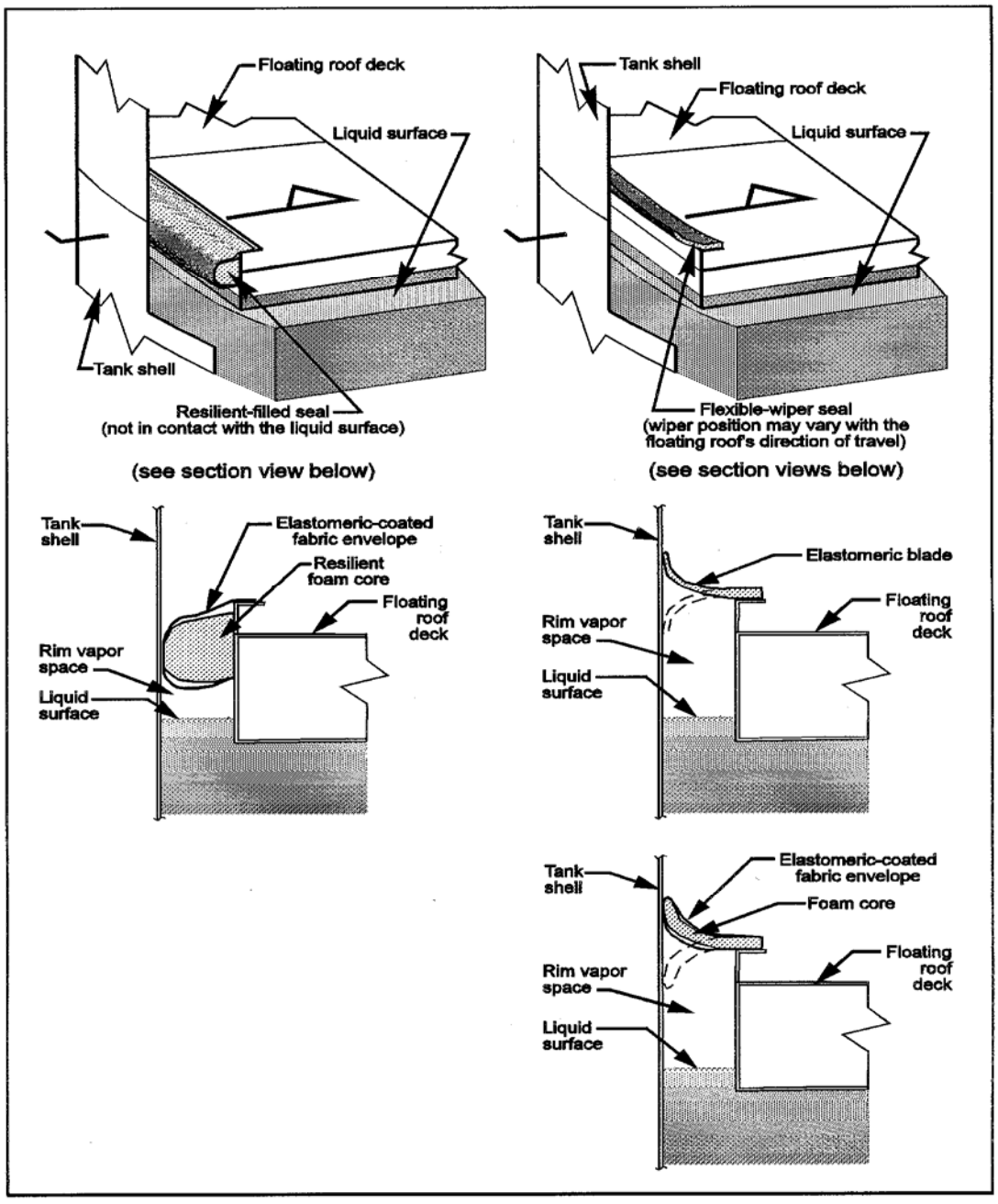

Figure 2-8. Vapor mounted primary seals.[11]

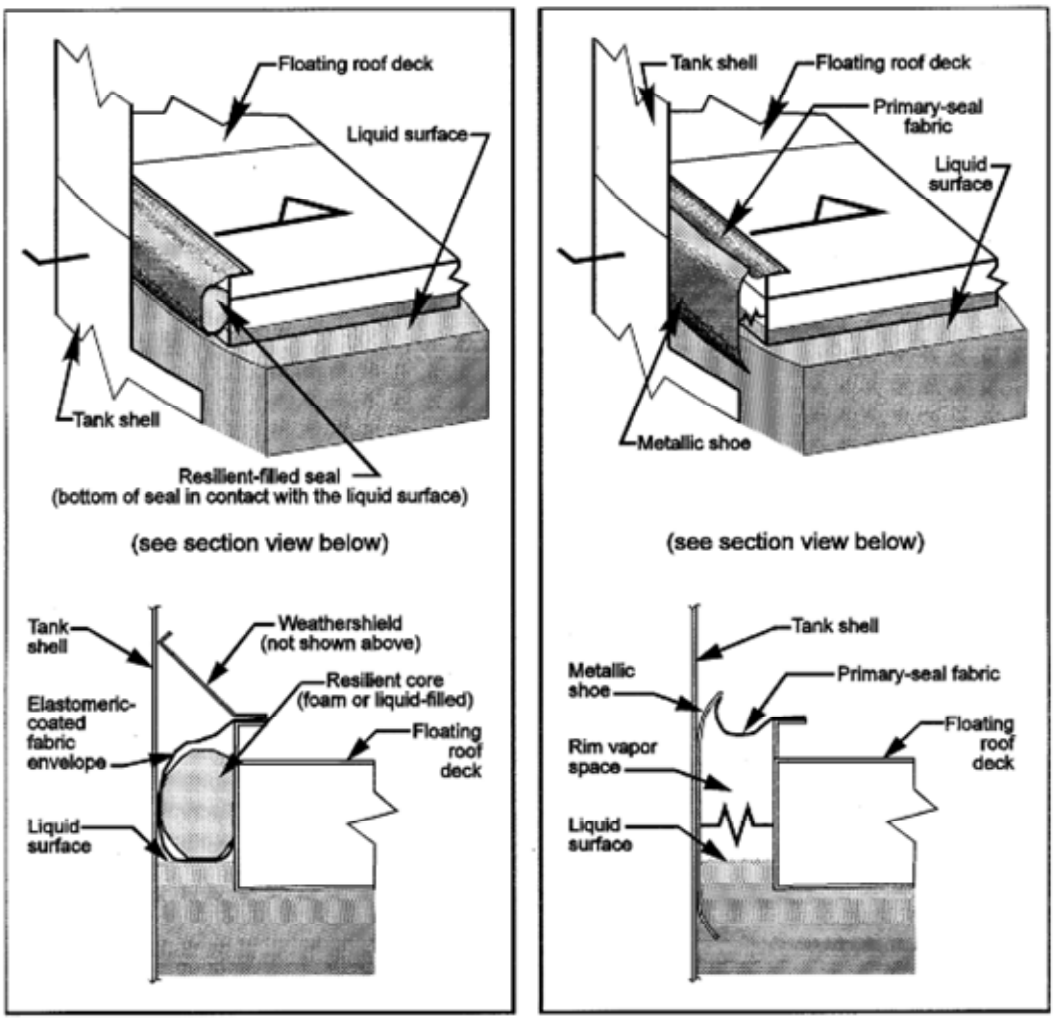

Figure 2-9. Liquid-mounted and mechanical shoe primary seals[11].

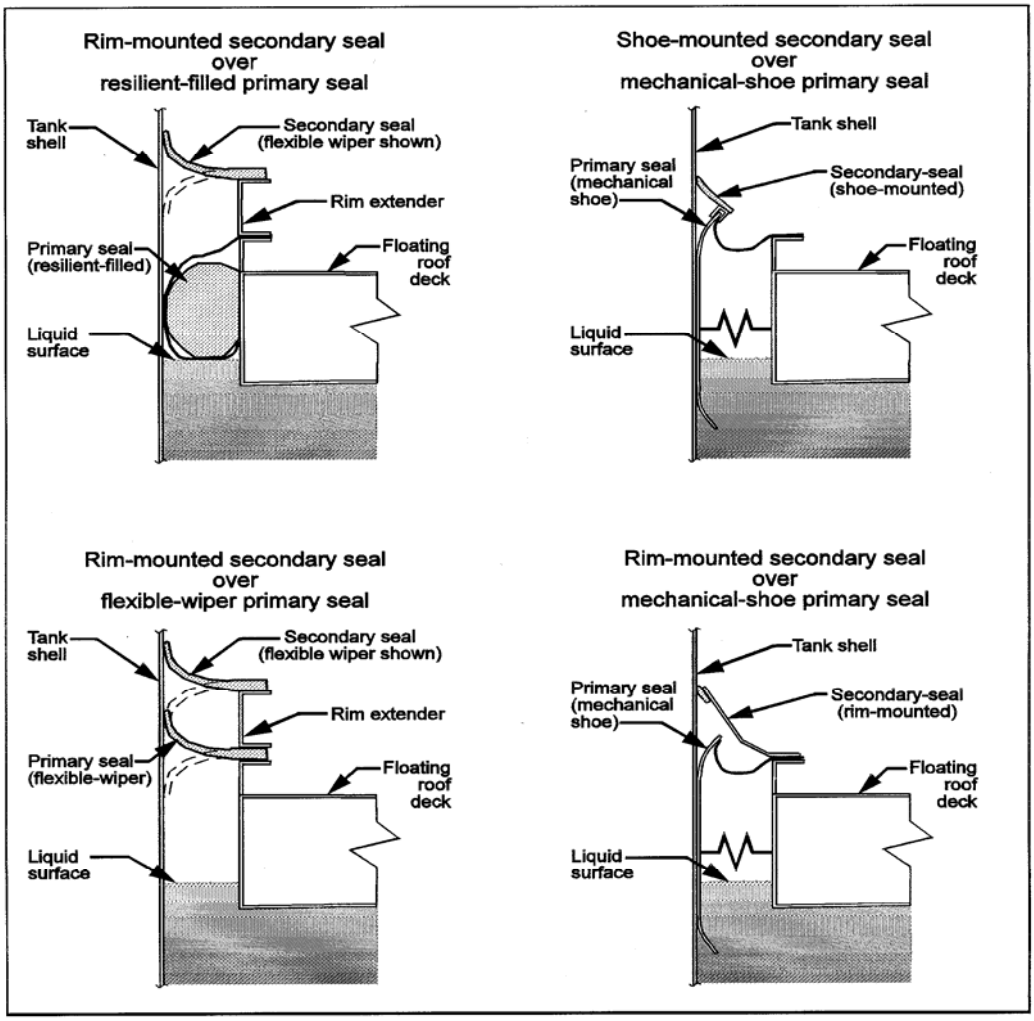

Figure 2-10. Secondary rim seals.[11]

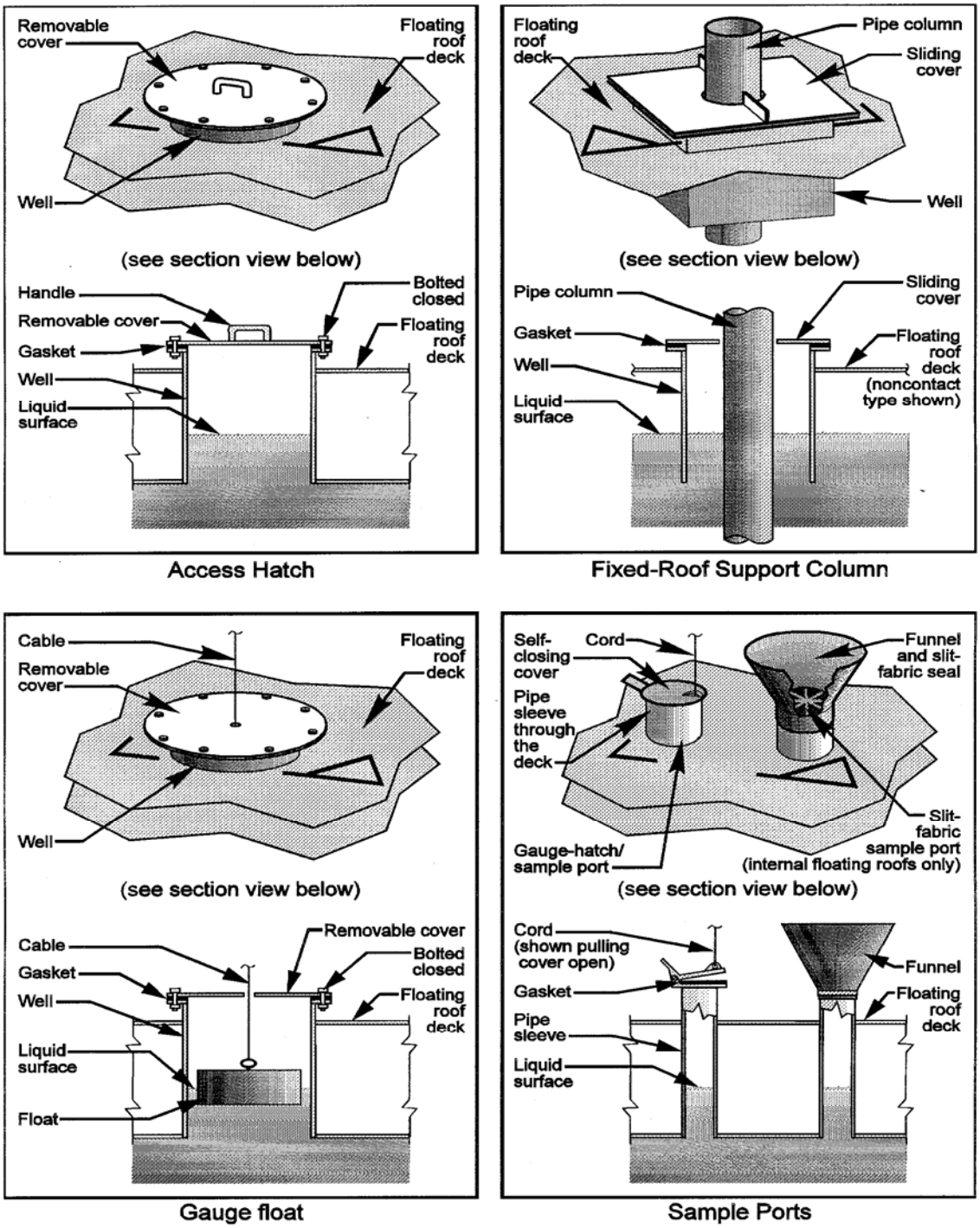

Figure 2-11. Deck fittings for floating roof tanks[11]

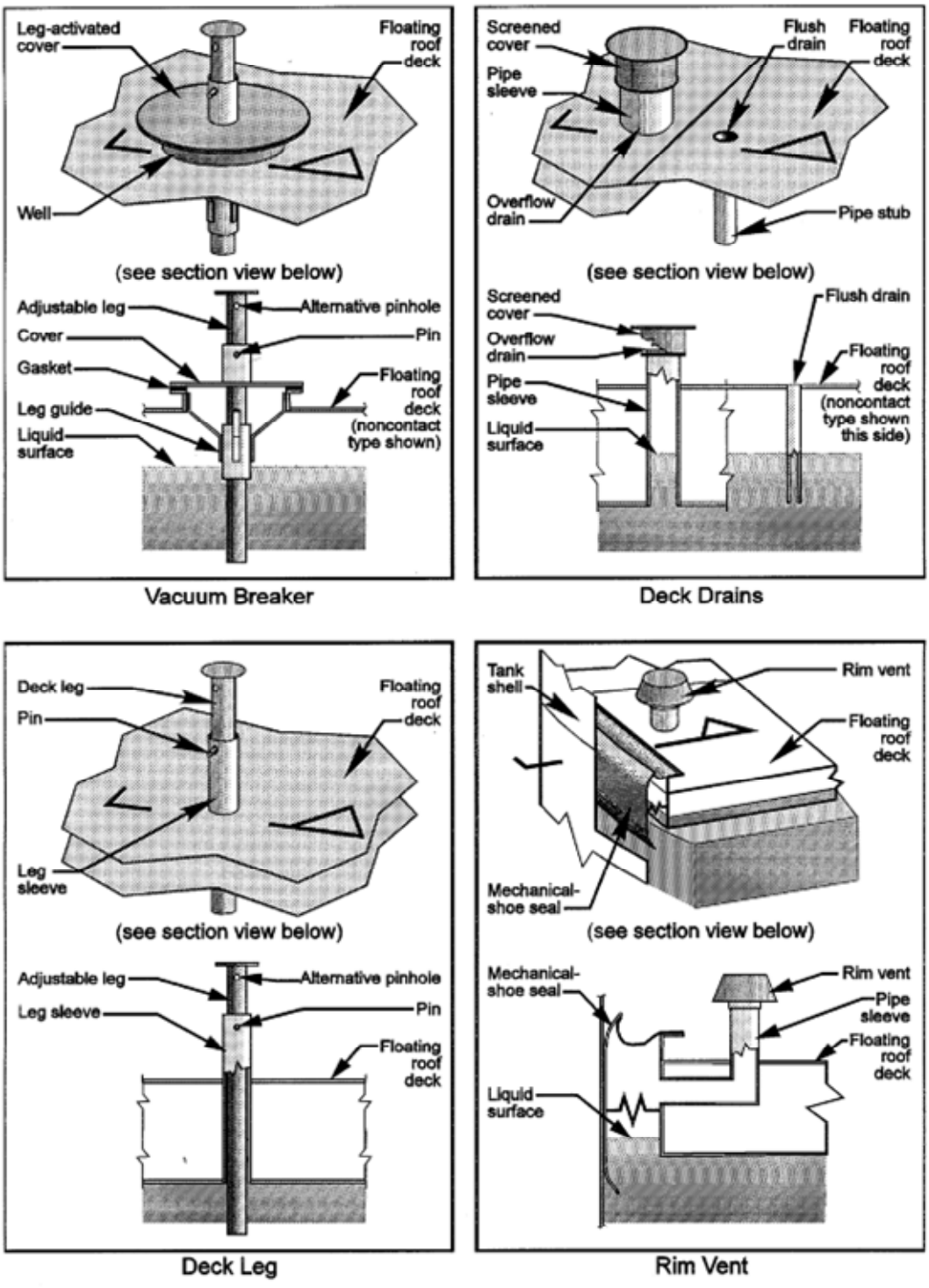

Figure 2-12. Deck fittings for floating roof tanks[11].

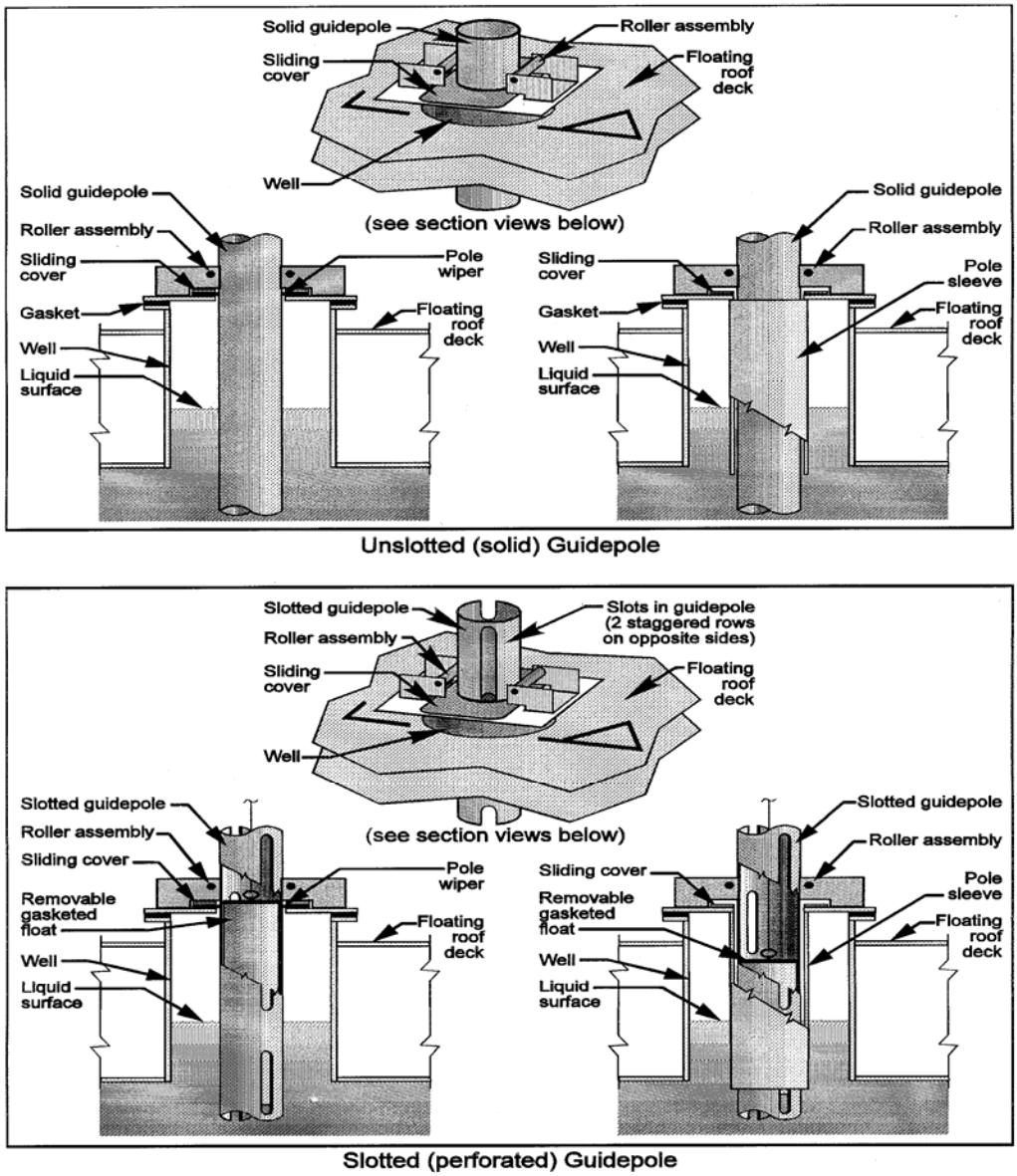

Figure 2-13. Slotted and unslotted guidepoles[11]

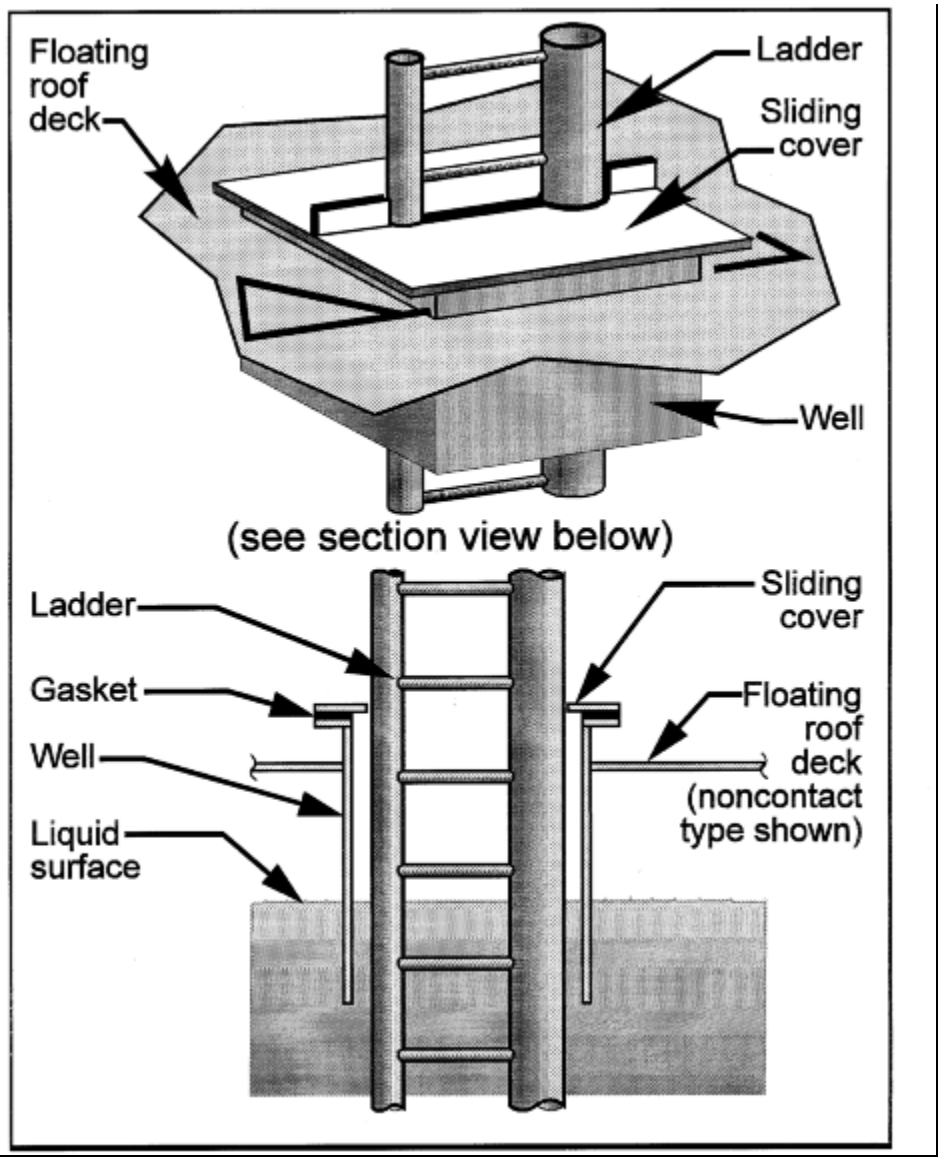

Figure 2-14. Ladder and well.[11]

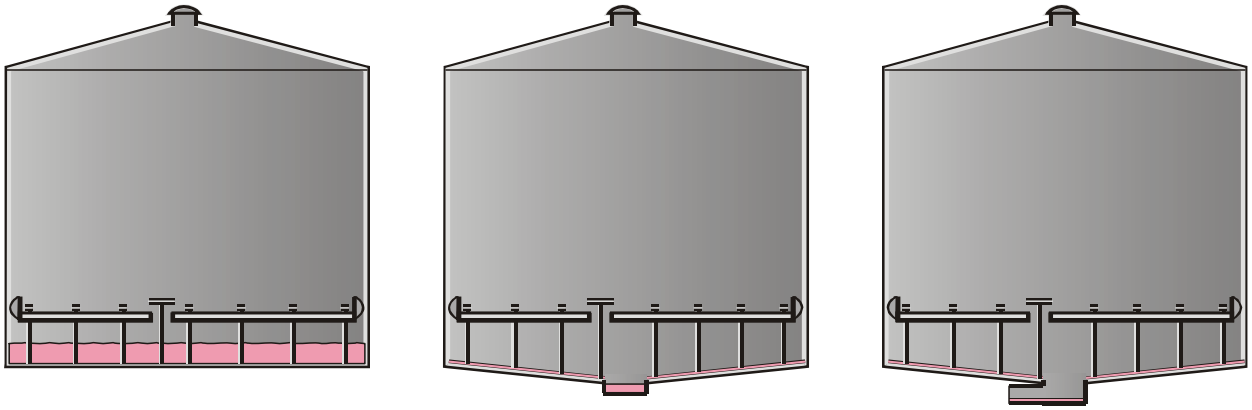

Full Liquid Heel
(standing liquid
across the entire bottom)

Partial Liquid Heel
(standing liquid only
in or near a sump;
clingage elsewhere)

Drain Dry
(no standing liquid,
only liquid is clingage)

Figure 2-15. Bottom conditions for landing loss

2.5 REFERENCES

1. Evaporative Loss from Fixed-Roof Tanks, API Draft Publication 2518, Second Edition, American Petroleum Institute, Washington, DC, October 1991.

2. Evaporative Loss From External Floating Roof Tanks, API Publication 2517, Third Edition, American Petroleum Institute, Washington, DC, February 1989.

3. Evaporation Loss From Internal Floating Roof Tanks, API Publication 2519, Third Edition, American Petroleum Institute, Washington, DC, June 1983.

4. Ferry, R.L., Estimating Storage Tank Emissions--Changes are Coming, TGB Partnership, 1994.

5. Use of Variable Vapor Space Systems to Reduce Evaporation Loss, API Bulletin 2520, American Petroleum Institute, Washington, DC, September 1964.

6. VOC Emissions From Volatile Organic Liquid Storage Tanks - Background Information for Proposed Standards, EPA-450/3-81-003a, U. S. Environmental Protection Agency, Research Triangle Park, NC, July 1984.

7. Benzene Emissions From Benzene Storage Tanks - Background Information for Proposed Standards, EPA-450/3-80-034a, U. S. Environmental Protection Agency, Research Triangle Park, NC, December 1980.

8. Laverman, R.J., Emission Reduction Options for Floating Roof Tanks, Chicago Bridge and Iron Technical Services Company, presented at the Second International Symposium on Aboveground Storage Tanks, Houston, TX, January 1992.

9. Recommended Practices for Underground Storage of Petroleum, New York State Department of Environmental Conservation, Albany, NY, May 1984.

10. Toxic Substance Storage Tank Containment, Ecology and Environment, Inc., 1985.

11. Courtesy of R. Ferry, TGB Partnership, Hillsborough, NC.

3.0 EMISSION ESTIMATION PROCEDURES

3.1 INTRODUCTION

The following section presents the emission estimation procedures for fixed roof, external floating roof, domed external floating roof, and internal floating roof tanks. These procedures are valid for all petroleum liquids, pure volatile organic liquids, and chemical mixtures with similar true vapor pressures. It is important to note that in all the emission estimation procedures the physical properties of the vapor do not include the noncondensibles (e.g., air) in the gas but only refer to the condensible components of the stored liquid. To aid in the emission estimation procedures, a list of variables with their corresponding definitions was developed and is presented in Table 7.3-1.

The factors presented in AP-42 are those that are currently available and have been reviewed and approved by the U. S. Environmental Protection Agency. As storage tank equipment vendors design new floating decks and equipment, new emission factors may be developed based on that equipment. If the new emission factors are reviewed and approved, the emission factors will be added to AP-42 during the next update.

The emission estimation procedures outlined in this chapter have been used as the basis for the development of a software program to estimate emissions from storage tanks. The software program entitled "TANKS" is available through the CHIEF website maintained by the U. S. Environmental Protection Agency.

3.1.1 Total Losses From Fixed Roof Tanks[4,8-14] –

The following equations, provided to estimate standing storage and working loss emissions, apply to tanks with vertical cylindrical shells and fixed roofs. These tanks must be substantially liquid- and vapor-tight and must operate approximately at atmospheric pressure. The equations are not intended to be used in estimating losses from unstable or boiling stocks or from mixtures of hydrocarbons or petrochemicals for which the vapor pressure is not known or cannot be readily predicted. Total losses from fixed roof tanks are equal to the sum of the standing storage loss and working loss:

$$L_T = L_S + L_W \quad (3\text{-}1)$$

where:

L_T = total losses, lb/yr
L_S = standing storage losses, lb/yr, see Equation 3-2
L_W = working losses, lb/yr, see Equation 3-29

3.1.1.1 Standing Storage Loss

The standing storage loss, L_S, refers to the loss of stock vapors as a result of tank vapor space breathing. Fixed roof tank standing storage losses can be estimated from Equation 3-2, which comes from the previous edition of Chapter 7 of AP-42.

$$L_S = 365\ V_V\ W_V\ K_E\ K_S \quad (3\text{-}2)$$

where:

L_S = standing storage loss, lb/yr
V_V = vapor space volume, ft^3, see Equation 3-3
W_V = stock vapor density, lb/ft^3
K_E = vapor space expansion factor, dimensionless
K_S = vented vapor saturation factor, dimensionless
365 = constant, the number of daily events in a year, $(year)^{-1}$

Tank Vapor Space Volume, V_V - The tank vapor space volume is calculated using the following equation:

$$V_V = \left(\frac{\pi}{4} D^2\right) H_{VO} \quad (3\text{-}3)$$

where:

V_V = vapor space volume, ft^3
D = tank diameter, ft, see Equation 3-13 for horizontal tanks
H_{VO} = vapor space outage, ft, see Equation 3-15

The standing storage loss equation can be simplified by combining Equation 3-2 with Equation 3-3. The result is Equation 3-4.

$$L_S = 365 K_E \left(\frac{\pi}{4} D^2\right) H_{VO} K_S W_V \quad (3\text{-}4)$$

where:

L_S = standing storage loss, lb/yr
K_E = vapor space expansion factor, dimensionless, see Equation 3-5, 3-6, or 3-7
D = diameter, ft, see Equation 3-13 for horizontal tanks
H_{VO} = vapor space outage, ft, see Equation 3-15; use $H_E/2$ from Equation 3-14 for horizontal tanks
K_S = vented vapor saturation factor, dimensionless, see Equation 3-20
W_V = stock vapor density, lb/ft^3, see Equation 3-21
365 = constant, the number of daily events in a year, $(year)^{-1}$

Vapor Space Expansion Factor, K_E

The calculation of the vapor space expansion factor, K_E, depends upon the properties of the liquid in the tank and the breather vent settings. If the liquid stock has a true vapor pressure greater than 0.1 psia, or if the breather vent settings are higher than the typical range of ±0.03 psig, see Equation 3-7. If the liquid stored in the fixed roof tank has a true vapor pressure less than 0.1 psia and the tank breather vent settings are ±0.03 psig, use either Equation 3-5 or Equation 3-6.

If the tank location and tank color and condition are known, K_E is calculated using the following equation:

$$K_E = 0.0018 \Delta T_V = 0.0018 \left[0.72 (T_{AX} - T_{AN}) + 0.028 \alpha I\right] \quad (3\text{-}5)$$

where:

K_E = vapor space expansion factor, dimensionless
ΔT_V = daily vapor temperature range, °R
T_{AX} = daily maximum ambient temperature, °R
T_{AN} = daily minimum ambient temperature, °R
α = tank paint solar absorptance, dimensionless
I = daily total solar insolation on a horizontal surface, Btu/(ft^2 day)
0.0018 = constant, (°R)$^{-1}$
0.72 = constant, dimensionless
0.028 = constant, (°R ft^2 day)/Btu

If the tank location is unknown, a value of K_E can be calculated using typical meteorological conditions for the lower 48 states. The typical value for daily solar insolation is 1,370 Btu/(ft^2 day), the daily range of ambient temperature is 21°R, the daily minimum ambient temperature is 473.5 °R, and the tank paint solar absorptance is 0.17 for white paint in good condition. Substituting these values into Equation 3-5 results in a value of 0.04, as shown in Equation 3-6.

$$K_E = 0.04 \quad (3\text{-}6)$$

When the liquid stock has a true vapor pressure greater than 0.1 psia, a more accurate estimate of the vapor space expansion factor, K_E, is obtained by Equation 3-7. As shown in the equation, K_E is greater than zero. If K_E is less than zero, standing storage losses will not occur.

$$K_E = \frac{\Delta T_V}{T_{LA}} + \frac{\Delta P_V - \Delta P_B}{P_A - P_{VA}} > 0 \qquad (3\text{-}7)$$

where:

ΔT_V = daily vapor temperature range, °R; see Note 1
ΔP_V = daily vapor pressure range, psi; see Note 2
ΔP_B = breather vent pressure setting range, psi; see Note 3
P_A = atmospheric pressure, psia
P_{VA} = vapor pressure at daily average liquid surface temperature, psia; see Notes 1 and 2 for Equation 3-21
T_{LA} = daily average liquid surface temperature, °R; see Note 3 for Equation 3-21

Notes:

1. The daily vapor temperature range, ΔT_V, is calculated using the following equation:

$$\Delta T_V = 0.72\ \Delta T_A + 0.028\ \alpha\ I \qquad (3\text{-}8)$$

where:

ΔT_V = daily vapor temperature range, °R
ΔT_A = daily ambient temperature range, °R; see Note 4
α = tank paint solar absorptance, dimensionless; see Table 7.3-6
I = daily total solar insolation factor, Btu/ft^2 d; see Table 7.3-7

2. The daily vapor pressure range, ΔP_V, can be calculated using the following equation:

$$\Delta P_V = P_{VX} - P_{VN} \qquad (3\text{-}9)$$

where:

ΔP_V = daily vapor pressure range, psia
P_{VX} = vapor pressure at the daily maximum liquid surface temperature, psia; see Note 5
P_{VN} = vapor pressure at the daily minimum liquid surface temperature, psia; see Note 5

The following method can be used as an alternate means of calculating ΔP_V for petroleum liquids:

$$\Delta P_V = \frac{0.50\, B\, P_{VA}\, \Delta T_V}{T_{LA}^{\,2}} \qquad (3\text{-}10)$$

where:

ΔP_V = daily vapor pressure range, psia
B = constant in the vapor pressure equation, °R; see Note 2 to Equation 3-21
P_{VA} = vapor pressure at the daily average liquid surface temperature, psia; see Notes 1 and 2 to Equation 3-21
T_{LA} = daily average liquid surface temperature, °R; see Note 3 to Equation 3-21
ΔT_V = daily vapor temperature range, °R; see Note 1

3. The breather vent pressure setting range, ΔP_B, is calculated using the following equation:

$$\Delta P_B = P_{BP} - P_{BV} \qquad (3\text{-}11)$$

where:

ΔP_B = breather vent pressure setting range, psig
P_{BP} = breather vent pressure setting, psig
P_{BV} = breather vent vacuum setting, psig

If specific information on the breather vent pressure setting and vacuum setting is not available, assume 0.03 psig for P_{BP} and -0.03 psig for P_{BV} as typical values. If the fixed roof tank is of bolted or riveted construction in which the roof or shell plates are not vapor tight, assume that $\Delta P_B = 0$, even if a breather vent is used.

4. The daily ambient temperature range, ΔT_A, is calculated using the following equation:

$$\Delta T_A = T_{AX} - T_{AN} \qquad (3\text{-}12)$$

where:

ΔT_A = daily ambient temperature range, °R
T_{AX} = daily maximum ambient temperature, °R
T_{AN} = daily minimum ambient temperature, °R

Table 7.3-7 gives values of T_{AX} and T_{AN} for selected cities in the United States.

5. The vapor pressures associated with daily maximum and minimum liquid surface temperature, P_{VX} and P_{VN}, respectively, are calculated by substituting the corresponding temperatures, T_{LX} and T_{LN}, into the vapor pressure function discussed in Notes 1 and 2 to Equation 3-21. If T_{LX} and T_{LN} are unknown, Figure 7.3-17 can be used to calculate their values.

Diameter

For vertical tanks, the diameter is straightforward. If a user needs to estimate emissions from a horizontal fixed roof tank, some of the tank parameters can be modified before using the vertical tank emission estimating equations. First, by assuming that the tank is one-half filled, the surface area of the liquid in the tank is approximately equal to the length of the tank times the diameter of the tank. Next, assume that this area represents a circle, i.e., that the liquid is an upright cylinder. Therefore, the effective diameter, D_E, is then equal to:

$$D_E = \sqrt{\frac{L\,D}{\frac{\pi}{4}}} \tag{3-13}$$

where:

D_E = effective tank diameter, ft
L = length of the horizontal tank, ft (for tanks with rounded ends, use the overall length)
D = diameter of a vertical cross-section of the horizontal tank, ft

By assuming the volume of the tank to be approximately equal to the cross-sectional area of the tank times the length of the tank, an effective height, H_E, of an equivalent upright cylinder may be calculated as:

$$H_E = \frac{\pi}{4} D \tag{3-14}$$

D_E should be used in place of D in Equation 3-4 for calculating the standing storage loss (or in Equation 3-3, if calculating the tank vapor space volume). One-half of the effective height, H_E, should be used as the vapor space outage, H_{VO}, in these equations. This method yields only a very approximate value for emissions from horizontal storage tanks. For underground horizontal tanks, assume that no breathing or standing storage losses occur ($L_S = 0$) because the insulating nature of the earth limits the diurnal temperature change. No modifications to the working loss equation are necessary for either above-ground or underground horizontal tanks.

Vapor Space Outage

The vapor space outage, H_{VO} is the height of a cylinder of tank diameter, D, whose volume is equivalent to the vapor space volume of a fixed roof tank, including the volume under the cone or dome roof. The vapor space outage, H_{VO}, is estimated from:

$$H_{VO} = H_S - H_L + H_{RO} \quad (3\text{-}15)$$

where:

H_{VO} = vapor space outage, ft; use $H_E/2$ from Equation 3-14 for horizontal tanks
H_S = tank shell height, ft
H_L = liquid height, ft
H_{RO} = roof outage, ft; see Note 1 for a cone roof or Note 2 for a dome roof

Notes:

1. For a cone roof, the roof outage, H_{RO}, is calculated as follows:

$$H_{RO} = 1/3\ H_R \quad (3\text{-}16)$$

where:

H_{RO} = roof outage (or shell height equivalent to the volume contained under the roof), ft
H_R = tank roof height, ft

$$H_R = S_R\ R_S \quad (3\text{-}17)$$

where:

S_R = tank cone roof slope, ft/ft; if unknown, a standard value of 0.0625 is used
R_S = tank shell radius, ft

2. For a dome roof, the roof outage, H_{RO}, is calculated as follows:

$$H_{RO} = H_R \left[\frac{1}{2} + \frac{1}{6} \left[\frac{H_R}{R_S} \right]^2 \right] \quad (3\text{-}18)$$

where:

H_{RO} = roof outage, ft
R_S = tank shell radius, ft
H_R = tank roof height, ft

$$H_R = R_R - \left(R_R^2 - R_S^2 \right)^{0.5} \quad (3\text{-}19)$$

H_R = tank roof height, ft
R_R = tank dome roof radius, ft
R_S = tank shell radius, ft

The value of R_R usually ranges from 0.8D - 1.2D, where D = 2 R_S. If R_R is unknown, the tank diameter is used in its place. If the tank diameter is used as the value for R_R, Equations 3-18 and 3-19 reduce to $H_{RO} = 0.137\ R_S$ and $H_R = 0.268\ R_S$.

Vented Vapor Saturation Factor, K_S

The vented vapor saturation factor, K_S, is calculated using the following equation:

$$K_S = \frac{1}{1 + 0.053\, P_{VA}\, H_{VO}} \tag{3-20}$$

where:

K_S = vented vapor saturation factor, dimensionless
P_{VA} = vapor pressure at daily average liquid surface temperature, psia; see Notes 1 and 2 to Equation 3-21
H_{VO} = vapor space outage, ft, see Equation 3-15
0.053 = constant, $(\text{psia-ft})^{-1}$

Stock Vapor Density, W_V - The density of the vapor is calculated using the following equation:

$$W_V = \frac{M_V\ P_{VA}}{R\ T_{LA}} \tag{3-21}$$

where:

W_V = vapor density, lb/ft^3
M_V = vapor molecular weight, lb/lb-mole; see Note 1
R = the ideal gas constant, 10.731 psia ft^3/lb-mole °R
P_{VA} = vapor pressure at daily average liquid surface temperature, psia; see Notes 1 and 2
T_{LA} = daily average liquid surface temperature, °R; see Note 3

Notes:

1. The molecular weight of the vapor, M_V, can be determined from Table 7.3-2 and 7.3-3 for selected petroleum liquids and volatile organic liquids, respectively, or by analyzing vapor samples. Where mixtures of organic liquids are stored in a tank, M_V can be calculated from the liquid composition. The molecular weight of the vapor, M_V, is equal to the sum of the molecular weight, M_i, multiplied by the vapor mole fraction, y_i, for each component. The vapor mole fraction is equal to the partial pressure of component i divided by the total vapor pressure. The partial pressure of component i is equal to the true vapor pressure of component i (P) multiplied by the liquid mole fraction, (x_i). Therefore,

$$M_V = \sum M_i\ y_i = \sum M_i \left(\frac{P x_i}{P_{VA}} \right) \tag{3-22}$$

where:

P_{VA}, total vapor pressure of the stored liquid, by Raoult's Law, is:

$$P_{VA} = \sum P x_i \tag{3-23}$$

For more detailed information, please refer to Section 7.1.4.

2. True vapor pressure is the equilibrium partial pressure exerted by a volatile organic liquid, as defined by ASTM-D 2879 or as obtained from standard reference texts. Reid vapor pressure is the absolute vapor pressure of volatile crude oil and volatile nonviscous petroleum liquids, except liquified petroleum gases, as determined by ASTM-D-323. True vapor pressures for organic liquids can be determined from Table 7.3-3. True vapor pressure can be determined for crude oils using Figures 7.3-13a and 7.3-13b. For refined stocks (gasolines and naphthas), Table 7.3-2 or Figures 7.3-14a and 7.3-14b can be used. In order to use Figures 7.3-13a, 7.3-13b, 7.3-14a, or 7.3-14b, the stored liquid surface temperature, T_{LA}, must be determined in degrees Fahrenheit. See Note 3 to determine T_{LA}.

Alternatively, true vapor pressure for selected petroleum liquid stocks, at the stored liquid surface temperature, can be determined using the following equation:

$$P_{VA} = \exp\left[A - \left(\frac{B}{T_{LA}}\right)\right] \tag{3-24}$$

where:

exp = exponential function
A = constant in the vapor pressure equation, dimensionless
B = constant in the vapor pressure equation, °R
T_{LA} = daily average liquid surface temperature, °R
P_{VA} = true vapor pressure, psia

For selected petroleum liquid stocks, physical property data are presented in Table 7.3-2. For refined petroleum stocks, the constants A and B can be calculated from the equations presented in Figure 7.3-15 and the distillation slopes presented in Table 7.3-4. For crude oil stocks, the constants A and B can be calculated from the equations presented in Figure 7.3-16. Note that in Equation 3-24, T_{LA} is determined in degrees Rankine instead of degrees Fahrenheit.

The true vapor pressure of organic liquids at the stored liquid temperature can be estimated by Antoine's equation:

$$\log P_{VA} = A - \left(\frac{B}{T_{LA} + C} \right) \quad (3\text{-}25)$$

where:

A = constant in vapor pressure equation
B = constant in vapor pressure equation
C = constant in vapor pressure equation
T_{LA} = daily average liquid surface temperature, °C
P_{VA} = vapor pressure at average liquid surface temperature, mm Hg

For organic liquids, the values for the constants A, B, and C are listed in Table 7.3-5. Note that in Equation 3-25, T_{LA} is determined in degrees Celsius instead of degrees Rankine. Also, in Equation 3-25, P_{VA} is determined in mm of Hg rather than psia (760 mm Hg = 14.7 psia).

3. If the daily average liquid surface temperature, T_{LA}, is unknown, it is calculated using the following equation:

$$T_{LA} = 0.44T_{AA} + 0.56T_B + 0.0079\ \alpha\ I \quad (3\text{-}26)$$

where:

T_{LA} = daily average liquid surface temperature, °R
T_{AA} = daily average ambient temperature, °R; see Note 4
T_B = liquid bulk temperature, °R; see Note 5
α = tank paint solar absorptance, dimensionless; see Table 7.3-6
I = daily total solar insolation factor, Btu/(ft^2 day); see Table 7.3-7

If T_{LA} is used to calculate P_{VA} from Figures 7.3-13a, 7.3-13b, 7.3-14a, or 7.3-14b, T_{LA} must be converted from degrees Rankine to degrees Fahrenheit (°F = °R - 460). If T_{LA} is used to calculate P_{VA} from Equation 3-25, T_{LA} must be converted from degrees Rankine to degrees Celsius (°C = [°R - 492]/1.8). Equation 3-26 should not be used to estimate liquid surface temperature from insulated tanks. In the case of insulated tanks, the average liquid surface temperature should be based on liquid surface temperature measurements from the tank.

4. The daily average ambient temperature, T_{AA}, is calculated using the following equation:

$$T_{AA} = \left(\frac{T_{AX} + T_{AN}}{2} \right) \quad (3\text{-}27)$$

where:

T_{AA} = daily average ambient temperature, °R
T_{AX} = daily maximum ambient temperature, °R
T_{AN} = daily minimum ambient temperature, °R

Table 7.3-7 gives values of T_{AX} and T_{AN} for selected U.S. cities.

5. The liquid bulk temperature, T_B, is calculated using the following equation:

$$T_B = T_{AA} + 6\alpha - 1 \quad (3\text{-}28)$$

where:

T_B = liquid bulk temperature, °R
T_{AA} = daily average ambient temperature, °R, as calculated in Note 4
α = tank paint solar absorptance, dimensionless; see Table 7.3-6.

3.1.1.2 Working Loss

The working loss, L_W, refers to the loss of stock vapors as a result of tank filling or emptying operations. Fixed roof tank working losses can be estimated from:

$$L_W = 0.0010\, M_V\, P_{VA}\, Q\, K_N\, K_P \quad (3\text{-}29)$$

where:

L_W = working loss, lb/yr
M_V = vapor molecular weight, lb/lb-mole; see Note 1 to Equation 3-21
P_{VA} = vapor pressure at daily average liquid surface temperature, psia; see Notes 1 and 2 to Equation 3-21
Q = annual net throughput (tank capacity [bbl] times annual turnover rate), bbl/yr
K_N = working loss turnover (saturation) factor, dimensionless; see Figure 7.3-18
for turnovers >36, $K_N = (180 + N)/6N$
for turnovers ≤36, $K_N = 1$

N = number of turnovers per year, dimensionless

$$N = \frac{5.614\, Q}{V_{LX}} \quad (3\text{-}30)$$

where:

V_{LX} = tank maximum liquid volume, ft^3

$$V_{LX} = \frac{\pi}{4} D^2 H_{LX} \quad (3\text{-}31)$$

where:

D = diameter, ft
H_{LX} = maximum liquid height, ft
K_P = working loss product factor, dimensionless
for crude oils $K_P = 0.75$
for all other organic liquids, $K_P = 1$

Using the following steps, Equation 3-29 can be simplified to combine all variables into one equation.

Using Equation 3-21, the term "$M_V P_{VA}$" can be replaced with Equation 3-32.

$$M_V P_{VA} = W_V R T_{LA} \quad (3\text{-}32)$$

Using a combination of Equation 3-30 and Equation 3-31, the term "Q" can be replaced with Equation 3-33.

$$Q = \frac{N H_{LX}}{5.614} \left(\frac{\pi}{4}\right) D^2 \quad (3\text{-}33)$$

Assuming a standard value of R to be 10.731 ft^3 psia/(lb-mole °R), the result is Equation 3-34.

$$L_W = \left(\frac{0.0010}{5.614}\right)(10.731)\, T_{LA}\, N\, H_{LX} \left(\frac{\pi}{4}\right) D^2\, K_N\, K_P\, W_V \quad (3\text{-}34)$$

By assuming the temperature to be 60°F (520°R), and adding the vent setting correction factor, K_B, the result is Equation 3-35. The vent setting correction factor accounts for any reduction in emissions due to the condensation of vapors prior to the opening of the vent. This correction factor will only affect the calculation if the vent settings are greater than ±0.03 psig.

$$L_W = N\ H_{LX} \left(\frac{\pi}{4}\right) D^2\ K_N\ K_P\ W_V\ K_B \tag{3-35}$$

where:

L_W = working loss, lb/yr
N = number of turnovers per year, $(year)^{-1}$
H_{LX} = maximum liquid height, ft
D = diameter, ft
K_N = working loss turnover (saturation) factor, dimensionless; see Figure 7.3-18
for turnovers > 36, $K_N = (180 + N)/6N$
for turnovers ≤ 36, $K_N = 1$
K_P = working loss product factor, dimensionless
for crude oils $K_P = 0.75$
for all other organic liquids, $K_P = 1$
W_V = vapor density, lb/ft^3, see Equation 3-21
K_B = vent setting correction factor, dimensionless
for open vents and for a vent setting range up to ± 0.03 psig, $K_B = 1$

Vent Setting Correction Factor

When the breather vent settings are greater than the typical values of ± 0.03 psig, and the condition expressed in Equation 3-36 is met, a vent setting correction factor, K_B, must be determined using Equation 3-37. This value of K_B will be used in Equation 3-35 to calculate working losses.

When:

$$K_N \left[\frac{P_{BP} + P_A}{P_I + P_A}\right] > 1.0 \tag{3-36}$$

Then:

$$K_B = \left[\frac{\frac{P_I + P_A}{K_N} - P_{VA}}{P_{BP} + P_A - P_{VA}} \right] \quad (3\text{-}37)$$

where:

K_B = vent setting correction factor, dimensionless

P_I = pressure of the vapor space at normal operating conditions, psig
P_I is an actual pressure reading (the gauge pressure). If the tank is held at atmospheric pressure (not under a vacuum or held at a steady pressure) P_I would be 0.

P_A = atmospheric pressure, psia

K_N = working loss turnover (saturation) factor (dimensionless)
for turnovers > 36, $K_N = (180 + N)/6N$
for turnovers ≤ 36, $K_N = 1$

P_{VA} = vapor pressure at the daily average liquid surface temperature, psia; see Notes 1 and 2 to Equation 3-21

P_{BP} = breather vent pressure setting, psig.

3.1.2 Total Losses From Floating Roof Tanks[3-5,13,15-17] –

Total floating roof tank emissions are the sum of rim seal, withdrawal, deck fitting, and deck seam losses. The equations presented in this subsection apply only to floating roof tanks. The equations are not intended to be used in the following applications:

1. To estimate losses from unstable or boiling stocks or from mixtures of hydrocarbons or petrochemicals for which the vapor pressure is not known or cannot readily be predicted;

2. To estimate losses from closed internal or closed domed external floating roof tanks (tanks vented only through a pressure/vacuum vent); or

3. To estimate losses from tanks in which the materials used in the rim seal and/or deck fittings are either deteriorated or significantly permeated by the stored liquid.

This section contains equations for estimating emissions from floating roof tanks in two situations: during normal operation, and during roof landings.

3.1.2.1 Normal Operation

Total losses from floating roof tanks may be written as:

$$L_T = L_R + L_{WD} + L_F + L_D \quad (3\text{-}38)$$

where:

L_T = total loss, lb/yr
L_R = rim seal loss, lb/yr; see Equation 3-39
L_{WD} = withdrawal loss, lb/yr; see Equation 3-41
L_F = deck fitting loss, lb/yr; see Equation 3-42
L_D = deck seam loss (internal floating roof tanks only), lb/yr; see Equation 3-46

Loss factors may be estimated for deck fitting configurations that are not listed in Table 3-12, at the zero miles-per-hour wind speed condition (IFRTs and CFRTs), from the following equation:

$$K_{fai} = 0.27(A_{fi})^{0.86}$$

where:

K_{fai} = zero-wind-speed loss factor for a particular type of deck fitting, in pound-moles per year.
A_{fi} = liquid surface area within a particular type of deck fitting, in square inches. The liquid surface area is the area inside the deck fitting well or leg sleeve, less any area occupied by an obstruction in the deck fitting well or leg sleeve (such as a fixed-roof support column, unslotted guidepole, guidepole float, or deck support leg).

The coefficient, 0.27, has units of pound-moles per (square inches)$^{0.86}$-year, and the exponent, 0.86, is dimensionless.

This equation is only applicable when the distance from the liquid surface to the top of the deck fitting well or leg sleeve is 12 inches or greater. Shorter deck fitting wells or leg sleeves may result in higher loss rates. There are no similar algorithms available for estimating loss factors for shorter deck fitting wells or leg sleeves.

This equation is for an uncontrolled deck fitting. Effective deck fitting controls would be expected to result in lower loss factors than would be estimated by this equation, but there are no algorithms available for estimating the effectiveness of deck fitting controls.

This equation is for the zero miles-per-hour wind speed condition. There are no algorithms available for estimating loss factors at non-zero wind speeds (EFRTs).

Rim Seal Loss - Rim seal loss from floating roof tanks can be estimated using the following equation:

$$L_R = (K_{Ra} + K_{Rb} v^n) D P^* M_V K_C \quad (3\text{-}39)$$

where:

L_R = rim seal loss, lb/yr
K_{Ra} = zero wind speed rim seal loss factor, lb-mole/ft·yr; see Table 7.3-8
K_{Rb} = wind speed dependent rim seal loss factor, lb-mole/(mph)^{n}ft·yr; see Table 7.3-8
v = average ambient wind speed at tank site, mph; see Note 1
n = seal-related wind speed exponent, dimensionless; see Table 7.3-8
P^* = vapor pressure function, dimensionless; see Note 2

$$P^* = \frac{\frac{P_{VA}}{P_A}}{\left[1 + \left(1 - \frac{P_{VA}}{P_A}\right)^{0.5}\right]^2} \quad (3\text{-}40)$$

where:

P_{VA} = vapor pressure at daily average liquid surface temperature, psia;

See Notes 1 and 2 to Equation 3-21 and Note 3 below

P_A = atmospheric pressure, psia

D = tank diameter, ft
M_V = average vapor molecular weight, lb/lb-mole; see Note 1 to Equation 3-21,
K_C = product factor;
$K_C = 0.4$ for crude oils;
$K_C = 1$ for all other organic liquids.

Notes:

1. If the ambient wind speed at the tank site is not available, use wind speed data from the nearest local weather station or values from Table 7.3-9. If the tank is an internal or domed external floating roof tank, the value of v is zero.

2. P^* can be calculated or read directly from Figure 7.3-19.

3. The API recommends using the stock liquid temperature to calculate P_{VA} for use in Equation 3-40 in lieu of the liquid surface temperature. If the stock liquid temperature is unknown, API recommends the following equations to estimate the stock temperature:

Tank Color		Average Annual Stock Temperature, T_s (°F)
White		$T_{AA} + 0^a$
Aluminum		$T_{AA} + 2.5$
Gray		$T_{AA} + 3.5$
Black		$T_{AA} + 5.0$

[a] T_{AA} is the average annual ambient temperature in degrees Fahrenheit.

Withdrawal Loss - The withdrawal loss from floating roof storage tanks can be estimated using Equation 3-41.

$$L_{WD} = \frac{(0.943)QC_S W_L}{D}\left[1 + \frac{N_C F_C}{D}\right] \quad (3\text{-}41)$$

where:

L_{WD} = withdrawal loss, lb/yr
Q = annual throughput (tank capacity [bbl] times annual turnover rate), bbl/yr
C_S = shell clingage factor, bbl/1,000 ft^2; see Table 7.3-10
W_L = average organic liquid density, lb/gal; see Note 1
D = tank diameter, ft
0.943 = constant, 1,000 ft^3·gal/bbl^2
N_C = number of fixed roof support columns, dimensionless; see Note 2
F_C = effective column diameter, ft (column perimeter [ft]/π); see Note 3

Notes:

1. A listing of the average organic liquid density for select petrochemicals is provided in Tables 7.3-2 and 7.3-3. If W_L is not known for gasoline, an average value of 6.1 lb/gal can be assumed.

2. For a self-supporting fixed roof or an external floating roof tank:

$N_C = 0$.

For a column-supported fixed roof:

N_C = use tank-specific information or see Table 7.3-11.

3. Use tank-specific effective column diameter or

F_C = 1.1 for 9-inch by 7-inch built-up columns, 0.7 for 8-inch-diameter pipe columns, and 1.0 if column construction details are not known

Deck Fitting Loss - Deck fitting losses from floating roof tanks can be estimated by the following equation:

$$L_F = F_F P^* M_V K_C \quad (3\text{-}42)$$

where:

L_F = the deck fitting loss, lb/yr
F_F = total deck fitting loss factor, lb-mole/yr

$$F_F = [(N_{F_1} K_{F_1}) + (N_{F_2} K_{F_2}) + \ldots + (N_{F_{nf}} K_{F_{nf}})] \quad (3\text{-}43)$$

where:

N_{F_i} = number of deck fittings of a particular type ($i = 0,1,2,\ldots,n_f$), dimensionless
K_{F_i} = deck fitting loss factor for a particular type fitting ($i = 0,1,2,\ldots,n_f$), lb-mole/yr; see Equation 3-44
n_f = total number of different types of fittings, dimensionless
P^*, M_V, K_C are as defined for Equation 3-39.

The value of F_F may be calculated by using actual tank-specific data for the number of each fitting type (N_F) and then multiplying by the fitting loss factor for each fitting (K_F).

The deck fitting loss factor, K_{F_i} for a particular type of fitting, can be estimated by the following equation:

$$K_{F_i} = K_{Fa_i} + K_{Fb_i} (K_v v)^{m_i} \quad (3\text{-}44)$$

where:

K_{F_i} = loss factor for a particular type of deck fitting, lb-mole/yr
K_{Fa_i} = zero wind speed loss factor for a particular type of fitting, lb-mole/yr
K_{Fb_i} = wind speed dependent loss factor for a particular type of fitting, lb-mole/(mph)^m·yr
m_i = loss factor for a particular type of deck fitting, dimensionless
i = 1, 2, ..., n, dimensionless
K_v = fitting wind speed correction factor, dimensionless; see below
v = average ambient wind speed, mph

For external floating roof tanks, the fitting wind speed correction factor, K_v, is equal to 0.7. For internal and domed external floating roof tanks, the value of v in Equation 3-44 is zero and the equation becomes:

$$K_{Fi} = K_{Fai} \quad (3\text{-}45)$$

Loss factors K_{Fa}, K_{Fb}, and m are provided in Table 7.3-12 for the most common deck fittings used on floating roof tanks. These factors apply only to typical deck fitting conditions and when the average ambient wind speed is below 15 miles per hour. Typical numbers of deck fittings for floating roof tanks are presented in Tables 7.3-11, 7.3-12, 7.3-13, 7.3-14, and 7.3-15.

Deck Seam Loss - Neither welded deck internal floating roof tanks nor external floating roof tanks have deck seam losses. Internal floating roof tanks with bolted decks may have deck seam losses. Deck seam loss can be estimated by the following equation:

$$L_D = K_D S_D D^2 P^* M_V K_C \quad (3\text{-}46)$$

where:

K_D = deck seam loss per unit seam length factor, lb-mole/ft-yr
= 0.0 for welded deck
= 0.14 for bolted deck; see Note
S_D = deck seam length factor, ft/ft^2

$$= \frac{L_{seam}}{A_{deck}}$$

where:

L_{seam} = total length of deck seams, ft

A_{deck} = area of deck, $ft^2 = \frac{\pi \cdot D^2}{4}$

D, P^*, M_V, and K_C are as defined for Equation 3-39.

If the total length of the deck seam is not known, Table 7.3-16 can be used to determine S_D. For a deck constructed from continuous metal sheets with a 7-ft spacing between the seams, a value of 0.14 ft/ft^2 can be used. A value of 0.33 ft/ft^2 can be used for S_D when a deck is constructed from rectangular panels 5 ft by 7.5 ft. Where tank-specific data concerning width of deck sheets or size of deck panels are unavailable, a default value for S_D can be assigned. A value of 0.20 ft/ft^2 can be assumed to represent the most common bolted decks currently in use.

Note: Recently vendors of bolted decks have been using various techniques, such as gasketing the deck seams, in an effort to reduce deck seam losses. However, emission factors are not currently available in AP-42 that represent the emission reduction, if any, achieved by these techniques. Some vendors have developed specific factors for their deck designs; however, use of these factors is not recommended until approval has been obtained from the governing regulatory agency or permitting authority.

3.1.2.2 Roof Landings[21]

When using floating roof tanks, the roof floats on the surface of the liquid inside the tank and reduces evaporative losses during normal operation. However, when the tank is emptied to the point that the roof lands on deck legs, there is a period where the roof is not floating and other mechanisms must be used to estimate emissions. These emissions continue until the tank is refilled to a sufficient level to again float the roof. Therefore, these emission estimate calculations are applicable each time there is a landing of the floating roof.

This model does not address standing idle losses for partial days. It would be conservative (i.e., potentially overestimate emissions) to apply the model to episodes during which the floating roof remains landed for less than a day.

The total loss from floating roof tanks during a roof landing is the sum of the standing idle losses and the filling losses. This relationship may be written in the form of an equation:

$$L_{TL} = L_{SL} + L_{FL} \quad (3\text{-}47)$$

where:

L_{TL} = total losses during roof landing, lb per landing episode
L_{SL} = standing idle losses during roof landing, lb per landing episode
L_{FL} = filling losses during roof landing, lb per landing episode

The group of applicable equations to estimate the landing losses differs according to the type of floating roof tank that is being used. The equations needed to estimate landing losses from internal floating roof tanks are contained in Table 7.3-17; equations for external floating roof tanks are contained in Table 7.3-18; and equations for drain-dry floating roof tanks are contained in Table 7.3-19. The following sections explain these equations in more detail.

3.1.2.2.1 Standing Idle Losses

After the floating roof is landed and the liquid level in the tank continues to drop, a vacuum is created which could cause the floating roof to collapse. To prevent damage and to equalize the pressure, a breather vent is actuated. Then, a vapor space is formed between the floating roof and the liquid. The breather vent remains open until the roof is again floated, so whenever the roof is landed, vapor can be lost through this vent. These losses are called “standing idle losses.”

The three different mechanisms that contribute to standing idle losses are (1) breathing losses from vapor space, (2) wind losses, and (3) clingage losses. The specific loss mechanism is dependent on the type of floating roof tank.

For internal floating roof tanks with nominally flat bottoms (including those built with a slight upward cone), the breathing losses originate from a discernible level of liquid that remains in the tank at all times due to the flatness of the tank bottom and the position of the withdrawal line (a liquid “heel”). The liquid evaporates into the vapor space and daily changes in ambient temperature cause the tank to breathe in a manner similar to a fixed roof tank.

For external floating roof tanks, which are not shielded from the surrounding atmosphere, the wind can cause vapors to flow from beneath the floating roof. The higher the wind speeds, the more vapor that can be expelled. These are known as wind losses.

For tanks with a cone-down or shovel bottom, the floor of the tank is sloped to allow for more thorough emptying of the tank contents, therefore, the amount of liquid differs significantly from tanks with flat bottoms (see Figure 7.3-20). When the emptying operation drains the tank bottom, but leaves a heel of liquid in or near the sump, the tank is considered to have a partial heel. A drain-dry condition is attained only when all of the standing liquid has been removed, including from the bottom of the sump. However, due to sludge buildup and roughness of the inside of the tank, a small layer of liquid can remain clinging to the sloped bottom of a drain-dry tank. This layer of liquid will create vapor that can result in clingage losses. The amount of vapor produced within a drain-dry tank is directly related to this clingage. Clingage factors for various tank conditions are contained in Table 7.3-10.

Standing Idle Loss for Tanks with a Liquid Heel

A constraint on the standing idle loss is added for floating roof tanks with a liquid heel in that the total emissions cannot exceed the available stock liquid in the tank. This upper limit, represented as L_{SLmax}, is a function of the volume and density of the liquid inside the tank.

$$L_{SL\max} = \text{(area of tank) (height of liquid) (density of liquid)} \quad (3\text{-}48)$$

Assuming that the tank has a circular bottom and adding a volume conversion unit, the equation can be simplified to Equation 3-49 and Equation 3-50.

$$L_{SL\max} = \left(\frac{\pi}{4}\right) D^2 \; h_{le} \; W_l \; (7.48) \quad (3\text{-}49)$$

$$L_{SL\max} = 5.9 \; D^2 \; h_{le} \; W_l \quad (3\text{-}50)$$

where:

L_{SLmax} = limit on standing idle loss, lb per landing episode
7.48 = volume conversion factor, gal/ft^3
D = diameter of the tank, feet
h_{le} = effective height of the stock liquid, feet
W_l = density of the liquid inside the tank, lb/gal

Internal Floating Roof Tank with a Liquid Heel

For internal floating roof tanks with liquid heels, the amount of "standing idle loss" depends on the amount of vapor within the vapor space under the floating roof. Essentially, the mechanism is identical to the breathing losses experienced with fixed roof tanks. The mechanism shown in Equation 3-51 is identical to Equation 3-2.

$$L_{SL} = 365\, V_V\ W_V\ K_E\ K_S \tag{3-51}$$

where:

L_{SL} = annual breathing loss from standing storage during roof landing, lb/yr
365 = number of days in a year, days/yr
V_V = volume of the vapor space, ft^3
W_V = stock vapor density, lb/ft^3

$$W_V = \frac{M_V P}{RT} \tag{3-52}$$

M_V = stock vapor molecular weight, lb/lb-mole
P = true vapor pressure of the stock liquid, psia
R = ideal gas constant, 10.731 (psia-ft^3)/(lb-mole °R)
T = temperature, °R
K_E = vapor space expansion factor, dimensionless
K_S = saturation factor, dimensionless.

Assuming that n_d equals the number of days that the tank stands idle and substituting for the stock vapor density according to Equation 3-52, the equation is further simplified to Equation 3-53.

$$L_{SL} = n_d\ K_E \left(\frac{P\, V_V}{R\, T} \right) M_V\ K_S \tag{3-53}$$

The term with the highest amount of uncertainty is the saturation of the vapor within the tank. The factor, K_S, is estimated with the same method used to calculate the saturation factor for fixed roof tanks in Equation 3-20. In order to establish limits on the value of K_S, the estimated factor is assumed to be less than or equal to the saturation factor during filling (S). (For more information see Filling Losses.)

External Floating Roof Tank with a Liquid Heel

For external floating roof tanks with a liquid heel, wind affects emission releases from the tanks. As a starting point, begin with a basic equation based on rim-seal loss. The equation, shown as Equation 3-54, is equivalent to Equation 3-39.

$$L_{RL} = (K_{Ra} + K_{Rb}\, v^n) D\, P^*\, M_V\, K_C \qquad (3\text{-}54)$$

where:

L_{RL} = annual rim seal loss during roof landing, lb/yr
K_{Ra} = zero wind speed rim seal loss factor, lb-mole/ft-yr
K_{Rb} = wind speed dependent rim seal loss factor, lb-mole/((mph)^n-ft-yr))
n = seal-related wind speed loss exponent, dimensionless
(K_{Ra}, K_{Rb}, and n are specific to a given configuration of rim seal)
v = average ambient wind speed, mph
D = tank diameter, ft
M_V = stock vapor molecular weight, lb/lb-mole
K_C = product factor, dimensionless
P^* = a vapor pressure function, dimensionless

$$P^* = \frac{\frac{P_{VA}}{P_A}}{\left[1 + \left(1 - \frac{P_{VA}}{P_A}\right)^{0.5}\right]^2} \qquad (3\text{-}55)$$

where:

P_A = atmospheric pressure, psia
P = true vapor pressure of the stock liquid, psia.

Assuming that the stock properties included in the vapor pressure function will adequately account for differences in liquid product type, K_C is assumed to equal 1. Regardless of the type of rim seal that is in use, it is effectively rendered a 'vapor-mounted' seal when the liquid level falls such that the rim seal is no longer in contact with the liquid. The contribution of a secondary seal is neglected in that it is offset by emissions through the deck fittings. The emissions are therefore based on the case of a welded tank with an average-fitting vapor-mounted primary seal. According to Table 7.3-8, the values of K_{ra}, K_{rb}, and n are 6.7, 0.2, and 3.0, respectively. The variables were substituted and the equation was converted from annual emissions to daily emissions by dividing the equation by 365. A value of 10 mph is assigned to the wind speed, so that estimated standing idle losses from an external floating roof tank will not be less than for a typical internal floating roof tank. Lower values for the rim seal loss factors or the wind speed should not be used. The equation can be simplified for daily emissions to Equation 3-56.

$$L_{SLwind} = 0.57\, n_d\, D\, P^*\, M_V \quad (3\text{-}56)$$

where:

L_{SLwind} = daily standing idle loss due to wind, lb per day
nd = number of days that the tank is standing idle, days
D = tank diameter, ft
P* = a vapor pressure function, dimensionless
M_V = stock vapor molecular weight, lb/lb-mole

After the wind empties the vapor space above the remaining liquid heel, the liquid will continue to produce vapor. Thus, this standing idle loss will occur every day that the tank stands idle. This equation is adequate at this time, but could be revised as additional testing is conducted and studied.

Standing Idle Losses from Drain-Dry Tanks

When a drain-dry tank has been emptied, the only stock liquid available inside the tank is a small amount that clings to the wetted surface of the tank interior (if a heel of liquid remains in or near a sump, then the tank should be evaluated as having a partial heel, and not as drain dry – see Figure 7.3-20). The slope prevents a significant amount of stock liquid from remaining in the tank so that evaporation is much lower than from tanks with liquid heels. Due to the limited amount of liquid clinging to the interior of the tank, as shown in Figure 7.3-20, it is assumed that vapors would not be replenished as readily as in tanks with a liquid heel. For this model, standing idle loss due to clingage is a one-time event rather than a daily event.

The loss due to clingage is proportional to a clingage factor, which varies with the condition of the inside of the tank. A list of clingage factors are shown in Table 7.3-10. The factors are given in terms of barrels per thousand square feet. To convert the loss to pounds, the density of the liquid and the area of the tank must be taken into account, as shown in Equation 3-57.

$$L_C = 42\, C_S\, W_l\, (Area) \quad (3\text{-}57)$$

where:

L_C = clingage loss from the drain-dry tank, lb
42 = conversion factor, gal/bbl
C_S = clingage factor, bbl/1,000 ft^2
W_l = density of the liquid, lb/gal
Area = area of the tank bottom, ft^2

$$Area = \left(\frac{\pi\, D^2}{4} \right) \quad (3\text{-}58)$$

Among the conditions shown in Table 7.3-10, the one that best approximates a sludge-lined tank bottom is gunite-lined. Assuming that gasoline is being stored in the tank, a clingage factor of 0.15 and the area term in Equation 3-58 were substituted into Equation 3-57, which simplifies to Equation 3-59.

$$L_{SL} = 0.0063\, W_l\, \frac{\pi\, D^2}{4} \qquad (3\text{-}59)$$

The clingage loss should be constrained by an upper limit equal to the filling loss for an internal floating roof tank with a liquid heel. This is demonstrated in Equation 3-60.

$$L_{SL\,\max} = 0.60 \left(\frac{P\, V_V}{R\, T} \right) M_V \qquad (3\text{-}60)$$

where:

L_{SLmax} = maximum standing idle loss for drain-dry tanks due to clingage, lb
W_l = density of the liquid inside the tank, lb/gal
D = diameter of the tank, feet
P = true vapor pressure of the liquid inside the tank, psia
V_V = volume of the vapor space, ft^3
R = ideal gas constant, 10.731 psia ft^3 /lb-mole °R
T = average temperature of the vapor and liquid below the floating roof, °R (= T_{AA})
M_V = stock vapor molecular weight, lb/lb-mole

Therefore, the standing idle loss for drain-dry tanks, shown in Equation 3-59, must be less than or equal to Equation 3-393. This relationship is shown by Equation 3-361.

$$L_{SL} \le 0.60 \left(\frac{P\, V_V}{R\, T} \right) M_V \qquad (3\text{-}61)$$

3.1.2.2.2 Filling Losses

When a floating roof tank is refilled, there are additional emissions resulting from the roof being landed. These losses are called "filling losses" and continue until the liquid reaches the level of the floating roof.

The first contributor to filling losses is called the "arrival" component. As liquid flows into the tank, the vapor space between the liquid and the floating roof is decreased. The displaced vapors are expelled through the breather vent. Once the roof is refloated on the liquid surface, the breather vent closes.

The second contributor to filling losses is called the "generated" component. As the incoming liquid evaporates, additional vapors will be formed in the vapor space and will also be expelled through the breather vent.

Internal Floating Roof Tank with a Liquid Heel

For internal floating roof tanks with a liquid heel, the amount of vapor that is lost during filling is directly related to the amount of vapor space and the saturation level of the vapor within the vapor space, as shown in Equation 3-62.

$$L_{FL} = (vol\ of\ vapor\ space)(density\ of\ vapor)(mol\ wt\ of\ vapor)(satfactor) \quad (3\text{-}62)$$

After substituting for the major terms in Equation 3-62, the equation can be simplified to Equation 3-63.

$$L_{FL} = \left(\frac{P\,V_V}{R\,T}\right) M_V\ S \quad (3\text{-}63)$$

where:

L_{FL} = filling loss during roof landing, lb
P = true vapor pressure of the liquid within the tank, psia
V_V = volume of the vapor space, ft^3
R = ideal gas constant, 10.731 psia-ft^3/(lb-mole-°R)
T = average temperature of the vapor and liquid below the floating roof, °R
M_V = stock vapor molecular weight, lb/lb-mole
S = filling saturation factor, dimension less (0.60 for a full liquid heel; 0.50 for a partial liquid heel).

This equation accounts for the arrival losses and the generated losses. The main concern with this equation is the estimation of the saturation factor. All other components are based on the ideal gas laws. For consistency, an accepted value of 0.6, which is used elsewhere in Chapter 7, will be used for the case of a full liquid heel. A value of 0.5 has been demonstrated for the case of a partial liquid heel.

External Floating Roof Tank with a Liquid Heel

For external floating roof tanks with a liquid heel, the amount of vapor lost during filling will be less than the amount for internal floating roof tanks because of wind effects. The "arrival" component will be partially flushed out of the tank by the wind, so the preceding equation requires the addition of a correction factor, C_{sf} to the saturation factor as shown in Equation 3-64.

$$L_{FL} = \left(\frac{P\,V_V}{R\,T}\right) M_V\ (C_{sf}\ S) \quad (3\text{-}64)$$

The basic premise of the correction factor is that the vapors expelled by wind action will not be present in the vapor space when the tank is refilled, so the amount of saturation is lowered. This is demonstrated in Equation 3-65.

$$C_{sf} = 1 - \frac{(one\ day\ of\ wind\ driven\ standing\ idle\ loss) - (one\ day\ without\ wind\ standing\ idle\ loss)}{one\ day\ without\ wind\ total\ loss} \quad (3\text{-}65)$$

The equation for the saturation factor can be simplified based on other equations contained in this section as shown in Equation 3-66 and Equation 3-67.

$$C_{sf} = 1 - \left(\frac{(Equation\ 2-19) - (Equation\ 2-16)}{(Equation\ 2-16) + (Equation\ 2-26)} \right) \quad (3\text{-}66)$$

$$C_{sf} = 1 - \left(\frac{\left(0.57\ n_d\ D\ P^*\ M_V\right) - \left(n_d\ K_E \left(\frac{P\ V_V}{R\ T} \right) M_V\ K_S \right)}{\left(n_d\ K_E \left(\frac{P\ V_V}{R\ T} \right) M_V\ K_S \right) + \left(M_V\ S \left(\frac{P\ V_V}{R\ T} \right) \right)} \right) \quad (3\text{-}67)$$

where:

C_{sf} = filling saturation correction factor, dimensionless
n_d = number of days the tank stands idle with the floating roof landed, dimensionless
K_E = vapor space expansion factor, dimensionless

$$K_E = \frac{\Delta T_V}{T} \left(1 + \frac{0.50\ B\ P}{T\left(P_A - P\right)} \right) \quad (3\text{-}68)$$

ΔT_v = daily vapor temperature range, °R
T = average temperature of the vapor and liquid below the floating roof, °R
B = constant from the vapor pressure equation shown in Equation 3-24, °R (If B is unknown, K_E may be calculated from Equation 3-5, 3-6, or 3-7, as appropriate, with the value of ΔP_B set equal to zero.)
P = true vapor pressure of the stock liquid, psia
P_A = atmospheric pressure at the tank location, psia
V_V = volume of the vapor space, ft^3

$$V_V = \frac{h_v\ \pi\ D^2}{4} \quad (3\text{-}69)$$

h_v = height of the vapor space under the floating roof, ft
D = tank diameter, ft
R = ideal gas constant, 10.731 psia ft^3 / lb-mole R
M_V = stock vapor molecular weight, lb/lb-mole
K_S = standing idle saturation factor, dimensionless
S = filling saturation factor, dimensionless
P^* = vapor pressure function, dimensionless
W_l = stock liquid density, lb/gal

Drain-Dry Tanks

The "arrival" component of filling losses for drain-dry tanks is completely covered by the "clingage" loss. Once this initial loss occurs, there is no remaining liquid inside the tank. Therefore, there is no vapor in the tank that could be expelled by the incoming liquid.

However, the "generated" component remains a valid aspect of the model. Therefore, the filling loss calculations for drain-dry tanks are identical to the filling loss calculations for internal floating roof tanks with a liquid heel. Although the equations are the same, the saturation factor will be lower for drain-dry tanks due to the lack of an "arrival" component. AP-42 Chapter 5, *Petroleum Industry*, provides emission factors for the loading of gasoline and crude oil into compartments according to the prior state of the compartment. A drain-dry tank would be most similar to a tank that was cleaned before filling because a cleaned tank also lacks "arrival" losses. The emission factor (0.33 lb/1000 gallons) for this kind of tank can be converted to a saturation factor by assuming a pressure of 8 psia (the same assumption used in the formulation of the emission factor), and substituting the molecular weight of gasoline (64 lb/lb-mole). The resulting saturation factor is 0.15. The equation is the same as Equation 3-70 with a different assumed saturation factor.

$$L_{FL} = \left(\frac{PV_V}{RT} \right) M_V \, S \qquad (3\text{-}70)$$

where:

L_{FL} = filling loss during roof landing, lb
P = true vapor pressure of the liquid within the tank, psia
V_V = volume of the vapor space, ft^3
R = ideal gas constant, 10.731 psia-ft^3/(lb-mole-°R)
T = average temperature of the vapor and liquid below the floating roof, °R
M_V = stock vapor molecular weight, lb/lb-mole
S = filling saturation factor, dimension less (0.15 for a drain-dry tank).

3.1.3 Variable Vapor Space Tanks[18] –

Variable vapor space filling losses result when vapor is displaced by liquid during filling operations. Since the variable vapor space tank has an expandable vapor storage capacity, this loss is not as large as the filling loss associated with fixed roof tanks. Loss of vapor occurs only when the tank's vapor storage capacity is exceeded. Equation 3-1 assumes that one-fourth of the expansion capacity is available at the beginning of each transfer.

Variable vapor space system filling losses can be estimated from:

$$L_V = (2.40\times10^{-2})\left(\frac{M_V\ P_{VA}}{V_1}\right)\left[(V_1)-(0.25\ V_2\ N_2)\right] \quad (3\text{-}71)$$

where:

L_V = variable vapor space filling loss, lb/1,000 gal throughput
M_V = molecular weight of vapor in storage tank, lb/lb-mole; see Note 1 to Equation 3-21
P_{VA} = true vapor pressure at the daily average liquid surface temperature, psia; see Notes 1 and 2 to Equation 3-21
V_1 = volume of liquid pumped into system, throughput, bbl/yr
V_2 = volume expansion capacity of system, bbl; see Note 1
N_2 = number of transfers into system, dimensionless; see Note 2

Notes:

1. V_2 is the volume expansion capacity of the variable vapor space achieved by roof lifting or diaphragm flexing.

2. N_2 is the number of transfers into the system during the time period that corresponds to a throughput of V_1.

The accuracy of Equation 3-1 is not documented. Special tank operating conditions may result in actual losses significantly different from the estimates provided by Equation 3-1. For example, if one or more tanks with interconnected vapor spaces are filled while others are emptied simultaneously, all or part of the expelled vapors will be transferred to the tank, or tanks, being emptied. This is called balanced pumping. Equation 3-1 does not account for balanced pumping, and will overestimate losses under this condition. It should also be noted that, although not developed for use with heavier petroleum liquids such as kerosenes and fuel oils, the equation is recommended for use with heavier petroleum liquids in the absence of better data.

3.1.4 Pressure Tanks –

Losses occur during withdrawal and filling operations in low-pressure (2.5 to 15 psig) tanks when atmospheric venting occurs. High-pressure tanks are considered closed systems, with virtually no emissions. Vapor recovery systems are often found on low-pressure tanks. Fugitive losses are also associated with pressure tanks and their equipment, but with proper system maintenance, these losses are considered insignificant. No appropriate correlations are available to estimate vapor losses from pressure tanks.

3.1.5 Variations Of Emission Estimation Procedures –

All of the emission estimation procedures presented in Section 7.1.3 can be used to estimate emissions for shorter time periods by manipulating the inputs to the equations for the time period in question. For all of the emission estimation procedures, the daily average liquid surface temperature should be based on the appropriate temperature and solar insolation data for the time period over which the estimate is to be evaluated. The subsequent calculation of the vapor pressure should be based on the corrected daily liquid surface temperature. For example, emission calculations for the month of June would be based only on the meteorological data for June. It is important to note that a 3-month time frame is recommended as the shortest time period for which emissions should be estimated.

In addition to the temperature and vapor pressure corrections, the constant in the standing storage loss equation for fixed roof tanks would need to be revised based on the actual time frame used. The constant, 365, is based on the number of days in a year. To change the equation for a different time period, the constant should be changed to the appropriate number of days in the time period for which emissions are being estimated. The only change that would need to be made to the working loss equation for fixed roof tanks would be to change the throughput per year to the throughput during the time period for which emissions are being estimated.

Other than changing the meteorological data and the vapor pressure data, the only changes needed for the floating roof rim seal, deck fitting, and deck seam losses would be to modify the time frame by dividing the individual losses by the appropriate number of days or months. The only change to the withdrawal losses would be to change the throughput to the throughput for the time period for which emissions are being estimated.

Another variation that is frequently made to the emission estimation procedures is an adjustment in the working or withdrawal loss equations if the tank is operated as a surge tank or constant level tank. For constant level tanks or surge tanks where the throughput and turnovers are high but the liquid level in the tank remains relatively constant, the actual throughput or turnovers should not be used in the working loss or withdrawal loss equations. For these tanks, the turnovers should be estimated by determining the average change in the liquid height. The average change in height should then be divided by the total shell height. This adjusted turnover value should then be multiplied by the actual throughput to obtain the net throughput for use in the loss equations. Alternatively, a default turnover rate of four could be used based on data from these type tanks.

3.2 HAZARDOUS AIR POLLUTANTS (HAP's) SPECIATION METHODOLOGY

In some cases it may be important to know the annual emission rate for a component (e. g., HAP) of a stored liquid mixture. There are two basic approaches that can be used to estimate emissions for a single component of a stored liquid mixture. One approach involves calculating the total losses based upon the known physical properties of the mixture (i. e., gasoline) and then determining the individual component losses by multiplying the total loss by the weight fraction of the desired component. The second approach is similar to the first approach except that the mixture properties are unknown; therefore, the mixture properties are first determined based on the composition of the liquid mixture.

Case 1 — If the physical properties of the mixture are known (P_{VA}, M_V, M_L and W_L), the total losses from the tank should be estimated using the procedures described previously for the particular tank type. The component losses are then determined from either Equation 3-72 or 3-73. For fixed roof tanks, the emission rate for each individual component can be estimated by:

$$L_{T_i} = (Z_{V_i})(L_T) \tag{3-72}$$

where:

L_{T_i} = emission rate of component i, lb/yr
Z_{V_i} = weight fraction of component i in the vapor, lb/lb
L_T = total losses, lb/yr

For floating roof tanks, the emission rate for each individual component can be estimated by:

$$L_{T_i} = (Z_{V_i})(L_R + L_F + L_D) + (Z_{L_i})(L_{WD}) \tag{3-73}$$

where:

L_{T_i} = emission rate of component i, lb/yr
Z_{V_i} = weight fraction of component i in the vapor, lb/lb
L_R = rim seal losses, lb/yr
L_F = deck fitting losses, lb/yr
L_D = deck seam losses, lb/yr
Z_{L_i} = weight fraction of component i in the liquid, lb/lb
L_{WD} = withdrawal losses, lb/yr

If Equation 3-72 is used in place of Equation 3-73 for floating roof tanks, the value obtained will be approximately the same value as that achieved with Equation 3-73 because withdrawal losses are typically minimal for floating roof tanks.

In order to use Equations 4-1 and 4-2, the weight fraction of the desired component in the liquid and vapor phase is needed. The liquid weight fraction of the desired component is typically known or can be readily calculated for most mixtures. In order to calculate the weight fraction in the vapor phase, Raoult's Law must first be used to determine the partial pressure of the component. The partial pressure of the component can then be divided by the total vapor pressure of the mixture to determine the mole fraction of the component in the vapor phase. Raoult's Law states that the mole fraction of the component in the liquid (x_i) multiplied by the vapor pressure of the pure component (at the daily average liquid surface temperature) (P) is equal to the partial pressure (P_i) of that component:

$$P_i = (P)(x_i) \tag{3-74}$$

where:

P_i = partial pressure of component i, psia
P = vapor pressure of pure component i at the daily average liquid surface temperature, psia
xi = liquid mole fraction, lb-mole/lb-mole

The vapor pressure of each component can be calculated from Antoine's equation or found in standard references, as shown in Section 7.1.3.1. In order to use Equation 3-74, the liquid mole fraction must be determined from the liquid weight fraction by:

$$x_i = \left(\frac{Z_{Li} M_L}{M_i} \right) \tag{3-75}$$

where:

x_i = liquid mole fraction of component i, lb-mole/lb-mole
Z_{L_i} = weight fraction of component i in the liquid, lb/lb
M_L = molecular weight of liquid stock, lb/lb-mole
M_i = molecular weight of component i, lb/lb-mole

If the molecular weight of the liquid is not known, the liquid mole fraction can be determined by assuming a total weight of the liquid mixture (see Example 1 in Section 7.1.5).

The liquid mole fraction and the vapor pressure of the component at the daily average liquid surface temperature can then be substituted into Equation 3-74 to obtain the partial pressure of the component. The vapor mole fraction of the component can be determined from the following equation:

$$y_i = \frac{P_i}{P_{VA}} \tag{3-76}$$

where:

y_i = vapor mole fraction of component i, lb-mole/lb-mole
P_i = partial pressure of component i, psia
P_{VA} = total vapor pressure of liquid mixture, psia

The weight fractions in the vapor phase are calculated from the mole fractions in the vapor phase.

$$Z_{V_i} = \frac{y_i M_i}{M_V} \quad (3\text{-}77)$$

where:

Z_{V_i} = vapor weight fraction of component i, lb/lb
y_i = vapor mole fraction of component i, lb-mole/lb-mole
M_i = molecular weight of component i, lb/lb-mole
M_V = molecular weight of vapor stock, lb/lb-mole

The liquid and vapor weight fractions of each desired component and the total losses can be substituted into either Equations 4-1 or 4-2 to estimate the individual component losses.

Case 2 — For cases where the mixture properties are unknown but the composition of the liquid is known (i. e., nonpetroleum organic mixtures), the equations presented above can be used to obtain a reasonable estimate of the physical properties of the mixture. For nonaqueous organic mixtures, Equation 3-74 can be used to determine the partial pressure of each component. If Equation 3-75 is used to determine the liquid mole fractions, the molecular weight of the liquid stock must be known. If the molecular weight of the liquid stock is unknown, then the liquid mole fractions can be determined by assuming a weight basis and calculating the number of moles (see Example 1 in Section 7.1.5). The partial pressure of each component can then be determined from Equation 3-74.

For special cases, such as wastewater, where the liquid mixture is a dilute aqueous solution, Henry's Law should be used instead of Raoult's Law in calculating total losses. Henry's Law states that the mole fraction of the component in the liquid phase multiplied by the Henry's Law constant for the component in the mixture is equal to the partial pressure (P_i) for that component. For wastewater, Henry's Law constants are typically provided in the form of atm·m^3/g-mole.

Therefore, the appropriate form of Henry's Law equation is:

$$P_i = (H_A)\,(C_i) \quad (3\text{-}78)$$

where:

P_i = partial pressure of component i, atm
H_A = Henry's Law constant for component i, atm·m^3/g-mole
C_i = concentration of component i in the wastewater, g-mole/m^3; see Note

Section 4.3 of AP-42 presents Henry's Law constants for selected organic liquids. The partial pressure calculated from Equation 4-7 will need to be converted from atmospheres to psia (1 atm = 14.7 psia).

Note: Typically wastewater concentrations are given in mg/liter, which is equivalent to g/m^3. To convert the concentrations to g-mole/m^3 divide the concentration by the molecular weight of the component.

The total vapor pressure of the mixture can be calculated from the sum of the partial pressures:

$$P_{VA} = \sum P_i \quad (3\text{-}79)$$

where:

P_{VA} = vapor pressure at daily average liquid surface temperature, psia
P_i = partial pressure of component i, psia

This procedure can be used to determine the vapor pressure at any temperature. After computing the total vapor pressure, the mole fractions in the vapor phase are calculated using Equation 3-76. The vapor mole fractions are used to calculate the molecular weight of the vapor, M_V. The molecular weight of the vapor can be calculated by:

$$M_V = \sum M_i y_i \quad (3\text{-}80)$$

where:

M_V = molecular weight of the vapor, lb/lb-mole
M_i = molecular weight of component i, lb/lb-mole
y_i = vapor mole fraction of component i, lb-mole/lb-mole

Another variable that may need to be calculated before estimating the total losses, if it is not available in a standard reference, is the density of the liquid, W_L. If the density of the liquid is unknown, it can be estimated based on the liquid weight fractions of each component (see Section 7.1.5, Example 3).

All of the mixture properties are now known (P_{VA}, M_V, and W_L). These values can now be used with the emission estimation procedures outlined in Section 7.1.3 to estimate total losses. After calculating the total losses, the component losses can be calculated by using either Equations 3-72 or 3-73. Prior to calculating component losses, Equation 3-77 must be used to determine the vapor weight fractions of each component.

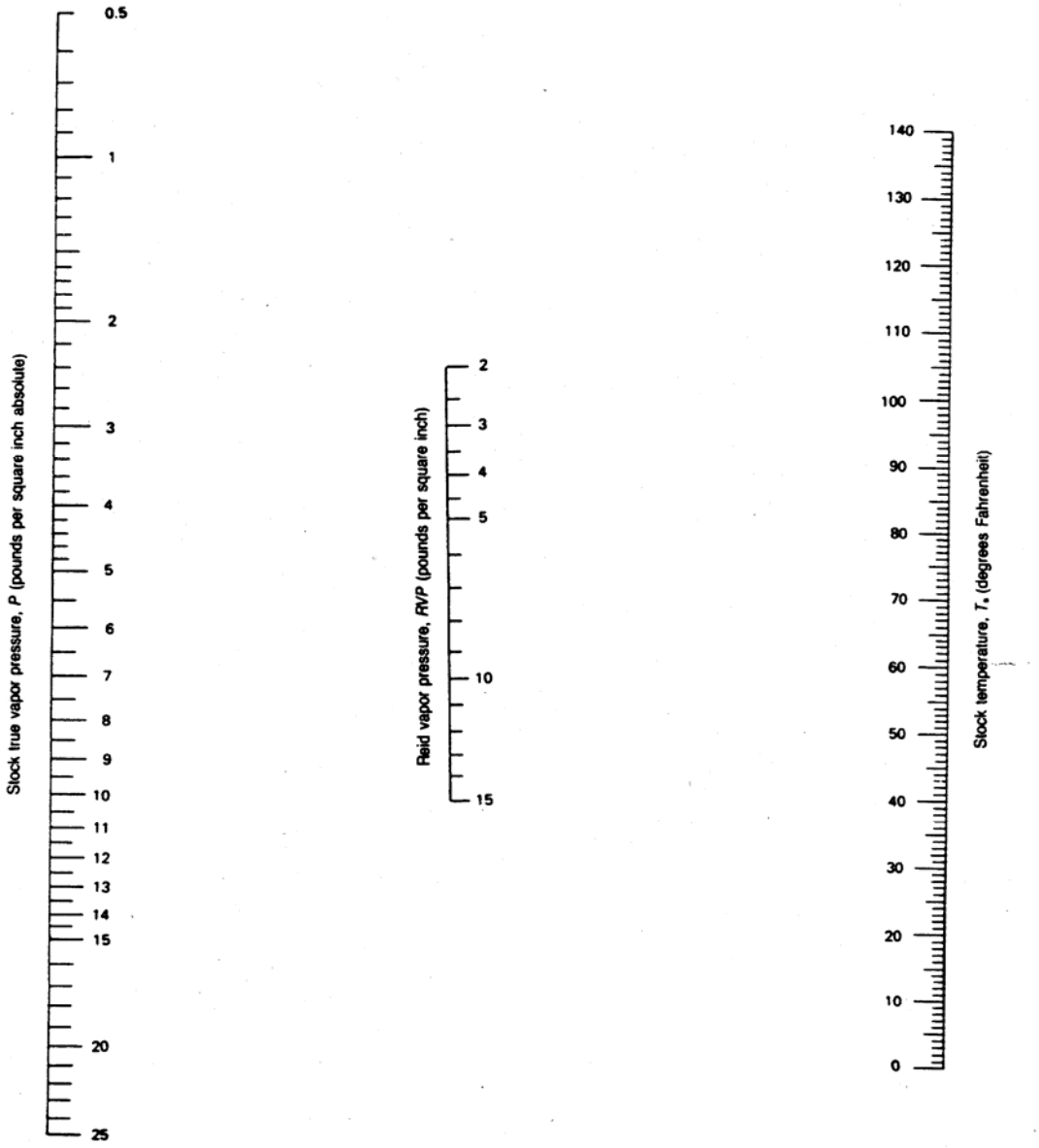

Figure 3-1. True vapor pressure of crude oils with a Reid vapor pressure of 2 to 15 pounds per square inch.[4]

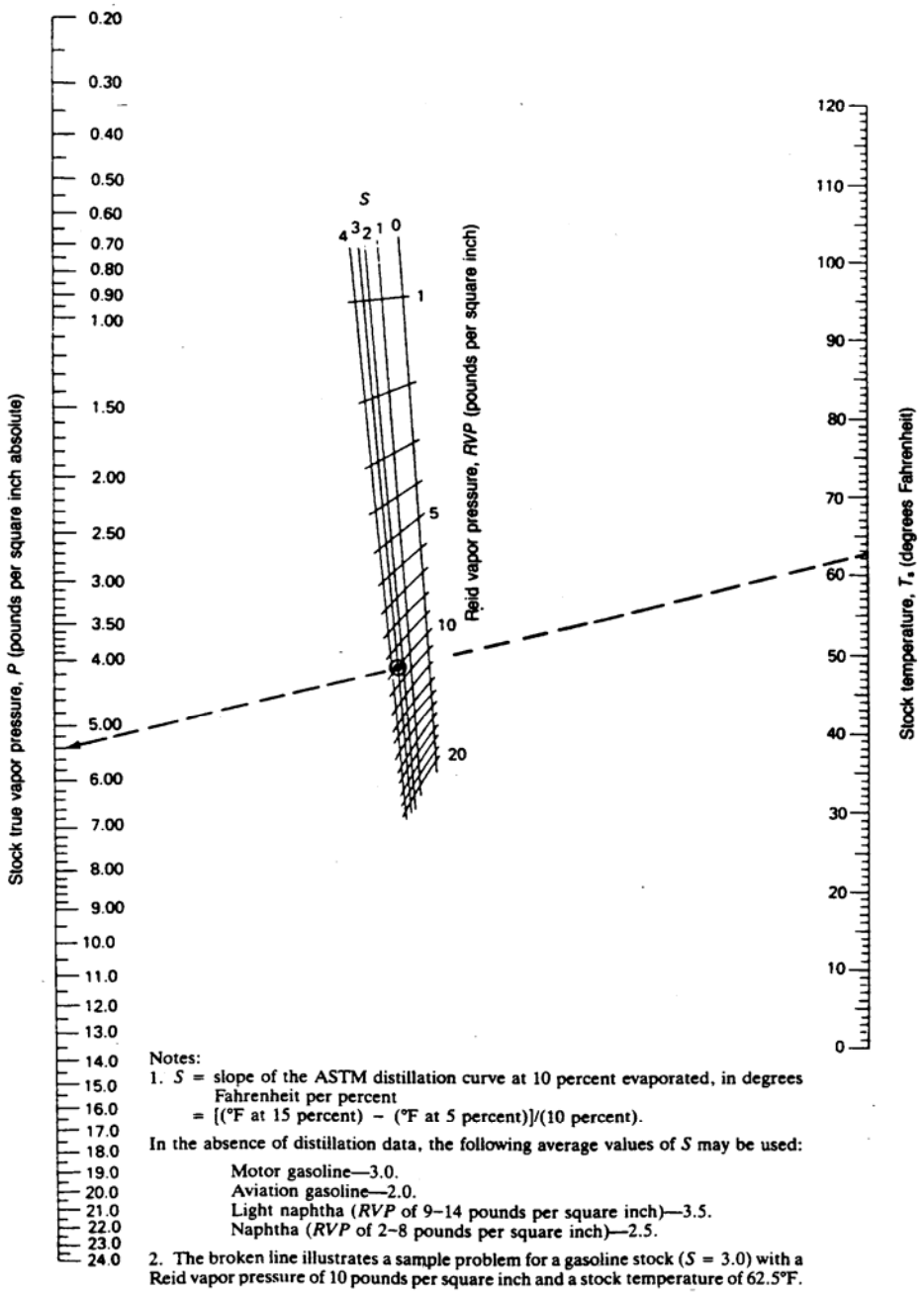

Notes:

1. S = slope of the ASTM distillation curve at 10 percent evaporated, in degrees Fahrenheit per percent
   = [(°F at 15 percent) − (°F at 5 percent)]/(10 percent).

In the absence of distillation data, the following average values of S may be used:

Motor gasoline—3.0.
Aviation gasoline—2.0.
Light naphtha (*RVP* of 9–14 pounds per square inch)—3.5.
Naphtha (*RVP* of 2–8 pounds per square inch)—2.5.

2. The broken line illustrates a sample problem for a gasoline stock (S = 3.0) with a Reid vapor pressure of 10 pounds per square inch and a stock temperature of 62.5°F.

Figure 3.-2. True vapor pressure of refined petroleum stocks with a Reid vapor pressure of 1 to 20 pounds per square inch.[4]

$$P = \exp\left\{\left[\left(\frac{2{,}799}{T+459.6}\right) - 2.227\right]\log_{10}(RVP) - \left(\frac{7{,}261}{T+459.6}\right) + 12.82\right\}$$

Where:

P = stock true vapor pressure, in pounds per square inch absolute.
T = stock temperature, in degrees Fahrenheit.
RVP = Reid vapor pressure, in pounds per square inch.

Note: This equation was derived from a regression analysis of points read off Figure 7.1-13a over the full range of Reid vapor pressures, slopes of the ASTM distillation curve at 10 percent evaporated, and stock temperatures. In general, the equation yields *P* values that are within +0.05 pound per square inch absolute of the values obtained directly from the nomograph.

Figure 3-1b. Equation for true vapor pressure of crude oils with a Reid vapor pressure of 2 to 15 pounds per square inch.[4]

$$P = \exp\left\{\left[0.7553 - \left(\frac{413.0}{T+459.6}\right)\right]S^{0.5}\log_{10}(RVP) - \left[1.854 - \left(\frac{1{,}042}{T+459.6}\right)\right]S^{0.5}\right.$$

$$\left. + \left[\left(\frac{2{,}416}{T+459.6}\right) - 2.013\right]\log_{10}(RVP) - \left(\frac{8{,}742}{T+459.6}\right) + 15.64\right\}$$

Where:

P = stock true vapor pressure, in pounds per square inch absolute.
T = stock temperature, in degrees Fahrenheit.
RVP = Reid vapor pressure, in pounds per square inch.
S = slope of the ASTM distillation curve at 10 percent evaporated, in degrees Fahrenheit per percent.

Note: This equation was derived from a regression analysis of points read off Figure 7.1-14a over the full range of Reid vapor pressures, slopes of the ASTM distillation curve at 10 percent evaporated, and stock temperatures. In general, the equation yields *P* values that are within +0.05 pound per square inch absolute of the values obtained directly from the nomograph.

Figure 3-2b. Equation for true vapor pressure of refined petroleum stocks with a Reid vapor pressure of 1 to 20 pounds per square inch.[4]

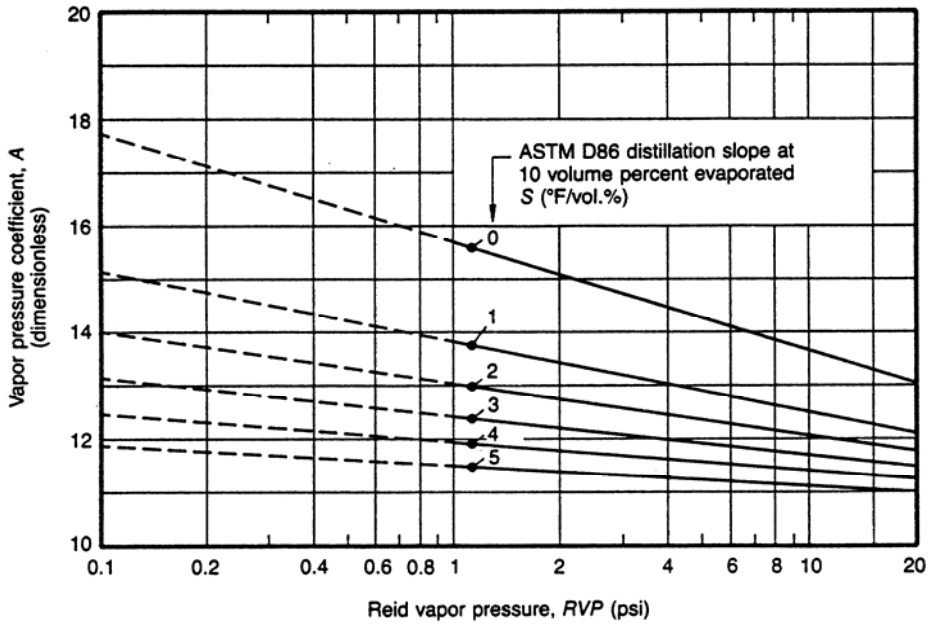

Figure 3-3. Vapor pressure function coefficient (A) of refined petroleum stocks with a Reid vapor pressure of 1 to 20 psi, extrapolated to 0.1 psi.[1]

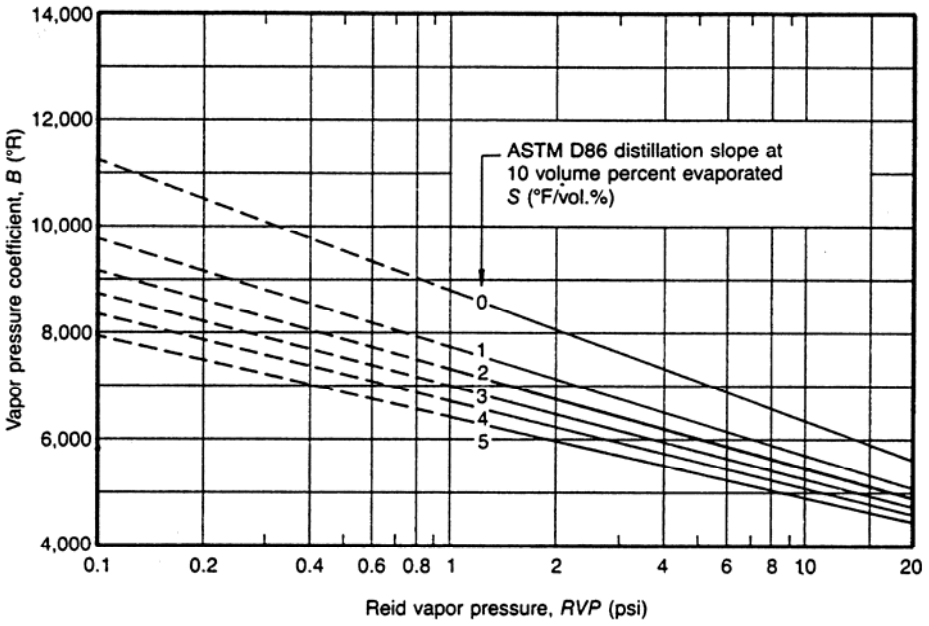

Figure 3-4. Vapor pressure function coefficient (B) of refined petroleum stocks with a Reid vapor pressure of 1 to 20 psi, extrapolated to 0.1 psi.[1]

$$A = 15.64 - 1.854\ S^{0.5} - (0.8742 - 0.3280\ S^{0.5})\ln(RVP)$$
$$B = 8{,}742 - 1{,}042\ S^{0.5} - (1{,}049 - 179.4\ S^{0.5})\ln(RVP)$$

where:

RVP = stock Reid vapor pressure, in pounds per square inch
ln = natural logarithm function
S = stock ASTM-D86 distillation slope at 10 volume percent evaporation (°F/vol %)

Figure 3-5. Equations to determine vapor pressure constants A and B for refined petroleum stocks.[8]

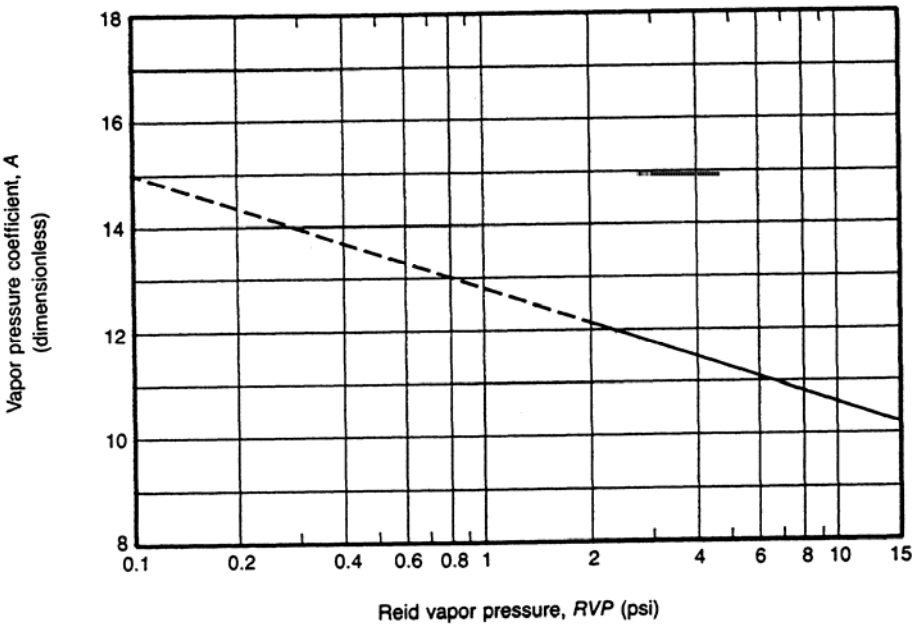

Figure 3-6. Vapor pressure function coefficient (A) of crude oil stocks with a Reid vapor pressure of 2 to 15 psi, extrapolated to 0.1 psi.[1]

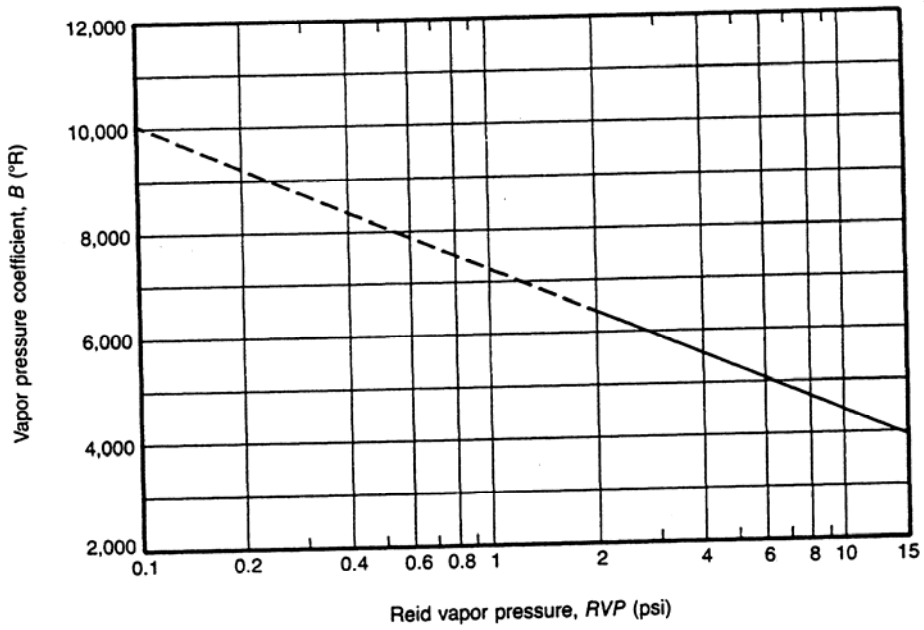

Figure 3-7. Vapor pressure function coefficient (B) of crude oil stocks with a Reid vapor pressure of 2 to 15 psi, extrapolated to 0.1 psi[1]

$$A = 12.82 - 0.9672 \ln (RVP)$$

$$B = 7{,}261 - 1{,}216 \ln (RVP)$$

where:

RVP = Reid vapor pressure, psi
ln = natural logarithm function

Figure 3-8. Equations to determine vapor pressure Constants A and B for crude oil stocks.[8]

Daily Maximum and Minimum Liquid Surface Temperature, (°R)

$$T_{LX} = T_{LA} + 0.25\ \Delta T_V$$

$$T_{LN} = T_{LA} - 0.25\ \Delta T_V$$

where:

T_{LX} = daily maximum liquid surface temperature, °R
T_{LA} is as defined in Note 3 to Equation 1-21
ΔT_V is as defined in Note 1 to Equation 1-7
T_{LN} = daily minimum liquid surface temperature, °R

Figure 3-9. Equations for the daily maximum and minimum liquid surface temperatures.[8]

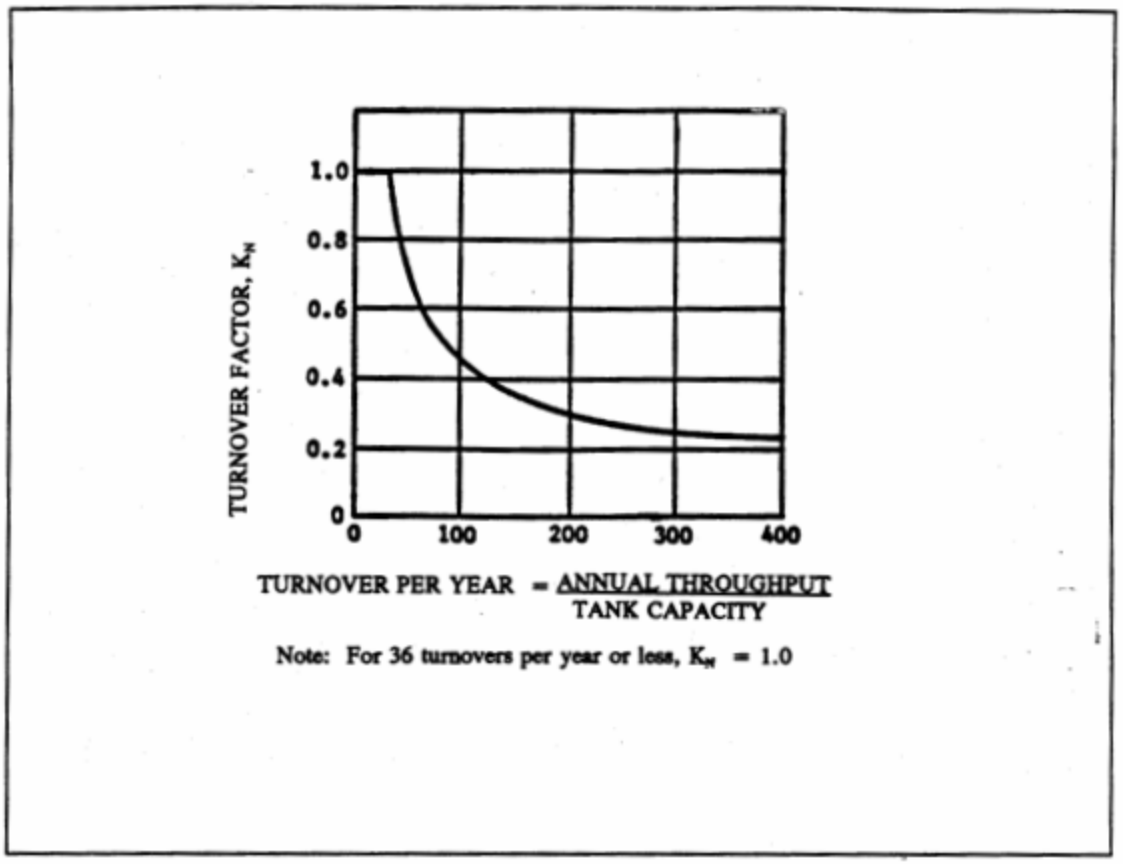

Figure 3-10. Turnover Factor (KN) for fixed roof tanks.[8]

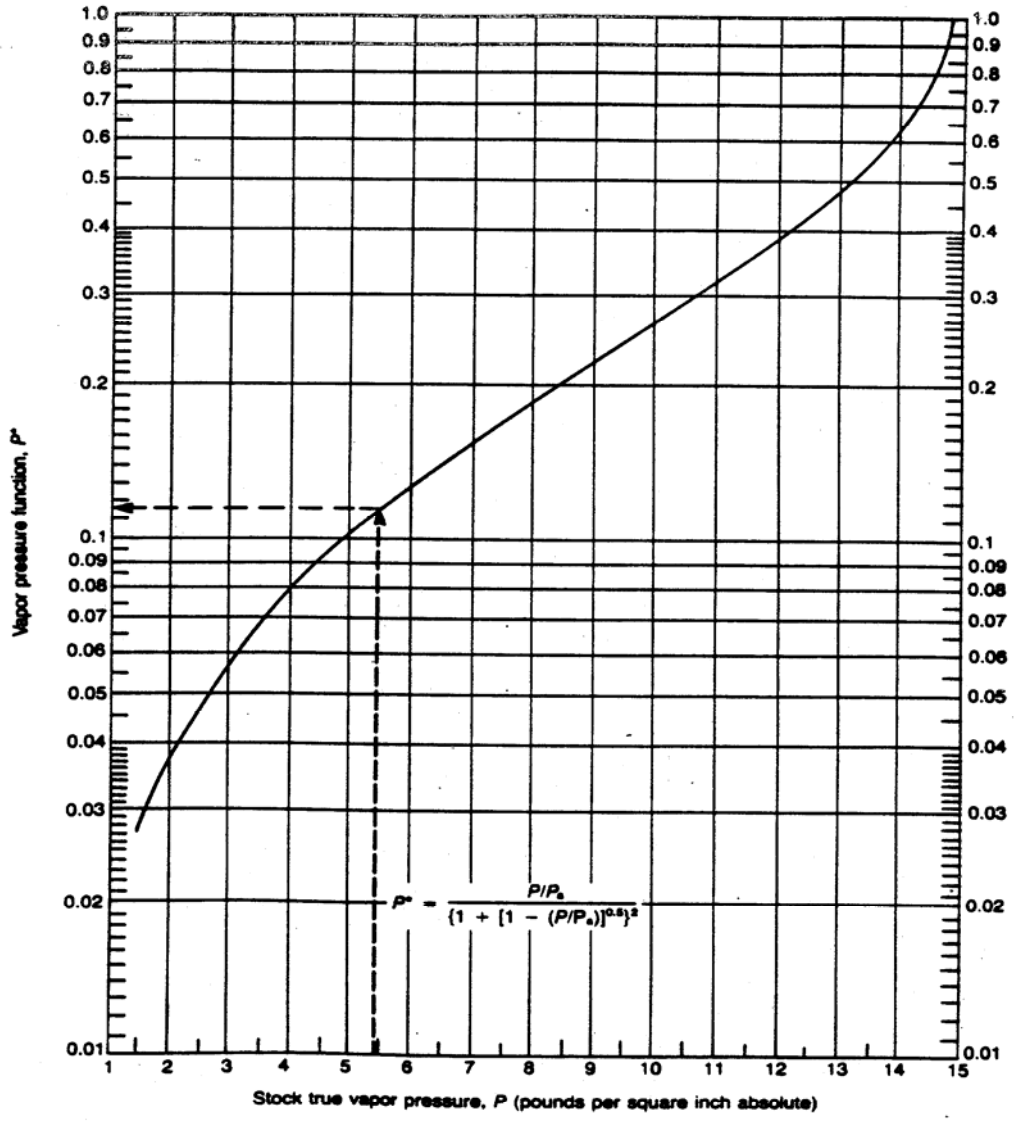

Notes:

1. Broken line illustrates sample problem for $P = 5.4$ pounds per square inch absolute.
2. Curve is for atmospheric pressure, P_a, equal to 14.7 pounds per square inch absolute.

Figure 3-11. Vapor pressure function.[4]

Table 3-1. LIST OF ABBREVIATIONS USED IN THE TANK EQUATIONS

Variable	Description
α	tank paint solar absorptance, dimensionless
π	constant, (3.14159)
A	constant in vapor pressure equation, dimensionless
A_{deck}	area of deck, ft^2
A_{fi}	liquid surface area within a particular type of deck fitting, in^2
B	constant in vapor pressure equation, °R or °C
C	constant in vapor pressure equation, °R or °C
C_S	shell clingage factor, bbl/1,000 ft^2
C_{sf}	filling saturation factor
D	tank diameter, ft
D_E	effective tank diameter, ft
F_C	effective column diameter, ft
F_F	total deck fitting loss factor, lb-mole/yr
F_R	rim deck loss factor, lb-mole/ft·yr
H_L	liquid height, ft
H_{LX}	maximum liquid height, ft
H_R	tank roof height, ft
H_{RO}	roof outage, ft
H_S	tank shell height, ft
H_{VO}	vapor space outage, ft
i	1,2,.....n, dimensionless
I	daily total solar insolation factor, Btu/ft^2·d
K_C	product factor for floating roof tanks, dimensionless
K_D	deck seam loss per unit seam length factor, lb-mole/ft-yr
K_E	vapor space expansion factor, dimensionless
K_{fai}	zero wind speed loss factor
K_{F_i}	loss factor for a particular type of deck fitting, lb-mole/yr
K_N	turnover factor, dimensionless
K_P	working loss product factor for fixed roof tanks, dimensionless
K_{Ra}	zero wind speed rim seal loss factor, lb-mole/ft·yr
K_{Rb}	wind speed dependent rim seal loss factor, lb-mole/ $(mph)^n$ft·yr
K_S	vented vapor saturation factor, dimensionless
K_v	fitting wind speed correction factor, dimensionless
L	length of tank, ft
L_C	clingage factor for drain dry tanks
L_D	deck seam loss, lb/yr
L_F	deck fitting loss, lb/yr
L_{FL}	filling loss during roof landing, lb/landing event
L_R	rim seal loss, lb/yr
L_{RL}	rim seal loss during roof landing, lb/landing event
L_S	standing storage losses, lb/yr
L_{seam}	total length of deck seam, ft
L_{SL}	standing loss during roof landing, lb/landing event
L_T	total losses, lb/yr
L_{T_i}	emission rate of component i, lb/yr
L_{TL}	total loss during roof landing, lb/landing event
L_V	variable vapor space filling loss, lb/1,000 gal throughput
L_W	working losses, lb/yr
L_{WD}	withdrawal loss, lb/yr
m_i	loss factor for a particular type of deck fitting, dimensionless
M_i	molecular weight of component i, lb/lb-mole
M_L	molecular weight of liquid mixture, lb/lb-mole
M_V	vapor molecular weight, lb/lb-mole
N	number of turnovers per year, dimensionless
n	seal-related wind speed exponent, dimensionless
N_2	number of transfers into system, dimensionless
N_c	number of columns
N_C	number of columns, dimen-sionless
N_d	number of drains
n_f	total number of different types of fittings, dimensionless
N_{Fa_i}	zero wind speed loss factor for a particular type of deck fitting, lb-mole/yr
N_{Fb_i}	wind speed dependent loss factor for a particular type of fitting, lb-mole/ mph^m·yr
N_{F_i}	number of deck fittings of a particular type, dimensionless
N_l	number of deck legs
N_{TOTAL}	total number of moles in mixture, lb-mole
N_{vb}	number of vacuum breakers
P	true vapor pressure of component i, psia
P^*	vapor pressure function, dimensionless
P_A	atmospheric pressure, psi
ΔP_B	breather vent pressure setting range, psig
P_{BP}	breather vent pressure setting, psig
P_{BV}	breather vent vacuum setting, psig

3-44

Table 3-1 (cont.).

Variable	Description	Variable	Description
P_I	gauge pressure within the vapor space, psig	T_B	liquid bulk temperature, °R
P_i	partial pressure of component i, psia	T_{LA}	daily average liquid surface temperature, °R
ΔP_V	daily vapor pressure range, psi	ΔT_V	daily vapor temperature range, °R
P_{VA}	vapor pressure at daily average liquid surface temperature, psia	v	average wind speed, mph
P_{VN}	vapor pressure at the daily minimum liquid surface temperature, psia	V_1	volume of liquid pumped into system, bbl/yr
P_{VX}	vapor pressure at the daily maximum liquid surface temperature, psia	V_2	volume expansion capacity, bbl
Q	annual net throughput, bbl/yr	V_{LX}	tank maximum liquid volume, ft^3
R	ideal gas constant, (10.731 psia·ft^3/lb-mole·°R)	V_V	vapor space volume, ft^3
R_R	tank dome roof radius, ft	W_i	liquid density of component i, lb/ft^3
R_S	tank shell radius, ft	W_L	average organic liquid density, lb/gal
S_D	deck seam length factor, ft/ft^2	W_V	vapor density, lb/ft^3
S_R	tank cone roof slope, ft/ft	x_i	liquid mole fraction of component i, lb-mole/lb-mole
ΔT_A	daily ambient temperature range, °R	y_i	vapor mole fraction of component i, lb-mole/lb-mole
T_{AA}	daily average ambient temperature, °R	Z_{L_i}	liquid weight fraction of component i, lb/lb
T_{AN}	daily minimum ambient temperature, °R	Z_{V_i}	vapor weight fraction of component i, lb/lb
T_{AX}	daily maximum ambient temperature, °R		

TABLE 3-2. PROPERTIES (M_V, W_{VC}, W_L, P_V) OF SELECTED PETROLEUM LIQUIDS[a]

Petroleum Liquid	Vapor Molecular Weight at 60°F, M_V (lb/lb-mole)	Liquid Density At 60°F, W_L (lb/gal)	True Vapor Pressure, P_{VA} (psi)						
			40°F	50°F	60°F	70°F	80°F	90°F	100°F
Crude oil RVP 5	50	7.1	1.8	2.3	2.8	3.4	4.0	4.8	5.7
Distillate fuel oil No. 2	130	7.1	0.0031	0.0045	0.0065	0.0090	0.012	0.016	0.022
Gasoline RVP 7	68	5.6	2.3	2.9	3.5	4.3	5.2	6.2	7.4
Gasoline RVP 7.8	68	5.6	2.5929	3.2079	3.9363	4.793	5.7937	6.9552	8.2952
Gasoline RVP 8.3	68	5.6	2.7888	3.444	4.2188	5.1284	6.1891	7.4184	8.8344
Gasoline RVP 10	66	5.6	3.4	4.2	5.2	6.2	7.4	8.8	10.5
Gasoline RVP 11.5	65	5.6	4.087	4.9997	6.069	7.3132	8.7519	10.4053	12.2949
Gasoline RVP 13	62	5.6	4.7	5.7	6.9	8.3	9.9	11.7	13.8
Gasoline RVP 13.5	62	5.6	4.932	6.0054	7.2573	8.7076	10.3774	12.2888	14.4646
Gasoline RVP 15.0	60	5.6	5.5802	6.774	8.1621	9.7656	11.6067	13.7085	16.0948
Jet kerosene	130	7.0	0.0041	0.0060	0.0085	0.011	0.015	0.021	0.029
Jet naphtha (JP-4)	80	6.4	0.8	1.0	1.3	1.6	1.9	2.4	2.7
Residual oil No. 6	190	7.9	0.00002	0.00003	0.00004	0.00006	0.00009	0.00013	0.00019

[a] References 10 and 11

Table 3-3. PHYSICAL PROPERTIES OF SELECTED PETROCHEMICALS[a]

Name	Formula	Molecular Weight	Boiling Point At 1 Atmosphere (°F)	Liquid Density At 60°F (lb/gal)	Vapor Pressure (psia) At						
					40°F	50°F	60°F	70°F	80°F	90°F	100°F
Acetone	CH_3COCH_3	58.08	133.0	6.628	1.682	2.185	2.862	3.713	4.699	5.917	7.251
Acetonitrile	CH_3CN	41.05	178.9	6.558	0.638	0.831	1.083	1.412	1.876	2.456	3.133
Acrylonitrile	CH_2:CHCN	53.06	173.5	6.758	0.812	0.967	1.373	1.779	2.378	3.133	4.022
Allyl alcohol	CH_2:$CHCH_2OH$	58.08	206.6	7.125	0.135	0.193	0.261	0.387	0.522	0.716	1.006
Allyl chloride	CH_2:$CHCH_2Cl$	76.53	113.2	7.864	2.998	3.772	4.797	6.015	7.447	9.110	11.025
Ammonium hydroxide (28.8% solution)	NH_4OH--H_2O	35.05	83.0	7.481	5.130	6.630	8.480	10.760	13.520	16.760	20.680
Benzene	C_6H_6	78.11	176.2	7.365	0.638	0.870	1.160	1.508	1.972	2.610	3.287
iso-Butyl alcohol	$(CH_3)_2CHCH_2OH$	74.12	227.1	6.712	0.058	0.097	0.135	0.193	0.271	0.387	0.541
tert-Butyl alcoholv	$(CH_3)_3COH$	74.12	180.5	6.595	0.174	0.290	0.425	0.638	0.909	1.238	1.702
n-Butyl chloride	$CH_3CH_2CH_2CH_2Cl$	92.57	172.0	7.430	0.715	1.006	1.320	1.740	2.185	2.684	3.481
Carbon disulfide	CS_2	76.13	115.3	10.588	3.036	3.867	4.834	6.014	7.387	9.185	11.215
Carbon tetrachloride	CCl_4	153.84	170.2	13.366	0.793	1.064	1.412	1.798	2.301	2.997	3.771
Chloroform	$CHCl_3$	119.39	142.7	12.488	1.528	1.934	2.475	3.191	4.061	5.163	6.342
Chloroprene	CH_2:CCl·CH:CH_2	88.54	138.9	8.046	1.760	2.320	2.901	3.655	4.563	5.685	6.981
Cyclohexane	C_6H_{12}	84.16	177.3	6.522	0.677	0.928	1.218	1.605	2.069	2.610	3.249
Cyclopentane	C_5H_{10}	70.13	120.7	6.248	2.514	3.287	4.177	5.240	6.517	8.063	9.668
1,1-Dichloroethane	CH_3CHCl_2	98.97	135.1	9.861	1.682	2.243	2.901	3.771	4.738	5.840	7.193
1,2-Dichloroethane	CH_2ClCH_2Cl	98.97	182.5	10.500	0.561	0.773	1.025	1.431	1.740	2.243	2.804
cis-1,2- Dichloro-ethylene	CHCl:CHCl	96.95	140.2	10.763	1.450	2.011	2.668	3.461	4.409	5.646	6.807
trans-1,2-Dichloro-ethylene	CHCl:CHCl	96.95	119.1	10.524	2.552	3.384	4.351	5.530	6.807	8.315	10.016
Diethylamine	$(C_2H_5)_2NH$	73.14	131.9	5.906	1.644	1.992	2.862	3.867	4.892	6.130	7.541
Diethyl ether	$C_2H_5OC_2H_5$	74.12	94.3	5.988	4.215	5.666	7.019	8.702	10.442	13.342	Boils
Di-*iso*-propyl ether	$(CH_3)_2CHOCH(CH_3)_2$	102.17	153.5	6.075	1.199	1.586	2.127	2.746	3.481	4.254	5.298
1,4-Dioxane	O·$CH_2CH_2OCH_2CH_2$	88.10	214.7	8.659	0.232	0.329	0.425	0.619	0.831	1.141	1.508
Dipropyl ether	$CH_3CH_2CH_2OCH_2CH_2CH_3$	102.17	195.8	6.260	0.425	0.619	0.831	1.102	1.431	1.876	2.320
Ethyl acetate	$C_2H_5OOCCH_3$	88.10	170.9	7.551	0.580	0.831	1.102	1.489	1.934	2.514	3.191
Ethyl acrylate	C_2H_5OOCCH:CH_2	100.11	211.8	7.750	0.213	0.290	0.425	0.599	0.831	1.122	1.470
Ethyl alcohol	C_2H_5OH	46.07	173.1	6.610	0.193	0.406	0.619	0.870	1.218	1.682	2.320

3-47

Table 3-3. (con't).

Name	Formula	Molecular Weight	Boiling Point At 1 Atmosphere (°F)	Liquid Density At 60°F (Pounds Per Gallon)	Vapor Pressure (Pounds Per Square Inch Absolute) At						
					40°F	50°F	60°F	70°F	80°F	90°F	100°F
Freon 11	CCl_3F	137.38	75.4	12.480	7.032	8.804	10.900	13.40	16.31	19.69	23.60
n-Heptane	$CH_3(CH_2)_5CH_3$	100.20	209.2	5.727	0.290	0.406	0.541	0.735	0.967	1.238	1.586
n-Hexane	$CH_3(CH_2)_4CH_3$	86.17	155.7	5.527	1.102	1.450	1.876	2.436	3.055	3.906	4.892
Hydrogen cyanide	HCN	27.03	78.3	5.772	6.284	7.831	9.514	11.853	15.392	18.563	22.237
Isopentane	$(CH_3)_2CHCH_2CH_3$	72.15	82.1	5.199	5.878	7.889	10.005	12.530	15.334	18.370	21.657
Isoprene	$(CH_2):C(CH_3)CH:CH_2$	68.11	93.5	5.707	4.757	6.130	7.677	9.668	11.699	14.503	17.113
Isopropyl alcohol	$(CH_3)_2{\cdot}CHOH$	60.09	180.1	6.573	0.213	0.329	0.483	0.677	0.928	1.296	1.779
Methacrylonitrile	$CH_2:CH(CH_3)CN$	67.09	194.5	6.738	0.483	0.657	0.870	1.160	1.470	1.934	2.456
Methyl acetate	CH_3OOCCH_3	74.08	134.8	7.831	1.489	2.011	2.746	3.693	4.699	5.762	6.961
Methyl acrylate	$CH_3OOCCH:CH_2$	86.09	176.9	7.996	0.599	0.773	1.025	1.354	1.798	2.398	3.055
Methyl alcohol	CH_3OH	32.04	148.4	6.630	0.735	1.006	1.412	1.953	2.610	3.461	4.525
Methylcyclohexane	$CH_3{\cdot}C_6H_{11}$	98.18	213.7	6.441	0.309	0.425	0.541	0.735	0.986	1.315	1.721
Methylcyclopentane	$CH_3C_5H_9$	84.16	161.3	6.274	0.909	1.160	1.644	2.224	2.862	3.616	4.544
Methylene chloride	CH_2Cl_2	84.94	104.2	11.122	3.094	4.254	5.434	6.787	8.702	10.329	13.342
Methyl ethyl ketone	$CH_3COC_2H_5$	72.10	175.3	6.747	0.715	0.928	1.199	1.489	2.069	2.668	3.345
Methyl methacrylate	$CH_3OOC(CH_3):CH_2$	100.11	212.0	7.909	0.116	0.213	0.348	0.541	0.773	1.064	1.373
Methyl propyl ether	$CH_3OC_3H_7$	74.12	102.1	6.166	3.674	4.738	6.091	7.058	9.417	11.602	13.729
Nitromethane	CH_3NO_2	61.04	214.2	9.538	0.213	0.251	0.348	0.503	0.715	1.006	1.334
n-Pentane	$CH_3(CH_2)_3CH_3$	72.15	96.9	5.253	4.293	5.454	6.828	8.433	10.445	12.959	15.474
n-Propylamine	$C_3H_7NH_2$	59.11	119.7	6.030	2.456	3.191	4.157	5.250	6.536	8.044	9.572
1,1,1-Trichloroethane	CH_3CCl_3	133.42	165.2	11.216	0.909	1.218	1.586	2.030	2.610	3.307	4.199
Trichloroethylene	$CHCl:CCl_2$	131.40	188.6	12.272	0.503	0.677	0.889	1.180	1.508	2.030	2.610
2,2,4-trimethyl pentane (isooctane)	$(CH_2)_3CCH_2CH(CH_3)_2$	114.23	210.6	5.76			0.596				
Toluene	$CH_3{\cdot}C_6H_5$	92.13	231.1	7.261	0.174	0.213	0.309	0.425	0.580	0.773	1.006
Vinyl acetate	$CH_2:CHOOCCH_3$	86.09	162.5	7.817	0.735	0.986	1.296	1.721	2.262	3.113	4.022
Vinylidene chloride	$CH_2:CCl_2$	96.5	89.1	10.383	4.990	6.344	7.930	9.806	11.799	15.280	23.210

3-48

TABLE 3-4. ASTM DISTILLATION SLOPE FOR SELECTED REFINED PETROLEUM STOCKS

Refined petroleum stock	Reid vapor pressure (RVP), psia	ASTM distillation slope at 10 volume percent evaporated,(°F/vol%)
Aviation gasoline	ND	2.0
Naphtha	3-45	2.5
Motor gasoline	ND	3.0
Light naphtha	9-14	3.5

[a]Reference 1. ND = no data.

TABLE 3-5. VAPOR PRESSURE EQUATION CONSTANTS FOR ORGANIC LIQUIDS[a]

Name	Vapor pressure equation constants		
	A	B	C
	(dimensionless)	(°C)	(°C)
Acetaldehyde	8.005	1600.017	291.809
Acetic acid	7.387	1533.313	222.309
Acetic anhydride	7.149	1444.718	199.817
Acetone	7.117	1210.595	229.664
Acetonitrile	7.119	1314.4	230
Acrylamide	11.2932	3939.877	273.16
Acrylic acid	5.652	648.629	154.683
Acrylonitrile	7.038	1232.53	222.47
Aniline	7.32	1731.515	206.049
Benzene	6.905	1211.033	220.79
Butanol (iso)	7.4743	1314.19	186.55
Butanol-(1)	7.4768	1362.39	178.77
Carbon disulfide	6.942	1169.11	241.59
Carbon tetrachloride	6.934	1242.43	230
Chlorobenzene	6.978	1431.05	217.55
Chloroform	6.493	929.44	196.03
Chloroprene	6.161	783.45	179.7
Cresol(-M)	7.508	1856.36	199.07
Cresol(-O)	6.911	1435.5	165.16
Cresol(-P)	7.035	1511.08	161.85
Cumene (isopropylbenzene)	6.963	1460.793	207.78
Cyclohexane	6.841	1201.53	222.65
Cyclohexanol	6.255	912.87	109.13
Cyclohexanone	7.8492	2137.192	273.16
Dichloroethane(1,2)	7.025	1272.3	222.9
Dichloroethylene(1,2)	6.965	1141.9	231.9
Diethyl (N,N) aniline	7.466	1993.57	218.5
Dimethyl formamide	6.928	1400.87	196.43
Dimethyl hydrazine (1,1)	7.408	1305.91	225.53
Dimethyl phthalate	4.522	700.31	51.42
Dinitrobenzene	4.337	229.2	-137
Dioxane(1,4)	7.431	1554.68	240.34

Table 3-5. (con't).

Epichlorohydrin	8.2294	2086.816	273.16
Ethanol	8.321	1718.21	237.52
Ethanolamine(mono-)	7.456	1577.67	173.37
Ethyl acetate	7.101	1244.95	217.88
Ethyl acrylate	7.9645	1897.011	273.16
Ethyl benzene	6.975	1424.255	213.21
Ethyl chloride	6.986	1030.01	238.61
Ethyl ether	6.92	1064.07	228.8
Formic acid	7.581	1699.2	260.7
Furan	6.975	1060.87	227.74
Furfural	6.575	1198.7	162.8
Heptane(iso)	6.8994	1331.53	212.41
Hexane(-N)	6.876	1171.17	224.41
Hexanol(-1)	7.86	1761.26	196.66
Hydrocyanic acid	7.528	1329.5	260.4
Methanol	7.897	1474.08	229.13
Methyl acetate	7.065	1157.63	219.73
Methyl ethyl ketone	6.9742	1209.6	216
Methyl isobutyl ketone	6.672	1168.4	191.9
Methyl metharcrylate	8.409	2050.5	274.4
Methyl styrene (alpha)	6.923	1486.88	202.4
Methylene chloride	7.409	1325.9	252.6
Morpholine	7.7181	1745.8	235
Naphthalene	7.01	1733.71	201.86
Nitrobenzene	7.115	1746.6	201.8
Pentachloroethane	6.74	1378	197
Phenol	7.133	1516.79	174.95
Picoline(-2)	7.032	1415.73	211.63
Propanol (iso)	8.117	1580.92	219.61
Propylene glycol	8.2082	2085.9	203.5396
Propylene oxide	8.2768	1656.884	273.16
Pyridine	7.041	1373.8	214.98
Resorcinol	6.9243	1884.547	186.0596
Styrene	7.14	1574.51	224.09
Tetrachloroethane(1,1,1,2)	6.898	1365.88	209.74
Tetrachloroethane(1,1,2,2)	6.631	1228.1	179.9
Tetrachloroethylene	6.98	1386.92	217.53
Tetrahydrofuran	6.995	1202.29	226.25
Toluene	6.954	1344.8	219.48
Trichloro(1,1,2)trifluoroethane	6.88	1099.9	227.5
Trichloroethane(1,1,1)	8.643	2136.6	302.8
Trichloroethane(1,1,2)	6.951	1314.41	209.2
Trichloroethylene	6.518	1018.6	192.7

Trichlorofluoromethane	6.884	1043.004	236.88
Trichloropropane(1,2,3)	6.903	788.2	243.23
Vinyl acetate	7.21	1296.13	226.66
Vinylidene chloride	6.972	1099.4	237.2
Xylene(-M)	7.009	1426.266	215.11
Xylene(-O)	6.998	1474.679	213.69
[a]Reference 11.			

TABLE 3-6. PAINT SOLAR ABSORPTANCE FOR FIXED ROOF TANKS[a]

Paint Color	**Paint Shade or Type**	**Paint Factors (α)**	
		Paint Condition	
		Good	**Poor**
Aluminum	Specular	0.39	0.49
Aluminum	Diffuse	0.60	0.68
Aluminum[b]	Mill finish, unpainted	0.10	0.15
Beige/Cream		0.35	0.49
Brown		0.58	0.67
Gray	Light	0.54	0.63
Gray	Medium	0.68	0.74
Green	Dark	0.89	0.91
Red	Primer	0.89	0.91
Rust	Red iron oxide	0.38	0.50
Tan		0.43	0.55
White	NA	0.17	0.34

Notes:

[a] Reference 8. If specific information is not available, a white shell and roof, with the paint in good condition, can be assumed to represent the most common or typical tank surface in use. If the tank roof and shell are painted a different color, α is determined from $\alpha = (\alpha_R + \alpha_S)/2$; where α_R is the tank roof paint solar absorptance and α_S is the tank shell paint solar absorptance.

[b]This refers to aluminum as the base metal, rather than aluminum-colored paint.

NA = not applicable.

Table 3-7. METEOROLOGICAL DATA (T_{AX}, T_{AN}, I) FOR SELECTED U.S. LOCATIONS[a]

Location	Property		Monthly Averages												Annual Average
	Symbol	Units	Jan.	Feb.	Mar.	Apr.	May	June	July	Aug.	Sept.	Oct.	Nov.	Dec.	
Birmingham, AL	T_{AX}	°F	52.7	57.3	65.2	75.2	81.6	87.9	90.3	89.7	84.6	74.8	63.7	35.2	73.2
	T_{AN}	°F	33.0	35.2	42.1	50.4	58.3	65.9	69.8	69.1	63.6	50.4	40.5	55.9	51.1
	I	Btu/ft^2·d	707	967	1296	1674	1857	1919	1810	1724	1455	1211	858	661	1345
Montgomery, AL	T_{AX}	°F	57.0	60.9	68.1	77.0	83.6	89.8	91.5	91.2	86.9	77.5	67.0	59.8	75.9
	T_{AN}	°F	36.4	38.8	45.5	53.3	61.1	68.4	71.8	71.1	66.4	53.1	43.0	37.9	53.9
	I	Btu/ft^2·d	752	1013	1341	1729	1897	1972	1841	1746	1468	1262	915	719	1388
Homer, AK	T_{AX}	°F	27.0	31.2	34.4	42.1	49.8	56.3	60.5	60.3	54.8	44.0	34.9	27.7	43.6
	T_{AN}	°F	14.4	17.4	19.3	28.1	34.6	41.2	45.1	45.2	39.7	30.6	22.8	15.8	29.5
	I	Btu/ft^2·d	122	334	759	1248	1583	1751	1598	1189	791	437	175	64	838
Phoenix, AZ	T_{AX}	°F	65.2	69.7	74.5	83.1	92.4	102.3	105.0	102.3	98.2	87.7	74.3	66.4	85.1
	T_{AN}	°F	39.4	42.5	46.7	53.0	61.5	70.6	79.5	77.5	70.9	59.1	46.9	40.2	57.3
	I	Btu/ft^2·d	1021	1374	1814	2355	2677	2739	2487	2293	2015	1577	1151	932	1869
Tucson, AZ	T_{AX}	°F	64.1	67.4	71.8	80.1	88.8	98.5	98.5	95.9	93.5	84.1	72.2	65.0	81.7
	T_{AN}	°F	38.1	40.0	43.8	49.7	57.5	67.4	73.8	72.0	67.3	56.7	45.2	39.0	54.2
	I	Btu/ft^2·d	1099	1432	1864	2363	2671	2730	2341	2183	1979	1602	1208	996	1872
Fort Smith, AR	T_{AX}	°F	48.4	53.8	62.5	73.7	81.0	88.5	93.6	92.9	85.7	75.9	61.9	52.1	72.5
	T_{AN}	°F	26.6	30.9	38.5	49.1	58.2	66.3	70.5	68.9	62.1	49.0	37.7	30.2	49.0
	I	Btu/ft^2·d	744	999	1312	1616	1912	2089	2065	1877	1502	1201	851	682	1404
Little Rock, AR	T_{AX}	°F	49.8	54.5	63.2	73.8	81.7	89.5	92.7	92.3	85.6	75.8	62.4	53.2	72.9
	T_{AN}	°F	29.9	33.6	41.2	50.9	59.2	67.5	71.4	69.6	63.0	50.4	40.0	33.2	50.8
	I	Btu/ft^2·d	731	1003	1313	1611	1929	2107	2032	1861	1518	1228	847	674	1404
Bakersfield, CA	T_{AX}	°F	57.4	63.7	68.6	75.1	83.9	92.2	98.8	96.4	90.8	81.0	67.4	57.6	77.7
	T_{AN}	°F	38.9	42.6	45.5	50.1	57.2	64.3	70.1	68.5	63.8	54.9	44.9	38.7	53.3
	I	Btu/ft^2·d	766	1102	1595	2095	2509	2749	2684	2421	1992	1458	942	677	1749
Long Beach, CA	T_{AX}	°F	66.0	67.3	68.0	70.9	73.4	77.4	83.0	83.8	82.5	78.4	72.7	67.4	74.2
	T_{AN}	°F	44.3	45.9	47.7	50.8	55.2	58.9	62.6	64.0	61.6	56.6	49.6	44.7	53.5
	I	Btu/ft^2·d	928	1215	1610	1938	2065	2140	2300	2100	1701	1326	1004	847	1598
Los Angeles AP, CA	T_{AX}	°F	64.6	65.5	65.1	66.7	69.1	72.0	75.3	76.5	76.4	74.0	70.3	66.1	70.1
	T_{AN}	°F	47.3	48.6	49.7	52.2	55.7	59.1	62.6	64.0	62.5	58.5	52.1	47.8	55.0
	I	Btu/ft^2·d	926	1214	1619	1951	2060	2119	2308	2080	1681	1317	1004	849	1594
Sacramento, CA	T_{AX}	°F	52.6	59.4	64.1	71.0	79.7	87.4	93.3	91.7	87.6	77.7	63.2	53.2	73.4
	T_{AN}	°F	37.9	41.2	42.4	45.3	50.1	55.1	57.9	57.6	55.8	50.0	42.8	37.9	47.8
	I	Btu/ft^2·d	597	939	1458	2004	2435	2684	2688	2368	1907	1315	782	538	1643
San Francisco AP, CA	T_{AX}	°F	55.5	59.0	60.6	63.0	66.3	69.6	71.0	71.8	73.4	70.0	62.7	56.3	64.9
	T_{AN}	°F	41.5	44.1	44.9	46.6	49.3	52.0	53.3	54.2	54.3	51.2	46.3	42.2	48.3
	I	Btu/ft^2·d	708	1009	1455	1920	2226	2377	2392	2117	1742	1226	821	642	1608

3-53

Table 3-7 (cont.).

Location	Property		Monthly Averages												Annual Average
	Symbol	Units	Jan.	Feb.	Mar.	Apr.	May	June	July	Aug.	Sept.	Oct.	Nov.	Dec.	
Santa Maria, CA	T_{AX}	°F	62.8	64.2	63.9	65.6	67.3	69.9	72.1	72.8	74.2	73.3	68.9	64.6	68.3
	T_{AN}	°F	38.8	40.3	40.9	42.7	46.2	49.6	52.4	53.2	51.8	47.6	42.1	38.3	45.3
	I	Btu/ft^2·d	854	1141	1582	1921	2141	2349	2341	2106	1730	1353	974	804	1608
Denver, CO	T_{AX}	°F	43.1	46.9	51.2	61.0	70.7	81.6	88.0	85.8	77.5	66.8	52.4	46.1	64.3
	T_{AN}	°F	15.9	20.2	24.7	33.7	43.6	52.4	58.7	57.0	47.7	36.9	25.1	18.9	36.2
	I	Btu/ft^2·d	840	1127	1530	1879	2135	2351	2273	2044	1727	1301	884	732	1568
Grand Junction, CO	T_{AX}	°F	35.7	44.5	54.1	65.2	76.2	87.9	94.0	90.3	81.9	68.7	51.0	38.7	65.7
	T_{AN}	°F	15.2	22.4	29.7	38.2	48.0	56.6	63.8	61.5	52.2	41.1	28.2	17.9	39.6
	I	Btu/ft^2·d	791	1119	1554	1986	2380	2599	2465	2182	1834	1345	918	731	1659
Wilmington, DE	T_{AX}	°F	39.2	41.8	50.9	63.0	72.7	81.2	85.6	84.1	77.8	66.7	54.8	43.6	63.5
	T_{AN}	°F	23.2	24.6	32.6	41.8	51.7	61.2	66.3	65.4	58.0	45.9	36.4	27.3	44.5
	I	Btu/ft^2·d	571	827	1149	1480	1710	1883	1823	1615	1318	984	645	489	1208
Atlanta, GA	T_{AX}	°F	51.2	55.3	63.2	73.2	79.8	85.6	87.9	87.6	82.3	72.9	62.6	54.1	71.3
	T_{AN}	°F	32.6	34.5	41.7	50.4	58.7	65.9	69.2	68.7	63.6	51.4	41.3	34.8	51.1
	I	Btu/ft^2·d	718	969	1304	1686	1854	1914	1812	1709	1422	1200	883	674	1345
Savannah, GA	T_{AX}	°F	60.3	63.1	69.9	77.8	84.2	88.6	90.8	90.1	85.6	77.8	69.5	62.5	76.7
	T_{AN}	°F	37.9	40.0	46.8	54.1	62.3	68.5	71.5	71.4	67.6	55.9	45.5	39.4	55.1
	I	Btu/ft^2·d	795	1044	1399	1761	1852	1844	1784	1621	1364	1217	941	754	1365
Honolulu, HI	T_{AX}	°F	79.9	80.4	81.4	82.7	84.8	86.2	87.1	88.3	88.2	86.7	83.9	81.4	84.2
	T_{AN}	°F	65.3	65.3	67.3	68.7	70.2	71.9	73.1	73.6	72.9	72.2	69.2	66.5	69.7
	I	Btu/ft^2·d	1180	1396	1622	1796	1949	2004	2002	1967	1810	1540	1266	1133	1639
Chicago, IL	T_{AX}	°F	29.2	33.9	44.3	58.8	70.0 48.1	79.4	83.3	82.1	75.5	64.1	48.2	35.0	58.7
	T_{AN}	°F	13.6	18.1	27.6	38.8	1789	57.7	62.7	61.7	53.9	42.9	31.4	20.3	39.7
	I	Btu/ft^2·d	507	760	1107	1459		2007	1944	1719	1354	969	566	402	1215
Springfield, IL	T_{AX}	°F	32.8	38.0	48.9	64.0	74.6	84.1	87.1	84.7	79.3	67.5	51.2	38.4	62.6
	T_{AN}	°F	16.3	20.9	30.3	42.6	52.5	62.0	65.9	63.7	55.8	44.4	32.9	23.0	42.5
	I	Btu/ft^2·d	585	861	1143	1515	1866	2097	2058	1806	1454	1068	677	490	1302
Indianapolis, IN	T_{AX}	°F	34.2	38.5	49.3	63.1	73.4	82.3	85.2	83.7	77.9	66.1	50.8	39.2	62.0
	T_{AN}	°F	17.8	21.1	30.7	41.7	51.5	60.9	64.9	62.7	55.3	43.4	32.8	23.7	42.2
	I	Btu/ft^2·d	496	747	1037	1398	1638	1868	1806	1644	1324	977	579	417	1165
Wichita, KS	T_{AX}	°F	39.8	46.1	55.8	68.1	77.1	87.4	92.9	91.5	82.0	71.2	55.1	44.6	67.6
	T_{AN}	°F	19.4	24.1	32.4	44.5	54.6	64.7	69.8	67.9	59.2	46.9	33.5	24.2	45.1
	I	Btu/ft^2·d	784	1058	1406	1783	2036	2264	2239	2032	1616	1250	871	690	1502

3-54

Table 3-7 (cont.).

Location	Property		Monthly Averages												Annual Average
	Symbol	Units	Jan.	Feb.	Mar.	Apr.	May	June	July	Aug.	Sept.	Oct.	Nov.	Dec.	
Louisville, KY	T_{AX}	°F	40.8	45.0	54.9	67.5	76.2	84.0	87.6	86.7	80.6	69.2	55.5	45.4	66.1
	T_{AN}	°F	24.1	26.8	35.2	45.6	54.6	63.3	67.5	66.1	59.1	46.2	36.6	28.9	46.2
	I	Btu/ft^2·d	546	789	1102	1467	1720	1904	1838	1680	1361	1042	653	488	1216
Baton Rouge, LA	T_{AX}	°F	61.1	64.5	71.6	79.2	85.2	90.6	91.4	90.8	87.4	80.1	70.1	63.8	78.0
	T_{AN}	°F	40.5	42.7	49.4	57.5	64.3	70.0	72.8	72.0	68.3	56.3	47.2	42.3	57.0
	I	Btu/ft^2·d	785	1054	1379	1681	1871	1926	1746	1677	1464	1301	920	737	1379
Lake Charles, LA	T_{AX}	°F	60.8	64.0	70.5	77.8	84.1	89.4	91.0	90.8	87.5	80.8	70.5	64.0	77.6
	T_{AN}	°F	42.2	44.5	50.8	58.9	65.6	71.4	73.5	72.8	68.9	57.7	48.9	43.8	58.3
	I	Btu/ft^2·d	728	1010	1313	1570	1849	1970	1788	1657	1485	1381	917	706	1365
New Orleans, LA	T_{AX}	°F	61.8	64.6	71.2	78.6	84.5	89.5	90.7	90.2	86.8	79.4	70.1	64.4	77.7
	T_{AN}	°F	43.0	44.8	51.6	58.8	65.3	70.9	73.5	73.1	70.1	59.0	49.9	44.8	58.7
	I	Btu/ft^2·d	835	1112	1415	1780	1968	2004	1814	1717	1514	1335	973	779	1437
Detroit, MI	T_{AX}	°F	30.6	33.5	43.4	57.7	69.4	79.0	83.1	81.5	74.4	62.5	47.6	35.4	58.2
	T_{AN}	°F	16.1	18.0	26.5	36.9	46.7	56.3	60.7	59.4	52.2	41.2	31.4	21.6	38.9
	I	Btu/ft^2·d	417	680	1000	1399	1716	1866	1835	1576	1253	876	478	344	1120
Grand Rapids, MI	T_{AX}	°F	29.0	31.7	41.6	56.9	69.4	78.9	83.0	81.1	73.4	61.4	46.0	33.8	57.2
	T_{AN}	°F	14.9	15.6	24.5	35.6	45.5	55.3	59.8	58.1	50.8	40.4	30.9	20.7	37.7
	I	Btu/ft^2·d	370	648	1014	1412	1755	1957	1914	1676	1262	858	446	311	1135
Minneapolis-St. Paul, MN	T_{AX}	°F	19.9	26.4	37.5	56.0	69.4	78.5	83.4	80.9	71.0	59.7	41.1	26.7	54.2
	T_{AN}	°F	2.4	8.5	20.8	36.0	47.6	57.7	62.7	60.3	50.2	39.4	25.3	11.7	35.2
	I	Btu/ft^2·d	464	764	1104	1442	1737	1928	1970	1687	1255	860	480	353	1170
Jackson, MS	T_{AX}	°F	56.5	60.9	68.4	77.3	84.1	90.5	92.5	92.1	87.6	78.6	67.5	60.0	76.3
	T_{AN}	°F	34.9	37.2	44.2	52.9	60.8	67.9	71.3	70.2	65.1	51.4	42.3	37.1	52.9
	I	Btu/ft^2·d	754	1026	1369	1708	1941	2024	1909	1781	1509	1271	902	709	1409
Billings, MT	T_{AX}	°F	29.9	37.9	44.0	55.9	66.4	76.3	86.6	84.3	72.3	61.0	44.4	36.0	57.9
	T_{AN}	°F	11.8	18.8	23.6	33.2	43.3	51.6	58.0	56.2	46.5	37.5	25.5	18.2	35.4
	I	Btu/ft^2·d	486	763	1190	1526	1913	2174	2384	2022	1470	987	561	421	1325
Las Vegas, NV	T_{AX}	°F	56.0	62.4	68.3	77.2	87.4	98.6	104.5	101.9	94.7	81.5	66.0	57.1	79.6
	T_{AN}	°F	33.0	37.7	42.3	49.8	59.0	68.6	75.9	73.9	65.6	53.5	41.2	33.6	52.8
	I	Btu/ft^2·d	978	1340	1824	2319	2646	2778	2588	2355	2037	1540	1086	881	1864
Newark, NJ	T_{AX}	°F	38.2	40.3	49.1	61.3	71.6	80.6	85.6	84.0	76.9	66.0	54.0	42.3	62.5
	T_{AN}	°F	24.2	25.3	33.3	42.9	53.0	62.4	67.9	67.0	59.4	48.3	39.0	28.6	45.9
	I	Btu/ft^2·d	552	793	1109	1449	1687	1795	1760	1565	1273	951	596	454	1165

3-55

Table 3-7 (cont.).

Location	Property		Monthly Averages												Annual Average
	Symbol	Units	Jan.	Feb.	Mar.	Apr.	May	June	July	Aug.	Sept.	Oct.	Nov.	Dec.	
Roswell, NM	T_{AX}	°F	55.4	60.4	67.7	76.9	85.0	93.1	93.7	91.3	84.9	75.8	63.1	56.7	75.3
	T_{AN}	°F	27.4	31.4	37.9	46.8	55.6	64.8	69.0	67.0	59.6	47.5	35.0	28.2	47.5
	I	Btu/ft^2·d	1047	1373	1807	2218	2459	2610	2441	2242	1913	1527	1131	952	1810
Buffalo, NY	T_{AX}	°F	30.0	31.4	40.4	54.4	65.9	75.6	80.2	78.2	71.4	60.2	47.0	35.0	55.8
	T_{AN}	°F	17.0	17.5	25.6	36.3	46.3	56.4	61.2	59.6	52.7	42.7	33.6	22.5	39.3
	I	Btu/ft^2·d	349	546	889	1315	1597	1804	1776	1513	1152	784	403	283	1034
New York, NY (LaGuardia Airport)	T_{AX}	°F	37.4	39.2	47.3	59.6	69.7	78.7	83.9	82.3	75.2	64.5	52.9	41.5	61.0
	T_{AN}	°F	26.1	27.3	34.6	44.2	53.7	63.2	68.9	68.2	61.2	50.5	41.2	30.8	47.5
	I	Btu/ft^2·d	548	795	1118	1457	1690	1802	1784	1583	1280	951	593	457	1171
Cleveland, OH	T_{AX}	°F	32.5	34.8	44.8	57.9	68.5	78.0	81.7	80.3	74.2	62.7	49.3	37.5	58.5
	T_{AN}	°F	18.5	19.9	28.4	38.3	47.9	57.2	61.4	60.5	54.0	43.6	34.3	24.6	40.7
	I	Btu/ft^2·d	388	601	922	1350	1681	1843	1828	1583	1240	867	466	318	1091
Columbus, OH	T_{AX}	°F	34.7	38.1	49.3	62.3	72.6	81.3	84.4	83.0	76.9	65.0	50.7	39.4	61.5
	T_{AN}	°F	19.4	21.5	30.6	40.5	50.2	59.0	63.2	61.7	54.6	42.8	33.5	24.7	41.8
	I	Btu/ft^2·d	459	677	980	1353	1647	1813	1755	1641	1282	945	538	387	1123
Toledo, OH	T_{AX}	°F	30.7	34.0	44.6	59.1	70.5	79.9	83.4	81.8	75.1	63.3	47.9	35.5	58.8
	T_{AN}	°F	15.5	17.5	26.1	36.5	46.6	56.0	60.2	58.4	51.2	40.1	30.6	20.6	38.3
	I	Btu/ft^2·d	435	680	997	1384	1717	1878	1849	1616	1276	911	498	355	1133
Oklahoma City, OK	T_{AX}	°F	46.6	52.2	61.0	71.7	79.0	87.6	93.5	92.8	84.7	74.3	59.9	50.7	71.2
	T_{AN}	°F	25.2	29.4	37.1	48.6	57.7	66.3	70.6	69.4	61.9	50.2	37.6	29.1	48.6
	I	Btu/ft^2·d	801	1055	1400	1725	1918	2144	2128	1950	1554	1233	901	725	1461
Tulsa, OK	T_{AX}	°F	45.6	51.9	60.8	72.4	79.7	87.9	93.9	93.0	85.0	74.9	60.2	50.3	71.3
	T_{AN}	°F	24.8	29.5	37.7	49.5	58.5	67.5	72.4	70.3	62.5	50.3	38.1	29.3	49.2
	I	Btu/ft^2·d	732	978	1306	1603	1822	2021	2031	1865	1473	1164	827	659	1373
Astoria, OR	T_{AX}	°F	46.8	50.6	51.9	55.5	60.2	63.9	67.9	68.6	67.8	61.4	53.5	48.8	58.1
	T_{AN}	°F	35.4	37.1	36.9	39.7	44.1	49.2	52.2	52.6	49.2	44.3	39.7	37.3	43.1
	I	Btu/ft^2·d	315	545	866	1253	1608	1626	1746	1499	1183	713	387	261	1000
Portland, OR	T_{AX}	°F	44.3	50.4	54.5	60.2	66.9	72.7	79.5	78.6	74.2	63.9	52.3	46.4	62.0
	T_{AN}	°F	33.5	36.0	37.4	40.6	46.4	52.2	55.8	55.8	51.1	44.6	38.6	35.4	44.0
	I	Btu/ft^2·d	310	554	895	1308	1663	1773	2037	1674	1217	724	388	260	1067
Philadelphia, PA	T_{AX}	°F	38.6	41.1	50.5	63.2	73.0	81.7	86.1	84.6	77.8	66.5	54.5	43.0	63.4
	T_{AN}	°F	23.8	25.0	33.1	42.6	52.5	61.5	66.8	66.0	58.6	46.5	37.1	28.0	45.1
	I	Btu/ft^2·d	555	795	1108	1434	1660	1811	1758	1575	1281	959	619	470	1169

3-56

Table 3-7 (cont.).

Location	Property		Monthly Averages												Annual Average
	Symbol	Units	Jan.	Feb.	Mar.	Apr.	May	June	July	Aug.	Sept.	Oct.	Nov.	Dec.	
Pittsburgh, PA	T_{AX}	°F	34.1	36.8	47.6	60.7	70.8	79.1	82.7	81.1	74.8	62.9	49.8	38.4	59.9
	T_{AN}	°F	19.2	20.7	29.4	39.4	48.5	57.1	61.3	60.1	53.3	42.1	33.3	24.3	40.7
	I	Btu/ft^2·d	424	625	943	1317	1602	1762	1689	1510	1209	895	505	347	1069
Providence, RI	T_{AX}	°F	36.4	37.7	45.5	57.5	67.6	76.6	81.7	80.3	73.1	63.2	51.9	40.5	59.3
	T_{AN}	°F	20.0	20.9	29.2	38.3	47.6	57.0	63.3	61.9	53.8	43.1	34.8	24.1	41.2
	I	Btu/ft^2·d	506	739	1032	1374	1655	1776	1695	1499	1209	907	538	419	1112
Columbia, SC	T_{AX}	°F	56.2	59.5	67.1	77.0	83.8	89.2	91.9	91.0	85.5	76.5	67.1	58.8	75.3
	T_{AN}	°F	33.2	34.6	41.9	50.5	59.1	66.1	70.1	69.4	63.9	50.3	40.6	34.7	51.2
	I	Btu/ft^2·d	762	1021	1355	1747	1895	1947	1842	1703	1439	1211	921	722	1380
Sioux Falls, SD	T_{AX}	°F	22.9	29.3	40.1	58.1	70.5	80.3	86.2	83.9	73.5	62.1	43.7	29.3	56.7
	T_{AN}	°F	1.9	8.9	20.6	34.6	45.7	56.3	61.8	59.7	48.5	36.7	22.3	10.1	33.9
	I	Btu/ft^2·d	533	802	1152	1543	1894	2100	2150	1845	1410	1005	608	441	1290
Memphis, TN	T_{AX}	°F	48.3	53.0	61.4	72.9	81.0	88.4	91.5	90.3	84.3	74.5	61.4	52.3	71.6
	T_{AN}	°F	30.9	34.1	41.9	52.2	60.9	68.9	72.6	70.8	64.1	51.3	41.1	34.3	51.9
	I	Btu/ft^2·d	683	945	1278	1639	1885	2045	1972	1824	1471	1205	817	629	1366
Amarillo, TX	T_{AX}	°F	49.1	53.1	60.8	71.0	79.1	88.2	91.4	89.6	82.4	72.7	58.7	51.8	70.7
	T_{AN}	°F	21.7	26.1	32.0	42.0	51.9	61.5	66.2	64.5	56.9	45.5	32.1	24.8	43.8
	I	Btu/ft^2·d	960	1244	1631	2019	2212	2393	2281	2103	1761	1404	1033	872	1659
Corpus Christi, TX	T_{AX}	°F	66.5	69.9	76.1	82.1	86.7	91.2	94.2	94.1	90.1	83.9	75.1	69.3	81.6
	T_{AN}	°F	46.1	48.7	55.7	63.9	69.5	74.1	75.6	75.8	72.8	64.1	54.9	48.8	62.5
	I	Btu/ft^2·d	898	1147	1430	1642	1866	2094	2186	1991	1687	1416	1043	845	1521
Dallas, TX	T_{AX}	°F	54.0	59.1	67.2	76.8	84.4	93.2	97.8	97.3	89.7	79.5	66.2	58.1	76.9
	T_{AN}	°F	33.9	37.8	44.9	55.0	62.9	70.8	74.7	73.7	67.5	56.3	44.9	37.4	55.0
	I	Btu/ft^2·d	822	1071	1422	1627	1889	2135	2122	1950	1587	1276	936	780	1468
Houston, TX	T_{AX}	°F	61.9	65.7	72.1	79.0	85.1	90.9 70.2	93.6	93.1	88.7	81.9	71.6	65.2	79.1
	T_{AN}	°F	40.8	43.2	49.8	58.3	64.7	1898	72.5	72.1	68.1	57.5	48.6	42.7	57.4
	I	Btu/ft^2·d	772	1034	1297	1522	1775		1828	1686	1471	1276	924	730	1351
Midland-Odessa, TX	T_{AX}	°F	57.6	62.1	69.8	78.8	86.0	93.0	94.2	93.1	86.4	77.7	65.5	59.7	77.0
	T_{AN}	°F	29.7	33.3	40.2	49.4	58.2	66.6	69.2	68.0	61.9	51.1	39.0	32.2	49.9
	I	Btu/ft^2·d	1081	1383	1839	2192	2430	2562	2389	2210	1844	1522	1176	1000	1802
Salt Lake City, UT	T_{AX}	°F	37.4	43.7	51.5	61.1	72.4	83.3	93.2	90.0	80.0	66.7	50.2	38.9	64.0
	T_{AN}	°F	19.7	24.4	29.9	37.2	45.2	53.3	61.8	59.7	50.0	39.3	29.2	21.6	39.3
	I	Btu/ft^2·d	639	989	1454	1894	2362	2561	2590	2254	1843	1293	788	570	1603

3-57

Table 3-7 (cont.).

Location	Property		Monthly Averages												Annual Average
	Symbol	Units	Jan.	Feb.	Mar.	Apr.	May	June	July	Aug.	Sept.	Oct.	Nov.	Dec.	
Richmond, VA	T_{AX}	°F	46.7	49.6	58.5	70.6	77.9	84.8	88.4	87.1	81.0	70.5	60.5	50.2	68.8
	T_{AN}	°F	26.5	28.1	35.8	45.1	54.2	62.2	67.2	66.4	59.3	46.7	37.3	29.6	46.5
	I	Btu/ft^2 day	632	877	1210	1566	1762	1872	1774	1601	1348	1033	733	567	1248
Seattle, WA (Sea-Tac Airport)	T_{AX}	°F	43.9	48.8	51.1	56.8	64.0	69.2	75.2	73.9	68.7	59.5	50.3	45.6	58.9
	T_{AN}	°F	34.3	36.8	37.2	40.5	46.0	51.1	54.3	54.3	51.2	45.3	39.3	36.3	43.9
	I	Btu/ft^2 day	262	495	849	1294	1714	1802	2248	1616	1148	656	337	211	1053
Charleston, WV	T_{AX}	°F	41.8	45.4	55.4	67.3	76.0	82.5	85.2	84.2	78.7	67.7	55.6	45.9	65.5
	T_{AN}	°F	23.9	25.8	34.1	43.3	51.8	59.4	63.8	63.1	56.4	44.0	35.0	27.8	44.0
	I	Btu/ft^2 day	498	707	1010	1356	1639	1776	1683	1514	1272	972	613	440	1123
Huntington, WV	T_{AX}	°F	41.1	45.0	55.2	67.2	75.7	82.6	85.6	84.4	78.7	67.6	55.2	45.2	65.3
	T_{AN}	°F	24.5	26.6	35.0	44.4	52.8	60.7	65.1	64.0	57.2	44.9	35.9	28.5	45.0
	I	Btu/ft^2 day	526	757	1067	1448	1710	1844	1769	1580	1306	1004	638	467	1176
Cheyenne, WY	T_{AX}	°F	37.3	40.7	43.6	54.0	64.6	75.4	83.1	80.8	72.1	61.0	46.5	40.4	58.3
	T_{AN}	°F	14.8	17.9	20.6	29.6	39.7	48.5	54.6	52.8	43.7	34.0	23.1	18.2	33.1
	I	Btu/ft^2 day	766	1068	1433	1771	1995	2258	2230	1966	1667	1242	823	671	1491

[a] References 13 and 14

T_{AX} = daily maximum ambient temperature

T_{AN} = daily minimum ambient temperature

I = daily total solar insolation factor

3-58

TABLE 3-8. RIM-SEAL LOSS FACTORS, K_{Ra}, K_{Rb} and n,
FOR FLOATING ROOF TANKS[a]

Tank Construction And Rim-Seal System	Average-Fitting Seals		
	K_{Ra} (lb-mole/ft-yr)	K_{Rb} [lb-mole/(mph)^n-ft-yr]	n (dimensionless)
Welded Tanks			
Mechanical-shoe seal			
Primary only[b]	5.8	0.3	2.1
Shoe-mounted secondary	1.6	0.3	1.6
Rim-mounted secondary	0.6	0.4	1.0
Liquid-mounted seal			
Primary only	1.6	0.3	1.5
Weather shield	0.7	0.3	1.2
Rim-mounted secondary	0.3	0.6	0.3
Vapor-mounted seal			
Primary only	6.7[c]	0.2	3.0
Weather shield	3.3	0.1	3.0
Rim-mounted secondary	2.2	0.003	4.3
Riveted Tanks			
Mechanical-shoe seal			
Primary only	10.8	0.4	2.0
Shoe-mounted secondary	9.2	0.2	1.9
Rim-mounted secondary	1.1	0.3	1.5

[a]Reference 11.

[b]If no specific information is available, a welded tank with an average-fitting mechanical-shoe primary seal can be used to represent the most common or typical construction and rim-seal system in use for external and domed external floating roof tanks.

[c]If no specific information is available, this value can be assumed to represent the most common or typical rim-seal system currently in use for internal floating roof tanks.

TABLE 3-9. AVERAGE ANNUAL WIND SPEED (v) FOR SELECTED U. S. LOCATIONS[a]

Location	Wind Speed (mph)	Location	Wind Speed (mph)	Location	Wind Speed (mph)
Alabama		Arizona (continued)		Delaware	
Birmingham	7.2	Winslow	8.9	Wilmington	9.1
Huntsville	8.2	Yuma	7.8	District of Columbia	
Mobile	9.0			Dulles Airport	7.4
Montgomery	6.6	Arkansas		National Airport	9.4
		Fort Smith	7.6		
Alaska		Little Rock	7.8	Florida	
Anchorage	6.9			Apalachicola	7.8
Annette	10.6	California		Daytona Beach	8.7
Barrow	11.8	Bakersfield	6.4	Fort Meyers	8.1
Barter Island	13.2	Blue Canyon	6.8	Jacksonville	8.0
Bethel	12.8	Eureka	6.8	Key West	11.2
Bettles	6.7	Fresno	6.3	Miami	9.3
Big Delta	8.2	Long Beach	6.4	Orlando	8.5
Cold Bay	17.0	Los Angeles (City)	6.2	Pensacola	8.4
Fairbanks	5.4	Los Angeles Int'l Airport	7.5	Tallahassee	6.3
Gulkana	6.8	Mount Shasta	5.1	Tampa	8.4
Homer	7.6	Sacramento	7.9	West Palm Beach	9.6
Juneau	8.3	San Diego	6.9		
King Salmon	10.8	San Francisco (City)	8.7	Georgia	
Kodiak	10.8	San Francisco Airport	10.6	Athens	7.4
Kotzebue	13.0	Santa Maria	7.0	Atlanta	9.1
McGrath	5.1	Stockton	7.5	Augusta	6.5
Nome	10.7			Columbus	6.7
St. Paul Island	17.7	Colorado		Macon	7.6
Talkeetna	4.8	Colorado Springs	10.1	Savannah	7.9
Valdez	6.0	Denver	8.7		
Yakutat	7.4	Grand Junction	8.1	Hawaii	
		Pueblo	8.7	Hilo	7.2
Arizona				Honolulu	11.4
Flagstaff	6.8	Connecticut		Kahului	12.8
Phoenix	6.3	Bridgeport	12.0	Lihue	12.2
Tucson	8.3	Hartford	8.5		

Table 3-9. (cont.)

Location	Wind Speed (mph)	Location	Wind Speed (mph)	Location	Wind Speed (mph)
Idaho		Louisiana		Mississippi	
Boise	8.8	Baton Rouge	7.6	Jackson	7.4
Pocatello	10.2	Lake Charles	8.7	Meridian	6.1
		New Orleans	8.2		
Illinois		Shreveport	8.4	Missouri	
Cairo	8.5			Columbia	9.9
Chicago	10.3	Maine		Kansas City	10.8
Moline	10.0	Caribou	11.2	Saint Louis	9.7
Peoria	10.0	Portland	8.8	Springfield	10.7
Rockford	10.0				
Springfield	11.2	Maryland		Montana	
		Baltimore	9.2	Billings	11.2
Indiana				Glasgow	10.8
Evansville	8.1	Massachusetts		Great Falls	12.8
Fort Wayne	10.0	Blue Hill Observatory	15.4	Helena	7.8
Indianapolis	9.6	Boston	12.5	Kalispell	6.6
South Bend	10.3	Worcester	10.1	Missoula	6.2
Iowa		Michigan		Nebraska	
Des Moines	10.9	Alpena	8.1	Grand Island	11.9
Sioux City	11.0	Detroit	10.4	Lincoln	10.4
Waterloo	10.7	Flint	10.2	Norfolk	11.7
		Grand Rapids	9.8	North Platte	10.2
Kansas		Houghton Lake	8.9	Omaha	10.6
Concordia	12.3	Lansing	10.0	Scottsbuff	10.6
Dodge City	14.0	Muskegon	10.7	Valentine	9.7
Goodland	12.6	Sault Sainte Marie	9.3		
Topeka	10.0			Nevada	
Wichita	12.3	Minnesota		Elko	6.0
		Duluth	11.1	Ely	10.3
Kentucky		International Falls	8.9	Las Vegas	9.3
Cincinnati Airport	9.1	Minneapolis-Saint Paul	10.6	Reno	6.6
Jackson	7.2	Rochester	13.1	Winnemucca	8.0
Lexington	9.3	Saint Cloud	8.0		
Louisville	8.4				

Table 3-9. (cont.)

Location	Wind Speed (mph)	Location	Wind Speed (mph)	Location	Wind Speed (mph)
New Hampshire		Ohio		Rhode Island	
Concord	6.7	Akron	9.8	Providence	10.6
Mount Washington	35.3	Cleveland	10.6		
		Columbus	8.5	South Carolina	
New Jersey		Dayton	9.9	Charleston	8.6
Atlantic City	10.1	Mansfield	11.0	Columbia	6.9
Newark	10.2	Toledo	9.4	Greenville-Spartanburg	6.9
		Youngstown	9.9		
New Mexico				South Dakota	
Albuquerque	9.1	Oklahoma		Aberdeen	11.2
Roswell	8.6	Oklahoma City	12.4	Huron	11.5
		Tulsa	10.3	Rapid City	11.3
New York				Sioux Falls	11.1
Albany	8.9	Oregon			
Birmingham	10.3	Astoria	8.6	Tennessee	
Buffalo	12.0	Eugene	7.6	Bristol-Johnson City	5.5
New York (Central Park)	9.4	Medford	4.8	Chattanooga	6.1
New York (JFK Airport)	12.0	Pendleton	8.7	Knoxville	7.0
New York (La Guardia Airport)	12.2	Portland	7.9	Memphis	8.9
Rochester	9.7	Salem	7.1	Nashville	8.0
Syracuse	9.5	Sexton Summit	11.8	Oak Ridge	4.4
North Carolina		Pennsylvania		Texas	
Asheville	7.6	Allentown	9.2	Abilene	12.0
Cape Hatteras	11.1	Avoca	8.3	Amarillo	13.6
Charlotte	7.5	Erie	11.3	Austin	9.2
Greensboro-High Point	7.5	Harrisburg	7.6	Brownsville	11.5
Raleigh	7.8	Philadelphia	9.5	Corpus Christi	12.0
Wilmington	8.8	Pittsburgh Int'l Airport	9.1	Dallas-Fort Worth	10.8
		Williamsport	7.8	Del Rio	9.9
North Dakota				El Paso	8.9
Bismark	10.2	Puerto Rico		Galveston	11.0
Fargo	12.3	San Juan	8.4	Houston	7.9
Williston	10.1			Lubbock	12.4

Table 3-9. (cont.)

Location	Wind Speed (mph)	Location	Wind Speed (mph)
Texas (continued)		Wisconsin	
Midland-Odessa	11.1	Green Bay	10.0
Port Arthur	9.8	La Crosse	8.8
San Angelo	10.4	Madison	9.9
San Antonio	9.3	Milwaukee	11.6
Victoria	10.1		
Waco	11.3	Wyoming	
Wichita Falls	11.7	Casper	12.9
		Cheyenne	13.0
Utah		Lander	6.8
Salt Lake City	8.9	Sheridan	8.0
Vermont			
Burlington	8.9		
Virginia			
Lynchburg	7.7		
Norfolk	10.7		
Richmond	7.7		
Roanoke	8.1		
Washington			
Olympia	6.7		
Quillayute	6.1		
Seattle Int'l. Airport	9.0		
Spokane	8.9		
Walla Walla	5.3		
Yakima	7.1		
West Virginia			
Belkley	9.1		
Charleston	6.3		
Elkins	6.2		
Huntington	6.6		

[a] Reference 13.

TABLE 3-10. AVERAGE CLINGAGE FACTORS, *C*
(Barrels per 1,000 square feet)[a]

Product stored	Shell condition		
	Light rust	Dense rust	Gunite lining
Gasoline	0.0015	0.0075	0.15
Single-component stocks	0.0015	0.0075	0.15
Crude oil	0.0060	0.030	0.60

[a]Reference 10.

Note: If no specific information is available, the values in this table can be assumed to represent the most common or typical condition of tanks currently in use.

TABLE 3-11. TYPICAL NUMBER OF COLUMNS AS A FUNCTION OF TANK DIAMETER FOR INTERNAL FLOATING ROOF TANKS WITH COLUMN-SUPPORTED FIXED ROOFS[a]

Tank diameter range D, (ft)	Typical number of columns, N_C
$0 < D \leq 85$	1
$85 < D \leq 100$	6
$100 < D \leq 120$	7
$120 < D \leq 135$	8
$135 < D \leq 150$	9
$150 < D \leq 170$	16
$170 < D \leq 190$	19
$190 < D \leq 220$	22
$220 < D \leq 235$	31
$235 < D \leq 270$	37
$270 < D \leq 275$	43
$275 < D \leq 290$	49
$290 < D \leq 330$	61
$330 < D \leq 360$	71
$360 < D \leq 400$	81

[a]Reference 5. This table was derived from a survey of users and manufacturers. The actual number of columns in a particular tank may vary greatly with age, fixed roof style, loading specifications, and manufacturing prerogatives. Data in this table should not supersede information on actual tanks.

Table 3.1-12. DECK-FITTING LOSS FACTORS, K_{Fa}, K_{Fb}, AND m, AND TYPICAL NUMBER OF DECK FITTINGS, N_F[a]

Fitting Type And Construction Details	Loss Factors			Typical Number Of Fittings, N_F
	K_{Fa} (lb-mole/yr)	K_{Fb} (lb-mole/(mph)^m-yr)	m (dimensionless)	
Access hatch (24-inch diameter well)				1
Bolted cover, gasketed[b]	1.6	0	0	
Unbolted cover, ungasketed	36[c]	5.9	1.2	
Unbolted cover, gasketed	31	5.2	1.3	
Fixed roof support column well[d]				N_C
Round pipe, ungasketed sliding cover	31			(Table 7.1-11)
Round pipe, gasketed sliding cover	25			
Round pipe, flexible fabric sleeve seal	10			
Built-up column, ungasketed sliding cover[c]	51			
Built-up column, gasketed sliding cover	33			
Unslotted guide-pole and well (8-inch diameter unslotted pole, 21-inch diameter well)				1
Ungasketed sliding cover[b]	31	150	1.4	
Ungasketed sliding cover w/pole	25	2.2	2.1	
sleeveGasketed sliding cover	25	13	2.2	
Gasketed sliding cover w/pole wiper	14	3.7	0.78	
Gasketed sliding cover w/pole sleeve	8.6	12	0.81	
Slotted guide-pole/sample well (8-inch diameter slotted pole, 21-inch diameter well)[e]				f
Ungasketed or gasketed sliding cover	43	270	1.4	
Ungasketed or gasketed sliding cover, with float[g]	31	36	2.0	
Gasketed sliding cover, with pole wiper	41	48	1.4	
Gasketed sliding cover, with pole sleeve	11	46	1.4	
Gasketed sliding cover, with pole sleeve and pole wiper	8.3	4.4	1.6	
Gasketed sliding cover, with float and pole wiper[g]	21	7.9	1.8	
Gasketed sliding cover, with float, pole sleeve, and pole wiper[h]	11	9.9	0.89	
Gauge-float well (automatic gauge)				1
Unbolted cover, ungasketed[b]	14[c]	5.4	1.1	
Unbolted cover, gasketed	4.3	17	0.38	
Bolted cover, gasketed	2.8	0	0	
Gauge-hatch/sample port				1
Weighted mechanical actuation, gasketed[b]	0.47	0.02	0.97	
Weighted mechanical actuation, ungasketed	2.3	0	0	
Slit fabric seal, 10% open area[c]	12			
Vacuum breaker				N_{yb} (Table 7.1-13)[i]
Weighted mechanical actuation, ungasketed	7.8	0.01	4.0	Deck drain (3-inch diameter)
Weighted mechanical actuation, gasketed[b]	6.2[c]	1.2	0.94	Open[b]
				90% closed
				1.5
				1.8
				0.21
				0.14
				1.7
				$1.1N_d$ (Table 7.1-13)

Fitting Type And Construction Details	Loss Factors			Typical Number Of Fittings, N_F
	K_{Fa} (lb-mole/yr)	K_{Fb} (lb-mole/(mph)^m-yr)	m (dimensionless)	
Stub drain (1-inch diameter)[k]	1.2			N_d (Table 7.1-15)
Deck leg (3-inch diameter)				N_l (Table 7.1-15), (Table 7.1-14)
Adjustable, internal floating deck[c]	7.9			
Adjustable, pontoon area - ungasketed[b]	2.0	0.37	0.91	
Adjustable, pontoon area - gasketed	1.3	0.08	0.65	
Adjustable, pontoon area - sock	1.2	0.14	0.65	
Adjustable, center area - ungasketed[b]	0.82	0.53	0.14	
Adjustable, center area - gasketed[m]	0.53	0.11	0.13	
Adjustable, center area - sock[m]	0.49	0.16	0.14	
Adjustable, double-deck roofs	0.82	0.53	0.14	
Fixed	0	0	0	
Rim vent[n]				1
Weighted mechanical actuation, ungasketed	0.68	1.8	1.0	
Weighted mechanical actuation, gasketed[b]	0.71	0.10	1.0	
Ladder well				1[d]
Sliding cover, ungasketed[c]	98			
Sliding cover, gasketed	56			

Note: The deck-fitting loss factors, K_{Fa}, K_{Fb}, and m, may only be used for wind speeds below 15 miles per hour.

[a] Reference 5, unless otherwise indicated.

[b] If no specific information is available, this value can be assumed to represent the most common or typical deck fitting currently in use for external and domed external floating roof tanks.

[c] If no specific information is available, this value can be assumed to represent the most common or typical deck fitting currently in use for internal floating roof tanks.

[d] Column wells and ladder wells are not typically used with self supported fixed roofs.

[e] References 16,19.

[f] A slotted guide-pole/sample well is an optional fitting and is not typically used.

[g] Tests were conducted with floats positioned with the float wiper at and 1 inch above the sliding cover. The user is cautioned against applying these factors to floats that are positioned with the wiper or top of the float below the sliding cover ("short floats"). The emission factor for such a float is expected to be between the factors for a guidepole without a float and with a float, depending upon the position of the float top and/or wiper within the guidepole.

[h] Tests were conducted with floats positioned with the float wiper at varying heights with respect to the sliding cover. This fitting configuration also includes a pole sleeve which restricts the airflow from the well vapor space into the slotted guidepole. Consequently, the float position within the guidepole (at, above, or below the sliding cover) is not expected to significantly affect emission levels for this fitting configuration, since the function of the pole sleeve is to restrict the flow of vapor from the vapor space below the deck into the guidepole.

[j] N_{vb} = 1 for internal floating roof tanks.

[k] Stub drains are not used on welded contact internal floating decks.

[m] These loss factors were derived using the results from pontoon-area deck legs with gaskets and socks.

[n] Rim vents are used only with mechanical-shoe primary seals.

TABLE 3-13. EXTERNAL FLOATING ROOF TANKS: TYPICAL NUMBER OF VACUUM BREAKERS, N_{vb}, AND DECK DRAINS, N_d[a]

Tank Diameter D (feet)[b]	Number Of Vacuum Breakers, N_{vb}		Number Of Deck drains, N_d
	Pontoon Roof	Double-Deck Roof	
50	1	1	1
100	1	1	1
150	2	2	2
200	3	2	3
250	4	3	5
300	5	3	7
350	6	4	ND
400	7	4	ND

Note: This table was derived from a survey of users and manufacturers. The actual number of vacuum breakers may vary greatly depending on throughput and manufacturing prerogatives. The actual number of deck drains may also vary greatly depending on the design rainfall and manufacturing prerogatives. For tanks more than 300 feet in diameter, actual tank data or the manufacturer's recommendations may be needed for the number of deck drains. This table should not supersede information based on actual tank data.

[a]Reference 10. ND = no data.

[b]If the actual diameter is between the diameters listed, the closest diameter listed should be used. If the actual diameter is midway between the diameters listed, the next larger diameter should be used.

TABLE 3-14. EXTERNAL FLOATING ROOF TANKS: TYPICAL NUMBER OF DECK LEGS, N_L[a]

Tank diameter, *D* (feet)[b]	Pontoon roof		Number of legs on double-deck roof
	Number of pontoon legs	Number of center legs	
30	4	2	6
40	4	4	7
50	6	6	8
60	9	7	10
70	13	9	13
80	15	10	16
90	16	12	20
100	17	16	25
110	18	20	29
120	19	24	34
130	20	28	40
140	21	33	46
150	23	38	52
160	26	42	58
170	27	49	66
180	28	56	74
190	29	62	82
200	30	69	90
210	31	77	98
220	32	83	107
230	33	92	115
240	34	101	127
250	35	109	138
260	36	118	149
270	36	128	162
280	37	138	173
290	38	148	186
300	38	156	200
310	39	168	213
320	39	179	226
330	40	190	240
340	41	202	255
350	42	213	270
360	44	226	285
370	45	238	300
380	46	252	315
390	47	266	330
400	48	281	345

Note: This table was derived from a survey of users and manufacturers. The actual number of roof legs may vary greatly depending on age, style of floating roof, loading specifications, and manufacturing prerogatives. This table should not supersede information based on actual tank data.

[a]Reference 10.

[b]If the actual diameter is between the diameters listed, the closest diameter listed should be used. If the actual diameter is midway between the diameters listed, the next larger diameter should be used.

TABLE 3-15. INTERNAL FLOATING ROOF TANKS: TYPICAL NUMBER OF DECK LEGS, N_l, AND STUB DRAINS, N_d[a]

Deck fitting type	Typical number of fittings, N_F
Deck leg or hanger well[b]	$(5+\frac{D}{10}+\frac{D^2}{600})$
Stub drain (3-inch diameter)[c]	$(\frac{D^2}{125})$

[a]Reference 5.
[b]D = tank diameter, ft
[c]Not used on welded contact internal floating roof decks.

TABLE 3-16. DECK SEAM LENGTH FACTORS (S_D) FOR TYPICAL DECK CONSTRUCTIONS FOR INTERNAL FLOATING ROOF TANKS[a]

Deck construction	Typical deck seam length factor, S_D (ft/ft$_2$)
Continuous sheet construction[b]	
5 ft wide	0.20[c]
6 ft wide	0.17
7 ft wide	0.14
Panel construction[d]	
5 x 7.5 ft rectangular	0.33
5 x 12 ft rectangular	0.28

[a]Reference 5. Deck seam loss applies to bolted internal floating decks only.
[b]S_D = 1/W, where W = sheet width (ft).
[c]If no specific information is available, this value can be assumed to represent the most common bolted decks currently in use.
[d]S_D = (L+W)/LW, where W = panel width (ft) and L = panel length (ft).

Table 3-17. ROOF LANDING LOSSES FOR INTERNAL FLOATING ROOF TANK WITH A LIQUID HEEL

Standing Idle Loss	$L_{SL} = \frac{P V_V}{R T} n_d \ K_E \ M_V \ K_S$ Equation 2-16 $L_{SL} \le 5.9 \ D^2 \ h_{le} \ W_l$ Equation 2-13
Standing Idle Saturation Factor	$K_S = \frac{1}{1 + 0.053 \left(P \ h_v \right)}$ Equation 1-20 $K_S \le S$
Filling Loss Equation	$L_{FL} = \left(\frac{P V_V}{R T} \right) M_V \ S$ Equation 2-26
Filling Saturation Factor (S)	S = 0.60 for a full liquid heel S = 0.50 for a partial liquid heel

Table 3-18. ROOF LANDING LOSSES FOR EXTERNAL FLOATING ROOF TANK WITH A LIQUID HEEL

Standing Idle Loss	$L_{SL} = 0.57\ n_d\ D\ P^*\ M_V$ Equation 2-19 $L_{SL} \le 5.9\ D^2\ h_{le}\ W_l$ Equation 2-13
Standing Idle Saturation Factor	Not applicable
Filling Loss Equation	$L_{FL} = \left(\frac{P\,V_V}{R\,T}\right)\ M_V\ \left(C_{sf}\ S\right)$ Equation 2-27 $C_{sf} = 1 - \left(\frac{\left(0.57\,n_d\,D\,P^*\,M_v\right) - \left(n_d\ K_E\left(\frac{P\,V_V}{RT}\right) M_V\ K_S\right)}{\left(n_d\ K_E\left(\frac{PV_V}{RT}\right) M_V\ K_S\right) + \left(M_V\ S\left(\frac{PV_V}{R\,T}\right)\right)}\right)$ Equation 2-30
Filling Saturation Factor (S)	S = 0.6 for a full liquid heel S = 0.5 for a partial liquid heel $C_{sf}\ S \ge 0.15$

Table 3-19. ROOF LANDING LOSSES FOR ALL DRAIN-DRY TANKS

Standing Idle Loss	$L_{SL} = 0.0063\, W_l \left(\frac{\pi\, D^2}{4}\right)$ Equation 2-22 $L_{SL} \le 0.60 \left(\frac{P\, V_V}{R\, T}\right) M_V$ Equation 2-23
Standing Idle Saturation Factor	Not applicable
Filling Loss Equation	$L_{FL} = \left(\frac{P\, V_V}{R\, T}\right) M_V\ S$ Equation 2-26
Filling Saturation Factor (S)	S = 0.15

where:

L_s = standing idle loss per landing episode (lb)
n_d = number of days the tank stands idle with the floating roof landed (dimensionless)
K_E = vapor space expansion factor (dimensionless)

$$K_E = \frac{\Delta T_V}{T}\left(1 + \frac{0.50\, B\, P}{T(P_A - P)}\right)$$

ΔT_v = daily vapor temperature range (°R)
T = average temperature of the vapor and liquid below the floating roof (°R)
B = constant from the vapor pressure equation shown in Equation 1-24 (°R)
P = true vapor pressure of the stock liquid (psia)
P_A = atmospheric pressure at the tank location (psia)
V_V = volume of the vapor space (ft^3)

$$V_V = \frac{h_v\ \pi\, D^2}{4}$$

h_v = height of the vapor space under the floating roof (ft)
D = tank diameter (ft)
R = ideal gas constant (psia ft^3 / lb-mole R) = 10.731
M_V = stock vapor molecular weight (lb/lb-mole)
K_S = standing idle saturation factor (dimensionless)
S = filling saturation factor (dimensionless)

P^* = vapor pressure function (dimensionless)

$$P^* = \frac{\frac{P_{VA}}{P_A}}{\left[1 + \left(1 - \frac{P_{VA}}{P_A}\right)^{0.5}\right]^2}$$

W_l = stock liquid density (lb/gal)
h_{le} = effective height of the stock liquid (ft)
L_F = filling loss per landing episode (lb)
C_{sf} = filling saturation correction factor (dimensionless)

TABLE 3-20. HENRY'S LAW CONSTANTS FOR SELECTED ORGANIC LIQUIDS

NO	FORMULA	NAME	Henry's Law Constant, H @ 25 C	H - atm/mol fraction BASIS
1	C2H4O	ACETALDEHYDE	4.8730000	Experimental
2	C2H5ON	ACETAMIDE	0.0000986	UNIFAC
3	C2H3N	ACETONITRILE	1.1076388	VLE Data
4	C8H8O	ACETOPHENONE	0.5089400	Solubility Data
5	C3H4O	ACROLEIN	4.5711400	Solubility Data
6	C3H5NO	ACRYLAMIDE	0.0000145	UNIFAC
7	C3H4O2	ACRYLIC ACID	0.0223962	VLE Data
8	C3H3N	ACRYLONITRILE	5.4484900	Solubility Data
9	C3H5CL	ALLYL CHLORIDE	515.4180500	Solubility Data
10	C6H7N	ANILINE	0.0977600	Solubility Data
11	C7H9NO	O-ANISIDINE	0.0092393	UNIFAC
12	C6H6	BENZENE	308.3400000	Experimental
13	C7H5CL3	BENZOTRICHLORIDE	54.5177107	UNIFAC
14	C7H7CL	BENZYL CHLORIDE	17.7286753	UNIFAC
15	C12H10	BIPHENYL	22.6700000	Experimental
16	C2H4CL2O	BIS(CHLOROMETHYL)ETHER	-------	Reaction with water
17	CHBR3	BROMOFORM	29.5600000	Experimental
18	C4H6	1,3-BUTADIENE	3961.1453000	Solubility Data
19	C6H11ON	CAPROLACTAM	0.0001639	UNIFAC
20	CS2	CARBON DISULFIDE	1064.0713500	Solubility Data
21	CCL4	CARBON TETRACHLORIDE	1677.7900000	Experimental
22	C2H3CLO2	CHLOROACETIC ACID	0.0036272	UNIFAC
23	C8H7CLO	2-CHLOROACETOPHENONE	1.5713000	Solubility - Estimated
24	C6H5CL	CHLOROBENZENE	209.4500000	Experimental
25	CHCL3	CHLOROFORM	221.3300000	Experimental
26	C4H5CL	CHLOROPRENE	51.6355560	UNIFAC
27	C7H8O	M-CRESOL	0.0394800	Solubility Data
28		CRESOLS/CRESYLIC ACID(ISOMERS & MIXTURES)	-------	
29	C7H8O	O-CRESOL	0.0911500	Solubility Data
30	C7H8O	P-CRESOL	0.0396800	Solubility Data
31	C9H12	CUMENE	727.7800000	Experimental
32	C6H4CL2	1,4-DICHLOROBENZENE	176.1100000	Experimental
33	C4H8CL2O	DICHLOROETHYL ETHER	1.1390000	Solubility Data
34	C3H4CL2	1,3-DICHLOROPROPENE	197.2200000	Experimental
35	C4H11NO2	DIETHANOLAMINE	0.0000001	UNIFAC
36	C8H11N	N,N-DIMETYLANILINE	0.7701322	UNIFAC
37	C4H10O4S	DIETHYL SULFATE	0.3405000	Solubility Data
38	C14H16N2	DIMETHYLBENZIDINE	0.1780100	Solubility - Estimated
39	C3H7NO	DIMETHYL FORMAMIDE	0.0098341	VLE Data
40	C2H8N2	1,1-DIMETHYLHYDRAZINE	0.0910756	VLE Data
41	C10H10O4	DIMETHYL PHTHALATE	0.0548542	UNIFAC
42	C2H6SO4	DIMETHYL SULFATE	0.2226700	Solubility Data
43	C6H3N2O5	2,4-DINITROPHENOL	0.4756000	Solubility Data
44	C7H6N2O4	2,4-DINITROTOLUENE	0.3996900	Solubility Data
45	C4H8O2	1,4-DIOXANE	0.3079797	VLE Data
46	C12H12N2	1,2-DIPHENYLHYDRAZINE	0.0135700	Solubility - Estimated
47	C3H5CLO	EPICHLOROHYDRIN	1.8590400	Solubility Data
48	C5H8O2	ETHYL ACRYLATE	14.1169500	Solubility Data
49	C8H10	ETHYLBENZENE	437.8100000	Experimental
50	C2H5CL	ETHYL CHLORIDE	672.2300000	Experimental

TABLE 3-20. (cont.)

NO	FORMULA	NAME	Henry's Law Constant, H @ 25 C	H - atm/mol fraction BASIS
51	C2H4BR2	ETHYLENE DIBROMIDE	36.1100000	Experimental
52	C2H4CL2	ETHYLENE DICHLORIDE	65.3800000	Experimental
53	C2H6O2	ETHYLENE GLYCOL	0.0001051	VLE Data
54	C2H4O	ETHYLENE OXIDE	13.2280793	VLE Data
55	C2H4CL2	ETHYLIDENE DICHLORIDE	312.2300000	Experimental
56	CH2O	FORMALDEHYDE	0.0187000	Experimental
57	C4H10O2	ETHYLENE GLYCOL DIMETHYL ETHER	1.9471264	VLE Data
58	C4H10O2	ETHYLENE GLYCOL MONOETHYL ETHER	0.0409170	VLE Data
59	C8H16O4	DIETHYLENE GLYCOL MONOETHYL ETHER ACETATE	0.0358406	UNIFAC
60	C6H12O3	ETHYLENE GLYCOL MONOETHYL ETHER ACETATE	0.0986300	Solubility Data
61	C6H14O3	DIETHYLENE GLYCOL MONOETHYL ETHER	0.0026793	UNIFAC
62	C5H10O3	ETHYLENE GLYCOL MONOMETHYL ETHER ACETATE*	0.1218685	UNIFAC
63	C8H18O3	DIETHYLENE GLYCOL MONOBUTYL ETHER	0.0012481	UNIFAC
64	C6H14O3	DIETHYLENE GLYCOL DIMETHYL ETHER	0.0837496	UNIFAC
65	C3H8O2	ETHYLENE GLYCOL MONOMETHYL ETHER	0.0405801	Correlation
66	C6H12O2	ETHYLENE GLYCOL MONOPROPYL ETHER	0.0474169	UNIFAC
67	C8H10O2	ETHYLENE GLYCOL MONOPHENYL ETHER	0.0037600	Solubility Data
68	C5H12O2	DIETHYLENE GLYCOL MONOMETHYL ETHER	0.0022577	UNIFAC
69	C8H18O3	DIETHYLENE GLYCOL DIETHYL ETHER	0.1189224	UNIFAC
70	C6H14O2	ETHYLENE GLYCOL MONOBUTYL ETHER	0.0292288	VLE Data
71	C8H18O4	TRIETHYLENE GLYCOL DIMETHYL ETHER	0.0025951	UNIFAC
72	C8H15O3	ETHYLENE GLYCOL MONOBUTYL ETHER ACETATE	0.2746400	Solubility Data
73	C6CL6	HEXACHLOROBENZENE	94.4500000	Experimental
74	C4CL6	HEXACHLOROBUTADIENE	572.2300000	Experimental
75	C2CL6	HEXACHLOROETHANE	463.8900000	Experimental
76	C6H14	HEXANE	42667.0100000	Experimental
77	C8H6O2	HYDROQUINONE	0.0000800	Solubility Data
78	C9H14O	ISOPHORONE	0.3682100	Solubility Data
79	C4H2O3	MALEIC ANHYDRIDE	0.0121651	UNIFAC
80	CH4O	METHANOL	0.2885032	VLE Data
81	CH3BR	METHYL BROMIDE	381.0578800	Solubility Data
82	CH3CL	METHYL CHLORIDE	490.0000000	Experimental
83	C2H3CL3	METHYL CHLOROFORM	966.6700000	Experimental
84	C4H8O	METHYL ETHYL KETONE	7.2200000	Experimental
85	CH6N2	METHYL HYDRAZINE	0.0248008	UNIFAC
86	C6H12O	METHYL ISOBUTYL KETONE	21.6700000	Experimental
87	C2H3NO	METHYL ISOCYANATE	-------	Reaction with water
88	C5H8O2	METHYL METHACRYLATE	7.8317700	Solubility - Estimated
89	C5H12O	METHYL TERT-BUTYL ETHER	30.8401800	Solubility Data
90	CH2CL2	METHYLENE CHLORIDE	164.4500000	Experimental
91	C15H10N2O2	METHYLENE DIPHENYL DIISOCYANATE**	0.0026600**	Solubility - Estimated
92	C13H14N2	4,4-METHYLENEDIANILINE	0.0284900	Solubility Data
93	C10H8	NAPHTHALENE	26.8300000	Experimental
94	C6H5NO2	NITROBENZENE	1.3300000	Experimental
95	C6H5NO3	4-NITROPHENOL	0.0064600	Solubility Data
96	C3H7NO2	2-NITROPROPANE	6.6111800	Solubility Data
97	C6H6O	PHENOL	0.0722000	Experimental
98	C6H8N2	P-PHENYLENEDIAMINE	0.0007700	Solubility Data
99	COCL2	PHOSGENE**	780.0225300**	Solubility Data
100	C8H4O3	PHTHALIC ANHYDRIDE	0.0441508	Solubility Data

TABLE 3-20. (cont.)

NO	FORMULA	NAME	Henry's Law Constant, H - atm/mol fraction H @ 25 C	BASIS
101	C3H4O2	BETA-PROPIOLACTONE	0.0063801	UNIFAC
102	C3H6O	PROPIONALDEHYDE	3.3224900	Solubility Data
103	C3H6CL2	PROPYLENE DICHLORIDE	158.7100000	Experimental
104	C3H6O	PROPYLENE OXIDE	19.7742986	VLE Data
105	C6H4O2	QUINONE	0.0576800	Solubility Data
106	C8H8	STYRENE	144.7155400	Solubility Data
107	C2H2CL4	1,1,2,2-TETRACHLOROETHANE	13.8900000	Experimental
108	C2CL4	TETRACHLOROETHYLENE	983.3400000	Experimental
109	C7H8	TOLUENE	356.6700000	Experimental
110	C7H10N2	2,4-TOLUENE DIAMINE	0.0000742	UNIFAC
111	C9H6N2O2	2,4-TOLUENE DIISOCYANATE**	0.0091900**	Solubility - Estimated
112	C7H9N	O-TOLUIDINE	0.1344600	Solubility Data
113	C6H3CL3	1,2,4-TRICHLOROBENZENE	106.6700000	Experimental
114	C2H3CL3	1,1,2-TRICHLOROETHANE	45.7700000	Experimental
115	C2HCL3	TRICHLOROTHYLENE	566.6700000	Experimental
116	C6H3CL3O	2,4,5-TRICHLOROPHENOL	0.4841100	Solubility Data
117	C6H15N	TRIETHYLAMINE	6.9428000	Solubility Data
118	C8H18	2,2,4-TRIMETHYLPENTANE	185451.3318600	Solubility Data
119	C4H6O2	VINYL ACETATE	28.2111800	Solubility Data
120	C2H3CL	VINYL CHLORIDE	1472.2300000	Experimental
121	C2H2CL2	VINYLIDENE CHLORIDE	1438.9000000	Experimental
122		XYLENES (ISOMERS & MIXTURES)	-------	
123	C8H10	M-XYLENE	413.3400000	Experimental
124	C8H10	O-XYLENE	270.5600000	Experimental
125	C8H10	P-XYLENE	413.3400000	Experimental

Notes:

1. * - Estimated values for coefficients in vapor pressure equation.

2. ** - Reacts with water.

3. For basis of UNIFAC, the estimation of the activity coefficient at infinite dilution makes use of the group contribution contribution method using the UNIFAC equations (Gmehling, J., P. Rasmussen and A. Fredenslund, Ind. Eng. Chem. Process Des. Dev., 21, 118 (1982)).

4. For basis of Solubility - Estimated, the estimation of water solubility makes use of experimental data which is available on reference compounds that are very close in molecular structure to the compound of interest. The addition of a molecular group (or groups) to the reference compound then provides a molecular structure that is identical to the molecular structure of the compound of interest (log S = log S_{ref} + ΔGroup).

TABLE 3-21. CORRECTION OF HENRY'S LAW FACTOR FOR A TEMPERATURE DIFFERENT FROM STANDARD

$$H_2 = \frac{MW}{10^6} * \frac{(T_2 - T_1)}{T_2} * \frac{H_1}{P^*_1} * \frac{T_1}{T_2} * P^*_2$$

where:

H_1 = Henry's Law Constant at standard temperature, atm-m^3/mol
H_2 = the Henry's Law Constant at the actual temperature, atm-m^3/mol
P^*_1 = the compound vapor pressure at standard temperature, atm
P^*_2 = the compound vapor pressure at actual temperature, atm
T_1 = the standard temperature, 298°K
T_2 = the actual temperature, °K
MW = the average molecular weight of the liquid, g/mole
10^6 = the density of water, g/m^3

Source: Lyman, Warren J., William Reahl, and David Rosenblatt. Handbook of Chemical Property Estimation Methods. McGraw-Hill Book Company, New York, New York, 1982. Section 14, pp. 3-25.

To convert from H in atm/vol fraction to:

H in atm/ (mol/m^3), divide by 55,556
H in mmHg/mol fraction, multiply by 760
H in psia/mol fraction, multiply by 19.7
H in kPa/mol fraction, multiply by 101.325
H in kPa/mol/m^3), multiply by 101.325/55,556

3.3 REFERENCES

1. *Evaporative Loss From Fixed-Roof Storage Tanks*, Bulletin No. 2518, Second Edition, American Petroleum Institute, Washington, DC, October 1991.

2. *Estimating Air Toxics Emissions From Organic Liquid Storage Tanks*, EPA-450/4-88-004, U. S. Environmental Protection Agency, Research Triangle Park, NC, October 1988.

3. Barnett, H.C., et al., *Properties of Aircraft Fuels*, NACA-TN 3276, Lewis Flight Propulsion Laboratory, Cleveland, OH, August 1956.

4. *Petrochemical Evaporation Loss From Storage Tanks*, Bulletin No. 2523, First Edition, American Petroleum Institute, Washington, DC, 1969.

5. *Evaporation Loss From Internal Floating Roof Tanks*, Bulletin No. 2519, Third Edition, American Petroleum Institute, Washington, DC, June 1983.

6. *Manual of Petroleum Measurement Standards: Chapter 19-Evaporative Loss Management, Section 2--Evaporative Loss from Floating Roof Tanks*, Draft Publication, American Petroleum Institute, Washington, DC, December 1994.

7. *SIMMS Data Base Management System*, U. S. Environmental Protection Agency, Research Triangle Park, NC.

8. *Comparative Climate Data Through 1990*, National Oceanic and Atmospheric Administration, Asheville, NC, 1990.

9. *Input for Solar Systems*, National Oceanic and Atmospheric Administration, Asheville, NC, November 1987.

10. *Evaporation Loss From External Floating Roof Tanks*, Bulletin No. 2517, Third Edition, American Petroleum Institute, Washington, DC, February 1989.

11. Ferry, R. L., *Documentation of Rim Seal Loss Factors for the Manual of Petroleum Measurement Standards*, American Petroleum Institute, Washington, DC, April 1995.

12. Memorandum from A. Parker, R. Neulicht, Midwest Research Institute, to D. Beauregard, U. S. Environmental Protection Agency, *Fitting Wind Speed Correction Factor for External Floating Roof Tanks*, September 22, 1995.

13. Memorandum from R. Jones, et al., Midwest Research Institute, to D. Beauregard, U. S. Environmental Protection Agency, *Final Fitting Loss Factors for Internal and External Floating Roof Tanks*, May 24, 1995.

14. Memorandum from A. Parker, Midwest Research Institute, to D. Beauregard, U. S. Environmental Protection Agency, *Final Deck Fitting Loss Factors for AP-42 Section 7.1*, February 15, 1996.

15. Memorandum from A. Marshall, Midwest Research Institute, to D. Beauregard, U. S. Environmental Protection Agency, *Review of New Loss Factor Data*, December 20, 1996.

16. *Use of Variable Vapor Space Systems to Reduce Evaporation Loss*, Bulletin No. 2520, American Petroleum Institute, New York, NY, 1964.

17. Yaws, C.L., *Henry's Law Constants for HAPs*, U. S. Environmental Protection Agency, September 30, 1992.

4.0 EMISSION ESTIMATION PROCEDURES FOR FIXED ROOF TANKS

Two emission estimation procedures were examined for estimating standing storage or breathing loss emissions from fixed roof tanks. The first equation is a version of that developed by the American Petroleum Institute (API) in 1962.[1] This breathing loss equation was used in both the industry and regulatory communities for 30 years. More recently, API proposed a new equation for predicting breathing losses from fixed roof tanks.[2] This chapter presents the results of a comparative evaluation of the two equations to determine the most accurate method for predicting breathing losses from fixed roof tanks. In order to evaluate the effectiveness of the equations in predicting actual breathing losses, the equations were used to estimate breathing losses in two scenarios. In the first scenario, actual parameters recorded during previous emissions testing are the variables used in the estimating equations. In the second scenario, default values that are likely to be used in the regulated community are the variables used in the estimating equations. In addition to evaluating the predictive abilities of each of the equations, the sensitivity of each equation to various parameters was analyzed using default values and a typical range of data points for each parameter.

4.1 BREATHING LOSS EQUATIONS

The standing storage or breathing loss equation that has been used historically is based on the assumption that the breathing loss is a function of the vapor pressure of the stored liquid, tank diameter, vapor space outage, ambient temperature, and the tank paint color and condition. The old breathing loss equation* is as follows:

$$L_b = 2.26\,x\,10^{-2}\,Mv\left(\frac{P}{[PA-P]}\right)^{0.68} D^{1.73}\,H^{0.51}\,\Delta T^{0.50}\,F_p\,C\,K_c \qquad (4\text{-}1)$$

where:

L_b = breathing loss, lb/yr
M_V = stock vapor molecular weight, lb/lb-mole
P = vapor pressure of stored liquid at bulk liquid conditions, psia
P_A = average atmospheric pressure at tank location, psia
D = tank diameter, ft
H = average vapor space height, including roof volume correction, ft
$\hat{I}T$ = average ambient diurnal temperature change, EF
F_p = paint factor, dimensionless
C = adjustment factor for small diameter tanks, D<30 ft, dimensionless
K_C = product factor, dimensionless

*Note: This equation was updated as described on the following page in Supplement E of the 4th edition of AP42, October 1992.

The new breathing loss equation proposed by API was developed based on theoretical equations and is a function of the following parameters:

1. K_E = the vapor space expansion factor;
2. K_S = the vapor space saturation factor;
3. V_V = the tank vapor space volume; and
4. W_V = the stock vapor density.

The expressions describing each of the above parameters were derived from theoretical equations and are themselves functions of tank diameter, vapor space outage, stock molecular weight, vapor pressure, and environmental conditions. The expression developed for K_S contains a mass transfer coefficient for which no value is available. Therefore, a correlation based on EPA, Western Oil and Gas Association (WOGA), and API data was developed to describe K_S.[2] The theoretical derivation was used as a guide in developing the data-based correlation. Thus, K_E, V_V, and W_V are based on theoretical derivations and K_S is based on actual test data. The following is the new breathing loss (standing storage loss) equation that has been developed by API:

$$L_S = 365\ V_V\ W_V\ K_E\ K_S \qquad (4\text{-}2)$$

where:

L_S = standing storage loss, lb/yr

$V_V = \left(\frac{\pi}{4} D^2\right) H_{VO}$

$W_V = \frac{M_V\ P_{VA}}{R\ T_{LA}}$

$K_E = \frac{\Delta TV}{T_{LA}} + \frac{\Delta P_V - \Delta P_B}{P_A - P_{VA}}$

$K_S = \frac{1}{1 + 0.053 P_{VA} H_{VO}}$

365 = constant, the number of daily events in a year, $(year)^{-1}$

π = constant, 3.1459

D = tank diameter, ft

H_{VO} = vapor space outage, ft

M_V = stock vapor molecular weight, lb/lb-mole

P_{VA} = vapor pressure at daily average liquid surface temperature, psia

R = ideal gas constant, 10.731 psi•ft^3/lb-mole•ER

T_{LA} = daily average liquid surface temperature, ER

ΔT_V = daily vapor temperature range, ER

ΔP_V = daily vapor pressure range, psia

ΔP_B = breather vent pressure setting range, psia

P_A = atmospheric pressure, psia

Of the above parameters, D, H_{VO}, M_V, P_V, ΔP_B, and R are readily available or can be determined using basic assumptions, tables, or figures. The remaining parameters, however, are not readily available and are themselves functions of the following variables:

T_{AA} = daily average ambient temperature, ER

Of the above parameters, D, H_{VO}, M_V, P_V, $\triangle P_B$, and R are readily available or can be determined using basic assumptions, tables, or figures. The remaining parameters, however, are not readily available and are themselves functions of the following variables:

T_{AA} = daily average ambient temperature, °R

T_B = liquid bulk temperature, °R

α = tank paint solar absorptance, dimensionless

I = daily total solar insolation, Btu/ft^2·d

The above values may not be readily available, but default values are provided by API.

4.2 COMPARISON OF PREDICTIVE ABILITY OF TWO EQUATIONS

The predictive ability of the two breathing loss equations was evaluated under two sets of circumstances. In the first situation, data collected for the WOGA, EPA, and API studies were used in each equation to generate breathing loss emission estimates for comparison against actual measured values. In the second situation, typical default values that are likely to be used by the regulated community were used in each breathing loss equation. The breathing loss calculated by each equation, based on default values, was then compared against actual measured values.

The emissions estimated by the two breathing loss equations were compared in Section H of the Documentation File for API 2518, second edition.[3] The WOGA, EPA, and API test data that were used in each equation are identified in Section H. The API test data used in this analysis are the same as the test data presented in Section H of the API 2518 documentation file and are for tanks storing fuel oil No. 2. The WOGA test data used in this analysis are taken from the document entitled "Hydrocarbon Emissions From Fixed Roof Petroleum Tanks," prepared by Engineering Science for WOGA in July 1977.[4] This report is the original report containing the data and field data sheets from the emission testing. The data in the Engineering Science report are, in some instances, different from those presented in Section H of the API 2518 documentation file. However, the data in the Engineering Science report were used because this report is assumed to be the most accurate source. These data are for tanks storing crude oil. The EPA data used in the report are also slightly different from those presented in Section H of the API 2518 documentation file. The EPA data used in this analysis were taken from the document entitled "Breathing Loss Emissions From Fixed-Roof Petrochemical Storage Tanks" (Third Draft), prepared by Engineering Science for EPA in December 1978.[5] As with the WOGA data, this document contains the original field data sheets and is therefore assumed to be the most accurate source of information. These data describe tanks storing several different petrochemicals.

4.2.1 Predictive Ability--Actual Data

A summary of breathing loss estimates calculated by the two equations is presented in Table 4-1 for fuel oil (API data base), Table 4-2 for crude oil (WOGA data base), and Table 4-3 for petrochemicals (EPA data base). The breathing loss values presented were calculated using actual measured parameters, not default values. Also presented in these tables are the stock type contained in test tanks, the measured vapor pressure of the stock, and the actual breathing loss emissions measured. The measured breathing losses were compared to those calculated using the two emission estimation equations by establishing the bias, standard deviation, and root mean squared error of the models, which are the emission estimation equations. The bias is used to describe the systematic error in a certain model, for example, whether the model consistently overpredicts or underpredicts the actual measured emission loss. The standard deviation describes the precision or reproducibility of the model. If the standard deviation is large, this indicates that there is a lot of scatter in the data base, or in the case of the breathing loss equations, that the equation has poor reproducibility. The root mean squared error is an expression that is used to incorporate both types of error in an equation, the bias and the standard deviation. The root mean squared error of each model is expressed in one number. The bias, standard deviation, and root mean squared error are all expressed in pounds per day (lb/d) for each emission estimation procedure.

From the first "row" of data presented in Table 4-4, which corresponds to the aggregate of data from all three data bases, the revised equation (Equation 4-2) has less bias and a smaller variability than Equation 4-1. Based on all tanks in the data base, Equation 4-1 underestimates actual measured emissions by approximately 49 lb/d and has a standard deviation of 116 lb/d. The root mean squared error is 126 lb/d. In comparing measured breathing losses to those calculated using the revised breathing loss estimating equation, and considering all tanks in the data base, Equation 4-2 underestimates by only 2.5 lb/d and has a standard deviation of 52.9 lb/d. The root mean squared error of Equation 4-2 is also 52.9 lb/d.

It is imperative that, when reviewing the data presented in Table 4-4, the reader note how the two equations predict breathing losses for individual stock types, and consider the number of data points associated with each stock type. For example, the fuel oil No. 2 (API data base) and crude oil (WOGA data base) comparisons are based on 10 and 8 data points, respectively. The other comparisons--isopropanol, ethanol, acetic acid, ethyl benzene, and cyclohexane (all from the EPA data base)--only comprise 2 or 3 data points each. If one equation happens to show better predictability in a stock type that has a large number of data points, as is the case with Equation 4-2 for crude oil, the overall (aggregate) results will be biased. Therefore, even though the overall (aggregate) results indicate that Equation 4-2 is a better predictor of breathing losses, the two equations are for the most part comparable, except in the case of crude oil, in which Equation 4-2 clearly is a better predictor (both equations underpredict, with Equation 4-1 being a substantially worse predictor than Equation 4-2).

A comparison of the calculated breathing losses as a function of vapor pressure is shown in Table 4-5. From the table, Equation 4-1 appears to be a better predictor for liquids having a vapor pressure of less than 0.5 psia and Equation 4-2 appears to be a better predictor for liquids with vapor pressures above 2 psia. In the vapor pressure range between 0.5 and 2.0 psia, the two equations are comparable predictors. However, based on the product type analysis, the difference between the two equations may be more a result of product type than vapor pressure. For example, no data points for crude oil fall within the vapor pressure range less than 0.5 psia, which happens to coincide with the vapor pressure range where Equation 4-1 appears to be a better predictor. On the other hand, four data points from crude oil fall within the vapor pressure range greater than 2.0 psia where Equation 4-2 is a better predictor.

4.2.2 Predictive Ability--Default Values

It is assumed that many users of the breathing loss equation have only basic information about a particular tank. This information would include the physical characteristics of the tank (size, color), the location of the tank, and the tank stock. Therefore, many of the parameters needed to use either breathing loss estimation procedure are default values provided in AP-42 or API 2518. These default values may be given specifically or presented in tables and figures. In the case of Equation 4-1, values of M_V, P_V, T_{AA}, $\triangle T$, and F_p are obtained from tables and figures. The value of H is obtained by assuming H equals one-half of the actual tank shell height. In the case of Equation 4-2, the same assumptions as for Equation 4-1 are made. The vapor space height, H, is denoted as the vapor space outage, H_{VO}, in Equation 4-2. However, additional parameters of α and I are based on tables provided in API 2518; these parameters would not typically be measured.

A summary of the estimates calculated by the two breathing loss estimating equations (using default values) is presented for the WOGA and EPA data bases in Tables 4-6 and 4-7. In the API testing, the test tank was located indoors. Therefore, no default meteorological data could be assumed and no comparison with the WOGA and EPA default value data bases is possible. Also presented in Tables 4-6 and 4-7 are the stock type contained in the test tanks and the actual breathing loss emissions measured. Overall, as compared to measured data, Equation 4-1 (using default values) underpredicts by approximately 67.9 lb/d and has a standard deviation of 127.9 lb/d. The root mean squared error is 144.8 lb/d. Equation 4-2 (using default values) underpredicts by approximately 16.2 lb/d and has a standard deviation of 85 lb/d. The root mean squared error is 86.5 lb/d.

A summary of the bias, standard deviation, and root mean squared error is presented in Table 4-8 for three cases. The first case compares the two equations using all actual data. The second compares the two equations using actual and default values, when the fuel oil data base is excluded (this is done because default values were not entered for the API-fuel oil testing). In the third case, the two equations with actual and default data are compared, excluding the fuel oil and crude oil data. This was done because the revised equation, Equation 4-2, is obviously a better predictor in the case of crude oil.

A summary of the comparison between the two equations by product type is provided in Table 4-9. There are no important differences between the equations' performance for any product except crude oil. Using the default values for the parameters in the equations improved the performance of Equation 4-1 and resulted in a slightly worse performance for the revised equation, Equation 4-2. However, for crude oil, Equation 4-2 is still better than Equation 4-1. The major difference is in the bias. The precision of the equations is comparable.

In summary, with the likely use of the default values for the parameters in the equations, the Equation 4-1 is a slightly better predictor for the products in the data base with the exception of crude oil. For crude oil, the revised equation, Equation 4-2, is better.

4.3 SENSITIVITY ANALYSIS

As indicated by the above discussion, both breathing loss equations are basically functions of the same variables; they differ in the extent to which they depend on those variables. In order to assess the extent to which each of the equations depends on its independent variables, a sensitivity analysis was conducted. The results of that analysis are discussed below.

The sensitivity of Equation 4-1 was evaluated with respect to molecular weight (M_V), vapor

pressure (P_V), vapor space height (H), average ambient temperature change ($\triangle T$), and the paint factor (F_p). A sensitivity analysis had previously been done for the new breathing loss equation developed by API, as documented in Section G of the documentation file for API 2518, second edition.[2] The parameters that were evaluated included M_V, P_V, H, and $\triangle T$ as well as the following parameters:

1. Tank diameter (D);
2. Solar insolation (I);
3. Solar absorptance (α);
4. Ambient temperature;
5. Breather vent pressure and vacuum settings; and
6. Reid vapor pressure.

The sensitivity of the two breathing loss equations to the various parameters was evaluated by maintaining all parameters constant except for the one being evaluated. The baseline case that was used for the sensitivity analysis was the WOGA test conducted on May 18, 1977, involving a crude oil storage tank.[4] Parameters of diameter, Reid vapor pressure, stock type, tank location, and tank color were obtained from field data sheets. These parameters are the parameters that are assumed to be available to all end users. For all other parameters (molecular weight, vapor pressure, vapor space height, temperature data, and solar insolation), it was assumed that default values would be used by the end users. A summary of the baseline values for the sensitivity equation is provided in Table 4-10.

For each equation, the sensitivity evaluation of each parameter was conducted using the following procedure. First, for each parameter, the default value was identified. Then, based on actual data (EPA, WOGA, and API data bases), the amount by which the default value is likely to vary was determined. For example, the default value for the molecular weight of crude oil is 50 pounds/pound-mole (lb/lb-mole). Actual data indicated that the measured molecular weight may be as high as 70 lb/lb-mole. Therefore, the default value range was assumed to be 20 lb/lb-mole. Once the default range was determined, the corresponding change in the calculated breathing loss was calculated using each equation. For example, in a 20 lb/lb-mole range of molecular weight, the breathing loss calculated by Equation 4-1 differs by approximately 64 pounds. The same analysis was conducted for each parameter using both breathing loss estimating equations. The results are summarized in Table 4-11 and Figures 4-1 to 4-11. Note that because one baseline case is being used in the sensitivity analysis, the actual measured breathing loss is the same in all cases, 574 lb/d, as shown in Figures 4-1 to 4-11. Also note that all figures have different scales.

As previously stated, the actual molecular weight of crude oil may vary by 20 lb/lb-mole. The sensitivity of Equation 4-1 to changes in the molecular weight (all other parameters held constant) is provided in Figure 4-1. As indicated in Figure 4-1, the relationship between molecular weight and breathing loss is linear. Using the default value of 50 lb/lb-mole, a breathing loss of 159.3 lb/d is estimated. Based on Figure 4-1, a difference of 20 lb/lb-mole in the molecular weight would result in breathing loss emissions ranging between 159.3 and 223.1, a difference of approximately 64 lb/d in breathing loss emissions. Figure 4-2 shows the sensitivity of the revised equation to variance in molecular weight. Again, the relationship is linear. Using the default value of 50 lb/lb-mole, a breathing loss of 377.9 lb/d is estimated. Based on a difference of 20 lb/lb-mole in the molecular weight value used in the equation, the breathing loss would range between 377.9 and 529.1 lb/d, a difference of approximately 150 lb/d.

The vapor pressure of the stored material is also a parameter for which a default value from a reference table is used. (The default values are a function of temperature and therefore vary with the stored liquid temperature.) The WOGA data base indicates that the Reid vapor pressure of the same type

of stock, stored in the same tank, can vary considerably. Thus, the vapor pressure, which is a function of the Reid vapor pressure, will also vary even at a constant stored temperature. For example, in WOGA tests 7b and 8a, breathing losses from the same tank storing crude oil were measured. The Reid vapor pressure during the first test was measured as 1.2 psi. During the second test, 3 months later, the Reid vapor pressure was measured as 3.4 psi. Assuming a constant default value for ambient temperature, the true vapor pressure varies from 0.5 psi to 2.0 psi, a difference of 1.5 psi. The sensitivity of Equation 4-1 to changes in the stock vapor pressure is linear, as shown in Figure 4-3. Based on a 1.5 psi difference in the vapor pressure value used in the equation, the difference in the breathing loss in the 0.5 to 2.0 psi range varies between 37.5 and 103.9 lb/d, a difference of approximately 64 lb/d. Performing the same analysis with the revised equation, the difference in the calculated breathing loss ranges between 79.2 and 236.6 lb/d, a difference of approximately 158 lb/d. The sensitivity of the revised equation to vapor pressure changes is also linear, as depicted graphically in Figure 4-4.

A value for the average vapor space height, or outage (H_{VO}), is required as an input for both equations (it is required as H in Equation 4-1). If this value is not available, it is recommended that H_{VO} be assumed to equal one-half the tank height. The API 2518 bulletin does not direct the user as to what value to use if the actual H_{VO} is unavailable. Based on the available data, a typical tank height is 40 feet; thus, a typical value for H_{VO} would be 20 feet. In the baseline case, the value of H_{VO} is 20.75 feet, one-half of the actual tank height of 41.5 feet. Based on the H_{VO} value measured at tanks with a height of approximately 40 feet, the actual H_{VO} varied from approximately 5 to 35 feet. This reflects a difference in $\pm$15 feet from the default value. The sensitivity of the two equations to various H_{VO} values, all other parameters held constant, is depicted graphically in Figures 4-5 and 4-6, respectively. As indicated in both figures, the relationship between H_{VO} and breathing loss is nonlinear. Thus, in using either equation to calculate breathing loss, the difference between measured and calculated emissions depends on whether the value used in the equation is less than or greater than the default value. Using Equation 4-1, if a value of 5 feet (-15 feet) is assumed for H_{VO}, a breathing loss of 77.1 lb/d is obtained. Using the default value of 20 feet, a breathing loss of 156.4 lb/d is obtained; the difference in breathing loss emission estimates is approximately 80 lb/d. If a value of 35 feet (+15 feet) is assumed for H_{VO}, a breathing loss of 208 lb/d is estimated. As compared to the estimate of 156.4 lb/d using the default value, the difference in breathing loss is approximately 50 lb/d. Performing the same analysis using Equation 4-2, the difference in breathing loss emissions is again found to depend on whether the value for H_{VO} is less than or greater than the default value. If the value used for H_{VO} is 5 feet, the breathing loss is estimated as 226 lb/d. Using a default value of 20 feet, the breathing loss estimated by the revised equation is 374.9 lb/d, a difference of approximately 150 lb/d. If the value used for H_{VO} in the revised equation is 35 feet, a breathing loss of 413.9 lb/d is estimated. The difference as compared to the default value is approximately 40 lb/d.

Both of the estimating equations also incorporate a value for average daily ambient temperature ($\triangle T$) into the emission estimating equation. In Equation 4-1, the breathing loss is directly related to the value of $\triangle T$ raised to the 0.5 power; the relationship is approximately linear. In the revised equation, the value of $\triangle T$ is not used directly in the emission estimating equation. It is, however, used to calculate values for the daily vapor temperature change and the liquid surface temperature; these parameters are used directly in calculating the breathing loss emissions. Thus, the relationship between $\triangle T$ and breathing loss is different for each equation. The tank in the baseline case, which is considered in this analysis, is located in California. The default $\triangle T$ value of 15°F was obtained by using meteorological data for the areas that are contained in both AP-42 and API 2518. Based on actual measured temperature changes of 20° to 40°F in the same area, the value of ambient temperature change may vary by 25°F. The sensitivity of the two equations to changes in the value of $\triangle T$ is shown graphically in Figures 4-7 and 4-8, respectively. As indicated by these figures, the relationship between $\triangle T$ and breathing loss is approximately linear in both cases. Using Equation 4-1 and a default value of 15°F, the breathing loss is estimated as 159.3 lb/d. Based on an increase of 25°F in the value of $\triangle T$, the emission rate predicted by

the old equations is 259.3, a difference of 100 lb/d. Using Equation 4-2 and a default value of 15°F, a breathing loss of 377.9 is estimated. With an increase in $\triangle T$ of 25°F, the calculated breathing loss is 642.8 lb/d, a difference of approximately 265 lb/d.

The effect of tank color on the breathing loss emission rate is accounted for in both equations. In Equation 4-1, the breathing loss is directly related to the value for the paint factor (F_p) that is used in the equation. The value for F_p depends on tank shell and roof paint color and paint condition. The values for F_p were developed based on testing that involved measurement of solar reflectance and an evaluation of the relationship between solar reflectance and emission rates. In the revised equation, the effect of tank shell and roof paint color and paint condition is described by the solar absorptance (α) of the paint. A linear relationship exists between the values of α and F_p. The values of α provided in API 2518, second edition, were calculated using this relationship. However, Equation 4-2 incorporates the α value much differently than Equation 4-1 uses the paint factor, F_p. A value of α is not used directly in calculating the breathing loss emission rate. It is used to calculate the liquid bulk temperature, the average liquid surface temperature, and the vapor temperature range. These parameters are all used in the emission estimating equation; thus, the relationship between α and the emission rate is complicated, and α and F_p are not directly comparable.

For the baseline case used in this analysis, the tank shell was white and the tank roof was light gray. The paint condition was reported as good/poor (good condition was assumed). Based on this information and tabular listings of F_p and α values in AP-42 and API 2518, a value of 1.3 was used for F_p and a value of 0.355 was used for α. Both the AP-42 and API 2518 documents state that if information is not known, assume a white shell and roof, with the paint in good condition. If these conditions are assumed, a value of 1.0 is used for F_p and a value of 0.17 for α. The sensitivity of the breathing loss emission rate calculated by Equation 4-1 to changes in the value of F_p is linear, as shown in Figure 4-9. Using the actual value of 1.3 for F_p, a breathing loss of 159.3 lb/d is estimated. Using the default value of 1 for F_p (a change of 0.3), the breathing loss is estimated as 122.6 lb/d. Using the default value, the breathing loss emission rate varies by approximately 37 lb/d.

The sensitivity of the breathing loss emission rate calculated by Equation 4-2 to changes in the α value is also linear, as shown in Figure 4-10. Using the actual value of 0.355 for α, a breathing loss of 377.9 lb/d is estimated. Using the default value of 0.17 for alpha, the breathing loss is estimated as 259.8 lb/d, a difference of 188 lb/d.

One parameter that is used in Equation 4-2 but is not used in any way in Equation 4-1 is the daily solar insolation (I). The value of I is not used directly in the revised equation, Equation 4-2, to estimate breathing loss emissions but is used to calculate bulk storage temperature, average liquid surface temperature, and the vapor temperature range. The value of I depends on the tank location. Default values for I are provided in API 2518, based on the city and State in which the tank is located. It is assumed that the default values of I will be used by the regulated community. In the baseline case, a value of 1,594 Btu/ft^{2}d was used due to location of the tank in California. Based on actual values for I that were measured at the same location, the values of I may vary from 933 to 2,050 Btu/ft^{2}d. The sensitivity of the revised equation to changes in the value of I is linear, as shown in Figure 4-11. Based on a variance of 600 Btu/ft^{2}d as the value of I, the breathing loss estimated would range between 336.2 lb/d at I = 1,300 and 421 lb/d at I = 1,900. The difference in the emission rate calculated by the revised equation varies by approximately 85 lb/d.

Based on the results of the sensitivity analysis, it is concluded that for both equations, the predicted emission rates decrease when a lower value than the default value is used and increase when a higher value than the default value is used. In general, the revised equation, Equation 4-2, for estimating

emissions from fixed roof storage tanks, is more sensitive to variations in the values of molecular weight, vapor pressure, temperature change, and in some instances, vapor space height, than Equation 4-1. Both equations account for the effect of tank shell and roof paint color and condition on the breathing loss emission rate. In Equation 4-2, the effect is described by alpha. In Equation 4-1, the effect is described by F_p. Variations in the value of α will affect the resultant calculated emission rate much more than variations in the value of F_p used in Equation 4-1 to describe the same effect. However, F_p and α are not directly comparable. Finally, a new parameter, I, is introduced into the Equation 4-2. The breathing loss emission rate calculated by Equation 4-2 is sensitive to changes in the value of I that is used.

Based on the sensitivity analysis, it is concluded that use of Equation 4-2 would result in more uncertainty or variability in the predicted value if any of the variables are subject to uncertainty or error.

4.4 CONCLUSIONS AND RECOMMENDATIONS

For all stock types other than crude oil, Equation 4-1 is an adequate predictor of breathing loss. For crude oil stocks, the revised equation is a clearly superior predictive equation. In the case of crude oil, the Equation 4-2 underpredicts by 55.6 lb/d, as compared to the underprediction of 179.5 lb/d of Equation 4-1. Equation 4-2 is very sensitive to the value of α that is used. In a situation in which the default value of α is incorrect, an underprediction of 118 lb/d may occur. Adding this factor to the underprediction of 55.6 lb/d in the case of crude oil, Equation 4-2 underpredicts by 173.6 lb/d, comparable to Equation 4-1. However, it is recommended that the revised equation, Equation 4-2, be incorporated in the AP-42 for estimating emissions from fixed roof tanks as it is a better predictor for crude oil and is comparable to Equation 4-1 for other stored materials.

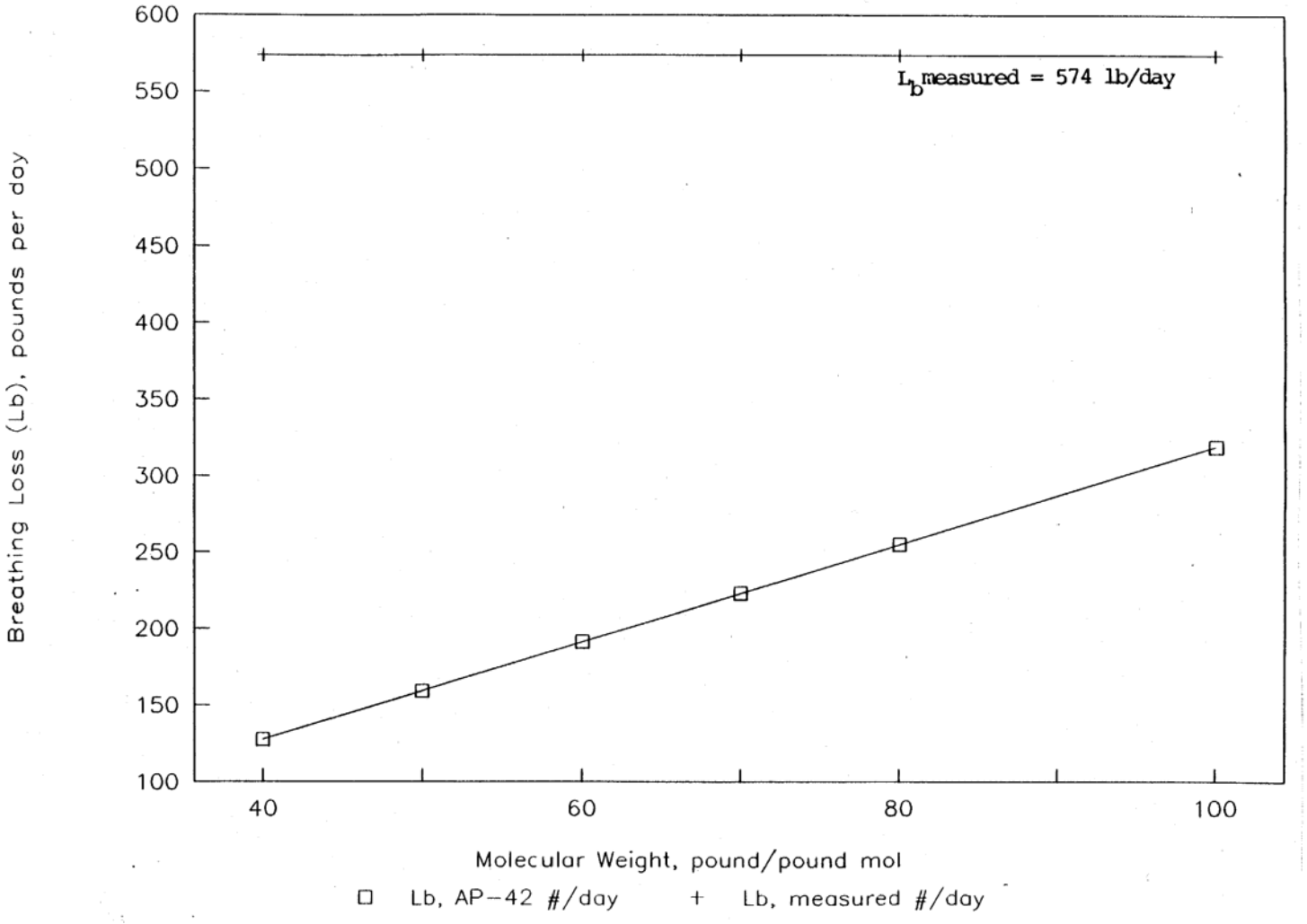

Figure 4-1. Sensitivity of Equation 4-1 to changes in molecular weight (M_V).

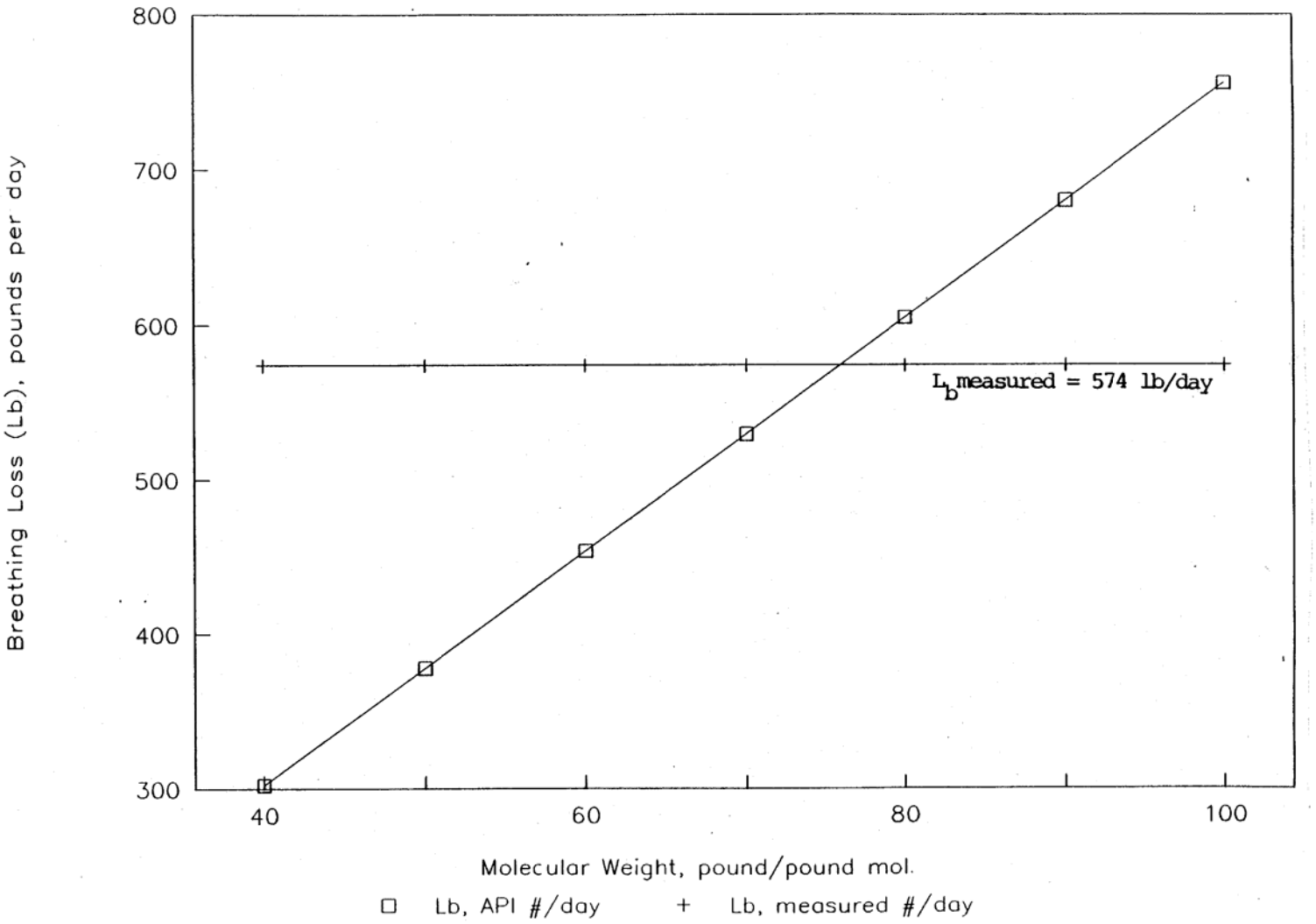

Figure 4-2. Sensitivity of Equation 4-2 to changes in molecular weight (M_V).

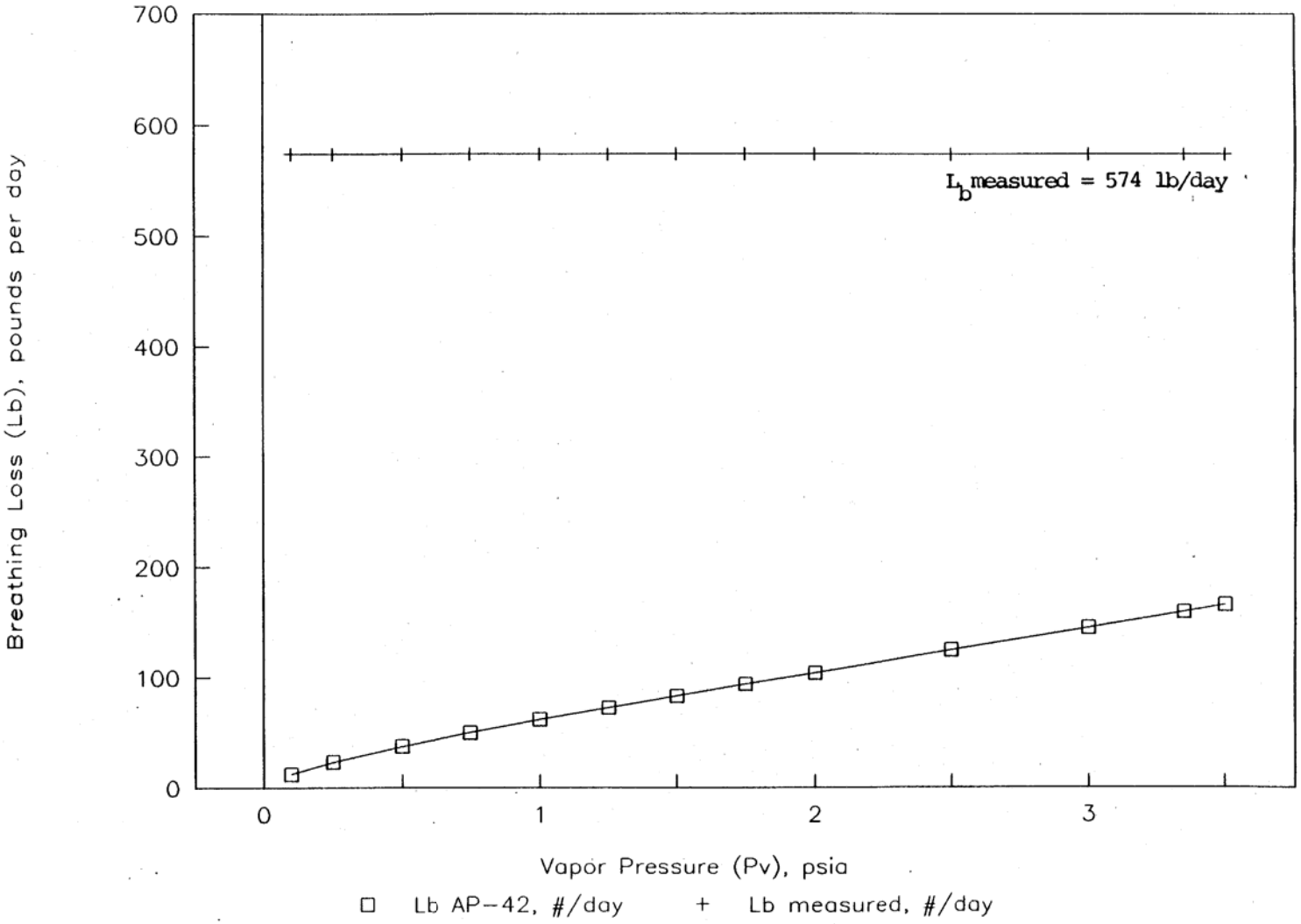

Figure 4-3. Sensitivity of Equation 4-1 to changes in vapor pressure (P_V).

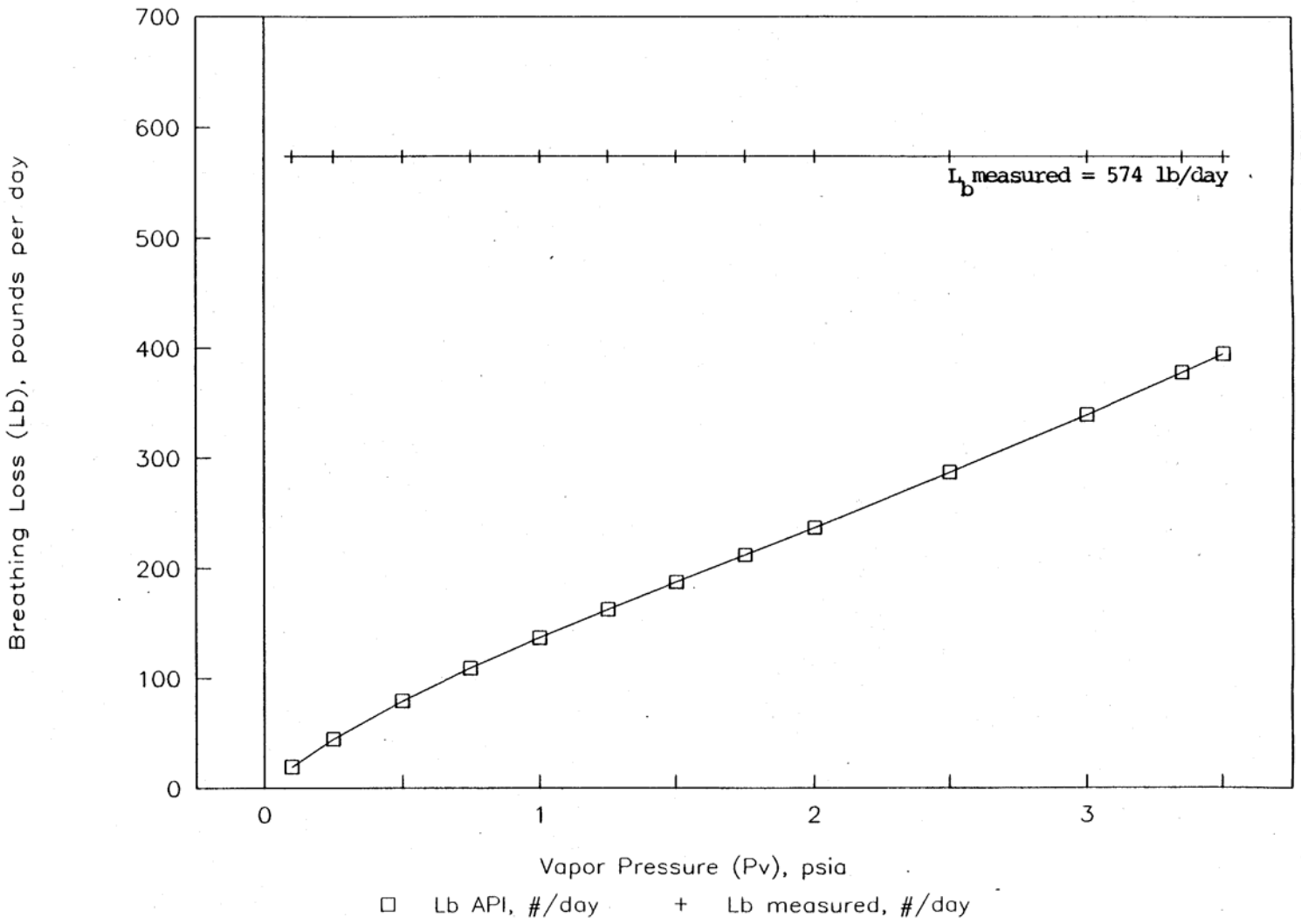

Figure 4-4. Sensitivity of Equation 4-2 to changes in vapor pressure (P_V).

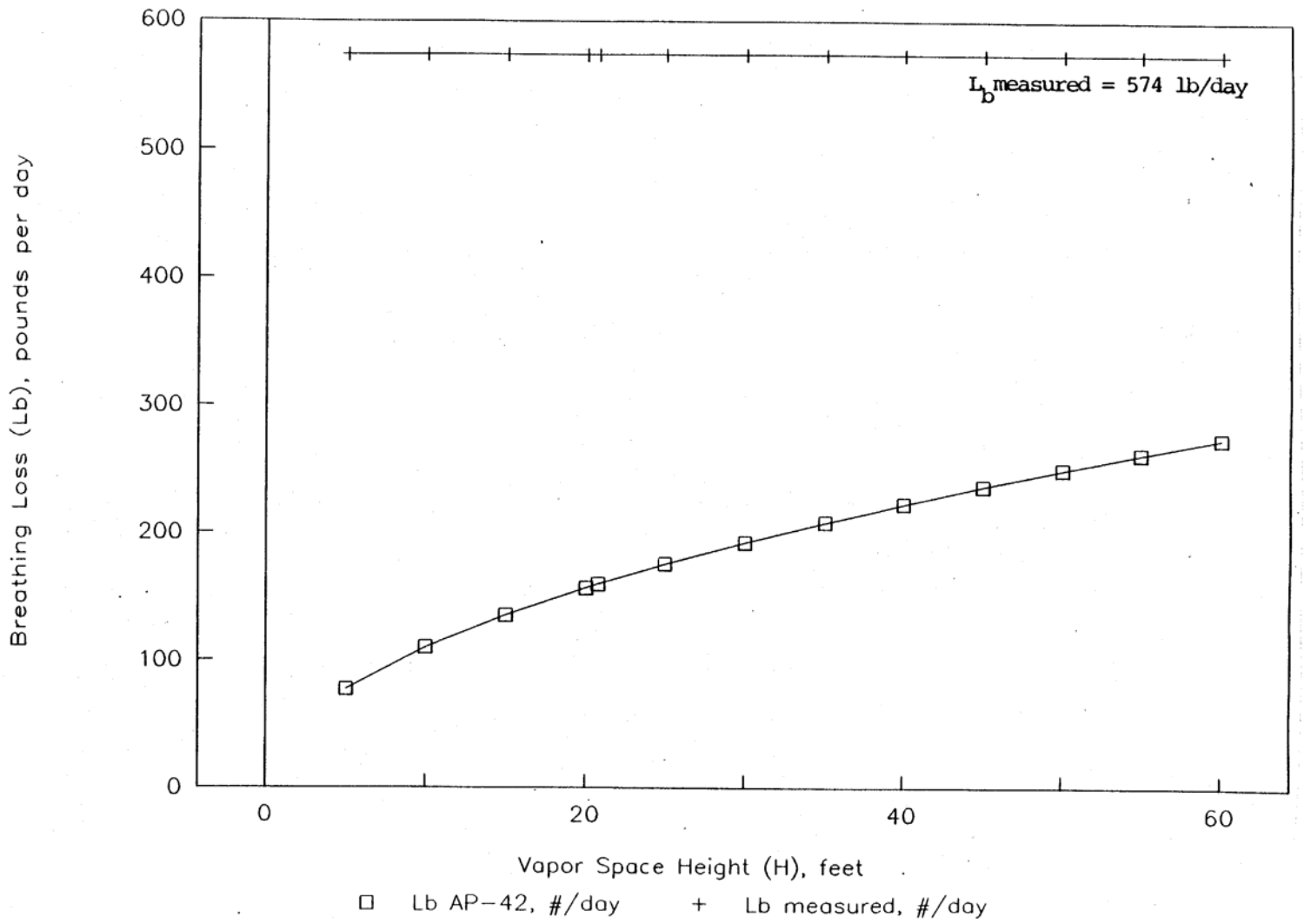

Figure 4-5. Sensitivity of Equation 4-1 to changes in the vapor space outage (H_{VO}).

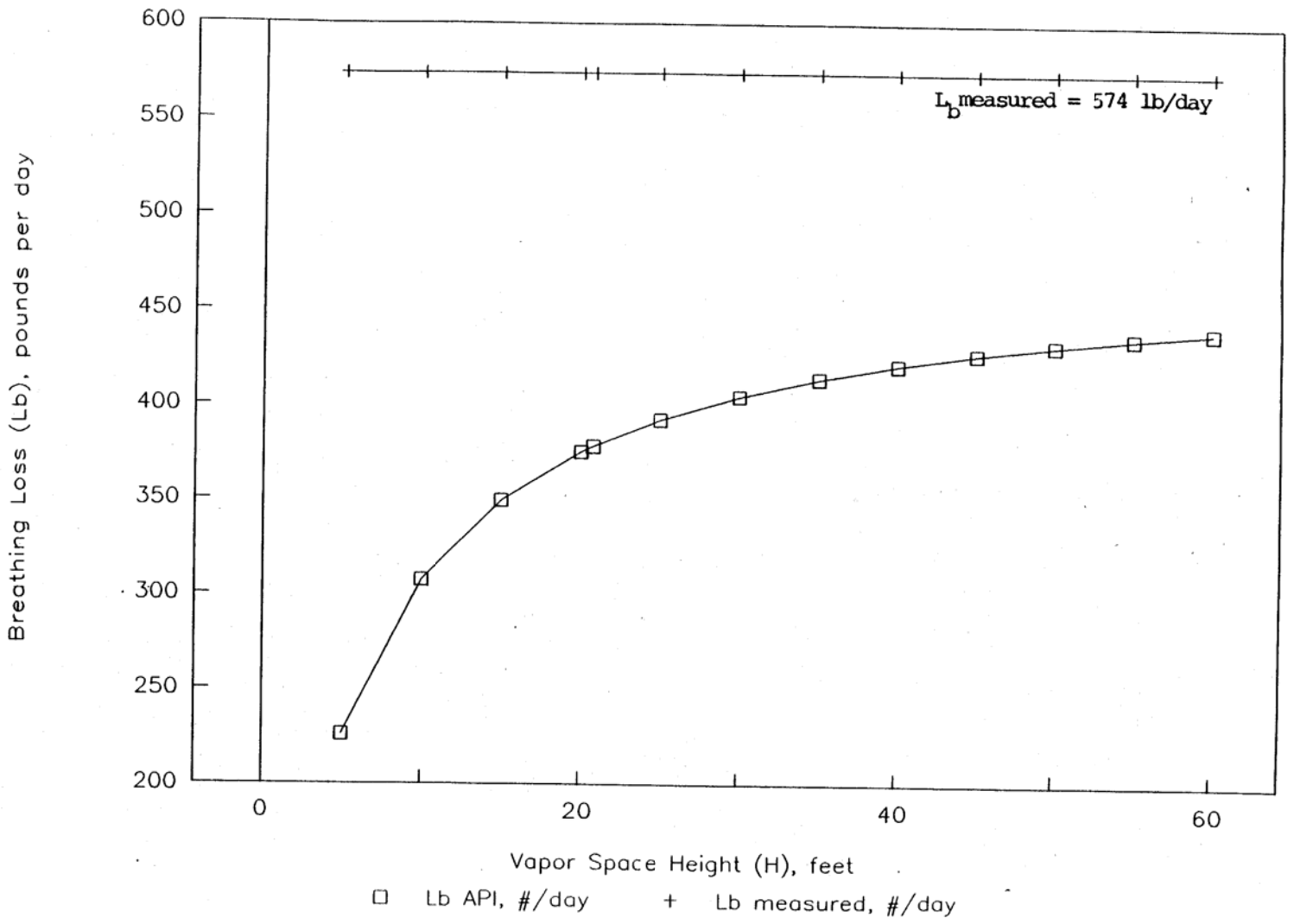

Figure 4-6. Sensitivity of Equation 4-2 to changes in the vapor space outage (H_{VO}).

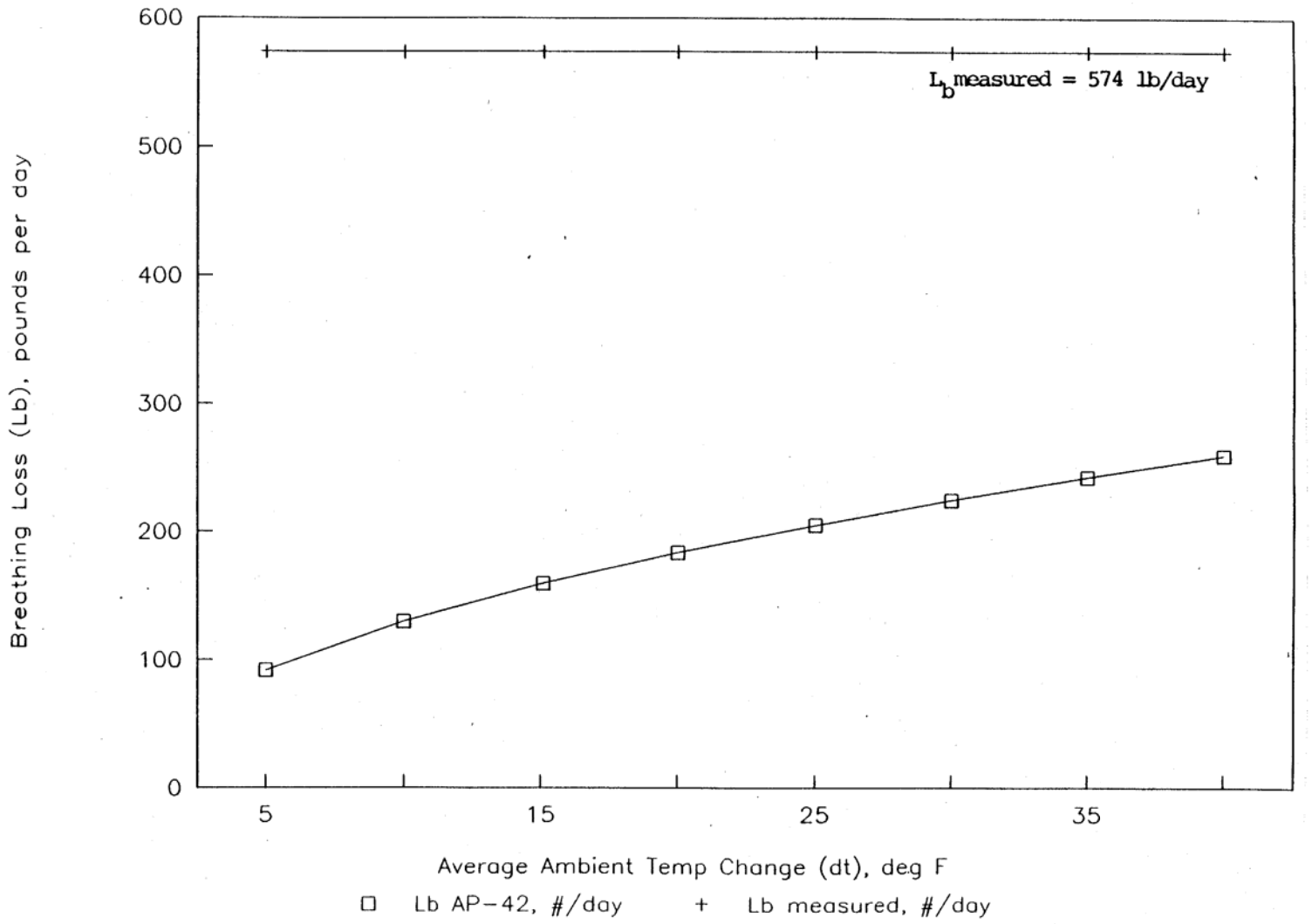

Figure 4-7. Sensitivity of Equation 4-1 to changes in the average ambient temperature range (ΔT).

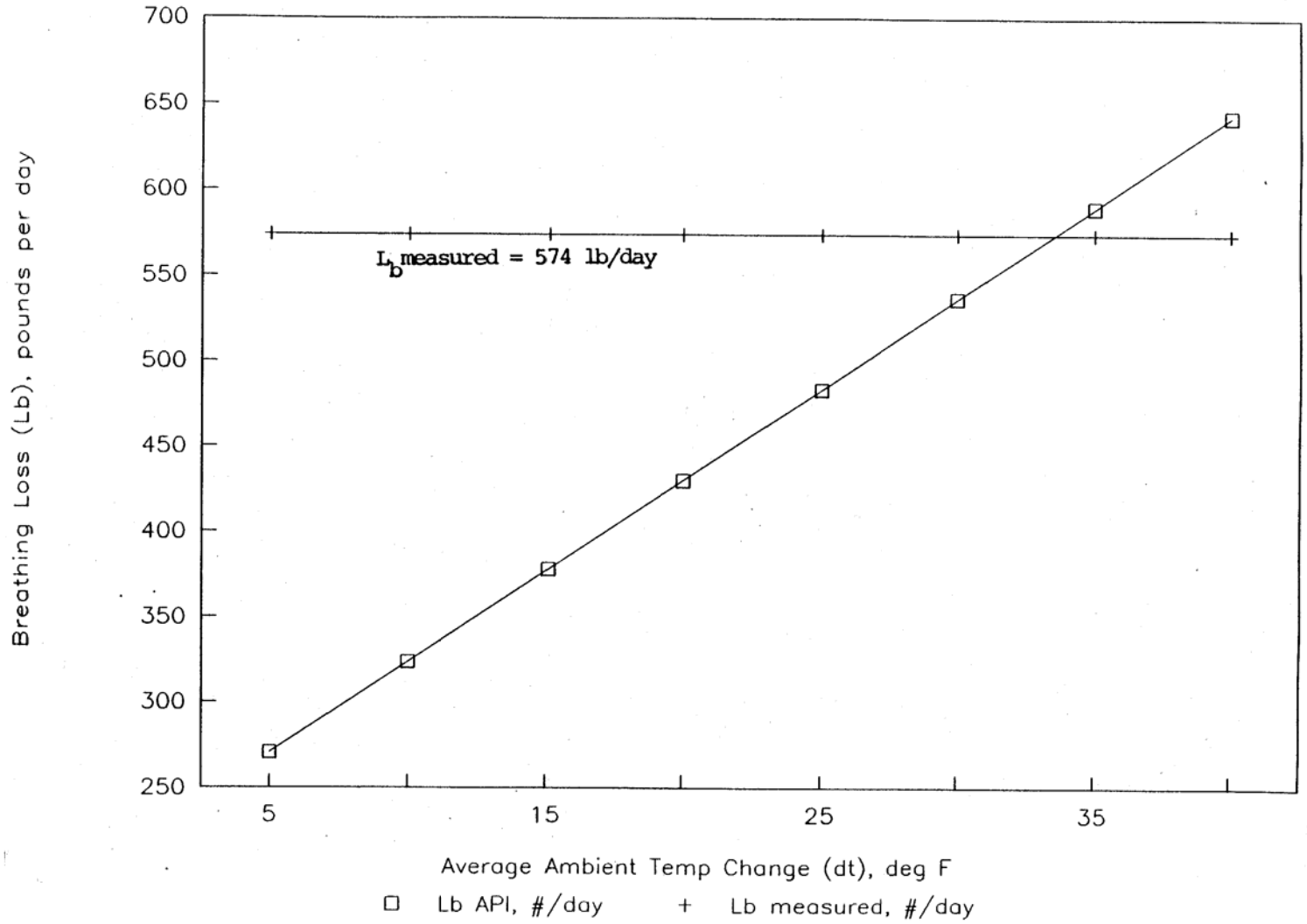

Figure 4-8. Sensitivity of Equation 4-2 to changes in the average ambient temperature range (ΔT).

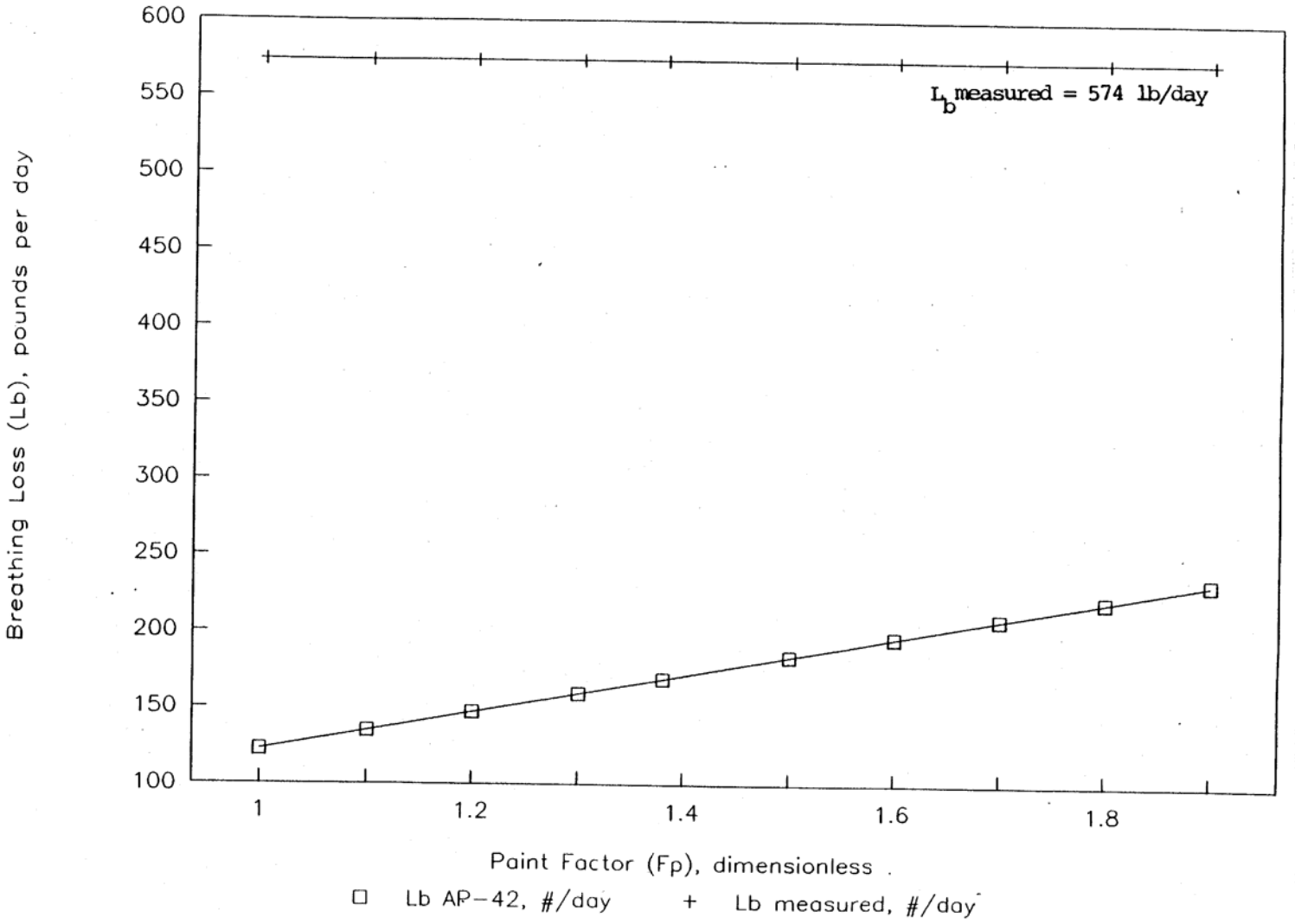

Figure 4-9. Sensitivity of Equation 4-1 to changes in the paint factor values (F_P).

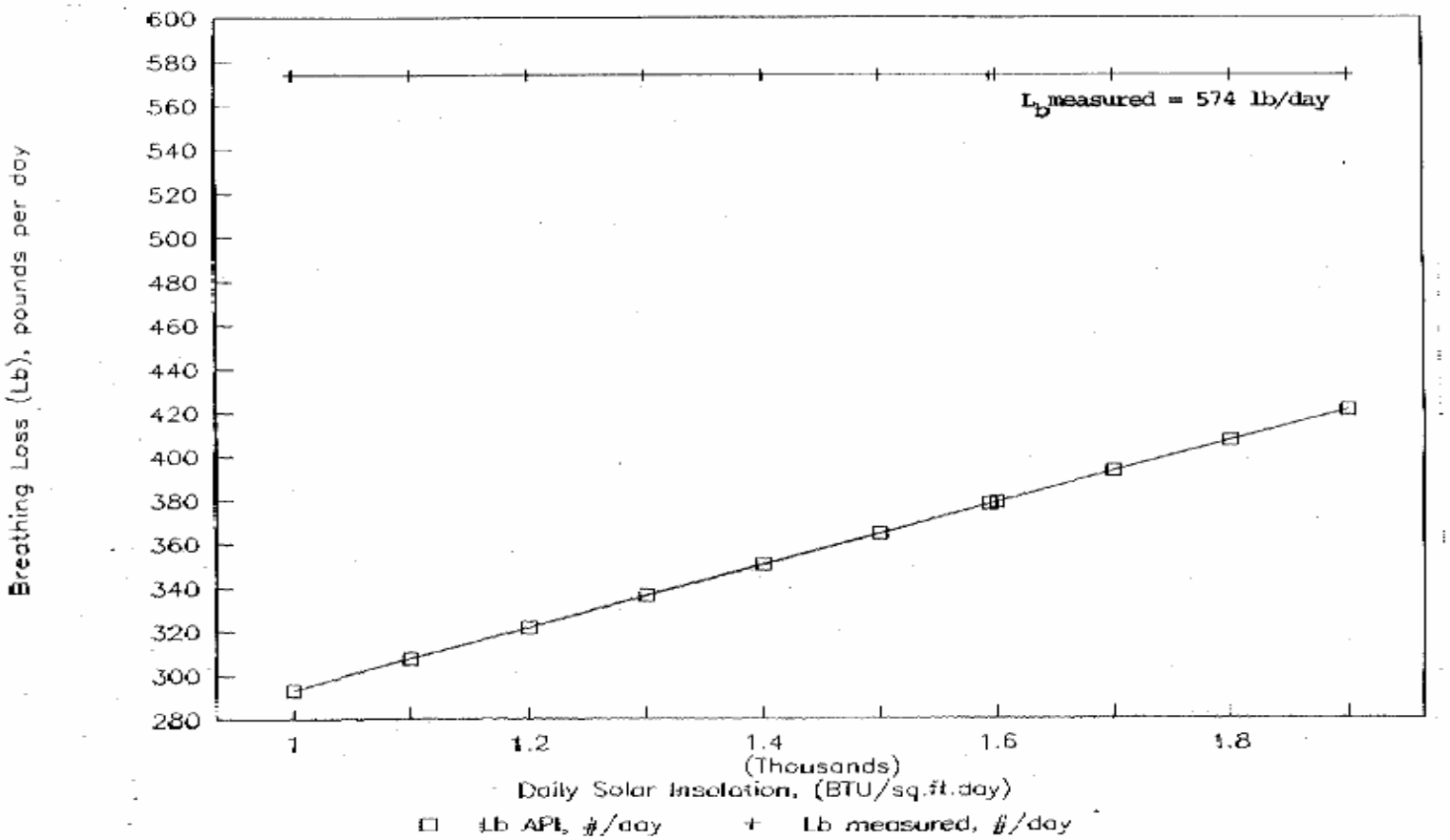

Figure 4-10. Sensitivity of Equation 4-2 to changes in the solar absorptance (∝).

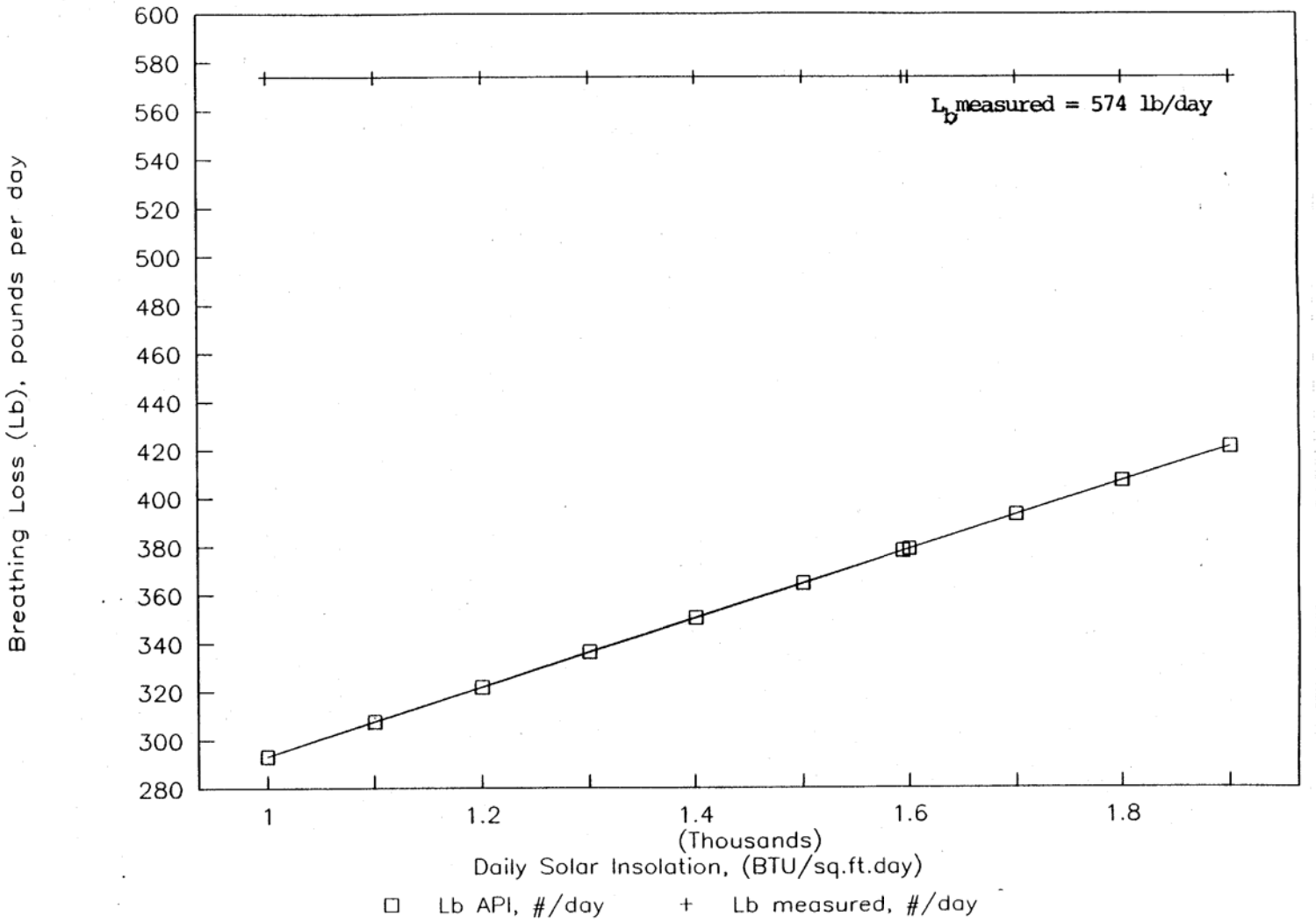

Figure 4-11. Sensitivity of Equation 4-2 to changes in the daily solar insolation factors (I).

TABLE 4-1. FIXED ROOF TANK BREATHING LOSS--COMPARISON OF ESTIMATING EQUATIONS--API DATA BASE

Test description	Stock type	Vapor pressure, psia	Breathing loss, lb/d		
			Eqn. 4-1	Eqn. 4-2	Actual
API-1	Fuel Oil No. 2	0.0049	0.0523	0.011	0.0152
API-2	Fuel Oil No. 2	0.0049	0.0575	0.0145	0.017
API-3	Fuel Oil No. 2	0.0050	0.0715	0.0172	0.0216
API-4	Fuel Oil No. 2	0.0051	0.0708	0.0171	0.0219
API-5	Fuel Oil No. 2	0.0051	0.0701	0.0155	0.0179
API-6	Fuel Oil No. 2	0.0051	0.0425	0.0053	0.0079
API-7	Fuel Oil No. 2	0.0075	0.0874	0.0374	0.0334
API-8	Fuel Oil No. 2	0.0101	0.1302	0.053	0.0502
API-9	Fuel Oil No. 2	0.0101	0.1112	0.0397	0.0478
API-10	Fuel Oil No. 2	0.0101	0.0890	0.0382	0.0441

TABLE 4-2. FIXED ROOF TANK BREATHING LOSS -- COMPARISON OF ESTIMATING EQUATIONS -- WOGA DATA BASE

Test description	Stock type	Vapor pressure, psia	Breathing loss, lb/d		
			Eqn. 4-1	Eqn. 4-2	Actual
WOGA-7B	Crude oil	1.5	136.3	254.6	196
WOGA-8A	Crude oil	0.6	46.5	145.2	80
WOGA-13A	Crude oil	0.8	17.7	22.0	129
WOGA-13B	Crude oil	0.8	14.0	19.5	146
WOGA-16A	Crude oil	2.7	99.8	282.7	177
WOGA-16B	Crude oil	2.7	98.7	278.7	256
WOGA-17A	Crude oil	3.4	122.9	448	574
WOGA-17B	Crude oil	3.4	129.2	446	576

TABLE 4-3. FIXED ROOF TANK BREATHING LOSS--COMPARISON OF ESTIMATING EQUATIONS--EPA DATA BASE

Test description	Stock type	Vapor pressure, psia	Breathing loss, lb/d		
			Eqn. 4-1	Eqn. 4-2	Actual
EPA-1A	Isopropanol	0.65	9.71	13.35	15
EPA-1B	Isopropanol	0.715	9.04	12.15	17
EPA-2A	Ethanol	0.895	11.03	12.99	6
EPA-2B	Ethanol	0.895	12.65	16.73	3.4
EPA-2C	Ethanol	0.895	10.35	10.42	5.7
EPA-3A	Acetic acid	0.23	22.12	45.64	24
EPA-3B	Acetic acid	0.23	27.44	70.5	45
EPA-5A	Ethyl benzene	0.2	9.67	13.56	11
EPA-5B	Ethyl benzene	0.2	10.64	15.59	15
EPA-6A	Cyclohexane	1.97	38.28	48.64	20
EPA-6B	Cyclohexane	1.97	31.08	48.64	17
EPA-6C	Cyclohexane	1.97	34.04	48.41	14

TABLE 4-4. COMPARISON OF EMISSION ESTIMATING EQUATIONS WITH BREATHING LOSS AS A FUNCTION OF STOCK TYPE

Aggregate of data	Equation 4-1	Equation 4-2
Bias, lb/d	-48.7	-2.5
Standard deviation, lb/d	115.9	52.9
Root mean squared error, lb/d	125.7	52.9
Fuel oil No. 2		
Bias, lb/d	0.051	-0.003
Standard deviation, lb/d	0.013	0.004
Root mean squared error, lb/d	0.052	0.005
No. of data points	10.0	10.0
Isopropanol		
Bias, lb/d	-6.6	-3.3
Standard deviation, lb/d	1.3	1.6
Root mean squared error, lb/d	6.8	3.6
No. of data points	2.0	2.0
Ethanol		
Bias, lb/d	6.3	8.3
Standard deviation, lb/d	2.1	3.6
Root mean squared error, lb/d	6.6	9.1
No. of data points	3.0	3.0
Acetic Acid		
Bias, lb/d	-9.7	23.6
Standard deviation, lb/d	7.8	1.9
Root mean squared error, lb/d	12.5	23.6
No. of data points	2.0	2.0
Ethyl benzene		
Bias, lb/d	-2.8	1.6
Standard deviation, lb/d	1.5	1.0
Root mean squared error, lb/d	3.2	1.9
No. of data points	2.0	2.0
Cyclohexane		
Bias, lb/d	17.5	31.6
Standard deviation, lb/d	2.5	2.4
Root mean squared error, lb/d	17.6	31.7
No. of data points	3.0	3.0
Crude oil		
Bias, lb/d	-186.9	-29.7
Standard deviation, lb/d	155.3	95.2
Root mean squared error, lb/d	243.0	99.7
No. of data points	8.0	8.0

TABLE 4-5. COMPARISON OF EMISSION ESTIMATING EQUATIONS WITH BREATHING LOSS AS A FUNCTION OF VAPOR PRESSURE

Vapor pressure range, psia	Equation 4-1	Equation 4-2
VP < 0.5		
Bias, lb/d	-1.8	3.6
Standard deviation, lb/d	4.5	8.2
Root mean squared error, lb/d	4.9	9.0
No. of data points	14	14
0.5 < VP < 1.0		
Bias, lb/d	-34.5	-18.7
Standard deviation, lb/d	52.4	60.4
Root mean squared error, lb/d	62.8	63.2
No. of data points	8	8
1.0 < VP < 2.0		
Bias, lb/d	-4.5	38.3
Standard deviation, lb/d	38.2	11.9
Root mean squared error, lb/d	38.5	40.1
No. of data points	4	4
VP > 2.0		
Bias, lb/d	-285.8	-31.9
Standard deviation, lb/d	165.5	100.5
Root mean squared error, lb/d	330.2	105.4
No. of data points	4	4

TABLE 4-6. FIXED ROOF TANK BREATHING LOSS -- COMPARISON OF ESTIMATING EQUATIONS -- WOGA DATA BASE DEFAULT VALUES

Test description	Stock type	Vapor pressure, psia	Breathing loss, lb/d		
			Eqn. 4-1	Eqn. 4-2	Actual
WOGA-7B	Crude oil	1.5	54.7	168.9	196
WOGA-8A	Crude oil	0.6	19.9	56.8	80
WOGA-13A	Crude oil	0.8	7.7	11.8	129
WOGA-13B	Crude oil	0.8	7.7	11.8	146
WOGA-16A	Crude oil	2.7	144.8	341.9	177
WOGA-16B	Crude oil	2.7	144.8	341.9	256
WOGA-17A	Crude oil	3.4	159.3	377.9	574
WOGA-17B	Crude oil	3.4	159.3	377.9	576

TABLE 4-7. FIXED ROOF TANK BREATHING LOSS--COMPARISON OF ESTIMATING EQUATIONS--EPA DATA BASE DEFAULT VALUES

Test description	Stock type	Vapor pressure, psia	Breathing loss, lb/d		
			Eqn. 4-1	Eqn. 4-2	Actual
EPA-1A	Isopropanol	0.65	9.9	10.1	15
EPA-1B	Isopropanol	0.715	9.9	10.1	17
EPA-2A	Ethanol	0.895	16.1	20.1	6
EPA-2B	Ethanol	0.895	16.1	20.1	3.4
EPA-2C	Ethanol	0.895	16.1	20.1	5.7
EPA-3A	Acetic acid	0.23	25.7	33.7	24
EPA-3B	Acetic acid	0.23	25.7	33.7	45
EPA-5A	Ethyl benzene	0.2	10.2	7.9	11
EPA-5B	Ethyl benzene	0.2	10.2	7.9	15
EPA-6A	Cyclohexane	1.97	43.5	50.4	20
EPA-6B	Cyclohexane	1.97	43.5	50.4	17
EPA-6C	Cyclohexane	1.97	43.5	50.4	14

TABLE 4-8. SUMMARY OF STATISTICAL ANALYSIS VALUES

Statistical analysis, lb/d	All data		Excluding fuel oil data				Excluding fuel oil data and crude oil data			
	Actual data		Actual data		Default data		Actual data		Default data	
	EQN 4-1	EQN 4-2	EQN 4-1	EQN 4-2	EQN 4-1	EQN 4-2	EQN 4-1	EQN 4-2	EQN 4-1	EQN 4-2
Bias	-48.7	-2.5	-73.1	-3.7	-67.9	-16.2	2.7	13.6	6.4	10.2
Standard deviation	115.9	52.9	135.5	64.7	127.9	85	10.8	13.5	14.4	16.2
Root mean squared error	125.7	52.9	153.9	64.8	144.8	86.5	11.1	19.2	15.7	19.2

TABLE 4-9. COMPARISON OF BREATHING LOSS ESTIMATING EQUATIONS (USING DEFAULT VALUES)--PREDICTIVE ABILITY AS A FUNCTION OF PRODUCT TYPE

Product	WOGA and EPA data bases, lb/d	
	Equation 4-1	Equation 4-2
Isopropanol		
Bias, lb/d	-6.1	-5.9
Standard deviation, lb/d	1.0	1.0
Root mean squared error, lb/d	6.2	6.0
Data points	2	2
Ethanol		
Bias, lb/d	11.1	15.1
Standard deviation, lb/d	1.2	1.2
Root mean squared error, lb/d	11.1	15.1
Data points	3	3
Acetic Acid		
Bias, lb/d	-8.8	-0.8
Standard deviation, lb/d	10.5	10.5
Root mean squared error, lb/d	13.7	10.5
Data points	2	2
Ethyl benzene		
Bias, lb/d	-2.8	-5.1
Standard deviation, lb/d	2.0	2.0
Root mean squared error, lb/d	3.4	5.5
Data points	2	2
Cyclohexane		
Bias, lb/d	26.5	33.4
Standard deviation, lb/d	2.4	2.4
Root mean squared error,lb/d	26.6	33.5
Data points	3	3
Crude oil		
Bias, lb/d	-179.5	-55.6
Standard deviation, lb/d	140.9	122.7
Root mean squared error, lb/d	228.2	134.8
Data points	8	8

TABLE 4-10. BREATHING LOSS ESTIMATING EQUATIONS FIXED ROOF TANKS SENSITIVITY ANALYSIS--COMPARISON BETWEEN THE AP-42 AND NEW API EQUATION BASELINE CONDITIONS

Parameter	Default value
Molecular weight (M_V)	50 lb/lb mole
Reid vapor pressure (RVP)	5.5 psia
Vapor pressure (P_V)	3.35 psia
Tank diameter (D)	175.8 ft
Vapor space height (H or H_{VO})	20.75 ft
Average ambient temperature (T_{AA})	62.6°F
Average ambient temperature change ($\triangle T$)	15.1°F
alpha	0.355
Paint factor (F_p)	1.3
Solar isolation (I)	1,594 Btu/ft^2 d
Breather vent pressure/vacuum difference ($\triangle P_B$)	0.06 psig
Small diam. adjustment (C)	1
Product factor (K_C)	0.65

TABLE 4-11. BREATHING LOSS ESTIMATING EQUATIONS FIXED ROOF TANKS SENSITIVITY ANALYSIS

Parameter	Baseline (default) value	Units	Difference in calculated breathing loss, lb/d			Change in emissions/change in default variable	
			Typical variance of default value	Current equation	Revised equation	Current equation	Revised equation
Molecular weight	50	lb/lb-mole	20	64	150	3.2 lb/lb-mole	7.5 lb/lb-mole
Vapor pressure	3.35	psia	1.5	64	158	42.7 lb/psia	105.3 lb/psia
Vapor space height	20.75	ft	-15 +15	80 50	150 36	-80 lb/-15 ft +50 lb/+15 ft	-150 lb/-15 ft +36 lb/+15 ft
Ambient temperature change	15.1	°F	25	100	265	100 lb/10°F	265 lb/10°F
Paint color/ condition Fp (AP-42 equation) alpha (API equation)	1.3 0.355	NA NA	0.3 0.18	37 NA	NA 118	+37 lb/0.3 NA	NA 118 lb/0.18
Solar insolation	1,594	$Btu/ft^2 \cdot d$	600	NA	85	NA	85 lb/600 $Btu/ft^2 \cdot d$

4.5 REFERENCES

1. *Evaporation Loss from Fixed-Roof Tanks*, Bulletin 2518, First Edition, American Petroleum Institute, Washington, DC, June 1962.

2. *Evaporative Loss from Fixed-Roof Tanks*, Bulletin 2518, Second Edition, American Petroleum Institute, Washington, DC, October 1991.

3. *Evaporative Loss from Fixed-Roof Tanks; Documentation File for API Publication 2518*, Second Edition, American Petroleum Institute, Washington, DC, September 1990.

4. *Hydrocarbon Emissions from Fixed-Roof Petroleum Tanks*, Engineering Science, Inc., prepared for the Western Oil and Gas Association, July 1977.

5. *Breathing Loss Emissions from Fixed-Roof Petrochemical Storage Tanks*, Third Draft, Engineering Science, Inc., prepared for the U. S. Environmental Protection Agency, December 1978.

6. *Compilation of Air Pollution Emission Factors*, AP-42, Supplement E, Chapter 12. September 1992.

5. EMISSION ESTIMATION PROCEDURES FOR FLOATING ROOF TANKS

The purpose of this chapter is to present the statistical analyses that were performed on the floating roof tank emission estimation procedures. In the first section, a discussion of the results of the statistical analyses on the test tank data performed by API in developing the emission estimation equations is presented. The second section documents the results of a statistical analysis to determine how well the procedures predict emissions based on actual tank test data. The third section documents the results of sensitivity analyses performed on selected variables in the emission estimating procedures. The fourth section presents the conclusions from the overall analyses.

5.1 STATISTICAL ANALYSES - API TANK TEST DATA

The first step in the analysis of the floating roof tank emission estimating factors and equations was a comprehensive review and evaluation of the procedures that the American Petroleum Institute (API) and their contractors, Chicago Bridge & Iron Company (CBI); Cermak, Peterka, Peterson, Inc. (CPP); and the TGB Partnership used to develop them. The primary objectives of the analysis were to assure that valid statistical procedures were used to evaluate the data and to develop better information on the precision of the coefficients that were developed for the estimating equations. Information on the precision of the coefficients can provide some indication of the uncertainty of the emission estimates generated by the equations. The primary sources of information used in the analysis were API Publications 2517 and 2519 and their associated background documentation files.[1-4] Additional sources of information were two draft documents API submitted to EPA which summarized the procedures API used for revising the evaporative loss estimating procedures and factors. These documents are: Manual of Petroleum Measurement Standards Chapter 19--Evaporative Loss Measurements, Section 2--Evaporative Loss From Floating-Roof Tanks; and Documentation of Rim-seal Loss Factors for the Manual of Petroleum Measurement Standards, Chapter 19--Evaporative Loss from Floating-Roof Tanks.[5-6]

Personnel at API were extremely helpful in providing the background information needed for the analysis. However, documentation was lacking on the basis of the development of clingage factors. The analyses focused on seven components of the floating roof tank estimating equations--the development of the rim-seal loss factors, the diameter function, the product factors, the deck fitting loss factors, the fitting wind speed correction factor, the IFRT deck seam loss factors, and the vapor pressure function. The evaluations of the analyses for each of these seven components are discussed in the following sections.

5.1.1 Evaluation of Rim-seal Loss Factors

5.1.1.1 Development Methodology. The rim-seal loss equation and factors introduced in the Second Edition of API Publication 2517 and used in the previous version of AP-42 Section 7.1 (July 1995) did not allow for a total rim-seal loss factor other than 0 at a wind speed of 0 miles per hour (mph) and were not considered to be valid at wind speeds below 2 mph. The new floating roof tank rim-seal loss estimating equation developed by API involves three rim-seal loss factors: (1) the zero wind speed rim-seal loss factor, K_{Ra}; (2) the wind speed dependent rim-seal loss factor, K_{Rb}; and (3) the rim-seal wind speed exponent, n. In the new equation, the K_{Ra} term extends the applicability of the equation and allows for a nonzero value of the 0 mph loss factor:

$$F_R = K_{Ra} + K_{Rb} v^n$$

where:

F_R = total rim-seal loss factor, lb-mole/yr
K_{Ra} = zero wind speed rim-seal loss factor, lb-mole/yr
K_{Rb} = wind speed dependent rim-seal loss factor, lb-mole/(mph)^n-yr
v = site ambient wind speed, mph
n = seal wind speed exponent, dimensionless

Sets of these new factors were developed by API for 12 distinct tank construction/rim-seal configurations for average fitting rim-seals and 9 distinct tank construction/rim-seal configurations for tight fitting rim-seals. The data used to develop estimates for the rim-seal loss factors were obtained from the documentation file for API Publication 2517.[2] This file contains data from a test program conducted for API by CBI on a 20 foot diameter test tank. In that test program, emission estimates were generated based on hydrocarbon measurements downstream from the test tank under steady state conditions and a constant wind speed. Test runs were conducted for a number of primary and secondary rim-seal configurations and gap speeds at wind speeds that ranged from 2.2 to 13.1 mph.

For each rim-seal configuration, information for tanks with two to four sets of gap sizes were averaged to obtain the final loss factors for average fitting rim-seals and the 0 gap size data were used to obtain loss factors for tight fitting rim-seals. Two distinct computational procedures were used, depending on the availability of information. In the first case, data were available for the specific combination of primary and secondary rim-seal of interest for all gap sizes included in the analysis. In the second case, data were unavailable for the specific combination of primary and secondary rim-seal of interest, so secondary rim-seal emission reductions were estimated from analogous configurations. Procedures used for each case are outlined below.

For cases with data available for the combination of primary and secondary rim-seal of interest, estimating equation coefficients (K_{Ra}, K_{Rb}, and n) were obtained using a three step process. The first two steps generated coefficients for specific gap sizes, while the third step averaged across the gap sizes of interest. However, prior to the first step, the raw data from the documentation file were modified by replacing emission rates for replicate tests at the same wind speed with the average emission rate for all replicates at that wind speed. The three steps used to obtain the final coefficient estimates are outlined below.

In the first step, the values of S_{Ra} (a coefficient analogous to the zero wind speed loss, K_{Ra}, but in units of lb/d) were determined using an iterative process. First, an exponential curve fit routine was used to estimate a starting value for S_{Ra}. Using that estimate of S_{Ra}, net emission rates were calculated for each test by subtracting S_{Ra} from the measured value of the emission rate. A standard least squares regression routine was then used to fit a linear equation with the log transform of the net emission rate as the dependent variable and the net wind speed as the independent variable. The estimate of S_{Ra} was then changed iteratively and the process was repeated. The estimate which yielded the best fit linear equation was assumed to be the best estimate of S_{Ra}.

In the second step, the estimate of S_{Ra} obtained from Step 1 was subtracted from the measured emission rate for each test to generate a net emission rate (E_{net}) for the test. Both the net emission rate and the measured wind speed for the test were log transformed and an equation of the following form was fit, where E_{net} and S_{Rb} have units of lb/d rather than lb-mole/ft-yr.

$$\log(E_{net}) = \log(S_{Rb}) + n^* \log(v)$$

If the value of E_{net} obtained was less than 0, that test was eliminated from the analyses. Least squares regression was used to obtain estimates of n and $\log(S_{Rb})$, which were then exponentiated to obtain an estimate of S_{Rb} (analogous to K_{Rb}, the wind dependent loss factor).

In the third step, estimates of the percentage of tanks represented by each gap size used in Steps 1 and 2 were used to generate a weighted average estimating equation for each rim-seal configuration. For each gap size considered, the equations generated in Steps 1 and 2 were used to generate estimated emission rates in lb/d at wind speeds of 0, 4, and 10 mph. The percentage weights were then applied to obtain average emission rates in lb/d at each of these wind speeds. The value obtained for a wind speed of 0 mph was used as the estimate of S_{Ra}. To obtain the estimates of n and S_{Rb}, net emission rates were calculated by subtracting the estimate of S_{Ra} from the average emission rates at 4 and 10 mph. The resulting net emission rates at two wind speeds were log transformed and a linear equation was fit to the two points to obtain estimates of n and $\log(S_{Rb})$, which was exponentiated to obtain an estimate of S_{Rb}. Finally, S_{Ra} and S_{Rb} were converted to K_{Ra} and K_{Rb}.

For six of the primary/secondary combinations of interest, no test data were available. However, test data were generally available for all primary rim-seals of interest with no secondary rim-seal and all secondary rim-seals of interest applied in combination with at least one of the primary rim-seals. Consequently, loss factors for the primary/secondary combinations without test data were developed by applying the reduction, or "control efficiency," achieved by the secondary seal of interest applied in combination with a different type primary rim-seal to the "uncontrolled" emissions from the primary rim-seal of interest.

Table 5-1 provides an overview of the data that were used to develop the rim-seal loss factors for floating roof tanks; the comment column indicates the factors that were calculated indirectly. The actual factors are presented in Table 5-2, and those factors that were calculated indirectly, by applying a secondary rim-seal control efficiency, are denoted by an asterisk.

TABLE 5-1. BASIS OF RIM-SEAL LOSS FACTORS

Tank construction	Rim seal system		Gap area (in.)		Gap percent	Tests/ points	Case	Comments
	Basic	Extension	Prim.	Sec.				
Welded	Mechanical shoe primary	Primary only	0	NA	10	10/47	1a1	
			1.7, 3.8	NA	80	3/10	1a2	
			9.4	NA	10	1/5	1a3	
		Shoe-mounted secondary	0	0	75	1/6	1b1	
			0	0.4	25	1/6	1b2	
		Rim-mounted secondary	0, 1.7, 3.8	0	75	NA	1c1	Calculated from a set of rim mounted secondary data on a LRMF applied to reduce emissions for mechanical shoe primary seal only data.
			1.7, 3.8	0	25	NA	1c2	
	LMRF seal[a]	Primary only	0	NA	65	1/7	2a1	
			1.3, 2.6	NA	35	3/22	2a2	
		Weather-shield	0, 1.3	>9<27	65	NA	2b1	One set only of weather-shield data on primary with 2.6 gap. Used these data to calculate reduction and applied to primary tight-fitting and average fitting data.
			1.3, 2.6	>9<27	35	NA	2b2	
		Rim-mounted secondary	0, 1.3	0	75	NA	2c1	One set of data for rim mount secondary on primary with 2.6 gap. Used these data tight fitting and average fitting to calculate reduction and applied to primary data.
			1.3, 2.6	0	25	NA	2c2	
	VMRF seal[b]	Primary only	0	NA	65	10/57	3a1	
			1	NA	35	1/13	3a2	
		Weather shield	0	>9<27	A		3b1	Efficiencies from weathershield on LMRF primary applied to VMRF primary seal.
			1	>9<27	NA		3b2	
		Rim-mounted secondary	0, 1	0	75	4/20	3c1	
			1	1	25	3/16	3c2	

5-4

TABLE 5-1. (continued)

Tank construction	Rim seal system		Gap area (in.)		Gap percent	Tests/ points	Case	Comments
	Basic	Extension	Prim.	Sec.				
Riveted	Mechanical shoe primary	Primary only	0	NA	5	10/47	4a1	
			1.7, 3.8	NA	55	3/10	4a2	
			9.4	NA	35	1/5	4a3	
			13.3	NA	5	1/5	4a4	
		Shoe-mounted secondary	0-13.3	0.4		NA	4b1	Calculated control efficiency using primary seal only (three tests) and one test with a secondary seal; applied this control efficiency to the average primary only factor
		Rim-mounted secondary	0-3.8	0	20	NA	4c1	
			1.7-3.8	0	70	NA	4c2	Efficiency of rim-mounted secondary seal with LMRF primary applied to selected mechanical shoe primary seal only data
			9.4	0.76-2.66	10	NA	4c3	

[a]Liquid-mounted, resilient foam seals.
[b]Vapor-mounted, resilient foam seals.

5-5

TABLE 5-2. SUMMARY OF RIM-SEAL LOSS FACTORS, K_{Ra}, K_{Rb}, AND n

Tank construction and rim-seal system	Average-fitting seals			Tight-fitting seals		
	K_{Ra}	K_{Rb}	n	K_{Ra}	K_{Rb}	n
	lb-mole/mph^{n}ft·yr	lb-mole/ft·yr	(dimensionless)	lb-mole/mph^{n}ft·yr	lb-mole/ft·yr	(dimensionless)
Welded tanks						
Mechanical-shoe seal						
Primary only	5.8[a]	0.3[a]	2.1[a]	1.5	0.4	1.9
Shoe-mounted secondary	1.6	0.3	1.6	1.0	0.4	1.5
Rim-mounted secondary	0.6*	0.4*	1.0*	0.4*	0.4*	1.0*
Liquid-mounted resilient-filled seal						
Primary only	1.6	0.3	1.5	1.0	0.08	1.8
Weather shield	0.7*	0.3*	1.2*	0.4*	0.2*	1.3*
Rim-mounted secondary	0.3*	0.6*	0.3*	0.2*	0.4*	0.4*
Vapor-mounted resilient-filled seal						
Primary only	6.7[b]	0.2	3.0	5.6	0.2	2.4
Weather shield	3.3*	0.1*	3.0*	2.8*	0.1*	2.3*
Rim-mounted secondary	2.2	0.003	4.3	2.2	0.02	2.6
Riveted tanks						
Mechanical-shoe seal						
Primary only	10.8	0.4	2.0	c	c	c
Shoe-mounted secondary	9.2*	0.2*	1.9*	c	c	c
Rim-mounted secondary	1.1*	0.3*	1.5*	c	c	c

Note: The rim-seal loss factors K_{Ra}, K_{Rb}, and n may only be used for wind speeds below 15 miles per hour. Factors calculated indirectly are denoted by an asterisk.

[a]If no specific information is available, a welded tank with an average-fitting mechanical-shoe primary seal only can be assumed to represent the most common or typical construction and rim-seal system in use for external and domed external floating roof tanks.

[b]If no specific information is available, this value can be assumed to represent the most common or typical rim-seal system currently in use for internal floating roof tanks.

[c]No evaporative-loss information is available for riveted tanks with consistently tight fitting rim-seal systems.

5-6

5.1.1.2 Evaluation. The complete results of the evaluation of rim-seal loss factors are documented in a report prepared for MRI entitled: Evaluation of Rim-seal Loss Factors for AP-42 Use, prepared by Dr. Dennis Wallace and dated September 1995.[7]

The verification of the API estimating equations addressed three questions: (1) whether the computations performed by API could be replicated; (2) whether the replacement of the raw test data with an average emission rate at a particular wind speed had a significant effect on the final estimates; and (3) whether the linearity assumed in the averaging process, particularly when ratio estimates were involved, had a significant effect on estimates. Also, analyses were conducted to assess the effect of primary seal type, primary seal gap size, and secondary seal gap size on secondary seal performance. Finally, uncertainty estimates were developed for two estimation scenarios (individual tanks and population means).

5.1.1.2.1 Verification of API computations. The computations performed by API were replicated using the raw data from the documentation file; no substantive problems were identified.

5.1.1.2.2 Replacement of the raw test data with an average emission rate. To address the second question, three alternative analyses were performed. First, nonlinear regression was used to estimate all three parameters. Second, the procedures used by API to compute estimates were replicated using the measured emission rates for each test, rather than the average emission rate for a particular wind speed. Third, the procedures used by API to compute estimates were replicated using average emission rates for a given wind speed, but with only a single observation at each wind speed rather than replication of the averages.

The results for the individual test conditions are presented in Table 5-3. Note that the coefficients generated using the nonlinear models are quite different than both the API coefficients and the coefficients generated by MRI using linear model analyses on log transformed data. Examination of the residuals from the different analyses suggested that the linear model approaches provided better fits and were more consistent with model assumptions than were the nonlinear model results. Consequently, the linear model approach used by API is considered appropriate.

TABLE 5-3. COMPARISON OF ESTIMATING EQUATION COEFFICIENTS: INDIVIDUAL CASES

Case	Number of tests[a]	API coefficients			Nonlinear model coefficients			Linear model coefficients					
								Test specific			Wind speed average		
		S_{Ra}	S_{Rb}	n	S_{Ra}	S_{Rb}	n	S_{Ra}	S_{Rb}	n	S_{Ra}	S_{Rb}	n
1a1	47 (39)	0.39	0.0956	1.976	2.383	0.00108	3.780	0.39	0.0947	1.974	0.39	0.0993	1.928
1a2	10 (9)	1.03	0.0491	2.130	1.103	0.0448	2.167	1.03	0.0456	2.162	1.03	0.0525	2.101
1a3	5	5.8	0.1522	1.972	4.011	0.4109	1.598	5.8	0.1522	1.972	--	--	--
1b1	6	0.24	0.0902	1.458	0.212	0.0981	1.428	0.24	0.0902	1.458	--	--	--
1b2	6	0.88	0.0380	1.994	0.186	0.2644	1.228	0.88	0.0380	1.994	--	--	--
1c1	57 (45)b	0.37	0.1049	1.922	2.168	0.00239	3.438	0.37	0.1033	1.923	0.37	0.1085	1.876
1c2													
2a1	7	0.241	0.0197	1.848	-0.062	0.1343	1.100	0.241	0.0197	1.848	--	--	--
2a2	22	0.68	0.1935	1.283	0.473	0.3179	1.121	0.68	0.1935	1.283	--	--	--
2b1	16	0.18	0.1001	1.340	0.475	0.0639	1.493	0.18	0.1001	1.340	--	--	--
2b2	c												
2c1	d												
2c2	c												
3a1	57*(43)	1.41	0.0484	2.390	0	0.599	1.326	1.41	0.0739	2.200	1.41	0.0542	2.342
3a2	13	2.14	0.0821	3.209	0	4.110	1.478	2.14	0.0821	3.209	--	--	--
3b1	e												
3b2	f												
3c1	20 (16)	0.55	0.0060	2.597	0.733	0.000357	3.859	0.55	0.00566	2.622	0.55	0.0058	2.631
3c2	16	0.52	0.0007	4.922	-10	0.329	2.418	0.52	0.00067	4.922	--	--	--

5-8

TABLE 5-3. (continued)

Case	Number of tests[a]	API coefficients			Nonlinear model coefficients			Linear model coefficients					
								Test specific			Wind speed average		
		S_{Ra}	S_{Rb}	n	S_{Ra}	S_{Rb}	n	S_{Ra}	S_{Rb}	n	S_{Ra}	S_{Rb}	n
4a1 4a2 4a3 4a4	g b h	1.46	0.1612	1.694	2.155	0.0653	2.046	1.46	0.1612	1.694	--	--	--
4b1	i	2.689	0.922	2.012	--	--	--	2.689	0.0631	1.9041	--	--	--
4c1 4c2 4c3	j a h												
C31	7	0.43	0.0372	1.113	--	--	--	0.43	0.0372	1.113	--	--	--
C36,C38	12	1.53	0.0179	2.457	-0.58	0.925	0.845	1.53	0.0179	2.457	--	--	--
C35	8	0.76	0.0170	2.191	0.557	0.0664	1.602	0.76	0.0170	2.191	----	----	----
W24,W25	16	0.12	0.0579	1.979	-4.2	1.478	0.8575	0.12	0.0579	1.979			

[a]Numbers in parentheses represent average wind speed.
[b]Same as Case 1a2
[c]Same as Case 2a2
[d]Same as Case 2b1
[e]Same as Case 3a1
[f]Same as Case 3a2
[g]Same as Case 1a1
[h]Same as Case 1a3
[i]Weighted average from 4a
[j]Same as Case 1c1

5-9

There were some differences in the specific coefficients for the different linear model approaches, but they were relatively minor. Furthermore, the values of S_{Rb} and n tend to adjust in opposite directions. Consequently, although using the actual data rather than the average data would have been more appropriate, the results differ so little that modification of the estimating equations is not warranted.

5.1.1.2.3 Linearity assumption. To address the third question, two alternative average estimates were computed. The first replicated the API procedures, but measured, rather than average, emission rates were used. The second procedure was fundamentally different in that emission rates were computed at 0.5 mph increments from 0.5 mph to 14 mph, weighted average emission rates were computed at each wind speed (using the appropriate ratio for secondary seal performance at that wind speed), and a linear regression equation was fit to log transformed net emissions and log transformed wind speeds to estimate coefficients. The results of the analyses are described below.

Estimating equation coefficients and estimated emission rates were calculated at wind speeds of 4, 8, and 12 mph in units of lb-mole/ft-yr for three averaging techniques. The first MRI technique was comparable to the API technique described above, but actual, rather than average, emission data were used in the computations. The second MRI technique involved computation of average emissions at wind speeds over the range of 0 to 14 mph and fitting a regression model to the computed values. The second MRI procedure provides better estimates if the ratio procedures used to estimate emissions result in extreme nonlinearities. Table 5-4 summarizes the results of using the alternative averaging techniques. The coefficients varied somewhat, but the effects on emissions were minimal, particularly in light of the uncertainties in the estimates. Average emissions for the 12 scenarios of interest varied little as a function of averaging method. Again, these analyses indicate that the equations generated by API are acceptable and provide no reason to modify the equations.

TABLE 5-4. COMPARISON OF ESTIMATING EQUATIONS FOR AVERAGE FITTING RIM-SEAL LOSS FACTORS

Case	Description	Method[a]	Coefficients			Emissions (lb-mole/ft-yr)		
			K_{Ra}	K_{Rb}	N	4mph	8mph	12mph
1A	Mechanical shoe--primary only	API	5.8	0.25	2.1	10.4	25.5	52.0
		MRI1	5.8	0.24	2.1	10.2	24.7	50.1
		MRI2	5.8	0.24	2.1	10.2	24.7	50.1
1b	Mechanical shoe--shoe-mounted secondary	API	1.6	0.29	1.6	4.3	9.7	17.1
		MRI1	1.6	0.29	1.6	4.3	9.7	17.1
		MRI2	1.6	0.30	1.6	4.4	10.0	17.6
1C	Mechanical shoe--rim-mounted secondary	API	0.60	0.38	1.0	2.1	3.6	5.2
		MRI1	0.60	0.37	1.0	2.1	3.6	5.0
		MRI2	0.60	0.19	1.3	1.8	3.4	5.4
2A	Liquid mounted seal--primary only	API	1.6	0.29	1.5	3.9	8.2	13.7
		MRI1	1.6	0.29	1.5	3.9	8.2	13.7
		MRI2	1.6	0.57	1.2	4.6	8.5	12.8
2B	Liquid mounted seal—weathershield	API	0.71	0.33	1.2	2.5	4.7	7.2
		MRI1	0.71	0.33	1.2	2.5	4.7	7.2
		MRI2	0.71	0.29	1.3	2.5	5.0	8.0
2C	Liquid mounted seal--rim-mounted secondary	API	0.34	0.57	0.33	1.2	1.5	1.6
		MRI1	0.34	0.57	0.33	1.2	1.5	1.6
		MRI2	0.34	0.23	0.75	1.0	1.4	1.8
3A	Vapor mounted seal--primary only	API	6.7	0.19	3.0	18.9	104	335
		MRI1	6.7	0.22	3.0	20.8	119	387
		MRI2	6.7	0.29	2.9	22.9	127	398
3B	Vapor mounted seal—weathershield	API	3.3	0.12	3.0	11.0	64.7	211
		MRI1	3.3	0.14	2.9	11.1	61.5	192
		MRI2	3.3	0.18	2.8	12.0	64.1	193
3C	Vapor mounted seal--rim-mounted secondary	API	2.2	0.0035	4.3	3.6	29.0	155
		MRI1	2.2	0.0034	4.3	3.5	28.2	151
		MRI2	2.2	0.012	3.7	4.2	28.5	120
4A	Riveted: mechanical shoe secondary	API	11	0.37	2.0	16.9	34.7	64.3
		MRI1	11	0.36	2.0	16.8	34.0	62.8
		MRI2	11	0.36	2.0	16.8	34.0	62.8
4B	Riveted: mechanical shoe shoe-mounted secondary	API	9.2	0.23	1.9	12.4	21.2	35.0
		MRI1	9.2	0.25	1.9	12.7	22.2	37.3
		MRI2	9.2	0.29	1.8	12.7	21.4	34.6
4C	Riveted: mechanical shoe rim-mounted secondary	API	1.1	0.27	1.5	3.3	7.2	12.3
		MRI1	1.1	0.26	1.5	3.2	6.9	11.9
		MRI2	1.1	0.21	1.6	3.0	7.0	12.3

5-11

5.1.1.2.4 Effect of rim-seal type and gap size on rim-seal performance. As noted previously, no specific test tank data were available for six of the primary/secondary rim-seal configurations. For each of those configurations, a comparison case was used to estimate the reduction in emissions associated with applying a secondary rim-seal. An assumption embedded in these computations is that the emission reduction, or the incremental control efficiency, achieved by a secondary rim-seal is not affected greatly by the type of primary rim-seal or rim-seal gap size. To evaluate this assumption, analyses were conducted to assess the effect of primary rim-seal type on secondary rim-seal performance, the effect of primary seal gap size on secondary rim-seal performance, and the effect of secondary seal gap size on secondary rim-seal performance.

To evaluate the effect of primary rim-seal type on secondary rim-seal performance, three cases were compared. The results are graphically presented in Figures 5-1 and 5-2, respectively. For both emission rates and reduction percentages, the rim-mounted secondary seal appears to perform comparably for mechanical shoe and liquid-mounted primary rim-seals (API estimate), but quite differently for vapor-mounted primary rim-seals. Because the comparison results were not used for vapor-mounted rim-seals in the API analyses, these results provide no basis for modifying any of those emission factors. However, they do suggest that care should be taken in evaluating secondary rim-seal performance on future tests conducted under the new protocol being developed by API for certifying loss factors for new rim-seal configurations.

To examine the effect of primary rim-seal gap size on secondary rim-seal performance, five cases were examined. Each case involved a rim-mounted secondary seal with no gap. The results are graphically presented in Figures 5-3 and 5-4. With the exception of the vapor-mounted seal with no primary gap, the data indicated some difference in efficiency at low wind speeds. However, for wind speeds above 6 to 7 mph, the data indicated that the primary seal gap size has little effect on efficiency. These results suggest that the primary seal gap will have little effect on the efficiency for cases generated by API, so no changes in the loss factors are recommended. However, the analyses again point to the anomalous results for vapor-mounted primary seals, raising some concerns about the reliability of those factors.

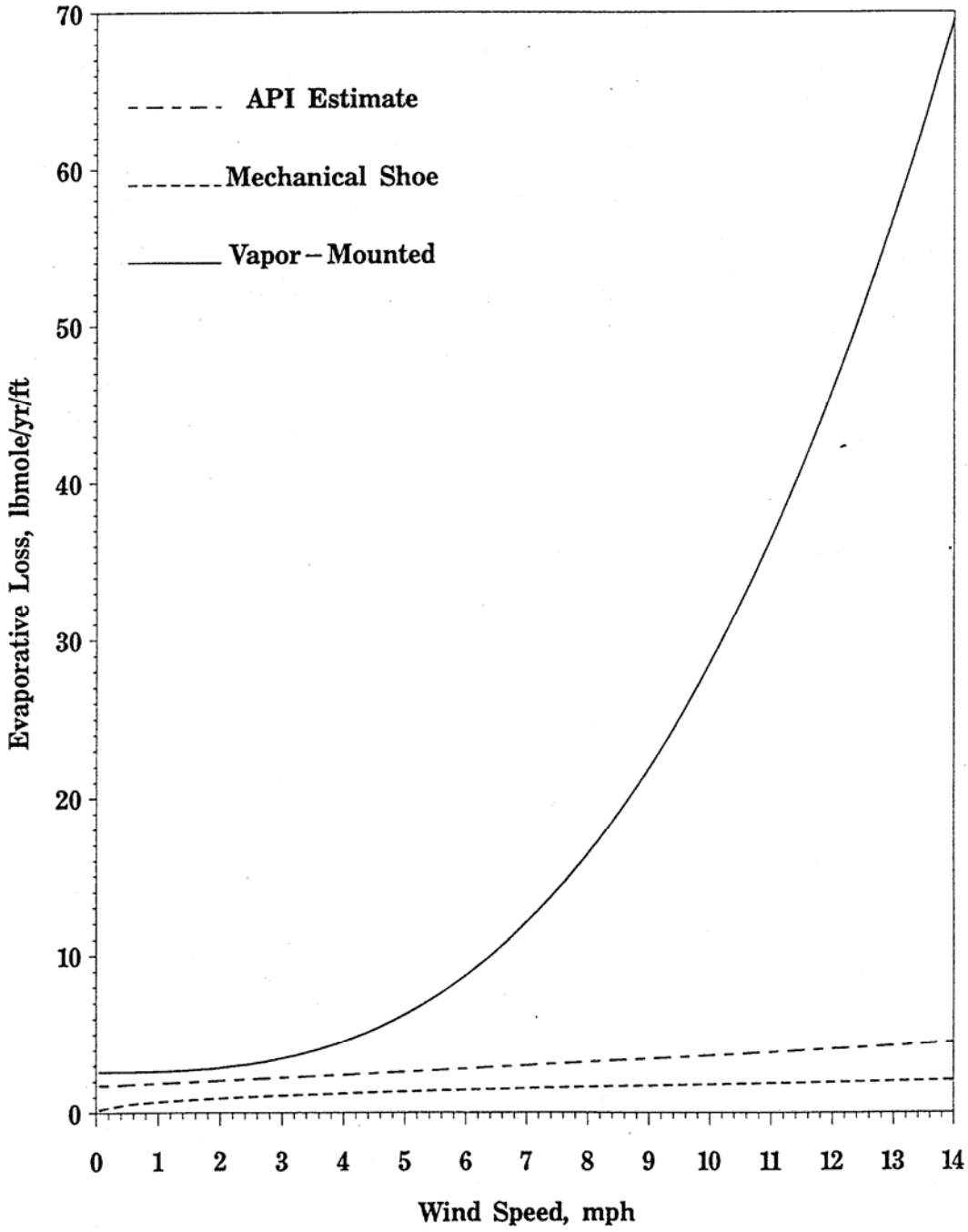

Figure 5-1. Emissions after a rim-mounted secondary seal as a function of primary seal type.

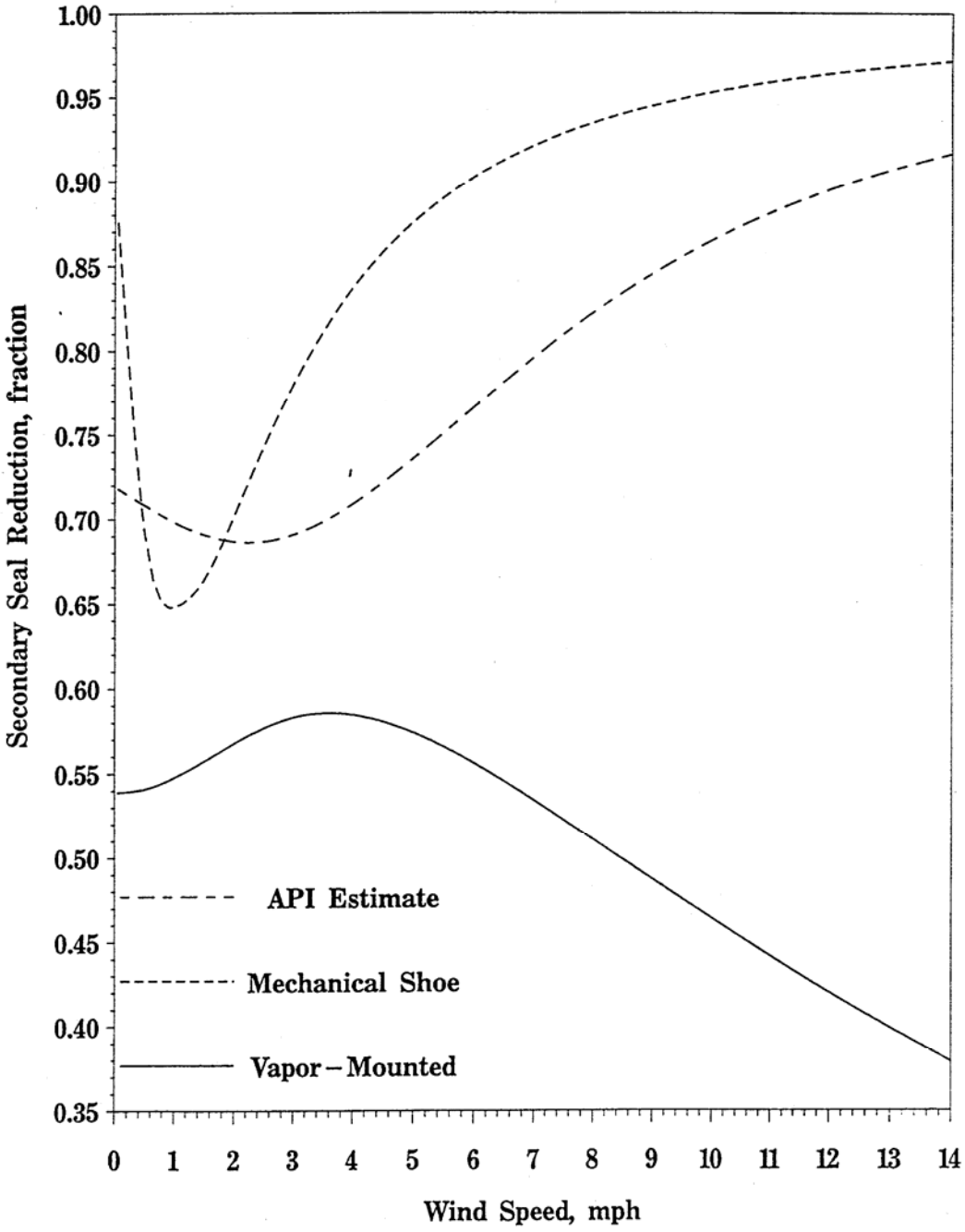

Figure 5-2. Efficiency of rim-mounted secondary seal as a function of primary seal type.

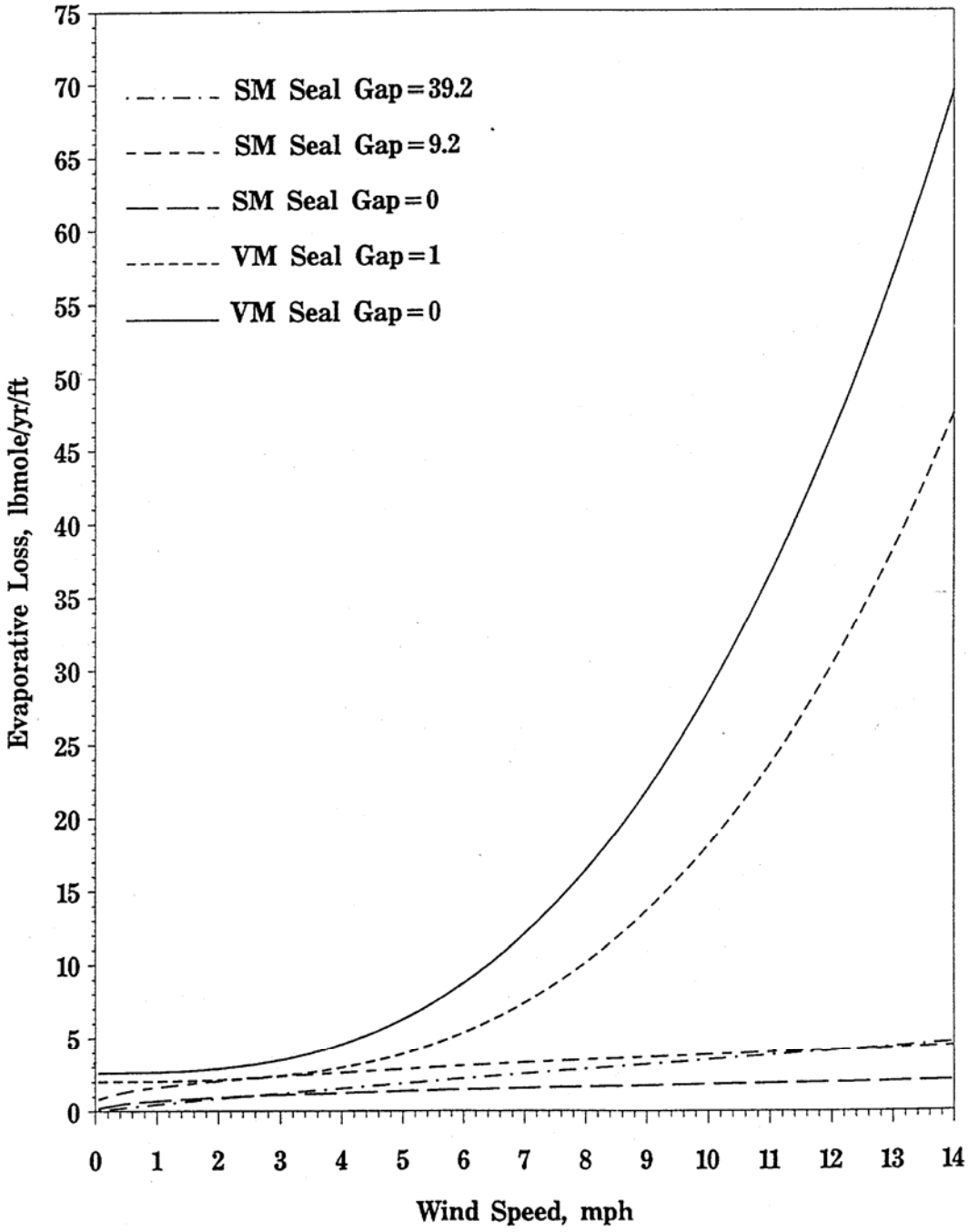

Figure 5-3. Emissions after a rim-mounted secondary seal as a function of primary seal gap size.

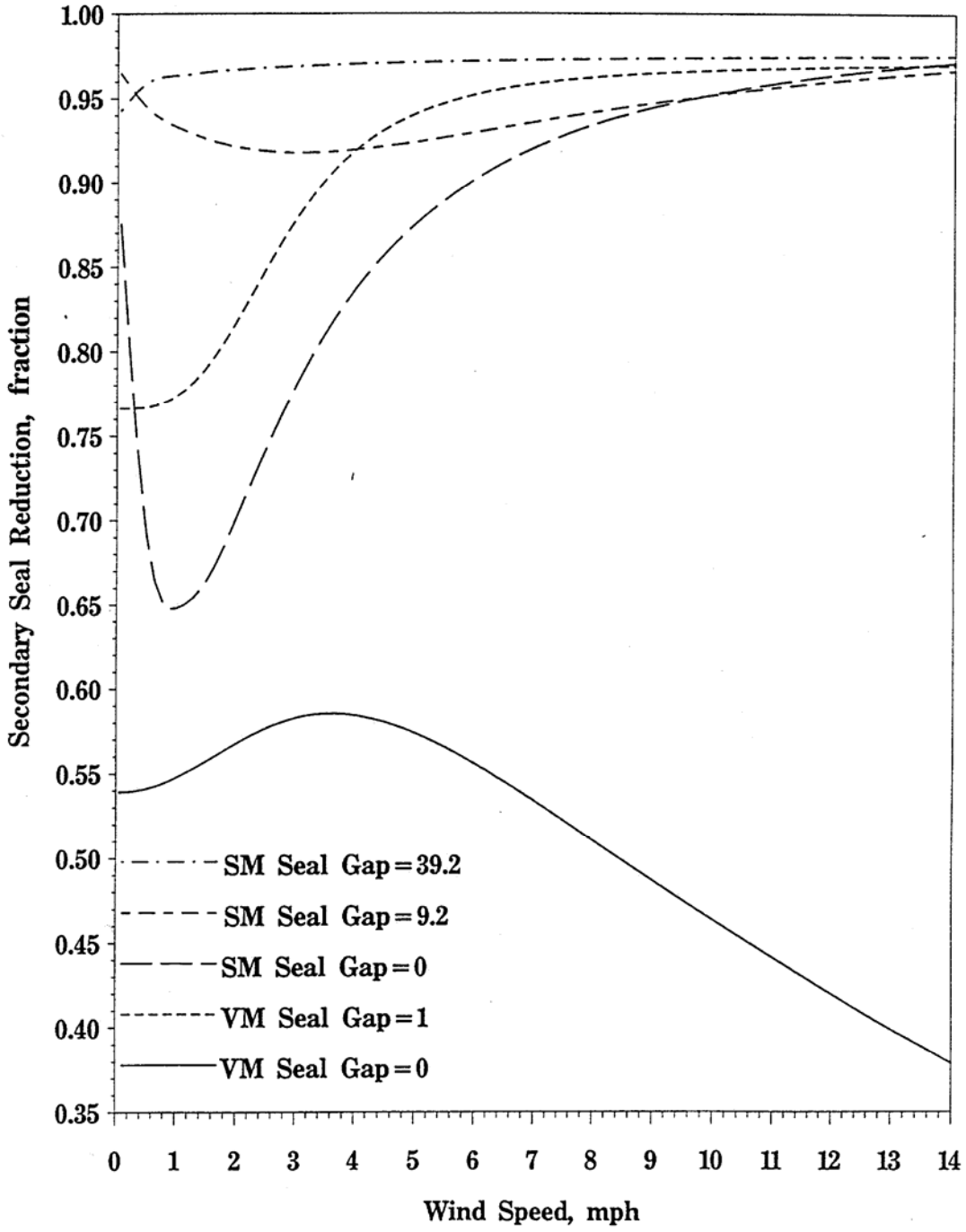

Figure 5-4. Efficiency of a rim-mounted secondary seal as a function of primary seal gap size.

Finally, the effect of secondary rim-seal gap size on secondary rim-seal performance was examined. A series of five cases were examined. The results are graphically presented in Figures 5-5, 5-6, 5-7, 5-8, and 5-9. The results suggest that even a small difference in secondary seal gap size can affect seal performance. Generally, the results show that performance improves with increasing wind speed for gap sizes 2 in^2/ft or less, but tends to deteriorate with increasing wind speed for larger gap sizes.

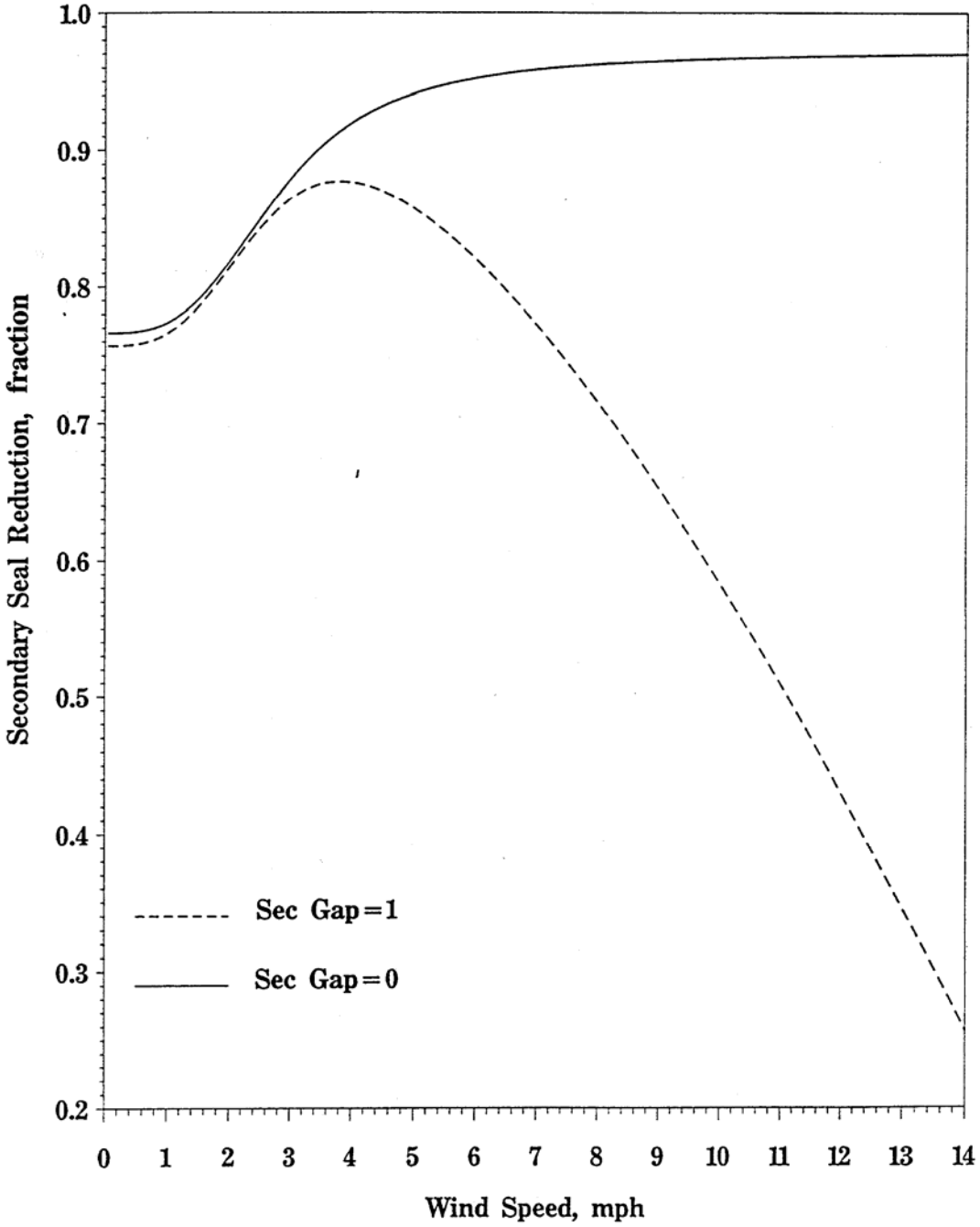

Figure 5-5. Effect of secondary gap on efficiency:
Case 1--vapor mounted primary with 1 inch gap.

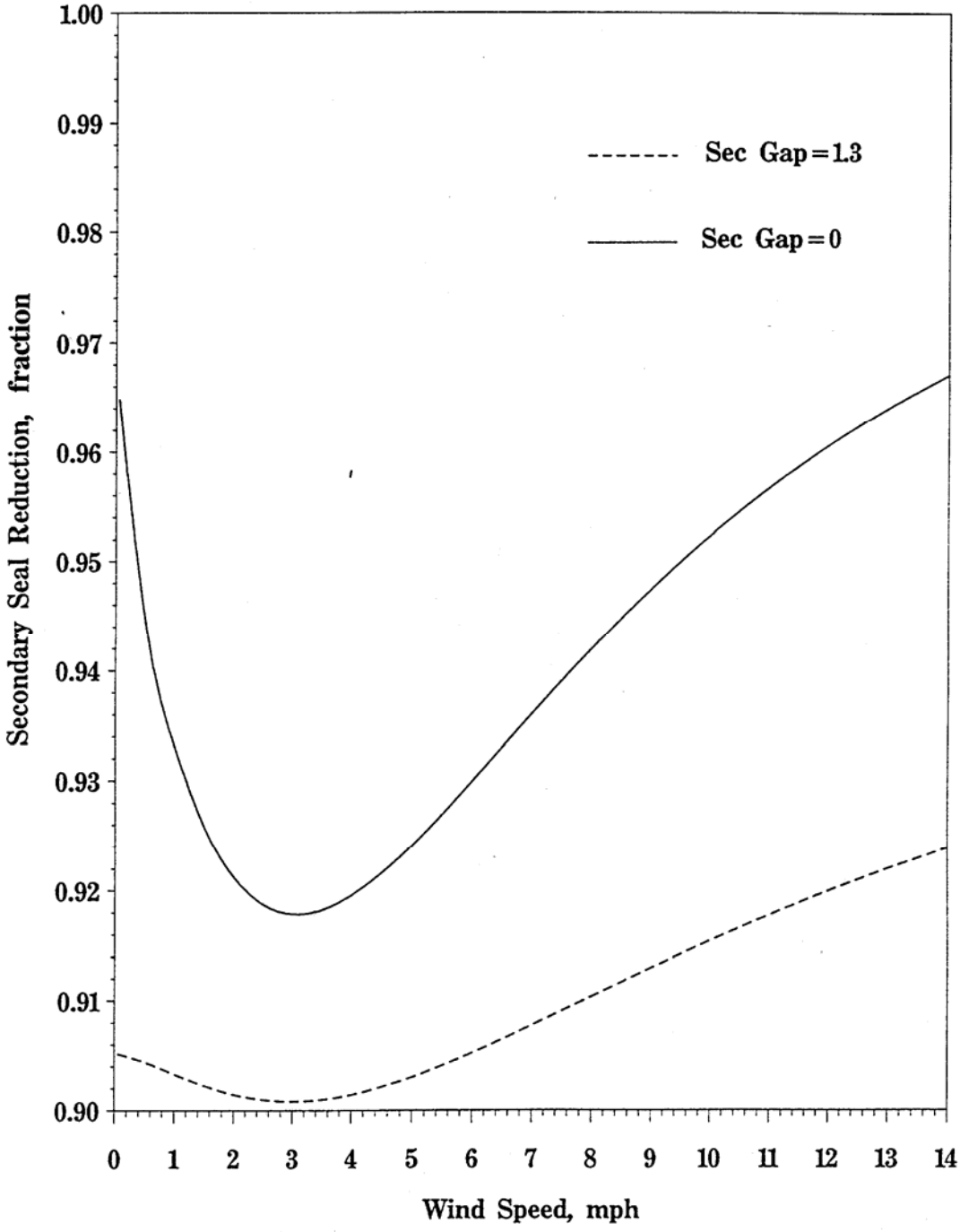

Figure 5-6. Effect of secondary gap on efficiency:
Case 2--shoe mounted primary with 9.4 inch gap

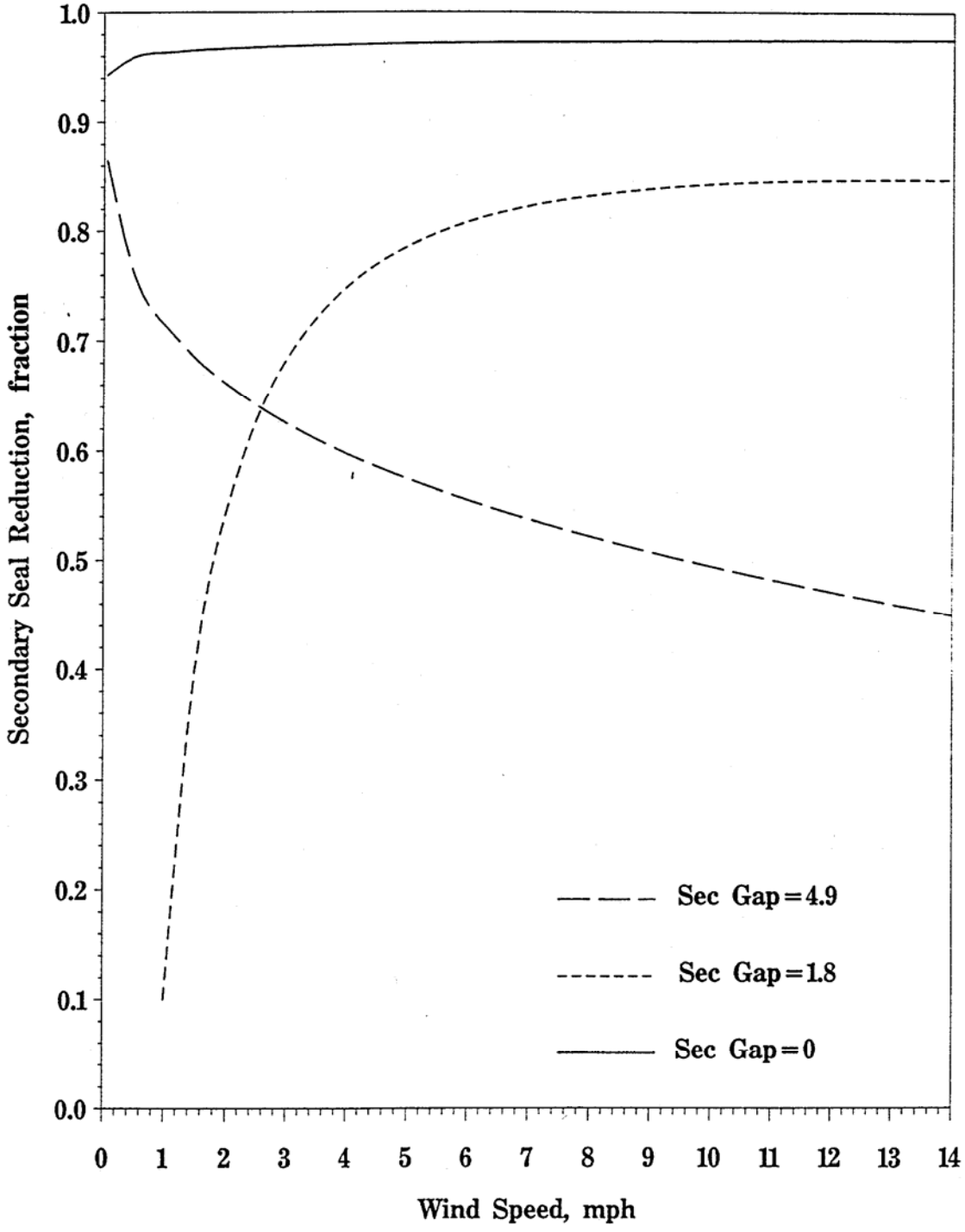

Figure 5-7. Effect of secondary gap on efficiency:
Case 3--shoe mounted primary with 39.2 inch gap.

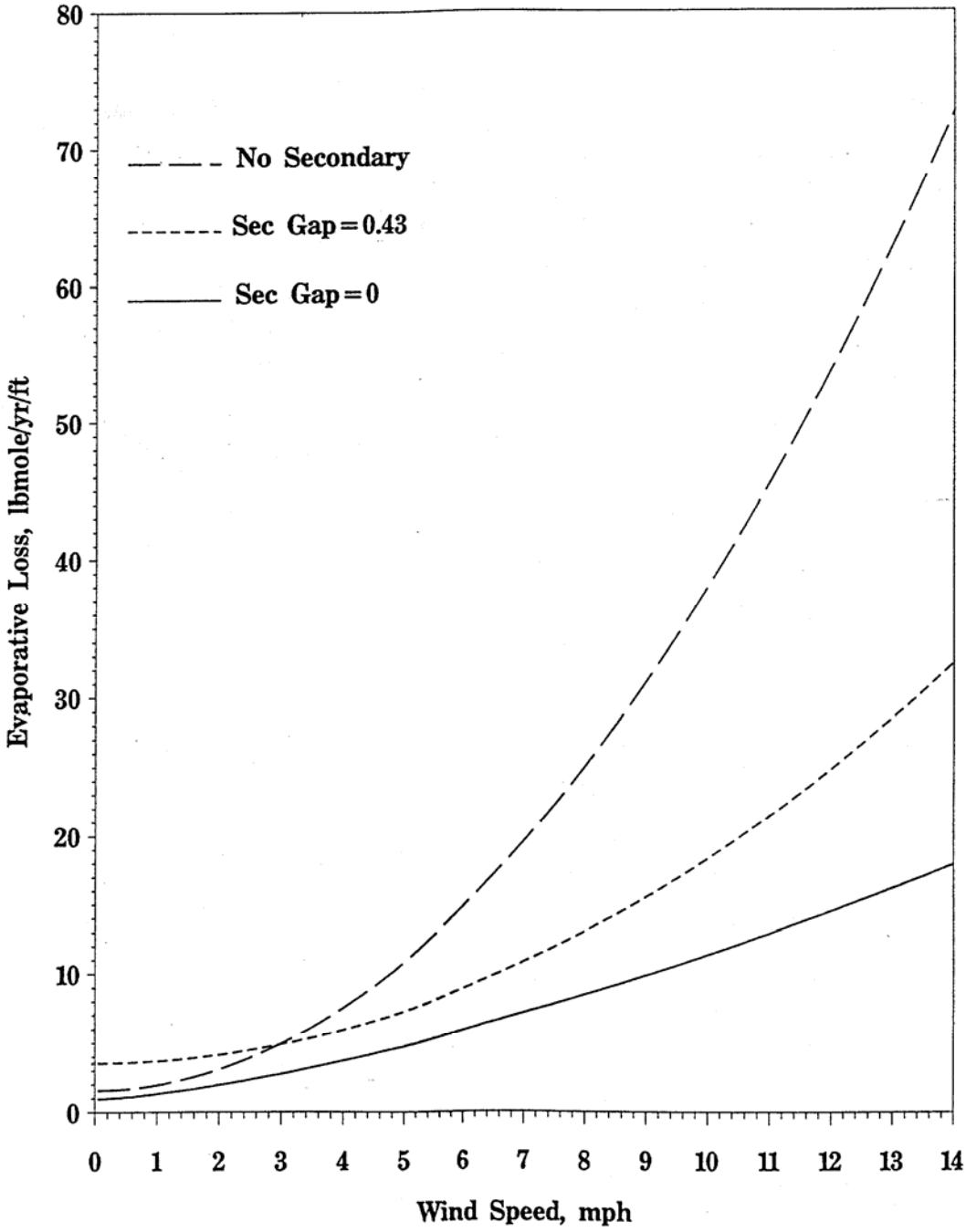

Figure 5-8. Effect of secondary gap on emissions:
Case 4--shoe mounted primary with 1 inch gap.

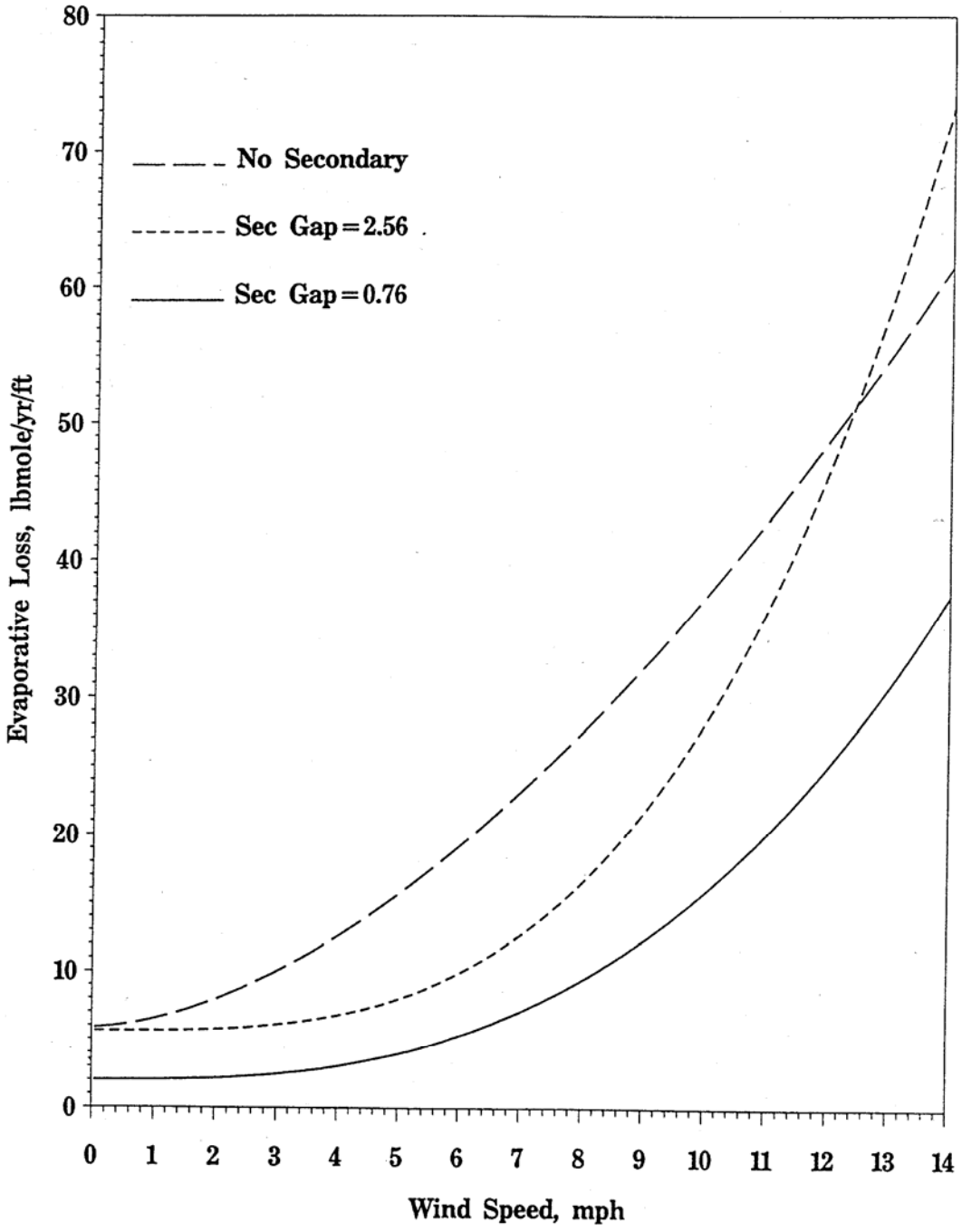

Figure 5-9. Effect of secondary gap on emissions:
Case 5--shoe mounted primary with 13.2 inch gap.

The analyses suggested that secondary rim-seal performance is strongly affected by gap size. Given the limitations in the current data base, no modifications to the loss factors based on these findings are recommended at this time. However, the strong effect of gap size on performance for vapor-mounted rim-seals suggests that further analysis of these rim-seals is warranted. Also, the effect of gap size on performance has implications for the design of test programs to demonstrate the performance of new rim-seal configurations.

5.1.1.2.5 Uncertainty estimates. Uncertainty estimates were developed at two levels (unique test cases and average estimating equations) for two estimation scenarios (individual tanks and a tank population mean). When the equations are applied to populations of tanks, the uncertainties are generally quite reasonable. However, the uncertainties for the equations when applied to individual tanks are quite large. Also, the uncertainties for vapor-mounted rim-seals are quite large in comparison to those for shoe-mounted and liquid-mounted rim-seals. With the exception of the vapor-mounted rim-seals, the upper bound for the population mean was generally within a factor of two of the point estimate.

In conclusion, the results of the analyses performed to verify and evaluate API's calculations indicate that the new rim-seal loss factors generated by API are acceptable for use in Section 7.1 of AP-42. Although the analyses do indicate that secondary seal gap size does affect rim-seal performance, limitations in the data base preclude any recommendation for modifications to the factors. However, due to the strong effect of wind speed and gap size on seal performance for vapor-mounted seals, further analysis of these seals may be warranted. The results of these analyses should also be considered in API's development of test methods to evaluate performance of new rim-seal designs.

5.1.2 Evaluation of Wind Speed Calculation

The relationship between emissions and wind speed in the floating roof tank estimating equations was developed by regressing daily emissions against fixed wind speeds under equilibrium conditions. The equation was then modified to generate annual emissions by embedding a multiple of 365.25 in the equation's constant coefficient and by assuming that as wind speed varied over the year, the average annual emissions could be obtained by evaluating the function at the average wind speed. Because emissions and wind speed are related nonlinearly, this latter assumption is not strictly correct. A sensitivity analysis was conducted to determine how using the estimating equations at average wind speeds rather than averaging the emissions obtained by applying the estimating equations over a typical wind speed distribution might affect the emission estimate.

Information presented by Justus, et al., and Corotis et al., indicates that wind speed distributions can be represented reasonably well by a two parameter Weibull distribution.[1,8] An analysis of the general form of the distribution indicated that the error in the emission estimate introduced by applying the estimating equation to the average wind speed rather than averaging emissions over the wind speed distribution depends only on the coefficient of variation of wind speed (i.e., the ratio of the standard deviation to the mean of wind speed) and the wind speed exponent in the estimating equation. The error in the estimate increases as the coefficient of variation increases and as the exponent moves away from 1. (Both methods produce the same result if the exponent equals 1). The Justus et al., and Corotis et al., papers also provided information on typical values for those parameters that could be used to evaluate possible errors. For an exponent of 1.5, the estimate obtained using the average wind speed was 7 to 11 percent lower than the estimate obtained by averaging over the wind speed distribution when the coefficient of variation was in the range of 0.45 to 0.6. For an exponent of 0.4 using the same range of coefficient of variation, the estimates obtained using the average were 2 to 5 percent higher than estimates obtained by averaging over wind speeds. However for an exponent of 2.6, the estimates obtained using

average wind speed were 30 to 45 percent lower than those obtained by averaging over wind speeds. These results suggest that if the estimating equations are used with exponents in the range of 0.4 to 1.5, using average wind speeds produces reasonable results. However, if the application involves larger exponents, the use of wind speed distribution data should be considered to improve the accuracy of the estimates.

5.1.3 Evaluation of Diameter Function and Product Factor

Because the data base that could be used to evaluate alternative diameter exponents for the floating roof tank estimating equations is quite sparse, the mathematical techniques used by API in the analysis are straightforward. As such neither the data nor the analytical procedures lend themselves to complicated statistical procedures. The procedures used by API are reasonable and the results of the analyses are supported. No change in the diameter exponent of 1 is recommended. However, the paragraphs below briefly describe the API analyses and summarize the available information on the uncertainty associated with the diameter exponent.

Field test emission data were collected for three tanks (denoted as C, T, and P) to evaluate the effect of tank diameter on emissions. To conduct the evaluation, API identified appropriate CBI test tank conditions that matched the field test conditions. For tanks T and P, CBI test conditions were found that closely matched the field tank. However, for tank C no directly applicable conditions were found, so multiple conditions were used to simulate the tank C conditions; consequently, the results for tank C are less reliable than those for tanks P and T. Estimating equations were then developed based on those field tank-specific test conditions, and emissions from the field tanks were estimated using those equations with different diameter exponents.

The results of the analyses, which are shown graphically in Figure 5-10, suggest that 1 is a reasonable exponent, particularly for tanks that are higher emitters. The error bands for the field tank emission estimates suggest that the exponent can reasonably be expected to be within the range of 0.7 to 1.2. If this range of exponents is applied to a 100 foot diameter tank, the emission estimate ranges from 25 percent to 250 percent of the estimate obtained for an exponent of 1. Hence, even though the exponent uncertainty is relatively small, it does introduce substantial uncertainty into the emission estimates.

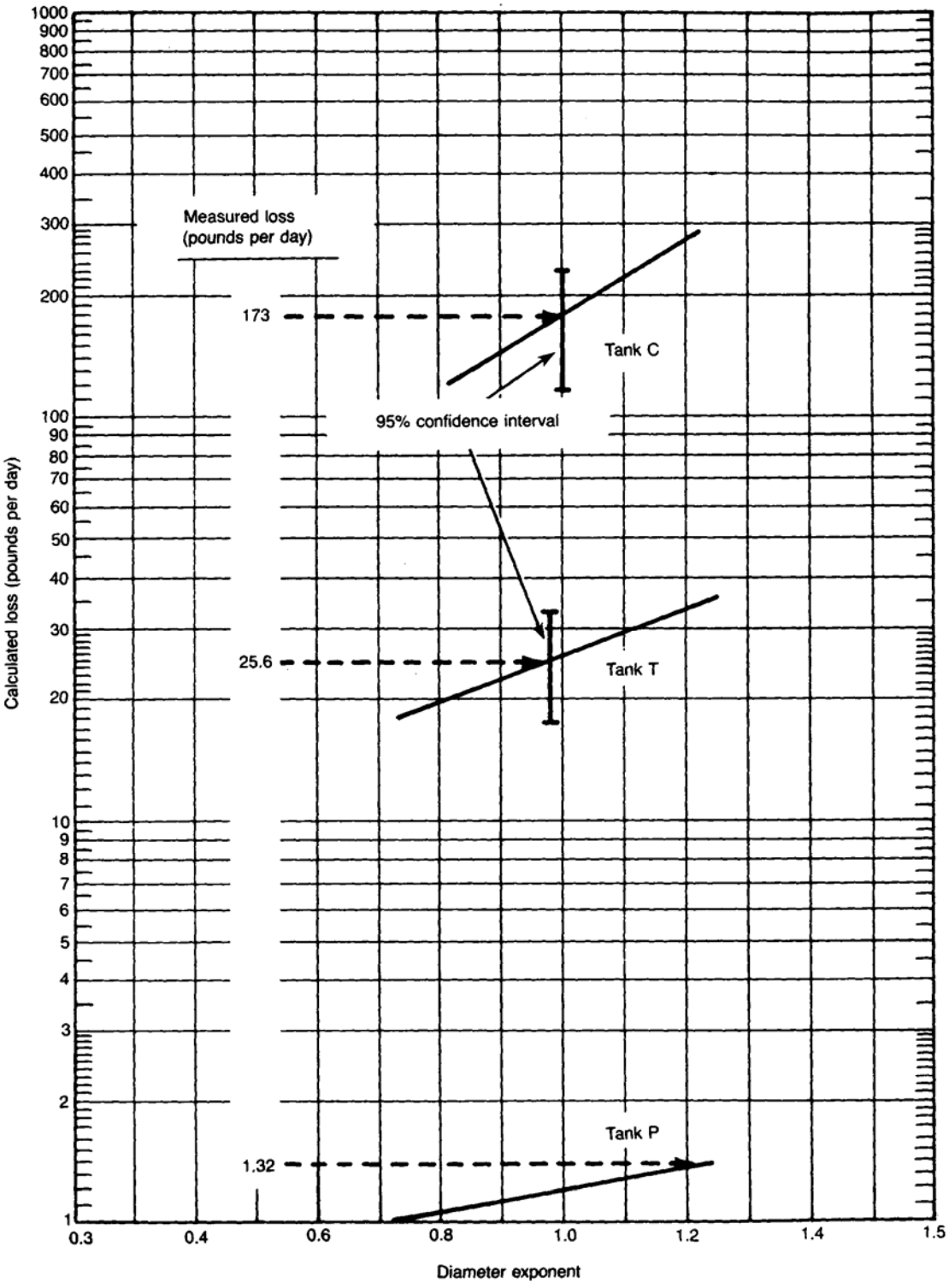

Figure 5-10. Calculated losses as a function of diameter exponent.

The procedures used by API to develop the product factors for crude oil and gasoline products are outlined in the documentation file of Appendix E of the 1983 Edition of API 2517.[2] The procedure relies on a straightforward comparison of paired test conditions that had the same seal configurations but different stored products. For the crude oil analysis, three test pairs that had different seal configurations and a wide variability in wind speeds were used. For each of the six test conditions, a regression model was fit for log emissions versus log wind speed. Resultant emission estimates at 5, 10, and 15 mph were then adjusted for vapor pressure and molecular weight and the ratio was compared. The results for the three scenarios produced product factor estimates of 0.28 and 0.32 for configurations with a primary seal only and 0.51 for a configuration with a secondary seal for an overall product factor of 0.4 for crude oil.

Replication of the regression analyses conducted by API verified these results. Furthermore, these analyses indicated that the uncertainty associated with the three individual product factors and the average factor was quite small. Based on the variances of the regression coefficiencies, the 95 percent confidence intervals for both the individual pairs and the average are estimated to be on the order of $\pm$ 10 percent. Hence, the product factor is likely to provide precise estimates over a large tank population. However, the large difference in the factor for different scenarios suggests that the factor could introduce substantial error for a single tank. Hence, the use of $K_C = 0.4$ for crude oil is recommended for AP-42.

During the IFRT, 20-ft diameter pilot scale studies conducted by CBI, several tests were conducted during each phase for which the only difference was the vapor pressure of the octane/propane mixture. Tests were available under the same conditions for the single-component stocks with n-hexane and n-octane stored in the tank. The emission data for each test condition were regressed against true vapor pressure. These regression lines were demonstrated graphically to provide a good fit to the octane/propane data. Furthermore, with one exception, the regression lines generated estimates for the single-component tests that were greater than or equal to the measured values. The single exception was an n-octane test during Phase I, under tight seal conditions, with a very low true vapor pressure (0.3 psia). Given these results, API determined that a product factor of 1.0 for single-component stocks provides a conservative emission estimate.

As a part of this review, MRI corroborated the API results. Given the limited quantity of data on single-component stocks, the procedures used by API are reasonable. The single problem point appears to be an anomalous data point. Hence, the use of $K_C = 1.0$ for single-component mixtures is recommended for AP-42.

5.1.4 Deck Fitting Loss Factors[9-13]

5.1.4.1 Development Methodology. The floating roof tank fitting loss estimating equations involve three loss factors: the zero wind speed loss factor, or equation intercept, (K_a), wind speed dependent loss factor (K_b), and wind speed exponent (m). Factors were developed for both slotted and unslotted guide poles under a variety of control scenarios that involved the application of gaskets, floats, float wipers, pole sleeves, and pole wipers. Other fittings used to develop the estimating equations were deck legs assumed to have a 3 in. diameter opening, a gauge hatch/sample port assumed to have a 8 in. diameter opening, a vacuum breaker assumed to have a 10 in. diameter opening, an access hatch assumed to have a 24 in. diameter opening, a gauge-float well assumed to have a 20 in. diameter opening, and a deck drain assumed to have a 3 in. diameter opening. With the exception of the deck leg and deck drain fittings, all fittings were tested with and without gasketing.

The tests were performed in a wind tunnel, at wind speeds of 0, 4.3, 8.5, and 11.9 miles per hour. The deck fitting was mounted on a product reservoir that rested on a digital platform scale. The top of the deck fitting extended into the wind tunnel. Precise measurements of the test facility weight were used to obtain data on cumulative evaporative loss over time; the duration of each test depended on the loss rate for a particular fitting. For slotted guide poles, tests were conducted with the slots oriented at different angles to the primary wind direction through the tunnel. Details of the guide pole test procedures and the raw data from the test are contained in the May 1994 addendum to API Publication No. 2517 and its background documentation.[9] Details of the other fitting test procedures can be found in Volume 1 of the Final Report, Testing Program to Measure Evaporative Losses from Floating Deck fittings, dated October 1, 1993.

The deck fitting loss factor estimating equations were developed by CBI/API using a three stage procedure, outlined below.

1. The raw data from each fitting test for cumulative loss versus time were fit to either a linear or quadratic polynomial in time using a least squares analysis, and the initial loss rate for each test was determined by evaluating the derivative of the polynomial at time zero.

2. For each combination of fitting and wind speed, an average initial loss rate was determined by taking the arithmetic average of all initial loss rates obtained for that combination of fitting and wind speed. This process generated four data points for each fitting, one point for each wind speed. Note, however, that in some cases, only one test was conducted, and this single test value was used as the average initial loss rate for that combination of fitting and wind speed.

3. For each fitting, a software package, "Table Curve for Windows™," was used to fit the four data points to a curve of the form:

$$K_F = K_{F_a} + K_{F_b} v^m$$

where:

K_F = Fitting loss factor, lb-mole/yr
K_{F_a} = Zero wind speed fitting loss factor, lb-mole/yr
K_{F_b} = Wind speed dependent fitting loss factor, lb-mole/(mph)^{n}yr

v = Ambient wind speed, mph
m = Wind-dependent loss exponent, dimensionless

The software used by API utilized a Levenburg-Marquardt algorithm, a standard technique for nonlinear curve fitting, to fit this curve. To force the intercept of the function (K_{F_a}) to fit the data exactly, the algorithm was modified to give a large weight to the zero wind speed data point.

The results of MRI's analyses of the deck fitting factors recommended by API are presented in the following sections. The analyses of guide pole fitting and other deck fittings are discussed separately.

5.1.4.3 Evaluation of the Guide Pole Deck Fitting Loss Factors. There were four primary concerns about the statistical methods used by API to evaluate the data. First, the method used to force the equation through the measured zero wind speed data point prevented obtaining meaningful information about the goodness of fit of the equation to the data. Because K_{F_a} is simply a linear transformation of the equation from the intercept, a much better method for forcing the equation through the zero wind speed data point is simply to subtract that intercept from the other data points and fit a two-parameter equation to the remaining three data points.

The next two concerns involved the method used to average the data. If the relationship between evaporative loss and wind speed is the hypothesized power function, then evaporative loss and wind speed are linearly related on a log-log scale. If that assumption holds, then averaging emissions on the log scale rather than the linear scale appears to be more appropriate. Also, the data indicate that loss rate is strongly related to slot orientation relative to wind direction. There were sometimes different numbers of tests for different slot orientations, so equal weighting of orientations rather than equal weighting of individual tests appears to be more appropriate.

The final concern was whether or not the use of an overall strategy that analyzed averaged data on a fitting-specific basis to obtain parameter estimates was more appropriate than the use of a more general modeling strategy that used individual test data modeled concurrently to obtain both parameter estimates and their standard errors. Use of averages masks the inherent variability among the tests and makes any assessment of the precision of the estimates unreliable, while a more general modeling strategy provides better insight into the relationship of the performance of the different control strategies. Outlined below are the approaches that were used to analyze the data and address the above concerns.

5.1.4.3.1 Slotted guide poles.

Fitting specific analysis. For slotted guide poles, three alternative fitting-specific modeling strategies were examined. For the first (MRI-1), the equation was forced through the measured data point by subtracting the zero wind speed value for a particular fitting from the nonzero wind speed values for that fitting. The resultant values were then averaged arithmetically, and the parameter estimates were obtained by fitting a linear equation to log transforms of loss rate and wind speed rather than fitting a nonlinear equation to the raw values. This first approach provides an assessment of modifying the approach to forcing the curve through a particular intercept and of using a linearized approach to fitting the equation rather than a nonlinear curve fit approach. The second and third approaches (MRI-2 and MRI-3) both used weighted regression approaches that employed test-specific loss rates rather than averages. This weighted approach resulted in "averaging" on the log transformed scale rather that on the linear scale. The MRI-2 approach gave equal weight to each test, while MRI-3 gave equal weight to each wind orientation.

Eleven different control scenarios that involved the application of gaskets, floats, float wipers, pole sleeves, and pole wipers to slotted guide poles were tested. Two additional tests, fitting Nos. 31 and C01, were conducted after these analyses were performed. Data from these tests were also used in developing slotted guide pole loss factors. Table 5-5 identifies each of the slotted guide pole fitting configurations and compares the parameter estimates for each of the analysis methods. For seven of the configurations, an equal number of tests was conducted at each slot orientation at any given wind speed, so the results for the last two methods are equal. From Table 5-5, it can be seen that parameter results produced by the different methods vary considerably. However, graphs of the estimating equations indicate that substantially different loss rates are estimated for most configurations only at low wind speeds. Only for fitting Nos. 20 and 30 are the loss rates at high wind speeds substantially different. Further, when the differences are substantial, the two methods that use "averaging" on the linear scale (API and MRI-1) consistently predict higher emissions than do the methods based on log scale analyses. This difference is a result of the greater relative weight given to the large values on a linear scale.

TABLE 5-5. COMPARISON OF SLOTTED GUIDE POLE PARAMETER ESTIMATES

	Control measure				Estimation technique[d]	Parameter estimate		
	Gasket[a]	Float[b]	Pole sleeve[a]	Pole wiper[c]		K_a	K_b	M
1	0	0	0	0	API MRI-1 MRI-2 MRI-3	45.4	698	0.974
						45.5	461	1.16
						45.5	186	1.54
						45.5	186	1.54
25	1	0	0	0	API MRI-1 MRI-2 MRI-3	40.7	311	1.29
						40.6	364	1.22
						40.6	386	1.17
						40.6	386	1.17
3	0	1	0	0	API MRI-1 MRI-2 MRI-3	35.7	102	1.71
						35.9	37.5	2.15
						35.9	26.4	2.29
						35.9	38.2	2.12
26	1	1	0	0	API MRI-1 MRI-2 MRI-3	25.8	9.06	2.54
						25.6	35.9	1.94
						25.6	33.1	1.94
						25.6	33.1	1.94
20	1	0	0	1	API MRI-1 MRI-2 MRI-3	41.2	130	1.23
						41.2	90.1	1.40
						41.2	47.9	1.45
						41.2	47.9	1.45
2	1	0	1	0	API MRI-1 MRI-2 MRI-3	16.3	132	1.19
						16.4	39.4	1.73
						16.4	4.92	2.45
						16.4	21.4	1.82

TABLE 5-5. (continued)

Fitting	Control measure				Estimation technique[d]	Parameter estimate		
30	1	3	0	1	API MRI-1 MRI-2 MRI-3	13.8	13.7	1.94
						13.8	9.47	2.10
23	1	2	0	1	API MRI-1 MRI-2 MRI-3	13.8	10.2	1.70
						13.8	10.4	1.67
						17.9	54.2	1.10
						17.9	16.9	1.62
						17.9	13.5	1.58
						17.9	13.5	1.58
						19.2	15.0	0.935
						19.2	6.99	1.19
29	1	1	1	2	API MRI-1 MRI-2 MRI-3	9.09	13.4	0.512
						9.09	15.0	0.457
						9.09	15.0	0.456
						9.09	15.0	0.456

[a]0 = control measure not implemented; and 1 = control measure implemented.
[b]0 = no float used; 1 = float with 0.25 inch gap and wiper 1 inch above cover; 2 = float with 0.25 inch gap; and wiper at cover elevation; and 3 = float with 0.125 inch gap and no wiper.
[c]0 = no pole wiper; 1 = pole wiper at sliding cover elevation; and 2 = pole wiper 6 inches above sliding cover.
[d]API = API estimates published in addendum to API Publication No. 2517; MRI-1 = results of MRI analyses using a linear regression technique with different wind orientations averaged on a linear scale; MRI-2 = results of MRI analyses using a linear regression technique with different wind orientations averaged on a log scale; and MRI-3 = results of MRI analyses using a linear regression technique with different wind orientations averaged on a log scale weighted so that each direction received equal weight.
[e]API excluded two tests (4BNF and 8AWG) from their analysis for fitting No. 4. MRI included these tests in the analysis. Subsequent conversations with API indicated that there were valid reasons for eliminating these tests.

The results of this analysis indicate that the estimating equations generated by API will provide conservative estimates of VOC loss rates. At wind speeds of 12 miles per hour or less, the positive bias will be relatively small for most fittings and will be less than a factor of 2 for all fittings except No. 30. This fitting had a float that fit tighter to the guide pole than is typical, but did not have a float wiper. This is not a design in actual use. The apparent rationale for this test was to determine whether this design could be considered equivalent to a standard float. The measured losses were slightly lower at 0 mph, but about twice as high at typical wind speed levels, as compared to a standard float.

General model analyses. The use of a more general modeling strategy that used individual test data modeled concurrently to obtain both parameter estimates and their standard errors was investigated. A general model analysis was performed to provide more information about the relative performance of the different control strategies and evaluate the precision of the parameter estimates. There were two stages in the analysis. The first was an analysis of the zero wind speed data to determine equation intercepts (K_{F_a}). The second used the nonzero wind speed data to determine the wind speed coefficient (K_{F_b}) and exponent (m). This approach was selected over a single modeling effort for two reasons. First, it assures that the intercept term will be nonnegative, which is a physical constraint of the system being modeled. Second, because measured emissions at zero wind speed were quite low for all fittings, any errors introduced by using only the zero wind speed data to generate the intercept are expected to be small relative to the overall errors in the data collection and analysis procedures.

Because only a single data point was obtained for each fitting at zero wind speed, the quantity of data was insufficient to model statistically. The data were examined visually, and engineering judgment based on the relative magnitude of the loss factor and the fitting configuration was used to determine which groups of data to average. An average zero wind speed loss was determined for fitting Nos. 2, 23, and 24; fitting Nos. 4 and 26; and fitting Nos. 25 and 20. For all other fittings the measured loss rate at zero wind speed was used for K_{F_a}.

Since K_{F_a} was fixed in stage 1, a linear model approach based on log transforms of loss rate and wind speed was used in stage 2 to determine K_{F_b} and m. The linear model approach has the advantage over a nonlinear modeling approach by having an exact analytical solution to the least squares normal equations. To develop the linear models, the appropriate value for K_{F_a} was subtracted from each initial loss rate and logs of the residual loss rate and wind speed were determined. Then a sequence of linear models was fit starting with a saturated model with individual estimates of K_{F_b} and m for each of the fittings. The saturated model was subsequently reduced by removing parameters that had no significant effect on the ability of the model to fit the measured data. A weighted regression approach was used, with each slot orientation equally weighted.

The saturated model generated the same parameter estimates as those generated by the weighted regression method MRI-1. The final reduced model contained six parameters: four to estimate K_{F_b} and two to estimate wind speed exponents. For all fittings except No. 29, which had a pole wiper 6 inches above the sliding cover instead of at the cover level, a single wind speed exponent of 1.6 fit the data well. Fitting No. 29 had a wind speed exponent of 0.45. The four parameters to estimate log K_{F_b} were found to be linear combinations of four types of fitting controls (gasket, float [with float location being unimportant], pole sleeve, and pole wiper at the sliding cover level). The resultant parameter estimates and their standard errors are presented in Table 5-6. For the uncontrolled fitting, the estimate of log (K_{F_b}) is 2.3. Adding a gasket reduces log (K_{F_b}) by 0.13, a float by 0.36, a pole sleeve by 0.63, and a wiper at the sliding cover by 0.72. The use of this method allows direct comparison of the effects of particular control options and reduces the standard errors of the parameter estimates, thereby providing more precise and stable estimates.

TABLE 5-6. SUMMARY OF RESULTS FOR LINEAR MODEL ANALYSES OF ALL FITTINGS

Fitting No.	Comparison of parameter estimates												
	K_a	Individual regression				Saturated model				Reduced model			
		Log K_b		m		Log K_b		m		Log K_b		m	
		Est.	s.e.	Est.	s.e.	Est.	s.e.	Est.	s.e.	Est.	s.e.	Est.	s.e.
1	45.5	2.27	0.36	1.54	0.40	2.27	0.58	1.54	0.64	2.30	0.18	1.6	0.18
25	40.9	2.58	0.28	1.17	0.31	2.58	0.58	1.17	0.64	2.17	0.17	1.6	0.18
3	35.9	1.59	0.28	2.12	0.31	1.58	0.58	2.12	0.64	1.95	0.18	1.6	0.18
26	25.9	1.52	0.32	1.94	0.36	1.52	0.58	1.94	0.64	1.81	0.17	1.6	0.18
20	40.9	1.68	1.01	1.45	1.12	1.68	0.58	1.45	0.64	1.44	0.18	1.6	0.18
2	17.8	1.32	0.77	1.83	0.86	1.32	0.58	1.83	0.64	1.54	0.17	1.6	0.18
30	13.8	1.02	0.93	1.67	1.03	1.02	0.58	1.67	0.64	1.09	0.17	1.6	0.18
23	17.8	1.13	0.69	1.58	0.77	1.13	0.58	1.58	0.64	1.09	0.17	1.6	0.18
4[a]	25.9 (2.42)	0.940 (0.669)	0.47	1.66 (1.93)	0.53	0.940 (0.669)	0.58	1.66 (1.93)	0.64	1.09	0.17	1.6	0.18
24	17.8	0.874	0.12	1.17	0.14	0.874	0.58	1.17	0.64	0.46	0.18	1.6	0.18
29	9.1	1.20	0.071	0.430	0.089	1.20	0.39	0.430	0.19	1.18	0.18	0.451	0.24
31	4.89	1.85	0.51	1.09	0.47	b	b	b	b	b	b	B	B
32	8.3	0.64	0.50	1.6	0.65	b	b	b	b	b	b	b	B
C01	4.86	0.97	0.06	1.03	0.11	b	b	b	b	b	b	b	B

[a]Note that MRI originally included the data from test runs 4BNF and 8AWG for fitting No. 4 in the analyses (Reference 16). Subsequently, it was determined that these were valid reasons for eliminating these tests from the analyses. The analysis results reported here are the original results including these two test runs; the values in parentheses for fitting four are the revised parameter values, excluding these two test runs.

[b]Tests 31, 32, and C01 were conducted after these analyses were performed so only the individual regression results are included here.

5-33

The results of the analyses showed that some of the control configurations tested were not statistically different (i.e., represented the same level of control). The control configurations tested and the corresponding control groups are shown in Table 5-7. As shown in Table 5-7, 13 guide pole configurations were tested that represented 7 distinct control levels. The results of the analysis showed that (1) the addition of a gasket to the sliding cover does not result in any appreciable reduction in emissions for the two configurations tested in both the gasketed and ungasketed condition, (2) the presence of a float in the guide pole tends to reduce emissions, however, for the two configurations tested (height of the float top or wiper at or 1 inch above the sliding cover) the height of the float wiper in the guide pole is not a critical factor, and (3) when a pole sleeve is employed, the height of the float or float wiper (at the sliding cover, 1-inch above the sliding cover, or 5-inches below the sliding cover) does not have a significant impact on emissions.

TABLE 5-7. RECOMMENDED GROUPING OF SLOTTED GUIDE POLE FITTINGS AND PARAMETERS FOR AP-42

Fitting No.	Control measure				Comment	Parameter estimates		
	Gasket[a]	Float[b]	Pole sleeve[a]	Pole wiper[c]		K_{F_a}	K_{F_b}	M
1	0	0	0	0	Presence of gasket had relatively little effect on emissions from configuration, compared to effect of other control measures.	43	270	1.4
25	1	0	0	0				
3	0	1	0	0	Presence of gasket had relatively little effect on emissions from configuration, compared to effects of other control measures.	31	36	2.0
26	1	1	0	0				
20	1	0	0	1		41	48	1.4
2	1	0	1	0		11	46	1.4
31	1	0	1	0				
23	1	2	0	1	Position of float wiper (at or 1 inch above cover) did not significantly affect emissions	21	7.9	1.8
4	1	1	0	1				
24	1	2	1	1	Positions of float and pole wipers did not significantly affect emissions when a pole sleeve was used	11	9.9	0.89
29	1	1	1	2				
CO1	1	4	1	1				
30	1	3	0	1	Configuration not included in analyses because configuration was atypical	14	10	1.7
32	1	0	1	1		8.3	4.4	1.6

[a]0 = control measure not implemented
1 = control measure implemented
[b]0 = no float used
1 = float with 0.25 inch gap and wiper 1 inch above cover
2 = float with 0.25 inch gap and wiper at cover elevation
3 = float with 0.125 inch gap and no wiper
4 = float 5 inches below sliding cover
[c]0 = no pole wiper
1 = pole wiper at sliding cover elevation
2 = pole wiper 6 inches above sliding cover

5-35

Conclusions. The general modeling approach does provide valuable information regarding the contribution of the different controls and was useful in providing information for deciding how to group the different fittings for establishing the AP-42 factors. However, in some cases, factor-specific linear regressions provide better estimates for the specific factor than the general model.

Furthermore, in the near future API plans on establishing test protocols that will allow manufacturers/users of tank components to evaluate evaporative losses from new deck fitting configurations. Consequently, establishing fitting-specific evaporative loss factors makes sense. Therefore, the factor-specific individual regression parameter estimates (Method MRI-3) are recommended for use in AP-42.

Since the analysis showed that the presence of a sliding cover gasket has relatively little effect on emissions, separate factors for gasketed and ungasketed covers are not warranted. Consequently, the parameter estimates from fitting Nos. 1 and 25, and 3 and 26 were combined to provide recommended AP-42 factors for slotted guide poles with a gasketed or ungasketed sliding cover and slotted guide poles with a gasketed or ungasketed sliding cover and a float, respectively. Similarly, because the analysis indicated that for the configuration tested float height had little effect on emissions, the parameter estimates for fitting Nos. 23 and 4 and for fitting Nos. 24, C01, and 29 were combined to provide the recommended AP-42 loss factors for sliding cover, with float and pole wiper and sliding cover with float, pole sleeve, and pole wiper, respectively. Data for fitting Nos. 2 and 31 were combined, since fitting No. 31 is identical to fitting No. 2, but was tested after the initial test program was completed. Since fitting No. 30 is not typical of fittings in use, a fitting factor for this fitting configuration is not being recommended for AP-42.

In cases where parameter estimates for fittings were combined, the calculation was as follows:

1. For (K_{F_a}), average of the K_{F_a} values estimated for the individual fittings;
2. For (K_{F_b}), average of the log(K_{F_b}) values estimated for the individual fittings; and
3. For (m), average of the m values estimated for the individual fittings.

Table 5-7 presents the recommended fitting factors for slotted guide poles.

5.1.4.3.2 Unslotted guide poles.

Data analysis. A single alternative modeling strategy was used to analyze the data gathered from the five unslotted guide pole configurations. First, for each fitting the zero wind speed loss estimate was subtracted from each data point. For the three resulting data points, a linear model was fit for the log of the loss factor versus the log of wind speed. This equation is equivalent to the power function defined earlier with the intercept removed. The parameter estimates obtained for unslotted guide pole fittings by API and by this alternative method are presented in Table 5-8. The parameter estimates obtained by the two methods differ somewhat but the resulting equations have very similar predicted emissions over the applicable wind speed range. The equations that do differ display the largest differences in absolute magnitude at wind speeds of 15 miles per hour. Since all the data used to generated the estimating equations were obtained at wind speeds less than 12 miles per hour, the reader is cautioned against applying the equations at wind speeds above 12 miles per hour. With this caution, the API equations for unslotted guide poles were found to provide acceptable estimates of VOC evaporative loss rates.

TABLE 5-8. COMPARISON OF UNSLOTTED GUIDE POLE PARAMETER ESTIMATES

Fitting	Control measure[a]				Estimation technique	Parameter estimate		
	Gasket	Float	Pole sleeve	Pole wiper		K_{Fa}	K_{Fb}	m
18	0	0	0	0	API	31.1	372	1.03
					MRI	31.2	148	1.44
28	0	0	1	0	API	25.0	0.0267	4.02
					MRI	24.9	2.21	2.12
27	1	0	0	0	API	25.0	1.05	3.26
					MRI	24.9	12.8	2.18
17	1	0	0	1	API	13.7	5.78	0.587
					MRI	13.7	3.73	0.781
19	1	0	1	0	API	8.63	13.8	0.755
					MRI	8.63	12.3	0.808

[a]0 = control measure not implemented; 1 = control measure implemented.

Conclusions. The unslotted guide pole parameters calculated by API using a curve fitting procedure provide reasonable predictions of VOC evaporative losses. Midwest Research Institute analyzed the data by an alternative approach using a simple linear regression. In order to force the intercept of the fitting equation through the measured loss rate at zero wind speed (K_{F_a}), the measured loss rate at zero wind speed was subtracted from the loss rates of other wind speeds. Then, the remaining nonzero wind speed data were plotted on a log-log scale and a linear regression performed to obtain the other loss factors (K_{F_b}, m). The emission estimating parameters calculated by MRI's procedure (and presented in Table 5-8) are recommended for AP-42.

5.1.4.4 Evaluation of Other External Deck Fitting Loss Factors. Fittings considered in these analyses were deck legs assumed to have a 3 in. diameter opening, a gauge hatch/sample port assumed to have a 8 in. diameter opening, a vacuum breaker assumed to have a 10 in. diameter opening, an access hatch assumed to have a 24 in. diameter opening, a gauge-float well assumed to have a 20 in. diameter opening, and a deck drain assumed to have a 3 in. diameter opening. With the exception of the deck leg and deck drain fittings, all fittings were tested under two conditions, one without gasketing (uncontrolled) and one with gasketing (controlled). Four deck leg tests were conducted. One set of tests was for an ungaskseted deck leg associated with the center of the deck on a double deck roof. The other three sets of tests were for the pontoon area under three different conditions--no control, gasket, and sock. The deck drain was tested under two conditions, open (uncontrolled) and 90 percent closed (controlled).

Three distinct sets of analyses were conducted. The first essentially replicated the procedures used by CBI to develop the coefficients for the EFRT estimating equations proposed by API. The second also replicated those results, but modified the procedure used to force the equation through the measured zero wind speed value for K_{F_a}. For the third set of analyses, a nonlinear model was fit to the data for all fittings to examine CBI's decision to model some of the fittings with a linear rather than a power function. Each of the analyses is described below.

As described earlier (Section 5.1.4.1), the fitting loss equations were developed by CBI/API using a three stage procedure. Because the raw data were unavailable at the time of the review, the first step of the procedure was not replicated, and all analyses began with the initial loss rates in units of lb-mole/yr generated by CBI. Note that for all fittings (except one) considered in these analyses only a single test was conducted at each wind speed, resulting in four data points for each fitting; one data point each at wind speeds of 0, 4.3, 8.5, and 11 mph. The MRI curve fitting analyses were performed using SAS procedures that employ the same curve fitting techniques as those used in the CBI software package.

For the first set of analyses, the zero wind speed data were given a weight of 3,000 and the other data points were given a weight of 1. The CBI procedure and MRI replication produce valid parameter estimates, but they produce incorrect measures of the precision of those estimates. First, by weighting a single point heavily to force the intercept (K_{F_a}) of the models to fit the measured zero wind speed emission rate, the majority of the "data" fit the curve exactly, giving an incorrect picture of the fit. Second, the use of the average emission rate rather than the actual calculated emission rate for each test artificially reduces the variability of the estimates (this only relates to fitting No. 5, 3 in. roof leg--pontoon area/no control; for all other fittings only one test was conducted at each wind speed).

The second set of analyses incorporated two modifications to overcome these problems. First, to force the models through the measured intercept, the calculated emissions at zero wind speed were subtracted from the calculated emissions at the other wind speeds. Then, simplified models that excluded the term K_{F_a} were fit using only the nonzero wind speed data. Second, the actual calculated values for each test were used in the analyses, rather than the average values at each wind speed. (Note that this second modification only affected fitting 5 because all other fittings had only one test at each wind speed.) This second set of analyses produced essentially the same parameter estimates as the first set, but it provided a more reliable measure of the precision of the estimates.

The final set of analyses was conducted using basically the same methods as the second set, but a power curve was fit for all fittings. The purpose of this last set was to examine the basis of the decisions by CBI to use a linear predictor rather than a power curve for some of the fittings.

The results of the first two sets of analyses are shown in Tables 5-9 and 5-10, respectively. Both analyses produced equivalent parameter estimates and replicated those reported by CBI. However, the confidence intervals for the second method, which are a much better reflection of the actual precision of the estimates, are much wider than those for the first method. Also, many of the intervals are quite wide relative to the parameter estimates.

TABLE 5-9. SUMMARY OF PARAMETER ESTIMATES - CB&I/API REPLICATE ANALYSES

Fitting No.	Fitting description	Parameter estimates				
		$A = K_a$	$B = K_b$		$C = m$	
		Estimate	Estimate	95% confidence interval	Estimate	95% confidence interval
5	Deck leg (3" dia.) -Pontoon Area/No control	2.012	0.3067	(0.3056, 0.3078)	1	--
6	Deck leg (3" dia.) - Center deck, Double Deck roof	0.825	0.0873	(0.0857, 0.0089)	1	--
7	Deck leg (3" dia.) – Pontoon Area/gasket	1.349	0.0365	(0.0361, 0.0369)	1	--
8	Deck leg (3" dia.) – Pontoon Area/sock	1.190	0.0614	(0.0610, 0.0618)	1	--
9	Gauge Hatch/Sample Port (8" dia.) – ungasketed	2.340	-0.0226	(-0.0239, -0.0213)	1	--
10	Vacuum breaker (10" dia.) – ungasketed	7.786	0.0287	(0.0282, 0.0291)	3.398	(3.392, 3.404)
11	Gauge-Float well (20" dia.) - unbolted, ungasketed	14.420	6.548	(6.528, 6.568)	1	--
12	Access Hatch (24" dia.) - unbolted/no gasket	36.440	8.545	(8.416, 8.583)	1	--
13	Gauge hatch/sample well (8" dia.) – gasketed	0.471	0.0205	(0.0201, 0.0209)	1	--
14	Vacuum breaker (10" dia.) – gasketed	6.174	0.9942	(0.9902, 0.9982)	1	--
15	Gauge float well (20" dia.) - unbolted/gasket	4.254	16.77	(10.73, 16.80)	0.3891	(0.3881, 0.3990)
16	Access Hatch (24" dia.) - unbolted/gasket	31.440	10.65	(10.52, 10.78)	1	--
21	Deck drain (3" dia.) – open	1.462	0.1376	(0.1349, 0.1402)	1.927	(1.919, 1.935)
22	Deck drain (3" dia.) - 90% closed	1.841	0.1951	(0.1926, 0.1976)	1	--

5-39

TABLE 5-10. SUMMARY OF PARAMETER ESTIMATES - MRI ANALYSES

Fitting No.	Fitting description	Parameter estimates				
		$A = K_a$	$B = K_b$		$C = m$	
		Estimate	Estimate	95% confidence interval	Estimate	95% confidence interval
5	Deck leg (3" dia.) -Pontoon Area/ungasketed	2.012	0.3067 [0.37]	(0.2276, 0.3858)	1 [0.91]	--
6	Deck leg (3" dia.) - Center deck, Double Deck roof/ungasketed	0.825	0.0873 [0.53]	(-0.0229, 0.1975)	1 [0.14]	--
7	Deck leg (3" dia.) - Pontoon Area/gasket	1.349	0.0365 [0.08]	(0.0101, 0.0629)	1 [0.65]	--
8	Deck leg (3" dia.) - Pontoon Area/sock	1.190	0.0614 [0.14]	(0.0362, 0.0866)	1 [0.65]	--
9	Gauge hatch/sample port (8" dia.) – ungasketed	2.340	-0.0226 [0.0]	(-0.110, -0.0648)	1 [0.0]	--
10	Vacuum breaker (10" dia.) – ungasketed	7.786	0.0287 [0.01]	(0.0952, 0.1525)	3.398 [4.0]	(1.632, 5.165)
11	Gauge-float well (20" dia.) - unbolted, ungasketed	14.420	6.548 [5.4]	(5.145, 7.951)	1 [1.1]	--
12	Access hatch (24" dia.) - unbolted/ ungasketed	36.440	8.544 [5.9]	(5.892, 11.20)	1 [1.2]	--
13	Gauge hatch/sample port (8" dia.) – gasketed	0.471	0.0206 [0.02]	(-0.0075, 0.0487)	1 [0.97]	--
14	Vacuum breaker (10" dia.) – gasketed	6.174	0.9943 [1.2]	(0.7195, 1.269)	1 [0.94]	--
15	Gauge-float well (20" dia.) - unbolted/gasketed	4.254	16.77 [17]	(6.326, 27.20)	0.3891 [0.38]	(0.1042, 0.6739)
16	Access hatch (24" dia.) - unbolted/gasketed	31.440	10.65 [5.2]	(1.46, 19.84)	1 [1.3]	--
21	Deck drain (3" dia.) – open	1.462	0.1376 [0.21]	(-0.6256, 0.900)	1.927 [1.7]	(-0.387, 4.242)
22	Deck drain (3" dia.) - 90% closed	1.841	0.1951 [0.14]	(0.0235, 0.3667)	1 [1.1]	--

5-40

To develop a better understanding of the effect of the uncertainty of these parameter estimates on the actual estimated emissions generated from the equations, MRI developed graphs of the estimating equations and 95 percent confidence intervals (95 percent CI's) for those estimates. The graphical results indicate that for the four roof leg conditions, there is virtually no difference among fitting Nos. 6, 7, and 8; subsequent statistical analysis showed that they can be modeled by a single equation. Generally, for each of the 6 types of fittings, at lower wind speeds particularly, the difference in the estimates for controlled and uncontrolled fittings is of the same order of magnitude as the uncertainty in emissions. This uncertainty could be the result of a small sample size or of the inherent variability in emissions.

Further examination of the data for access hatches, vacuum breakers, and gauge-float wells raised other concerns about the reliability of the emissions estimates produced by these equations. First, although the gauge-float well (20 in. diameter) is intermediate in size between the 10 in. diameter vacuum breaker and the 24 in. diameter access hatch, the emissions at high wind speed are lower than those from the other fittings. Also, the pattern in reduction from adding a gasket to the access hatch is much different than the patterns in reduction from adding gaskets to the vacuum breaker or the gauge-float well. The vacuum breaker and gauge-float well show substantial reductions at high wind speeds when a gasket is applied, while the access hatch shows essentially no difference.

The results presented in Table 5-10 indicate an estimated wind speed exponent (m) equal to 1 for all fittings except Nos. 10, 15, and 21. In other words, a linear correlation between evaporative loss and wind speed was assumed. This assumption is embedded in the approach followed by API in the data analysis submitted to MRI. Subsequently, as with the procedure used for other analyses (e.g., guide poles and rim-seals), both the net emission rate (at each wind speed) and the measured wind speed were log transformed and a least squares regression was performed in order to obtain estimates of m and log K_{F_b}. These estimates were then exponentiated to obtain an estimate of K_{F_b}. The fitting loss factors based on the linear regression of the log-transformed data are the factors recommended for AP-42. Table 5-10 presents these factors in brackets.

It should be noted that the results for the ungasketed gauge hatch/sample port were interpreted differently than the other fittings. If the raw test data for this fitting are used, the model would predict that emissions decrease as the wind speed increases. Since this result is contrary to good engineering judgement, the emission losses at varying wind speeds were averaged to determine a single zero-wind speed loss factor (K_{F_a} = 2.2) for this fitting. Using this approach, it is inherently assumed that there is no wind effect on this fitting configuration. Note that API recommended a factor based upon averaging the emission losses at zero wind speed only (K_{F_a} = 2.3).

The deck fitting evaporative loss data evaluated as described in the preceding paragraphs were obtained from the most recent test program conducted by API. However, this test program did not include evaluation of several external floating deck fitting configurations. These configurations include:

1. Rim vent, gasketed;
2. Rim vent, ungasketed;
3. Access hatch, bolted cover, gasketed;
4. Gauge-float well, bolted cover, gasketed;
5. Deck leg, adjustable, double deck roof;
6. Deck leg, fixed;
7. Deck leg, center area, gasketed; and
8. Deck leg, center area, sock.

For rim vents, gasketed and ungasketed, the factors from the previous edition of AP-42 are recommended:

(K_{F_a} = 0.71, K_{F_b} = 0.10, and m = 1.0 for gasketed rim vents; K_{F_a} = 0.68, K_{F_b} = 1.8, and m = 10 for ungasketed rim vents).

For an access hatch with a bolted, gasketed cover, fitting factors based on the original IFR test data for an access hatch with a bolted, gasketed cover are recommended (K_{F_a} = 1.6, K_{F_b} = 0, m = 0). Given the fact that the zero wind speed estimates for common fittings should be equivalent for both types of floating roofs, it is consistent to use the zero wind speed factor for an IFR tank for an EFR tank also. In addition, it is not anticipated that there would be any wind effects on an access hatch with a bolted, gasketed cover. In the case of the gauge-float well with a bolted, gasketed cover, the IFR factor from the previous AP-42 edition for the same fitting was also examined. The original zero wind speed (IFR) factor for the gauge-float well was 5.1. However, an examination of the basis of the original IFR factor revealed that the zero wind speed factor was based on a sum of the zero wind speed factor for an access hatch with a bolted, gasketed cover and three times the zero wind speed factor for a 1-in. stub drain. The rationale behind the development of this factor was that the gauge-float well was approximately the same size as the access hatch and the fact that there are typically three small penetrations in the top of the float well cover in an IFR tank. One of the small penetrations was for the cable that connected to the float in the well. Mr. Rob Ferry of TGB indicated that the other penetrations were sealed off for the most part. In reexamining the development of the zero wind speed factor for the gauge-float well, it was determined that the factor should be based on the sum of the zero wind speed factors for the access hatch with a bolted, gasketed cover and the 1-in. stub drain. Thus, the 1-in stub drain was added in only once and not three times. This revision is recommended because on EFR tanks there is typically only one small penetration in the gauge float well to allow the cable to pass through for the float; also, on IFR tanks to the remaining two penetrations are for the most part sealed off. The revised factors are K_{F_a} = 2.8, K_{F_b} = 0, m = 0.

The same factors for the adjustable deck leg, center area, are recommended for the adjustable deck leg for double deck roofs (K_{F_a} = 0.82, K_{F_b} = 0.53, m = 0.14). The fixed deck leg factors (0) from the previous edition remain unchanged.

Factors for center-area deck legs with gaskets and socks were developed using the factors for pontoon-area deck legs.[13] Loss factors were derived using a method similar to that used to develop rim seal loss factors when no test data were available for certain configurations. The percent reductions achieved by gaskets and socks on pontoon-area deck legs were applied to the ungasketed center-area leg at wind speeds of 0, v_i, and v_j mph (where $v_i = 10^{-100}$ mph and $v_j = 4$ mph) and the form of the loss equation was assumed to be:

$$E = K_{F_a} + K_{F_b} v^m$$

where:

E = deck leg loss, lb-mole/yr
K_{F_a} = zero wind speed loss factor, lb-mole/yr
K_{F_b} = wind-dependent loss factor, lb-mole/mph^m-yr
v = ambient wind speed, mph
m = wind speed exponent, dimensionless

By assigning the 0 mph loss value to K_{F_a}, K_{F_b} and m are determined using the derived loss values at v_i and v_j.

Note that 2½ in. deck legs were not tested during the most recent tests by API. This size roof leg is atypical; consequently, factors for these fittings are not recommended in this edition of AP-42.

Conclusions. The deck fitting parameters calculated by API using a simple linear regression provide reasonable predictions of evaporative losses. However, to be consistent with procedures used for determining the loss factors for other fittings, data analysis procedures based upon a linear regression of log-transformed wind speed and evaporative losses are recommended for developing factors for deck fittings. However, for the ungasketed gauge hatch/sample port fitting test data, this approach results in factors that predict decreasing emissions with increasing wind speed. Since this result is contrary to good engineering judgment, a single zero wind speed loss factor based upon the average losses measured at zero wind speed is recommended ($K_{F_a} = 2.3$).

5.1.4.5 Evaluation of Other Internal Floating Deck Fitting Factors. Internal floating roof tanks are equipped with a fixed roof; therefore, the wind effect on evaporative losses is mitigated. The individual fitting loss factors for internal floating roof tanks are represented by emission measurements at zero wind speed. Many of the fittings used on external roof tanks are also used on internal floating roof tanks (i.e., access hatches) or the fittings are of a similar construction between tank types (i.e., column wells on IFR's compared to guide pole wells on EFR's). Although the most recent API test program did not include internal floating deck fittings, the zero wind speed measurement data for similar fittings were used to revise the IFR factors, where applicable. Otherwise, the IFR fitting factors from the previous edition of AP-42 remain unchanged. Specifically:

1. Fixed roof support column well factor.

a. The round pipe fixed roof suport wells with and without a gasketed sliding cover are similar in design to the unslotted guide-pole wells with and without a gasketed sliding cover. Therefore, the new fitting factors developed for the unslotted guide pole wells are used for the round pipe fixed roof support column wells (K_{F_a} = 31 for ungasketed; K_{F_a} = 25 for gasketed).

b. The factor for a round pipe fixed roof support column well with a flexible fabric sleeve seal remains unchanged (K_{F_a} = 10).

c. The factors for built-up column fixed roof support wells with a gasketed sliding cover (K_{F_a} = 33) and without a gasketed sliding cover (K_{F_a} = 47) remain unchanged.

2. Gauge hatch/sample port with slit fabric seal. This factor remains unchanged (K_{F_a} = 12).

3. Stub drain (1 in.). This factor remains unchanged (K_{F_a} = 1.2).

4. Ladder well with sliding cover, with and without a gasket. These factors remain unchanged (K_{F_a} = 76 for ungasketed; K_{F_a} = 56 for gasketed).

5. Deck leg for internal floating deck. This factor remains unchanged (K_{F_a} = 7.9).

5.1.4.6 Recommended AP-42 Deck Fitting Loss Factors. The recommended deck fitting loss factors for AP-42 are summarized in Table 5-11.

TABLE 5-11. RECOMMENDED DECK-FITTING LOSS FACTORS, K_{Fa}, K_{Fb}, AND m[a]

Fitting Type And Construction Details	Loss Factors			Typical Number Of Fittings, N_F
	K_{Fa} (lb-mole/yr)	K_{Fb} (lb-mole/(mph)^m-yr)	m (dimensionless)	
Access hatch (24-inch diameter well)				1
Bolted cover, gasketed[b]	1.6	0	0	
Unbolted cover, ungasketed	36[c]	5.9	1.2	
Unbolted cover, gasketed	31	5.2	1.3	
Fixed roof support column well[d]				N_C (Table 7.1-11)
Round pipe, ungasketed sliding cover	31			
Round pipe, gasketed sliding cover	25			
Round pipe, flexible fabric sleeve seal	10			
Built-up column, ungasketed sliding cover[c]	51			
Built-up column, gasketed sliding cover	33			
Unslotted guide-pole and well (8-inch diameter unslotted pole, 21-inch diameter well)				1
Ungasketed sliding cover[b]	31	150	1.4	
Ungasketed sliding cover w/pole	25	2.2	2.1	
sleeveGasketed sliding cover	25	13	2.2	
Gasketed sliding cover w/pole wiper	14	3.7	0.78	
Gasketed sliding cover w/pole sleeve	8.6	12	0.81	
Slotted guide-pole/sample well (8-inch diameter slotted pole, 21-inch diameter well)[e]				f
Ungasketed or gasketed sliding cover	43	270	1.4	
Ungasketed or gasketed sliding cover, with float[g]	31	36	2.0	
Gasketed sliding cover, with pole wiper	41	48	1.4	
Gasketed sliding cover, with pole sleeve	11	46	1.4	
Gasketed sliding cover, with pole sleeve and pole wiper	8.3	4.4	1.6	
Gasketed sliding cover, with float and pole wiper[g]	21	7.9	1.8	
Gasketed sliding cover, with float, pole sleeve, and pole wiper[h]	11	9.9	0.89	
Gauge-float well (automatic gauge)				1
Unbolted cover, ungasketed[b]	14[c]	5.4	1.1	
Unbolted cover, gasketed	4.3	17	0.38	
Bolted cover, gasketed	2.8	0	0	
Gauge-hatch/sample port				1
Weighted mechanical actuation, gasketed[b]	0.47	0.02	0.97	
Weighted mechanical actuation, ungasketed	2.3	0	0	
Slit fabric seal, 10% open area[c]	12			
Vacuum breaker				N_{vb} (Table 7.1-13)[j]
Weighted mechanical actuation, ungasketed	7.8	0.01	4.0	
Weighted mechanical actuation, gasketed[b]	6.2[c]	1.2	0.94	

Table 5-11 (cont.)

Fitting Type And Construction Details	Loss Factors			Typical Number Of Fittings, N_F
	K_{Fa} (lb-mole/yr)	K_{Fb} (lb-mole/(mph)^m-yr)	m (dimensionless)	
Deck drain (3-inch diameter)				N_d (Table 7.1-13)
Open[b]	1.5	0.21	1.7	
90% closed	1.8	0.14	1.1	
Stub drain (1-inch diameter)[k]	1.2			N_d (Table 7.1-15)
Deck leg (3-inch diameter)				N_l (Table 7.1-15), (Table 7.1-14)
Adjustable, internal floating deck[c]				
Adjustable, pontoon area - ungasketed[b]	7.9	0.37	0.91	
Adjustable, pontoon area - gasketed	2.0	0.08	0.65	
Adjustable, pontoon area - sock	1.3	0.14	0.65	
Adjustable, center area - ungasketed[b]	1.2	0.53	0.14	
Adjustable, center area - gasketed[m]	0.82	0.11	0.13	
Adjustable, center area - sock[m]	0.53	0.16	0.14	
Adjustable, double-deck roofs	0.49	0.53	0.14	
Fixed	0.82	0	0	
	0			
Rim vent[n]				1
Weighted mechanical actuation, ungasketed	0.68	1.8	1.0	
Weighted mechanical actuation, gasketed[b]	0.71	0.10	1.0	
Ladder well				1[d]
Sliding cover, ungasketed[c]	98			
Sliding cover, gasketed	56			

5.1.5 Development of the Fitting Wind Speed Correction Factor[14-16]

Evaporative loss from external floating roof tanks has been shown to be wind dependent. The old EFRT fitting loss estimating equation included the assumption that the wind speed across the deck is equivalent to the local ambient wind speed. It is known from field experience, however, that the shell of the tank partially shields the floating roof from the wind. Therefore, the fitting wind speed correction factor has been added to the deck fitting loss equation to account for the reduction in wind speed across the floating roof as compared to the ambient wind speed. This addition results in the following form of the fitting loss estimating equation:

$$K_F = K_{F_a} + K_{F_b}(K_v v)^m$$

where:

K_F =loss factor for a given deck fitting, lb-mole/yr
K_{F_a} =zero wind speed loss factor, lb-mole/yr
K_{F_b} =wind speed dependent loss factor, lb-mole/mph^m-yr
K_v =fitting wind speed correction factor, dimensionless
v =average ambient wind speed at tank location, mph
m =deck fitting loss exponent, dimensionless

While this shielding effect was previously a known phenomenon, no data were available to quantify the reduction in wind speed across the deck. Therefore, wind tunnel testing, a roof height survey, and an evaluation of field data were conducted to determine the actual reduction.

The CPP wind tunnel test program modeled EFRT's of 48, 100, and 200 feet in diameter, with the floating roof positioned at three different heights in each tank.[14] The roof heights chosen were grouped to result in three ranges of roof height as follows:

$$0.35 \leq R/H \leq 0.75$$
$$0.80 \leq R/H \leq 0.90$$
$$R/H = 1.0$$

(The ratio R/H is the ratio of the floating roof height to the tank shell height.)

Average horizontal wind speeds were calculated for each roof height range at 28 locations across each floating roof. The test program concluded that a single factor could reasonably be used to account for the reduction in wind speeds for all areas of the floating roof, at all roof heights and tank diameters. This factor was determined by calculating separate correction factors for each of the roof height ranges and then calculating a weighted average of these three factors based on an assumed distribution of time that the floating roof would spend in each height range. The distribution was based on a complete cycle of a floating roof, where the tank begins empty, rises through each height range, and then empties back through each range. This assumption results in the following distribution:

$0.35 \leq R/H \leq 0.75$	40 percent
$0.80 \leq R/H \leq 0.90$	40 percent
$R/H = 1.0$	20 percent

This test program determined that the wind speed on the floating roof is about 0.4 times the ambient site wind speed in the first two height ranges, but increases to about 0.7 times the ambient at the third roof height. Although the third roof height (R/H = 1.0) is not a position that occurs in the normal operation of storage tanks, it was conservatively included in the calculation of the weighted average correction factor. A value of 0.52 was calculated by CPP for the single fitting wind speed correction factor.

To investigate the validity of the assumption regarding roof height distribution, a survey of roof heights was conducted. Forty tanks were evaluated based on 12 consecutive monthly records of liquid level. These liquid levels were then compared to the height of the tank shell, and the ratio of liquid level to shell height determined. Each ratio was then assigned to one of the height ranges from the wind tunnel study, with any readings not falling within a range being assigned to the next higher range. This approach resulted in tanks over 0.9 being assigned to the R/H = 1.0 range. The resulting distribution was as follows:

Assigned range	Assumed distribution, percent	Actual distribution, percent
$0.35 \leq R/H \leq 0.75$	40	77.7
$0.80 \leq R/H \leq 0.90$	40	15.6
$R/H = 1.0$	20	6.7

While the weighted average single factor had assumed the floating roof to be at the top of the tank shell 20 percent of the time, in the survey it was found to be in the top 10 percent of the shell height only 6.7 percent of the time. The distribution assumed in the wind tunnel test study was therefore conservative compared to the distribution determined from this survey.

Field wind speed data were also evaluated in the analysis of the fitting wind speed correction factor. Measurements of wind speed were taken at two external floating roof tanks at a petroleum refinery over an eleven month period. Site wind speed was measured at a platform located at the top of the shell of one of the tanks. Wind speed across the floating roof of each tank was measured at two locations on the deck, one near the perimeter and one near the center of the deck. Both horizontal and vertical wind speed were measured. Approximately 30 readings were taken per day.

Five months worth of data from one of these tanks were evaluated. Daily average wind speeds were determined at each of the two locations on the floating roof, as well as at the platform. However, in this analysis, only the horizontal wind speed measurements were used. Due to some interruptions in the data, only 142 days were included in the evaluation. The wind speeds were summed for each measurement location and the ratio of floating roof to ambient wind speed was calculated for the two deck locations. The resulting ratios were 0.45 for the outer area of the deck and 0.53 for the inner area. The resulting average, 0.49, corresponds well with the value of 0.52 calculated for the single factor in the wind tunnel test program. A correction factor of 0.5 was adopted by API and published in their draft Manual of Petroleum Measurement Standards, Chapter 19, Section 2.[5] A summary of the analysis and conclusions is presented in the report entitled "Documentation of the Fitting Wind-Speed Correction Factor."[15]

The single wind speed correction factor developed by API in the wind tunnel test program was determined using generally conservative procedures. As stated, the correction factor for the highest roof position was weighted at 20 percent, while the roof height survey indicated that the roof would be at this height less than 10 percent of the time. Further, the factor was developed based on wind speed at an isolated tank. For a tank farm scenario, the wind speed at the tank is expected to be only 80 percent of the site ambient wind speed.

The field data were evaluated and used by API to compare to the wind speed correction factor developed from the wind tunnel study. The field data were also evaluated by MRI; during MRI's review, several questions were raised. Those questions and MRI's evaluation of the field data are discussed in the following paragraphs.

During the wind tunnel study performed to determine evaporative loss rates from deck fittings, only a horizontal wind speed component was measured; however, the total wind speed was equal to the horizontal wind speed (i.e., there was no vertical component). The wind tunnel turbulence was much less than that expected on an actual tank (7 percent in the tunnel versus 20 to 100 percent expected).

Although the effect of turbulence on evaporative loss from fittings is unknown, the CPP report indicates that an increase in turbulence may cause an increase in evaporative loss. During the testing, the wind speed in the tunnel was held as constant as possible to reduce variability in loss rates and provide a stable estimate of the rate at each test condition. Also, only the horizontal wind speed vector was measured during the wind tunnel study performed to determine the fitting wind speed correction factor, although a vertical wind speed component may have been present. Development of the wind speed correction factor by API was based on the wind tunnel data and, consequently, only a horizontal wind speed vector.

The factor API developed from their analysis of the field data agrees well with the factor they developed from the wind tunnel study. However, both horizontal and vertical wind speed vectors were measured in the field study. Questions regarding what effect the vertical vector of the wind speed has on emissions and whether the vertical component should be incorporated into the calculation of the wind speed correction factor were raised during MRI's analysis. Since no data exists on the effects of the vertical component of wind speed on evaporative loss, it is difficult to assess whether that component should be included in the calculation of the wind speed correction factor.

Another issue concerns the accuracy of the field data. For example, there are some measurements of deck wind speed that are more than 10 times the ambient wind speed. In addition, no information was provided concerning the accuracy of the measurement devices. The field data were used as a validation of the wind tunnel study, but it is unclear whether or not the data are accurate.

Finally, the fitting loss factors in AP-42 Section 7.1 are applicable only for wind speeds up to 15 miles per hour. Average ambient wind speeds during the field test were generally low, with a maximum wind speed of about 6 m/s (13 mph). However, CPP's wind tunnel tests were conducted at wind speeds of greater than 6 m/s (13 mph).

Analyses of the field data were conducted by MRI to replicate API's analysis and to determine the value of the wind speed correction factor when the vertical wind speed component is included. The first analysis replicated API's analysis, using only the horizontal wind speed measurements. A correction factor of 0.5 resulted. The second analysis used both the horizontal and vertical vectors of the wind speed measured on the floating deck. Daily average wind speeds were calculated for the 5 month period used in the API analysis. A vector addition ($Horiz^2 + Vert^2 = Total^2$) was then performed to determine a total deck wind speed vector for each daily average at both inner and outer locations. The ratio of deck to ambient wind speed was calculated for each data point and measurement location. An average ratio was then determined for the inner and the outer locations. These two ratios were then averaged and an average fitting wind speed correction factor of 0.69 was calculated.

The field data indicate that a vertical wind speed component is present at the deck surface on an EFRT. However, no data are available to evaluate the effect of a vertical wind speed component on evaporative loss. Further, no wind tunnel data are available that quantify a vertical wind speed component for different tank configurations.

Previously, API recommended a wind speed correction factor of 0.5 based on their analyses of the wind tunnel and field data. Due to the fact that no data are available on the effects of the vertical wind speed component on evaporative loss, the most conservative approach is to use the factor calculated by MRI from the field data, even though the accuracy of the field data is uncertain, and the field data represent only one test condition. Therefore, the fitting wind speed correction factor recommended for use in AP-42 is 0.7.

5.1.6 Deck Seam Loss Factor[4,17-19]

In developing the IFRT deck seam loss factor, API assumed that deck seam losses from welded decks are zero. The deck seam loss factor for bolted decks was calculated based on the difference in the average emissions from two sets of pilot tank tests with all loss sources sealed and all loss sources but deck seams sealed. The IFRT deck seam loss factor previously in AP-42 was K_D = 0.34 lb-mole/ft-yr; it applied to both contact and noncontact internal floating decks with bolted deck seams. Additional testing has been conducted by CBI in their weight loss test facility on both contact and noncontact floating roof bolted deck seams of various sizes. The purpose of the additional testing was to develop and validate API's draft weight loss test method for the measurement of deck seam loss factors for internal floating roof tanks. The test data may be found in References 17-19.

5.1.5.1 Noncontact Deck Seam Data. The noncontact deck seam loss factor data include the pilot scale tank test data used in developing the old deck seam loss factor and data from laboratory scale tests conducted using different sizes of pan-type assemblies. The laboratory scale deck seam test assemblies consist of panels bolted together with deck seams and sealed over a rectangular reservoir which contains the test liquid. Two test assemblies are used: a blank test assembly with no deck seams and a deck seam test assembly. The test assemblies are filled with a volatile test liquid of known properties (normal hexane) and are suspended from load cells. The rate of weight loss from the test assembly is then measured over time and compared to the weight loss rate from a blank assembly without deck seams to determine the deck seam loss factor. It was observed that for deck seams, the weight loss versus time data could be correlated using a linear relationship. Data are adjusted so a correlation is obtained at the average test temperature. Table 5-12 describes each noncontact deck seam assembly tested.

The deck seam loss factor, K_D, for each test is determined as follows. First, the vapor pressure function is calculated for the deck seam test assembly and the blank using the mean stock vapor pressure and mean test room atmospheric pressure during the test:

$$P^* = \frac{\frac{P_{VA}}{P_A}}{\left[1 + \left(1 - \frac{P_{VA}}{P_A}\right)^{0.5}\right]^2}$$

where:

P^* = vapor pressure function, dimensionless
P = mean vapor pressure of test liquid, psia
P_a = mean atmospheric pressure in test room, psia

The loss factor for the test deck seam assembly is then determined using the loss rate, vapor pressure function, and stock vapor molecular weight, as follows:

$$F = E / P^* M_v K_c$$

where:

F =loss factor of the test assembly, lb-mole/hr
E =loss rate of the test assembly, lb/hr
P^* =vapor pressure function, dimensionless
M_v =vapor molecular weight of the test liquid, lb/lb-mole
K_c =product factor, dimensionless (for organics, $K_c = 1$)

The loss factor for the blank assembly is determined in the same manner.

The deck seam loss factor, K_D, for the test is then determined using the loss factors for the deck seam and blank test assemblies:

$$K_D = \frac{(365.25\ d/yr)(24\ hr/d)(\pi)(F_D - F_B)}{4\ L_D}$$

where:

K_D = deck seam loss factor, lb-mole/ft-yr
F_D = deck seam test assembly loss factor, lb-mole/yr
F_B = blank test assembly loss factor, lb-mole/yr
L_D = total length of the test deck seams, ft

Deck seam loss factors for each noncontact deck seam assembly tested are given in Table 5-12. The deck seam loss factors appear to vary with the size of the test assembly used. In addition, the perimeter seal loss rates for blank assembly tests 9 and 13 were an order of magnitude higher than expected, and CBI notes in the test report (Reference 18, Interim Report No. 7, October 7, 1996) that it was expected that the perimeter seal loss factors for these tests would be closer to those measured in tests 4, 4R, and 9R. It was discovered that the assembly used for blank test 13 had a substantial leak. However, the repeat test, 13R, showed an even higher perimeter seal loss rate, so CBI used the data from test 13 to calculate the deck seam loss factor for test 12 in the test report. In addition, the temperature coefficients calculated for tests 13 and 13R are negative, indicating that as temperature increases, weight loss decreases. Therefore, MRI discarded blank tests 13 and 13R. MRI recalculated the deck seam loss factor for test 12 using test 9R as the blank, resulting in a deck seam loss factor of 0.030 lb-mole/ft-yr, rather than 0.015 lb-mole/ft-yr.

TABLE 5-12. NONCONTACT DECK SEAM LOSS FACTORS BY TEST

Deck seam loss factor test	Test assembly description	Test Nos.		Deck seam loss factor, K_D (lb-mole/ft-yr)
		Deck seam	Blank	
Pilot scale tank[a]	18'10" diameter 7'x18' panels 2 deck seams	76R	77	0.12
Large test cells	6'x16'8" panels 2 deck seams	8R	9R	0.089
		8	9	0.016
	Average			0.053
	1'x16'8" panels 6 deck seams	12	9R	0.030
Small test cells	4"x4' panels 5 deck seams	1	4	0.017
		1R	4R	0.015
		2R	4R	0.010
		3	4	0.0051
		3R	4R	0.0064
	Average			0.011

[a]Used to develop old factor.

TABLE 5-13. CONTACT DECK SEAM LOSS FACTORS BY TEST

Deck seam loss factor test	Test assembly description	Test Nos.		Deck seam loss factor, K_D (lb-mole/ft-yr)
		Deck seam	Blank	
Pilot scale tank[a]	18'10" diameter 7'x18' panels 2 deck seams	56	55	0.57
Large test cell	2'4"x7' panels 6 deck seams	10	NA	0.13
Small test cell	4"x4' panels 5 deck seams	5R	7R	0.11
Petrex pan test	12"x20" panel 1 deck seam	2	1	0.12

[a] Used to develop old factor.

5.1.5.2 Contact Deck Seam Data. The deck seam test data for internal floating decks that contact the liquid surface include: (1) the pilot scale tank contact deck seam data used in the development of the current deck seam loss factor; (2) a "small" contact deck seam test assembly of the same dimensions as those in the noncontact deck seam tests; (3) a "large" contact deck seam test assembly; and (4) a small test assembly with one deck seam, tested by Petrex, Inc. in 1984. The test assemblies are described in Table 5-13.

A blank test assembly was not used for the "large" test assembly (test 10) because the perimeter seals were welded. Otherwise, the deck seam loss factors for each test assembly were calculated in the same manner as those for the noncontact deck seams. The loss factors for each contact deck seam assembly tested are presented in Table 5-13. With the exception of the pilot tank test, the loss factors are very similar for the contact deck seam tests.

5.1.5.3 Revised Deck Seam Loss Factor. It can be observed from Table 5-12 that the noncontact deck seam loss factors for the individual test assemblies vary with the size of the deck seam assembly tested. Sufficient data are not available to determine whether the variation is a direct result of the size of panel/assembly used, or due to some error or variation in test procedure or test assembly construction. However, the data available do suggest that as the size of the test assembly increases, the deck seam loss factor increases. The noncontact test data range in value from 0.0064 to 0.12 lb-mole/ft-yr. In contrast, the laboratory scale contact deck seam loss factors for the individual test assemblies are consistent with each other, ranging from 0.11 to 0.13 lb-mole/ft-yr. The pilot test tank, however, exhibited a much higher loss factor of 0.57 lb-mole/ft-yr.

There are a few possible explanations for the higher loss factors from the pilot scale tank. For the pilot tank tests, tests were conducted (a) with all loss sources sealed, and (b) with all loss sources sealed except deck seams. The deck seam loss rate was determined as the difference in loss rate for these two tests. However, the loss rate experienced when all loss sources were sealed was still considerable in comparison to the loss rate attributed to the deck seams (for the case of the noncontact bolted deck, the loss rate attributed to the deck seams was only about 4 percent of the total loss rate). On the other hand, in the laboratory scale testing, the blank assembly loss rates were an order of magnitude lower than the deck seam assembly loss rates.

There is a wide range in the data for the various test configurations. The data available are inconclusive in supporting the use of any particular size panel for loss factor development. In addition, a t-test showed that the means of the contact and noncontact data are not statistically different at the 95 percent confidence level. Therefore, an average deck seam loss factor was calculated for each test assembly construction and then those data were averaged to obtain a revised deck seam loss factor. The resulting average deck seam loss factor is 0.14 lb-mole/ft-yr. This value is approximately 40 percent of the old deck seam loss factor of 0.34 lb-mole/ft-yr.

5.1.6 Vapor Pressure Functions

Three alternative vapor pressure functions were considered for the vapor pressure scaling component of the floating roof tank equations. Those functions included two functions considered in different versions of API Publication 2519 and an alternative recommended by TRW. These three functions are:

$$P_1^* = \frac{P_V / 14.7}{\left[1 + \left(1 - \frac{P_V}{14.7}\right)^{0.5}\right]^2}$$

$$P_3^* = (P_V / 14.7)^N$$

$$P_2^* = \left[\frac{P_V / 14.7}{1 - P_V / 14.7}\right]^{0.7}$$

where:

P_V= true vapor pressure (psia)
N= a scaling exponent (optimal value to be determined from experimental data)

Data from the 20-ft diameter pilot tank studies conducted by CBI were used to evaluate the relative merits of the three functions.[17] These studies evaluated emissions for three types of IFRT decks--a bolted noncontact deck with vapor mounted flexible wiper seals (Phases 1 and 1R), a welded contact deck with a liquid-mounted, resilient-filled seal (Phases 2 and 2R), and a bolted, contact deck with a vapor-mounted, resilient-filled seal (Phases 3 and 3R). Tests were conducted primarily for octane/propane mixtures, but limited single-component testing was conducted using n-hexane and n-octane. The analyses of the vapor pressure function used only the octane/propane mixture data.

Evaluation of the vapor pressure functions was conducted in two stages. First, the data were evaluated to determine the optimal value of N for P_3^*. Then, using that value of N, linear regression analyses were performed for each of the three test phases (i) and each vapor pressure function (P_j^*) to estimate the slope b_{ij} for the equation:

$$E = b_{ij} P_j^*$$

These values, b_{ij}, were then used to predict emissions for each test data point, and the correlation between predicted and actual emissions was used to evaluate the different vapor pressure functions.

To determine the optimal value of N, API first used the average emissions and vapor pressure for each test sequence within a test phase to estimate b_i and N_i for the three different phases by fitting the equation:

$$E = b_i (P_V /14.7)^{N}i$$

Then the three values of N_i were averaged to obtain the optimal value of N. The estimates of N_i for the three phases ranged from 0.62 to 0.76 with an average of 0.68 (which API appropriately rounded to 0.7).

A better statistical approach to this problem is to fit a single model, which permits different b_i's but only a single N, to the complete data set. Using the data presented in documentation file B.1, MRI conducted such an analysis and obtained an optimal value for N of 0.71, which is consistent with the API results. Hence, the use of N = 0.7 for P_3^* appears to be reasonable.

In the second stage of the analyses, API fit separate regression models for each test phase and vapor pressure function and used these regression models to predict emissions for each test used in the analysis. Because the number of data points was quite small (4 to 8 per test phase) and the predictions were developed for the same data sets that were used to develop the models, the correlation coefficients were predictably quite high. Furthermore, over the range of vapor pressures used in the analysis (0.7 to 6 psia), the values of the three functions differ very little. Because the three functions provided comparable results, API chose to recommend P_1^* because it was being used in API Publications 2517 and 2519 at the time of the analysis.

As a part of this study MRI reviewed the API calculations and found them to be correct. However, the vapor pressure function has not been validated on an independent data set, so neither its validity nor its reliability is well established. Consequently, the performance of the function is uncertain. Furthermore, no information is available on its validity for vapor pressures greater than 6 psia. A footnote in AP-42 tables that cautions the reader about the lack of information on the performance of the vapor pressure function at true vapor pressures greater than 6 psia is recommended.

5.2 PREDICTIVE ABILITY - ACTUAL TANK TEST DATA

5.2.1 Standing Storage Loss

The standing storage loss equations (rim-seal and deck fitting losses) were used to predict emissions based on actual storage tank parameters recorded from external floating roof tanks tested by the Western Oil and Gas Association (WOGA) in 1977.[8] Table 5-14 presents the parameters recorded for each tank tested. As shown in Table 5-14, all of the tanks stored petroleum distillates. Therefore, possible biases in the emission estimation equation could be determined only for petroleum distillates. Analyses of the performance of this equation for different stored liquids were not possible.

TABLE 5-14. TANK PARAMETERS RECORDED DURING TESTS BY THE WESTERN OIL AND GAS ASSOCIATION

Tank	Product type	Tank diameter, ft	Type of deck	Tank construction	Seal configuration
WOGA 134	Gasoline (RVP 9)	153	Double deck	Riveted	Shoe-mounted
WOGA 1757	Gasoline (RVP 9)	67	Pontoon	Welded	"Tube"
WOGA 428	J.P. 4 (RVP 6)	78	Pontoon	Riveted	Shoe-mounted
WOGA 400 x 20	Gasoline (RVP 9)	85	Double deck	Welded	Shoe-mounted
WOGA 47	Gasoline (RVP 10)	90	Pontoon	Riveted	Shoe-mounted
WOGA 48	Gasoline (RVP 10)	90	Pontoon	Riveted	Shoe-mounted
WOGA 192	Gasoline (RVP 11)	115	Double deck	Riveted	Shoe-mounted
WOGA 20010	Gasoline (RVP 9)	55	Double deck	Welded	Shoe-mounted
WOGA 80210	Light Naphtha (RVP 12)	120	Pontoon	Welded	"Tube"
WOGA 330	Gasoline (RVP 9)	120	Double deck	Welded	"Tube"
WOGA 100514	Gasoline (RVP 9)	135	Pontoon	Riveted	Shoe-mounted

In the WOGA test report, both vapor-mounted and liquid-mounted rim-seals were characterized as "tube" seals. For the tanks that were reported to be equipped with "tube" seals, the emission estimation equations were used to predict emissions for two different assumed configurations--liquid- and vapor-mounted rim-seals. No specific information was available on the type and status (gasketed, covered, etc.) of deck fittings on each external floating roof tank tested. However, the test report did state that the fittings on all the tanks met the following conditions: (1) deck leg openings were sealed; (2) emergency deck drains were at least 90 percent covered; (3) slotted gauging devices were equipped with a floating type plug; (4) roof guide openings were closed; and (5) all tank gauging or sampling devices were covered, except at the time of sampling. Due to the limited information available on fittings and other tank parameters, some assumptions were made. For example, tanks with pontoon decks are typically not equipped with deck drains. Also, most storage tanks are equipped with unslotted guide poles rather than slotted guide poles. However to account for possible deviations from this practice, the emission estimation equations were used to develop separate emission predictions for both slotted and unslotted guide poles.

Table 5-15 presents the predicted and actual emissions from 11 tanks tested by WOGA. Column 1 presents the range in predicted emissions for liquid-mounted and vapor-mounted rim-seals for those tanks equipped with "tube" seals assuming the guide pole was slotted with an ungasketed cover and float. Column 2 presents the predicted emissions based on the assumption that all tanks are equipped with slotted guide poles with an ungasketed cover and float and Column 3 presents the predicted emissions assuming the guide pole is unslotted with a gasketed cover. For tanks equipped with "tube" seals in Columns 2 and 3, it was assumed that the tank was equipped with the type seal that more closely approximated actual emissions from the tank. This assumption will minimize the "estimation error", and if it is incorrect the error estimates will be biased low. For each tank, Column 4 presents the predicted emissions selected from either Column 2 or 3 that most closely approximated actual emissions from the tanks tested.

TABLE 5-15. PREDICTED AND ACTUAL EMISSION FROM TANKS TESTED BY THE WESTERN OIL AND GAS ASSOCIATION

Tank	Predicted emissions, lb/d[a] Column 1	Predicted emissions, lb/d[b] Column 2	Predicted emissions, lb/d[c] Column 3	Predicted emissions, lb/d Column 4	Default emissions, lb/d Column 5	Actual emissions, lb/d Column 6
WOGA 134	NA	86	97	86	79	33
WOGA 1757	54 - 103	54	109	54	60	49
WOGA 428	NA	58	63	63	57	108
WOGA 400 x 20	NA	72	78	72	79	35
WOGA 47	NA	73	86	73	74	32
WOGA 48	NA	73	86	73	74	33
WOGA 192	NA	100	115	115	96	265
WOGA 20010	NA	63	69	63	58	20
WOGA 80210	54 - 293	66	83	66	83	25
WOGA 330	41 - 220	41	52	52	51	52
WOGA 100514	NA	63	73	73	74	167

[a]Range of emissions assuming vapor-mounted and liquid-mounted seals. NA = not applicable.
[b]Assumes guide-pole was slotted with float.
[c]Assumes guide-pole was unslotted with ungasketed cover.

TABLE 5-16. RELATIVE ERRORS CALCULATED FOR PREDICTED EMISSIONS PRESENTED IN TABLE 5-15

Data point	Relative errors Column 2[a]	Relative errors Column 3[b]	Relative errors Column 4[c]	Relative errors Column 5[d]
WOGA 134	1.61	1.94	1.61	1.39
WOGA 1757	0.10	1.22	0.10	0.22
WOGA 428	-0.46	-0.42	-0.42	-0.47
WOGA 400 x 20	1.06	1.23	1.06	1.26
WOGA 47	1.28	1.69	1.28	1.31
WOGA 48	1.21	1.61	1.21	1.24
WOGA 192	-0.62	-0.57	-0.57	-0.64
WOGA 20010	2.15	2.45	2.15	1.90
WOGA 80210	1.64	2.32	1.64	2.32
WOGA 330	-0.21	0.00	0.00	-0.02
WOGA 100514	-0.62	-0.56	-0.56	-0.56

[a]Mean value = 0.65; standard deviation = 1.03; and variance = 1.05.
[b]Mean value = 0.99; standard deviation = 1.16; and variance = 1.36.
[c]Mean value = 0.68; standard deviation = 0.99; and variance = 0.98.
[d]Mean value = 0.72; standard deviation = 1.05; and variance = 1.10.

In order to determine the predictive ability of the emission estimation equations, the relative errors ([predicted emissions - actual emissions]/actual emissions) were calculated for Columns 2 through 4. The values for the relative errors are shown in Table 5-16. After computing the relative errors, the mean, standard deviation, and variance of the relative errors were calculated for each column of data. Table 5-16 also presents these values.

A comparison of the means and standard deviations of the relative errors for Columns 2 and 3 shows that the predicted emissions calculated assuming that the tanks were equipped with a slotted guide pole (Column 2) more closely approximate actual emissions than the predicted emissions calculated assuming that the tanks were equipped with an unslotted guide pole (Column 3). The predicted emissions based on slotted guide poles (Column 2) overestimated actual emissions by 65 percent on average; whereas, predicted emissions based on unslotted guide poles (Column 3) overestimated actual emissions by 99 percent on average. It should be noted that tanks are typically equipped with unslotted guide poles instead of slotted guide poles. Based on the mean relative error for Column 4, the best-estimate predicted emissions overestimated actual emissions by 68 percent on average.

In addition to using actual parameters recorded during emission testing, the emission estimation equations were used to predict emissions using default values for the tanks with the exception of the type of seal specified. Default parameters included the paint color (white), the fittings (typical), and the meteorological data (temperature and wind speed) based on the tank's location. The predicted emissions assuming default values are presented in Column 5 of Table 5-14. The predictive ability of the emission estimation equations assuming default values was determined from the relative errors presented in Column 5 of Table 5-16. In addition, Table 5-16 presents the mean, standard deviation, and variance of the relative errors in Column 5. On average the predicted emissions assuming default values overestimated emissions by 72 percent, compared to 68 percent using actual tank parameters.

5.2.2 Internal Floating Roof Emissions

In Appendix B of the API documentation file on internal floating roof tanks, information regarding the predictive ability of the internal floating roof tank emission estimation procedures is presented. The basis of this study was an emission test on an internal floating roof tank performed by Radian Corporation in May 1979.[20] Table 5-17 presents the tank configuration and stored liquid properties of the internal floating roof tank tested. The measured emissions were 77.6 lb/d.

TABLE 5-17. FIELD TEST TANK PARAMETERS

Tank description	
Type	Internal floating roof
Diameter	100 ft
Shell height	30 ft, 8 in.
Product volume	926,310 gallons
Product type	Regular, unleaded gasoline (RVP 10.4)
Distillation slope 10%	2.5
Product temperature, °F	77.5
Product vapor pressure, psia	7.4
Product molecular weight, lb/lb-mole	62.4
Internal floating roof description:	
Type	Welded, contact
Rim-seal type	Vapor-mounted, resilient foam-filled
Deck fittings	1 - Automatic gauge float well, unbolted cover, ungasketed
	13-Column well, built-up column, sliding cover, gasketed
	1 - Ladder well, sliding cover, gasketed
	28 - Adjustable deck legs
	1 - Sample Well, weighted mechanically actuated, ungasketed
	1 - Vacuum breaker, weighted mechanically actuated, ungaskested
	1 - Syphon drain

In most cases, detailed information on the deck fittings is not available to the extent shown in Table 5-17. Therefore, the emission estimation procedures were used to predict emissions assuming different levels of knowledge regarding the status of the fittings that more closely approximates what a user of the internal floating roof tank emission estimation procedures would do to model emissions.

In the first scenario, the emission estimation procedures were used to predict emissions by using the fitting factors presented in Chapter 3 for all fittings except the sample well and syphon drains. For these fittings, a vacuum breaker was used to model emissions for the sample well and 36 1-in. stub drains were used to model emissions from the syphon drain. The estimated emissions under this scenario are 48 lb/d. In the second scenario, the tank was assumed to be equipped with typical fittings and the default quantities of those fittings. The estimated emission calculated under the second scenario are 32 lb/d. Under the third scenario, the tank was assumed to be equipped with typical fittings but the number of the fittings was based on the actual tank data. The estimated emissions under this scenario are 42 lb/d. For all three scenarios, the estimated emissions underpredict the actual tank emissions of 77.6 lb/d and the amount of the underprediction ranged from 38 to 59 percent. Using these scenarios, it appears that the internal floating roof tank emission estimation procedures have a tendency to underpredict emissions if detailed information is not available for the tank. However, due to the limited availability of actual tank test data, no conclusive findings can be presented on the predictive ability of the internal floating roof tank procedures.

5.3 SENSITIVITY ANALYSES

A sensitivity analysis was performed on both internal and external floating roof tanks to determine the independent variables that have the most influence on the emission estimating procedures. The results of these analyses can be used to determine the relative importance of defining a particular parameter for a tank. If the variable has a strong influence on emissions then it is important to measure that variable explicitly for the tank for which the emissions are estimated. Alternatively, if the variable has only a minor influence on emissions, then the default value for the parameter can be used without substantially biasing the emission estimate. In order to determine the influence of the independent variables on EFRT and IFRT standing storage losses (fitting, rim-seal, and deck seam losses) and withdrawal losses, default tanks were used as baseline cases.

5.3.1 Standing Storage Loss

5.3.1.1 External Floating Roof Tank. The default external floating roof tank is 153 feet in diameter and has a pontoon floating roof with typical deck fittings. This default tank stores gasoline (RVP 10) with a vapor molecular weight of 66 lb/lb-mole. The shell and roof of the tank are painted white and the tank is located in Long Beach, California (wind speed = 6.4 mph). Table 5-18 presents the results of the sensitivity analyses on EFRT standing storage losses (deck fitting and rim-seal losses). The variables that have the strongest influence on standing storage losses from EFRT's are the rim-seal factor, the wind speed, and the guidepole fitting factor.

TABLE 5-18. RESULTS OF SENSITIVITY ANALYSIS FOR THE STANDING STORAGE LOSS EQUATION FOR EXTERNAL FLOATING ROOF TANKS

Independent variables	Standing storage losses, lb/d								
	Vapor-mounted primary rim-seal			Liquid-mounted primary rim-seal			Shoe-mounted primary rim-seal		
	None[a]	rm[b]	ws[c]	None[a]	rm[b]	ws[c]	None[a]	rm[b]	sm[d]
Default tank[e]	234	70	133	54	37	44	103	43	58
Tank characteristics									
1.Paint color									
a.Red primer	312	93	178	73	49	59	137	58	77
b.Aluminum/specular	255	76	145	59	40	48	112	47	63
2.Shell construction									
a.Welded	234	70	133	54	37	44	103	43	58
b.Riveted	NA	NA	NA	NA	NA	NA	125	53	87
3.Deck type									
a.Pontoon	234	70	133	54	37	44	103	43	58
b.Double deck	232	69	132	53	36	43	101	42	57
4.Fittings									
a.Typical	234	70	133	54	37	44	103	43	58
b.Controlled	05	42	105	26	9	16	74	15	30
c.Guide-pole									
(1)usug[f]	234	70	133	54	37	44	103	43	58
(2)usg[g]	214	50	113	35	17	25	83	24	38
(3)sug or sg w/o float[h]	255	91	155	76	59	66	124	65	79
(4)sug or sg w/float[i]	222	58	122	43	26	33	91	32	46
Meteorological conditions									
1.Wind speed									
a.2 mph	38	17	23	18	13	14	33	14	18
b.6.4 mph	234	70	133	54	37	44	103	43	58
c.10 mph	760	268	409	95	62	76	205	73	103
2.Temperature									
a.66° + 20°F	390	117	222	91	62	74	171	72	97
b.66°F	234	70	133	54	37	44	103	43	58
c.66° - 20°F	143	43	81	33	23	27	63	26	35
Liquid properties									
1.Vapor pressure									
a.vp = 3.84 psia	143	43	81	33	23	27	63	26	35
b.vp = 5.74 psia	234	70	133	54	37	44	103	43	58
c.vp = 8.32 psia	390	117	222	91	62	74	171	72	97

TABLE 5-18. (continued)

Independent variables	Standing storage losses, lb/d								
	Vapor-mounted primary rim-seal			Liquid-mounted primary rim-seal			Shoe-mounted primary rim-seal		
	None[a]	rm[b]	ws[c]	None[a]	rm[b]	ws[c]	None[a]	rm[b]	sm[d]
2.Vapor molecular weigh									
a.MW = 46 lb/lb-mole	163	49	93	38	26	31	71	30	40
b.MW = 66 lb/lb-mole	234	70	133	54	37	44	103	43	58
c.MW = 86 lb/lb-mole	304	93	173	71	48	58	134	56	75

[a]No secondary rim-seal.
[b]Rim-mounted secondary rim-seal.
[c]Weather shield.
[d]Shoe-mounted secondary rim-seal.
[e]The default tank is 153 feet in diameter and is located in Long Beach, California. The tank has a pontoon floating roof with typical deck fittings. The shell and roof of the tank are painted white. The stored liquid is gasoline (RVP 10) [VP = 5.74 at ambient conditions] with a vapor molecular weight of 66 lb/lb-mole. The wind speed at the tank site is 6.4 miles per hour. The mean liquid surface temperature is 66°F.
[f]Unslotted, ungasketed.
[g]Unslotted, gasketed.
[h]Slotted, ungasketed or gasketed without float.
[i]Slotted, ungasketed or gasketed with float.

Emission estimates were generated for the default EFR tank for each type of seal configuration. As shown in Table 5-15, the emission estimates ranged from 37 lb/d to 234 lb/d. Based on the emission estimates for the different types of primary rim-seals, it is most important to determine whether the rim-seal is a vapor-mounted seal versus a liquid- or shoe-mounted seal. In the case of vapor-mounted seals, it is also important to know whether a secondary rim-seal is used on the tank because of the wide variability in the emission estimates (70 to 234 lb/d) for a vapor mounted primary only seal and a vapor mounted primary with secondary rim-seals. For liquid-mounted seals, the variability with and without secondary rim-seals is not as significant as that for vapor-mounted rim-seals. The emission estimates for liquid-mounted rim-seals varied from 37 to 54 lb/d. For shoe-mounted rim-seals, the variability with and without secondary rim-seals is slightly more pronounced than that for liquid-mounted rim-seals ranging from 43 to 103 lb/d. Given the wide variability in the emission estimates among primary rim-seal configurations, the reliability of the emission estimates depends strongly on identifying the primary rim-seal type for the tank. The relative importance of the secondary rim-seal configuration depends on the type of primary rim-seal used.

The color of the shell is a variable in the emission estimation procedures. The color of the shell of the tank is used indirectly to determine the surface temperature of the stored liquid. For each color combination, a solar absorptivity factor is developed that accounts for the ability of the color to absorb or reflect heat. The lighter the color, the less heat absorbed and the lower the liquid surface temperature. The overall effect of shell color on the standing storage loss is fairly small for tanks that are painted with colors that have a high reflectivity such as white, aluminum, etc. The effect becomes more pronounced if the tank color is a dark color such as red primer. For example, the emissions estimate for the default EFR tank (painted white) with vapor-mounted primary seals was 234 lb/d. However, if the actual paint color had been red primer, the emissions would have been underestimated by 25 percent. On the other hand, if the actual paint color had been aluminum, the emissions would have been underestimated by only 8 percent.

The type of deck used, double-deck or pontoon, has no appreciable effect on the EFR emission estimates. The emission estimates assuming double-deck floating roofs are slightly lower (less than 0.1 percent) than those generated for pontoon decks.

A comparison of the emission estimates when the tank is assumed to be equipped with typical deck fittings versus being equipped with controlled fittings indicates that the emission estimates using controlled fittings are 12 to 75 percent less than the estimates using typical fittings. However, the one fitting that has a significant effect on the emission estimate is the guide pole. The use of a slotted guide pole rather than an unslotted guide pole can result in total emission increases from 10 to over 200 percent depending upon the type of rim-seal used on the tank. Emission estimates for tanks equipped with the more efficient rim-seal systems are more effected by inaccuracies associated with incorrect specification of the configuration of the guide pole than are those with inefficient rim-seal systems.

As expected, the wind speed at the tank's location is a dominant factor in the emission estimates from the storage tank. The wind speed of the default tank was 6.4 miles per hour (mph). The emission estimates for the default tank were recalculated assuming wind speeds of 2 and 10 mph. A wind speed of 10 mph is the default value recommended by API for use if no other data are available. The lower wind speed of 2 mph resulted in a 50 to 85 percent decrease in emissions from those estimated at a wind speed of 6.4 mph. The higher wind speed of 10 mph resulted in a 70 to 280 percent increase in emissions from these estimated at a wind speed of 6.4 miles per hour. These results highlight the importance of accurate wind speed measurements for estimating emissions.

The sensitivity of both the temperature and vapor pressure were examined concurrently since vapor pressure is dependent upon the liquid surface temperature. The base case temperature and vapor pressure conditions are 66°F and 5.74 psia. A temperature change of ±20°F degrees results in vapor pressures of 3.84 psia and 8.32 psia. At the lower temperature and vapor pressure, the emission estimates are reduced by about 40 percent from the base case. At the higher temperature and vapor pressure, the emission estimates are 65 to 69 percent higher than those estimated at the base case conditions.

A change in the vapor molecular weight of the mixture also results in changes in the emission estimates. Vapor molecular weights of crude oils and gasolines can vary by as much as 40 lb/lb-mole. The base case molecular weight is 66 lb/lb-mole. At the lower molecular weight of 46 lb/lb-mole, the emission estimates resulted in a 30 percent reduction from those calculated at 66 lb/lb-mole. At the higher molecular weight of 86 lb/lb-mole, the emission estimates increased by 30 percent from those generated at 66 lb/lb-mole.

5.3.1.3 Internal Floating Roof Tank. The default IFR tank is 50 feet in diameter and has a bolted deck with typical fittings. The default tank stores acetone, which has a molecular weight of 58 lb/lb-mole. The shell and roof of the tank are painted white and the tank is located in Greensboro, North Carolina. Table 5-19 presents the results of the sensitivity analyses on IFR standing storage losses (deck fitting, rim-seal, and deck seam losses). The variables that have the strongest influence on estimating IFR standing storage losses are the physical properties of the liquid (liquid type, vapor pressure, and molecular weight). For IFRT's, the configuration of the tank does not have as much influence on the estimated standing storage loss as for external floating roof tanks.

TABLE 5-19. RESULTS OF SENSITIVITY ANALYSIS FOR THE STANDING STORAGE LOSS EQUATION FOR INTERNAL FLOATING ROOF TANKS

Independent variables	Standing storage losses, lb/d			
	Vapor-mounted primary rim-seal		Liquid-mounted primary rim-seal	
	None[a]	ss[b]	None[a]	ss[b]
Default tank[c]	6.3	4.3	4.1	3.5
Tank characteristics				
1.Paint color				
a.Red primer	8.4	5.8	5.4	4.7
b.Aluminum	6.9	4.7	4.4	3.8
2.Roof type				
a.Column-supported	6.3	4.3	4.1	3.5
b.Self-supported	5.2	3.3	3.0	2.4
3.Deck type				
a.Bolted	6.3	4.3	4.1	3.5
b.Welded	4.6	2.6	2.4	1.8
4.Deck construction				
a.Cont. sheet 5 ft	6.3	4.3	4.1	3.5
b.Cont. sheet 6 ft	6.1	4.1	3.8	3.3
c.Cont. sheet 7 ft	5.9	3.9	3.6	3.1
d.Panel 5 x 7.5	7.3	5.3	5.1	4.5
e.Panel 5 x 12	6.9	4.9	4.7	4.1
5.Fittings				
a.Typical	6.3	4.3	4.1	3.5
b.Controlled	5.6	3.6	3.4	2.8
Meteorological conditions				
1.Temperature				
a.+20°F	11.2	7.7	7.2	6.2
b.-20°F	3.5	2.4	2.3	1.9
Liquid properties				
1.Vapor pressure				
a.vp = 2.91 psia	6.3	4.3	4.1	3.5
b.vp = 1.69 psia	3.5	2.4	2.3	1.9
c.vp = 4.76 psia	11.2	7.7	7.2	6.2
2.Vapor molecular weight				
a.MW = 38 lb/lb-mole	4.1	2.8	2.7	2.3
b.MW = 58 lb/lb-mole	6.3	4.3	4.1	3.5
c.MW = 78 lb/lb-mole	8.5	5.8	5.5	4.7
Liquid type				
a.Organic liquid (2.91 psia)	6.3	4.3	4.1	3.5
b.Gasoline (RVP 10)	13.7	9.4	8.9	7.6
c.Crude oil (RVP 5)	2.1	1.5	1.4	1.2

[a]No secondary rim-seal.

[b]Rim-mounted secondary rim-seal.

[c]The default tank is 50 feet in diameter and is located in Greensboro, North Carolina. The tank has a bolted deck with typical deck fittings. The shell and roof of the tank are painted white. The stored liquid is acetone [vp = 2.91 at ambient conditions] with a vapor molecular weight of 58 lb/lb-mole.

Emission estimates were generated for the default IFR tank for each type of rim-seal configuration. As shown in Table 5-19, the emission estimates ranged from 3.5 lb/d to 6.3 lb/d. With regard to rim-seal type, the estimated emissions for the rim-seal configurations presented in Table 5-16 indicate that it is most important to identify the use of a vapor-mounted primary seal without a secondary seal versus the use of all other seal configurations. For the vapor-mounted seal without a secondary seal, the emission estimate is 6.3 lb/d. For the vapor-mounted rim-seal with a secondary rim-seal and for the liquid-mounted rim-seal with and without a secondary rim-seal, the emission estimates are 4.3, 3.5, and 4.1 lb/d, respectively.

The color of the shell is a variable in the IFR emission estimation procedures. The emissions estimate for the default tank (white) with a vapor-mounted primary seal was 6.3 lb/d. However, if the actual paint color had been red primer, the emissions would have been underestimated by 25 percent; if the actual paint color had been aluminum, the emissions would have been underestimated by 9 percent.

The type of fixed roof used has a minor influence on the IFR standing storage loss emissions. Column-supported fixed roofs resulted in higher emission estimates than self-supported fixed roofs because of the deck penetration required to accommodate the columns in the tank. The emission estimates for column-supported fixed roofs are 23 to 27 percent higher than those for self-supported fixed roofs.

The type of deck used, bolted or welded, has a similar effect on the IFR emission estimates as the rim-seal configuration. The emission estimates assuming bolted decks are higher than those from welded decks because of the deck seam losses for bolted IFR decks. The emission estimates for welded decks are 25 to 40 percent lower than those for bolted decks. In addition, the construction of the bolted deck has a minor influence on the emission estimates. Five basic deck construction parameters were examined to determine the effect of the variation of the deck construction on IFR standing storage losses. The emission estimates can vary from an underestimate of 3 to 10 percent to an overestimate from 10 to 20 percent.

The sensitivity of the estimating equations to whether controlled or uncontrolled fittings are specified is small compared to other factors. The emission estimates are decreased by 11 to 20 percent when controlled fitting factors are used versus typical fitting factors.

The sensitivity of both the temperature and vapor pressure were examined concurrently because vapor pressure is dependent upon the liquid surface temperature. The base case temperature and vapor pressure are 66°F and 2.41 psia. A temperature change of $\pm$20°F resulted in vapor pressures of 1.69 psia and 4.76 psia. At the lower temperature and vapor pressure, the emission estimates were reduced by approximately 45 percent. At the higher temperature and vapor pressure, the emission estimates were 75 to 80 percent higher than those estimated at the base case conditions.

A change in the vapor molecular weight also results in changes to the emission estimates. At the lower vapor molecular weight selected for the sensitivity analysis, 38 lb/lb-mole, the estimated emissions are 35 percent less than the estimated emissions for the base case, 58 lb/lb-mole. At the higher molecular weight selected for the sensitivity analysis, 78 lb/lb-mole, the emission estimates increased by approximately 35 percent over those calculated at the base case molecular weight, 58 lb/lb-mole.

As expected, the type of liquid stored in the tank has the strongest influence on the IFR emission estimates. For example, if the tank had been storing crude oil (RVP 5) rather than acetone, the emission estimates would have been overestimated by 200 to 300 percent. If the tank had been storing gasoline (RVP 10) instead of acetone, the emission estimates would have been underestimated by approximately 46 percent. Therefore, it is very important to determine the type(s) of liquid(s) stored in the tank during the period over which the emission estimates are calculated.

5.3.2 Withdrawal Loss

In terms of overall emissions from floating roof tanks, the independent variables in the withdrawal loss equation have a fairly insignificant effect because the majority of the emissions occur from standing storage. Typically, withdrawal loss emissions account for less than 5 percent of the overall emissions from floating roof tanks. However, it should be noted that as the tank diameter increases, the sensitivity of the withdrawal loss equation to certain variables increases.

5.3.2.1 External Floating Roof Tanks. The independent variables evaluated during the sensitivity analysis of the withdrawal loss equation for external floating roof tanks consisted of the shell condition, the turnover rate, and the liquid type. The results of the analysis are presented in Table 5-20. All three factors have an effect on emissions, but shell condition has the greatest effect.

Table 5-20 shows that the condition of the tank shell (light rust, dense rust, or gunite lined) has a greater effect on estimated emissions from crude oils than from gasolines. The default value for the shell condition is light rust. However, if the tank is gunite lined, the withdrawal loss is dramatically underestimated compared to the base case, especially for crude oils (40 lb/yr versus 4,000 lb/yr).

The influence of the turnover rate on EFR emissions is fairly insignificant compared to the effect of the shell condition or the effect of turnovers on fixed roof tanks. At 10 turnovers per year, EFRT withdrawal losses were estimated to be 14 lb/yr. At 100 turnovers per year, withdrawal losses were estimated at 140 lb/yr.

The type of liquid stored in the tank has a small impact on estimating EFRT withdrawal losses. Estimated withdrawal losses for gasoline are 26 lb/yr less than those estimated for crude oil. The higher withdrawal loss estimate for crude oil is a result of the higher clingage factor for heavy crudes than for lighter gasolines. Heavy crude oils tend to cling to the tank shell more than the lighter gasolines.

TABLE 5-20. SENSITIVITY ANALYSIS OF WITHDRAWAL LOSSES FROM EXTERNAL FLOATING ROOF TANKS

Independent variables	Withdrawal loss, lb/yr
Shell condition[a]	
Gasoline (RVP 8.5)	
a.Light rust	14
b.Dense rust	67
c.Gunite lined	1,300
Crude Oil (RVP 5)	
a. light rust	40
b. dense rust	200
c. gunite lined	4,000
Turnover rate[b]	
a. 10 turnovers per year	14
b. 50 turnovers per year	67
c. 100 turnovers per year	140
Liquid type[a]	
a. Crude oil (RVP 5)	40
b. Gasoline (RVP 8.5)	14

[a]Based on 10 turnovers per year.
[b]Based on gasoline (RVP 8.5).

5.3.2.2 Internal Floating Roof Tanks. The independent variables evaluated during the sensitivity analysis of the withdrawal loss equation for IFRT's consisted of the column diameter, roof type, shell condition, and the turnover rate. The results of the analysis are presented in Table 5-21. Shell condition has the greatest effect on estimated withdrawal losses. Turnover rate also has an effect on estimated withdrawal loss. However, roof type essentially has no effect on estimated withdrawal loss.

Table 5-21 shows that the condition of the tank shell (light rust, dense rust, or gunite lined) has a greater effect on estimated withdrawal loss when storing crude oil than when storing other volatile organic liquids. The default value for the shell condition is light rust. However, if the tank is gunite lined, the withdrawal losses are underestimated dramatically compared to the base case, especially for crude oils (310 lb/yr versus 31,000 lb/yr).

The type of liquid stored in the tank has an impact on the estimated withdrawal losses. Estimated withdrawal losses for acetone were 2.7 times lower than the estimated losses for crude oils (110 lb/yr versus 310 lb/yr). The higher estimated losses for crude oil is a result of the higher clingage factor for heavy crudes than for lighter volatile organic liquids. Heavy crude oils tend to cling to the tank shell more than the lighter volatile organic liquids.

In the case of the turnover rate, the influence of the turnover rate on emissions is fairly insignificant compared to the effect of the shell condition or the effect of turnovers on fixed roof tanks. At 10 turnovers per year, estimated emissions are 23 lb/yr. At 100 turnovers per year, estimated emissions are 230 lb/yr.

The type of fixed roof has an insignificant effect on the withdrawal loss emissions. A column-supported fixed roof, in theory, has a higher withdrawal loss than that of a self-supported fixed roof because of the clingage of the liquid on the columns in the column-supported fixed roofs. However, the diameter of the columns are fairly small, therefore, the difference between the estimated withdrawal losses between the different roof types is insignificant (within two significant figures).

The column diameter also is a variable in IFR withdrawal loss for the same reason as that stated above for a column-supported internal floating roof tank. As with the column-supported fixed roofs, the column diameter has essentially no effect on the working loss emissions. Column diameters typically range from 0.8 to 1.1 ft. The use of the various column diameters did not produce any effect on the overall withdrawal loss estimate of 110 lb/d.

TABLE 5-21. SENSITIVITY ANALYSIS OF WITHDRAWAL LOSSES FROM INTERNAL FLOATING ROOF TANKS

Independent variables	Withdrawal loss, lb/yr
Shell condition	
Volatile organic liquids	
a.Light rust	110
b.Dense rust	570
c.Gunite lined	11,000
Crude oils	
a.Light rust	310
b.Dense rust	1,500
c.Gunite lined	31,000
Turnover rate	
a.10 turnovers per year	23
b.50 turnovers per year	110
c.100 turnovers per year	230
Roof type	
a.Column-supported	110
b.Self-supported	110
Column diameter	
a.Built-up	110
b.Pipe	110
c.Unknown	110

5.4 CONCLUSIONS

The results of these analyses support the continued use of the API floating roof tank estimating equations in AP-42. The estimating equations for tanks with mechanical shoe rim-seals appear to be very reliable for estimating emissions for large tank populations. The equations for the liquid- and vapor-mounted resilient-filled rim-seals are less reliable than those for mechanical shoe seals, but they provide reasonable estimates for large tank populations. While the equations do provide good estimates of emissions for tank populations, their ability to present reliable estimates for single tanks is limited. Assuming all input parameters for a single tank are correct, the inherent uncertainty in the coefficients used makes the emission estimate imprecise. The 95 percent confidence interval for annual emissions from a single tank typically spans an order of magnitude or more.

5.5 REFERENCES

1. *Evaporative Loss From External Floating Roof Tanks*, Bulletin No. 2517, Third Edition, American Petroleum Institute, Washington, DC, 1989.

2. *Evaporative Loss From External Floating Roof Tanks: Documentation File for API Publication 2517*, American Petroleum Institute, Washington, DC.

3. *Evaporative Loss from Internal Floating Roof Tanks*, API Publication 2519, American Petroleum Institute, Washington, DC, March 1990.

4. *Evaporative Loss from Internal Floating Roof Tanks: Documentation File for API Publication 2519*, American Petroleum Institute, Washington, DC.

5. *Manual of Petroleum Measurement Standards Chapter 19--Evaporative Loss Measurements; Section 2--Evaporative Loss Floating-Roof Tanks*, Preliminary Draft, American Petroleum Institute, December 31, 1994.

6. *Documentation of Rim-seal Loss Factors for the Manual of Petroleum Measurement Standards, Chapter 19--Evaporative Loss from Floating-Roof Tanks*, Revised draft, The TGB Partnership, Hillsborough, Hillsborough, NC, April 5, 1995.

7. Wallace, D., *Evaluation of Rim-Seal Loss Factors for AP-42 Use*, University of Alabama, Birmingham, AL, September 1995.

8. *Hydrocarbon Emissions Floating Roof Petroleum Tanks*, Engineering Science, Inc., prepared for Western Oil and Gas Association, Los Angeles, CA, January 1977.

9. *Addendum to Publication 2517--Evaporative Loss From External Floating Roof Tanks*, American Petroleum Institute, Washington, DC, May 1994.

10. Memorandum from R. Jones, D. Wallace, Midwest Research Institute, to D. Beauregard, U. S. Environmental Protection Agency, *Review of Fitting Analyses Conducted in Support of an Addendum to API Publication 2517 for External Floating Roof Tanks*, December 5, 1994.

11. Memorandum from R. Jones, D. Wallace, Midwest Research Institute, to A. Pope, U. S. Environmental Protection Agency *Review of Guide Pole Fittings Analyses Conducted in Support of*

an Addendum to API Publication 2517 for External Floating Roof Tanks, May 25, 1994.

12. Memorandum from A. Parker, Midwest Research Institute, to file, *Final Guidepole Fitting Factors: Revised Analysis*, November 8, 1995.

13. Memorandum from A. Parker, Midwest Research Institute, to D. Beauregard, U. S. Environmental Protection Agency, *Final Deck Fitting Loss Factors for Use in AP-42 Section 7.1*, February 23, 1996.

14. *Wind Tunnel Testing of External Floating Roof Storage Tanks*, Cermak, Peterka, Peterson, Inc., prepared for the American Petroleum Institute, CPP Reports 92-0869, 93-0934, and 93-1024.

15. *Documentation of the Fitting Wind-Speed Correction Factor*, The TGB Partnership, Hillsborough, NC, March 25, 1995.

16. Memorandum from A. Parker, Midwest Research Institute, to D. Beauregard, EPA, *Fitting Wind Speed Correction Factor for External Floating Roof Tanks*, September 22, 1995.

17. Laverman, R.J., Haynie, T.J., and Newbury, J.F., *Testing Program to Measure Hydrocarbon Emissions from a Controlled Internal Floating Roof Tank*, Chicago Bridge and Iron Company, March 1982.

18. Chicago Bridge & Iron Technical Services Company, *Loss Factor Measurements of Internal Floating Roof Deck Seams*, Interim Reports 1-7, Prepared for the American Petroleum Institute Committee on Evaporation Loss Measurement, September 1994-October 1996.

19. Petrex, Inc., *Test for Vapor Loss Through Clamp Bars Used on Petrex Internal Floating Roof System*, Prepared by Petrex, Inc., March 5, 1984.

20. *Field Testing Program to Determine Hydrocarbon Emissions from Floating Roof Tanks*, Final Report, Volumes I and II, Radian Corporation, May 1979.

6. SUMMARY OF CHANGES TO AP-42 SECTION

The following sections summarize the major changes made since the previous version of Section 7.1--Organic Liquid Storage Tanks (September 1997) of AP-42.

6.1 CHANGES TO EMISSION ESTIMATION PROCEDURES AND FACTORS FOR FIXED ROOF TANKS

An update of Section 7.1.3.1, mainly concerning low pressure tanks, was added. Table 7.1-6 was updated, giving new paint solar absorptance factors for additional tank colors. All changes are based on research performed by The American Petroleum Institute (API) and The TGB Partnership. For more information, the API *Manual of Petroleum Measurement Standards, Chapter 19.1 (API MPMS 19.1)* should be consulted.

6.2 CHANGES TO EMISSION ESTIMATION PROCEDURES AND FACTORS FOR FLOATING ROOF TANKS

A new section was added to address emissions that originate during the landing of a floating roof. All changes are based on research performed by The American Petroleum Institute (API) and The TGB Partnership. For more information, the API *Manual of Petroleum Measurement Standards, Chapter 19.2 (API MPMS 19.2)* should be consulted.